Aprofundiment en la relació estructura/funció de les metal·lotioneïnes (MTs). Estudi de la capacitat coordinant i de la influència de lligands no proteics en MT4 de mamífer i altres MTs relacionades

Tesi Doctoral

Laura Villarreal Tolchinsky

Setembre 2005

Abreujaments

aa	Aminoàcids
Cys	Cisteïna
DC	Dicroisme circular
ED	Espectres de diferència dels espectres d’absorció UV-Visible
eq	Equivalent molar
ESI-MS	Espectrometria de masses amb ionització per electrosprai
FPLC	Cromatografia de líquids amb columna de gel tou
GC-FPD	Cromatografia de gasos amb detector fotomètric de flama
His	Histidina
HPLC	Cromatografia de líquids d’alta resolució
ICP-AES	Espectroscòpia d’emissió atòmica de plasma acoblat per inducció
Lys	Lisina
Met	Metionina
MTs	Metal·lotioneïnes
N_{His}	Nitrogen histidínic
RMN	Ressonància Magnètica Nuclear
S_{Cys}	Sofre cisteínic
Tris	Tris(hidroximetil)aminometà
UV-Vis	Espectres d’absorció UV-Visible

ORGANITZACIÓ DEL MANUSCRIT

D’acord amb la normativa vigent, i prèvia acceptació de la Comissió de Doctorat de la Universitat Autònoma de Barcelona, aquesta memòria es presenta com a compendi d’articles publicats i presentats a la Comissió de Doctorat de la UAB el mes de Juny del 2005. Així mateix, amb l’interès de presentar una memòria el més completa possible, s’han inclòs en forma d’annex els treballs realitzats en el marc d’aquesta Tesi Doctoral que han estat enviats posteriorment i d’altres que estan en procés d’elaboració. Els treballs inclosos a la memòria són:

1. **Functional Differentiation in the Mammalian Metallothionein Gene Family. Metal binding features of mouse MT4 and comparison with its paralog MT1**
   Laura Tío, Laura Villarreal, Sílvia Atrian and Mercè Capdevila, *Journal of Biological Chemistry* (2004) **279**, 24403-24413.

2. **Influence of chloride ligands on the structure of Zn- and Cd-metallothionein species**
   Laura Villarreal, Laura Tío, Sílvia Atrian and Mercè Capdevila, *Archives of Biochemistry and Biophysics* (2005) **435**, 331-335.

3. **Zn- and Cd-Metallothionein Recombinant Species from the Most Diverse Phyla May Contain Sulfide (S^{2-}) Ligands**
   Mercè Capdevila, Jordi Domènech, Ayelen Pagani, Laura Tío, Laura Villarreal and Sílvia Atrian, *Angewandte Chemie International Edition* (2005) **44**, 4618

ANNEX

4. **Metallothionein (MT) differentiation in warm-blooded Vertebrates. Comparative Genomics and metal-binding analysis of chicken MT *vs.* mammalian forms**
   Laura Villarreal, Laura Tío, Mercè Capdevila and Sílvia Atrian, *FEBS Journal*
   Enviat 19/07/05
5. **Yeast Crs5: a putative ancestor in the Zn-thionein lineage**
   Laura Villarreal, Ayelen Pagani, Sívia Atrian and Mercè Capdevila, Manuscrit en preparació

ÍNDEX

1. **Introducció** ... 3
   - **1.1 Què són les metal·lotioneïnes?** ... 3
   - **1.2 Mètodes d'obtenció** ... 3
   - **1.3 Característiques estructurals** ... 4
   - **1.4 Classificació de les metal·lotioneïnes** ... 6
   - **1.5 Les metal·lotioneïnes en els organismes vius** ... 8
     - 1.5.1 MTs de mamífer ... 9
     - 1.5.2 MTs d'altres vertebrats ... 10
     - 1.5.3 MTs de llevat ... 11
     - 1.5.4 Altres MTs ... 13
   - **1.6 Reactivitat i funció fisiològica** ... 15
   - **1.7 Objectius** ... 16
2. **Resultats i Discussió** ... 19
   - **2.1 Capacitat coordinant de la isoforma MT4 de mamífer** ... 20
     - 2.1.1 Propietats coordinants de MT4 envers Zn(II) ... 21
     - 2.1.2 Propietats coordinants de MT4 envers Cd(II) ... 22
     - 2.1.3 Propietats coordinants de MT4 envers Cu(I) ... 24
   - **2.2 Influència dels lligands no proteics en l'estructura de les espècies metall-MT** ... 27
     - 2.2.1 Participació dels ions clorur (Cl^-) en els complexos metall-MT ... 27
     - 2.2.2 Participació dels ions sulfur (S^{2-}) en els complexos metall-MT ... 29
     - 2.2.3 Revisió dels resultats publicats sobre MT4 i MT1 ... 32
   - **2.3 Capacitat coordinant de la MT de pollastre, ckMT1** ... 35
     - 2.3.1 Propietats coordinants de ckMT1 envers Zn(II) i Cd(II) ... 35
     - 2.3.2 Propietats coordinants de ckMT1 envers Cu(I) ... 40
   - **2.4 Capacitat coordinant d'una MT de llevat, Crs5** ... 43
     - 2.4.1 Propietats coordinants de Crs5 envers Zn(II) i Cd(II) ... 43
     - 2.4.2 Propietats coordinants de Crs5 envers Cu(I) ... 45
3. **Conclusions** ... 53
4. **Bibliografia** ... 57
5. **Articles publicats** (acceptats per la Comissió de Doctorat, Juny 2005) ... 63
6. **Annex** (articles i manuscrits posteriors a la Comissió de Doctorat) ... 111

1. Introducció

1. INTRODUCCIÓ

1.1 Què són les metal·lotioneïnes?

L'any 1957, Margoshes i Vallee descobreixen i caracteritzen una proteïna associada a zinc i cadmi a partir de còrtex de ronyó de cavall, que van anomenar metal·lotioneïna degut al seu elevat contingut en sofre i ions metàl·lics.[1] Des d'aquest descobriment, el nombre de treballs dedicats a aquestes proteïnes ha crescut exponencialment, de tal manera que avui en dia es poden trobar en la literatura prop de 17.000 articles científics que cobreixen els resultats obtinguts tant pel que fa referència als seus aspectes químics, biològics i bioquímics com a d'altres de caire mediambiental, toxicològic, patològic o nutricional.[2]

Les metal·lotioneïnes (MTs) són unes proteïnes molt particulars, no només per la seva ubiqüitat (presents en la majoria d'organismes vius, apartat 1.5), sinó perquè, a més a més, es caracteritzen per tenir un baix pes molecular (3-10 kD) i un elevat nombre de cisteïnes (30% dels seus aminoàcids). Aquest alt contingut en Cys els confereix una elevada capacitat per enllaçar ions metàl·lics així com una considerable reactivitat. Cal destacar també el baix nombre de residus hidrofòbics (0-3%), histidina i arginina i l'absència, en la majoria de MTs, de residus aromàtics, la qual cosa facilita el seu estudi per tècniques espectroscòpiques. Les MTs natives enllacen metalls essencials, bàsicament Zn(II) i/o Cu(I), però també poden coordinar metalls tòxics, com Cd(II), Hg(II), Ag(I) o Pb(II). A més, amb independència de la seva composició metàl·lica inicial, les MTs poden enllaçar-se *in vitro* a una gran varietat d'ions metàl·lics, com Ag(I), Au(I), Bi(III), Cd(II), Co(II), Cu(I), Fe(II), Hg(II), Ni(II), Pb(II), Pt(II), Tc(IV) i Zn(II).[3]

1.2 Mètodes d'obtenció

El procediment tradicional d'obtenció de MTs, i fins fa uns anys el més emprat, es basa en la inducció de la seva síntesi en éssers vius i el seu posterior aïllament i purificació a partir dels òrgans on més es sintetitza la proteïna. La producció de MTs pot ser induïda per un gran nombre de factors, com per exemple la presència de metalls, agents radicals oxidants, exposició a radiació UV, determinades hormones, etc. Aquest mètode, però, presenta diversos inconvenients ja que comporta un procediment de purificació llarg i difícil que sovint dóna lloc a proteïnes de baixa concentració i puresa limitada.[4] Addicionalment, no és aplicable a tots els organismes i la composició metàl·lica de les proteïnes que se'n recuperen és funció del mètode

d'inducció emprat.

Una possibilitat emprada per tal de pal·liar els inconvenients de la metodologia anterior, però menys utilitzada que la primera, és la síntesi química de les cadenes peptídiques sobre suport sòlid. Si bé aquesta metodologia ha permès caracteritzar MTs de fongs[5] i els dominis per separat d'algunes MTs de crustaci[6] i de mamífer[7,8] també presenta les seves limitacions, com és la longitud de la cadena peptídica o el fet que s'obté la proteïna desmetal·lada i, per tant, té el requeriment d'haver de protegir els residus cisteínics per evitar la seva oxidació.

Una altra alternativa, molt més actual i àmpliament utilitzada avui en dia, consisteix en la biosíntesi de MTs mitjançant la tècnica de l'ADN recombinant. Aquesta es basa en la utilització de cèl·lules bacterianes o de llevat per sintetitzar productes heteròlegs, és a dir, propis d'una altra espècie. Així, l'aprofitament dels mecanismes cel·lulars de síntesi de proteïnes en bacteri o llevat permet obtenir quantitats elevades d'un producte que normalment no es sintetitza en aquestes cèl·lules. D'aquesta manera es poden obtenir MTs d'una gran puresa en elevades concentracions i en forma metal·lada, evitant així els inconvenients dels mètodes anteriors.[2]

Entre d'altres, el grup de recerca de la Universitat de Barcelona actualment dirigit per la Dra. Sílvia Atrian va posar a punt, cap a l'inici de la dècada dels 90, un mètode d'expressió de metal·lotioneïnes en *E.coli*. Des de llavors, s'han obtingut MTs d'una àmplia varietat d'organismes i fins i tot s'han pogut sintetitzar per separat els dominis constituents d'algunes MTs que s'estructuren en més d'un domini.[9,10] Així mateix, i en funció del metall amb què s'enriqueix el medi de cultiu, s'han obtingut MTs enllaçades a diferents ions metàl·lics, tot cercant aquells agregats metall-MT de rellevància fisiològica.

1.3 Característiques estructurals

La majoria de MTs presenten un baix grau d'estructura secundària i manca d'estructura terciària,[11] de manera que en absència de metall (forma apo) les MTs presenten una estructura desordenada (*random coil*).[12] Així, actualment és ben conegut que l'estructura tridimensional de les MTs ve determinada pel nombre i naturalesa dels ions metàl·lics coordinats, els quals donen lloc a complexos metall-tiolat polinuclears. Per tant, són les Cys de la cadena polipeptídica de les MTs les que coordinen els ions metàl·lics i és aquesta coordinació la que determina el replegament de la proteïna. No obstant això, la formació de complexos metall-MT estables només pot ser aconseguida si la cadena polipeptídica es plega de manera

que els àtoms de S_{Cys} quedin disposats en una situació espacial acceptable per a satisfer les geometries de coordinació específiques dels ions metàl·lics enllaçats i sense produir tensions excessives en la conformació de la proteïna.[3] Afortunadament, la gran plasticitat de l'estructura primària d'aquestes proteïnes els confereix la sorprenent propietat d'adaptar-se a metalls que difereixen força en el seu radi atòmic i preferències coordinatives sense provocar distorsions importants en la geometria de coordinació d'aquests ni en la conformació global de la proteïna.

Aquesta mateixa flexibilitat de la cadena polipeptídica, juntament amb la fluctuació dinàmica dels ions metàl·lics entre els dominis de les MTs, ha dificultat durant molt de temps l'estudi de l'estructura d'aquestes proteïnes mitjançant les tècniques convencionals. No obstant això, les tècniques de RMN de ^{111}Cd, ^{113}Cd i/o ^{1}H i de difracció de raigs X han permès disposar d'informació precisa sobre l'estructura tridimensional d'algunes MTs. Així, per RMN s'ha pogut resoldre l'estructura d'algunes MTs de mamífer,[13,14,15,16,17] i d'altres organismes com peixos,[18] crustacis,[19,20] equinoderms[21] o cianobacteris[22] enllaçades a metalls divalents (Zn i/o Cd). Amb aquests estudis s'ha pogut determinar que en les MTs de mamífer la cadena polipeptídica es replega donant lloc a dos dominis globulars d'aproximadament la mateixa mida, amb quiralitat oposada, i essencialment no interactius i en els que els residus hidrofílics estan orientats cap a l'exterior de la molècula (Figura 1.1). El fragment N-terminal forma l'agregat M_3S_9, domini β, amb 3 S_{Cys} pontals i 6 de terminals, i el fragment C-terminal dóna lloc a l'agregat M_4S_{11}, domini α, amb 5 S_{Cys} pontals i 6 de terminals. En ambdós dominis, els metalls presenten coordinació tetraèdrica. En les altres espècies esmentades, amb l'excepció de la MT de bacteri, també s'observa l'ordenació dels polipèptids en dos dominis, propers als de mamífer, però que tant el número com la posició dels residus de Cys és diferent, generant diferències estructurals i de reactivitat importants. Contràriament, la MT de cianobacteri, més curta que les anteriors, presenta un únic agregat $Zn_4(S_{Cys})_9(N_{His})_2$ de conformació similar al domini α de les MTs de mamífer.

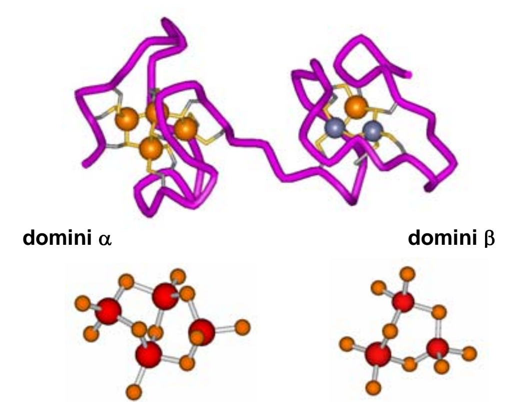

Figura 1.1.- Estructura de la Cd_5Zn_2-MT2 de fetge de rata i dels seus fragments α i β.

Les dificultats en l'obtenció de mostres cristalitzades, juntament amb la inexistència d'isòtops de Cu actius en RMN,[23] han fet que l'estructura de les MTs que contenen Cu sigui força menys coneguda. Tot i així, s'han determinat les estructures

tridimensionals de certes Cu-MTs, com la de Cup1 de *Saccharomyces cerevisiae*[24,25] (Figura 1.2.A) o la de NcMT de *Neurospora crassa*[11] (Figura 1.2.B). Encara que la primera conté 12 Cys, 10 de les quals enllacen entre 7 i 8 Cu(I), i NcMT conté 7 Cys enllaçades a 6 Cu(I),[26] ambdues s'estructuren en un únic domini (Figura 1.2).

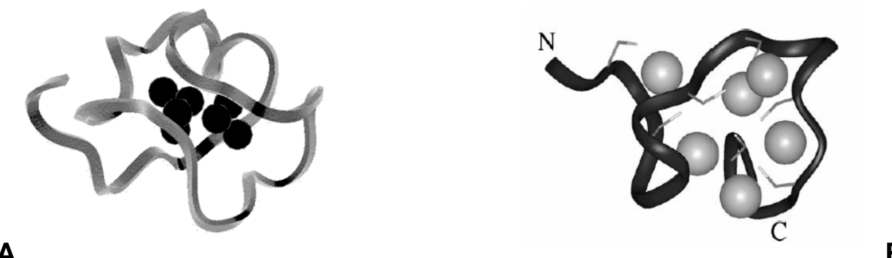

Figura 1.2.- Estructura 3D de: (A) Cu_7-MT de *Saccharomyces cerevisiae*, i (B) Cu_6-MT de *Neurospora crassa*.

La difracció de raigs X i la RMN són les tècniques d'elucidació estructural per excel·lència, però cal remarcar que les espectroscòpies de DC i d'emissió han proporcionat una informació considerable sobre la coordinació d'alguns metalls a les MTs. Així, a partir d'estudis realitzats amb Zn(II), Cd(II), Hg(II), Cu(I) o Ag(I),[3] s'han identificat diversos motius estructurals i s'ha determinat que la MT nativa de fetge de conill dóna lloc a agregats Zn_7-MT, Cd_7-MT, Cu_{12}-MT, Ag_{12}-MT, Ag_{18}-MT o Hg_{18}-MT.[2]

1.4 Classificació de les metal·lotioneïnes

Normalment les proteïnes es classifiquen segons la seva funcionalitat (proteases, oxigenases, reductases, etc). Aquest no és el cas de les MTs, la funció o funcions fisiològiques de les quals avui en dia encara no estan totalment definides (apartat 1.6). Per aquest motiu s'han fet diverses propostes de classificació en funció de les homologies de seqüència i característiques estructurals de les MTs conegudes.

La primera classificació, proposada l'any 1985, comporta tres grans grups de MTs en funció de les característiques de la seva estructura primària.[27]

- Classe I, MTs d'entre 59 i 63 aminoàcids, dels quals uns 20 són Cys. Aquest tipus de MTs es troba en la majoria de vertebrats i en alguns invertebrats. Són homòlogues a MT1 de ronyó de cavall i s'estructuren en dos dominis.
- Classe II, MTs que tot i conservar els residus de Cys, presenten una gran heterogeneïtat de seqüències, totes no alineables amb MT1 de cavall. Aquestes MTs es troben en plantes, fongs, invertebrats i alguns bacteris. La majoria es constitueixen en un únic domini.

- Classe III, cadistines, fitoquelatines i altres polipèptids de fórmula general $(\gamma\text{-Glu-Cys})_n\text{Gly}$, de síntesi enzimàtica, que es troben principalment en vegetals i organismes unicel·lulars.

Posteriorment es va proposar una altra classificació que considera similituds de seqüència globals a més a més de la de les cisteïnes. Aquesta classificació, molt més detallada, divideix les MTs en famílies, subfamílies, subgrups, isoformes i subisoformes.[28,29] Això, però, ha donat lloc a tants grups de MTs com grups taxonòmics hi ha en el regne animal i vegetal.

En qualsevol cas, cap de les dues classificacions esmentades proporciona informació funcional o evolutiva de les MTs, ja que ambdues es basen únicament en similituds de seqüència. Per aquest motiu, el grup de recerca en el qual s'ha realitzat aquesta tesi doctoral va proposar un nou model de classificació que es basa tant en la seqüència aminoacídica com en la preferència de les MTs envers els metalls essencials Zn i Cu. Si els ions metàl·lics coordinats a MT determinen la seva estructura (apartat 1.3), sembla probable que Zn(II) i Cu(I), amb característiques coordinatives pròpies, donin lloc a estructures metall-MT diferents. En conseqüència, en base a les relacions estructura/funció, cal esperar que estructures diferents dels seus agregats metàl·lics també determinin funcions diferents per a aquestes metal·loproteïnes.

D'acord amb la metodologia emprada per aquest grup, la preferència metàl·lica i la capacitat coordinant de les MTs s'avalua mitjançant la producció *in vivo* de cada MT recombinant en medis de cultiu enriquits amb diferents ions metàl·lics, l'estudi de la substitució *in vitro* dels ions metàl·lics inicialment coordinats i l'anàlisi qualitativa i quantitativa de la composició i estructura dels agregats metàl·lics formats tant *in vivo* com *in vitro*. D'aquesta manera les MT es classificarien en:

- **Zn-tioneïnes**: MTs que en medis enriquits en Cu s'expressen com a espècies heterometàl·liques Zn,Cu-MT i que, per tant, requereixen Zn(II) per estructurar-se. Així, MT1 de ratolí[30] i MTH de llamàntol[10] són Zn-tioneïnes.
- **Cu-tioneïnes**: MTs que en medis rics en Cu s'expressen com a espècies homometàl·liques Cu-MT i que, per tant, no requereixen Zn(II) per replegar-se. Totes les MTs de *Drosophila melanogaster*[31,32,33] i el fragment β de MT1[30] són Cu-tioneïnes.

L'interès a continuar validant la nostra proposta de classificació i a esbrinar les relacions entre Zn- i Cu-MTs i la funcionalitat fisiològica d'aquestes són alguns dels motius que han propiciat aquesta tesi.

1.5 Les metal·lotioneïnes en els organismes vius

Les MTs es troben presents en la totalitat dels organismes del regne animal i també en vegetals i procariotes.[34] Actualment es coneixen unes 200 MTs procedents d'unes 100 espècies diferents. D'entre aquestes, les més estudiades han estat les de mamífer, seguides de les de crustaci i llevat, però també hi ha estudis de caracterització, a diferents nivells, de MTs de peixos, aus, insectes, equinoderms, mol·luscs, anèl·lids, nematodes, fongs, protozous i bacteris. En la Taula 1.1 es donen detalls de la seqüència primària d'aquelles MTs de les quals es disposa d'alguna informació respecte els seus complexos metàl·lics des d'un punt de vista químic o estructural. Donat que per motius d'extensió no és possible descriure aquí tot el coneixement que es té actualment sobre aquestes MTs, únicament es comenten a continuació les dades més rellevats de les MTs estrictament relacionades amb aquesta tesi.

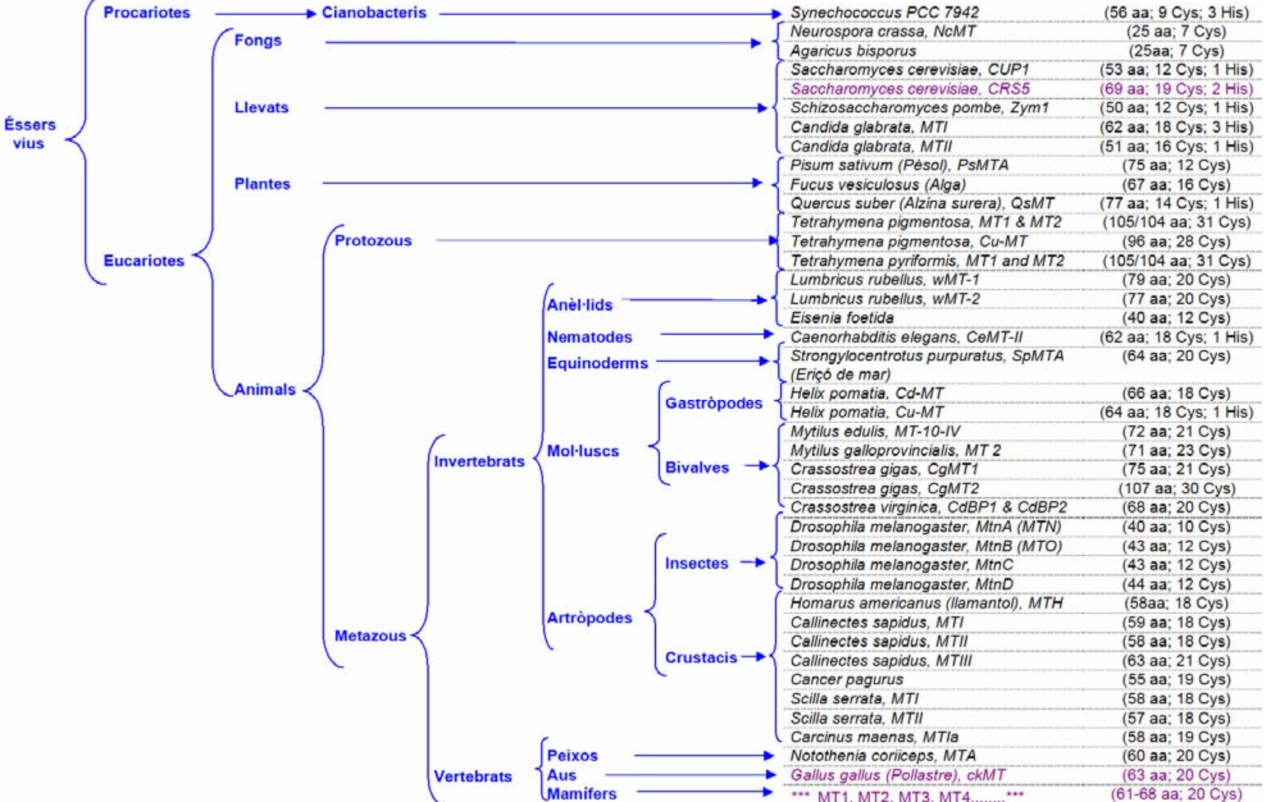

Taula 1.1.- MTs de diferents organismes i les corresponents subfamílies i famílies a les quals pertanyen.

*** per motius d'extensió, les dades de mamífer no s'inclouen en la taula però es comenten en el text.

1.5.1 MTs de mamífer

Les MTs de mamífer han estat llargament estudiades, de manera que avui en dia es té un ampli coneixement d'aquestes proteïnes. Així, en la literatura es troba una gran varietat de treballs tant a nivell biològic (purificació, patrons d'expressió, estudis genètics, clonatge heteròleg, etc) com químic (capacitat coordinant envers diferents metalls, caracterització dels agregats metàl·lics formats, reactivitat, estructuració, etc) referents a MTs de mamífer.[2]

En aquests organismes s'han aïllat fins a quatre gens codificants de MT (MT1, MT2, MT3 i MT4) i si bé en l'espècie humana la isoforma MT1 presenta encara un major grau de multiplicitat amb diferents subisoformes (MT1a, MT1b,...), en altres espècies de mamífer, com el ratolí, només es coneix un representant per a cadascuna de les quatre isoformes principals.

Les 4 isoformes de MT de mamífer presenten les 20 Cys en posicions totalment conservades (Figura 1.3) i una elevada similitud en la resta d'aminoàcids, però en canvi hi ha divergències importants pel que fa als seus patrons d'expressió. Mentre que MT1 i MT2 es sintetitzen ubíquament, MT3 i MT4 presenten expressions específiques, trobant-se únicament en el sistema nerviós i en l'epiteli escamós estratificat, respectivament.[35,36]

```
MT 1    MDP NCSCSTGGSCTCTSSCACKNCKCTSCKKSCCSCCPVGCSKCAQGCVCK          GAADKCTCCA   (61 aa)
MT 2    MDP NCSCASDGSCSCAGACKCKQCKCTSCKKSCCSCCPVGCAKCSQGCICK          EASDKCSCCA   (61 aa)
MT 3    MDPETCPCPTGGSCTCSDKCKCKGCKCTNCKKSCCSCCPAGCEKCAKDCVCKGEEGAKAEAEKCSCCQ   (68 aa)
MT 4    MDPGECTCMSGGICICGDNCKCTTCSCKTCRKSCCPCCPPGCAKCARGCICK          GGSDKCSCCP   (62 aa)
```

Figura 1.3.- Comparació de la seqüència aminoacídica de les 4 MTs de ratolí. S'han assenyalat en groc les Cys conservades en les diferents isoformes.

La MT1 de mamífer és, molt probablement, la MT més estudiada i, per tant, la més coneguda, i degut a la similitud de seqüències entre MT2 i MT1 el comportament descrit per MT1 pot fer-se extensiu a MT2 (apartat 1.3). En canvi, mentre que la isoforma MT3 està essent objecte d'estudis intensius[17,37,38] per la seva possible funció en el sistema nerviós central,[39] la informació de la qual es disposa actualment sobre la isoforma MT4 és molt reduïda.[35,36]

De totes les MTs de mamífer, MT4 és la que presenta diferències aminoacídiques més importants (dels seus 62 aa, entre 24 i 27 difereixen de la resta d'isoformes, mentre que per a MT3 només hi ha 15 diferències) però alhora és la més conservada entre espècies diferents. Això fa que en els arbres filogenètics construïts a partir de seqüències codificants d'ADN, MT4 aparegui en una posició separada de la resta de MTs de mamífer i més propera a les MTs d'aus (Figura 1.4), cosa que suggereix que MT4 podria ser la MT primitiva de mamífer.

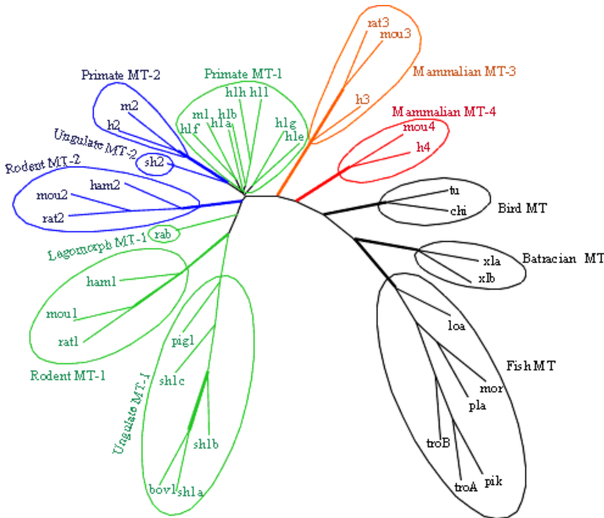

Figura 1.4.- Arbre filogenètic obtingut a partir de les seqüències dels exons de MTs de vertebrats. Extret de: http://www.unizh.ch/~mtpage/poster/postree.GIF

D'acord amb resultats d'aquest grup de recerca, MT1 recombinant de ratolí és una Zn-tioneïna,[10] formada per un domini α, també amb caràcter de Zn-tioneïna, i un domini β que es comporta aïlladament com una Cu-tioneïna.[40] D'acord amb dades bibliogràfiques anteriors obtingudes per a proteïnes natives,[2] quan la MT1 s'expressa en medis rics en Zn s'obté Zn_7-MT1, on els ions Zn(II) poden ser substituïts per Cd(II) per a donar l'agregat isoestructural Cd_7-MT1.[9,41] Per altra part, en medis rics en Cu la proteïna s'expressa com a Cu_7Zn_3-MT1, amb una distribució entre dominis d'acord amb Cu_3Zn_2-αMT1 i Cu_4Zn_1-βMT1.[30]

1.5.2 MTs d'altres vertebrats

Contrastant amb l'ampli coneixement que es té de les MTs de mamífer, la informació disponible sobre altres MTs és molt més limitada i bastant més dispersa.[2] Pel que fa a la resta de vertebrats, cal destacar que els treballs de caracterització química i/o estructural de MTs de peixos, amfibis, rèptils i aus (Taula 1.1) són pràcticament inexistents.

Estudis evolutius en vertebrats han posat de manifest un alt grau de proximitat entre les MTs d'aus i de mamífer (Figura 1.4), dos tipus d'organismes que han evolucionat paral·lelament durant pràcticament 310 milions d'anys,[42] cosa que ha portat a proposar que ambdós organismes contenen MTs originades per un ancestre comú.[43] El pollastre (*Gallus gallus*) és l'organisme model per a l'estudi de les aus i la seva MT, ckMT, ha estat considerada funcionalment equivalent a les MTs de mamífer.

La metal·loproteïna ckMT consta de 63 aminoàcids, dels quals 20 són Cys i 1 His, i presenta un 68% de similitud de seqüència i dues insercions aminoacídiques en

relació a MT1 de ratolí.[44] Addicionalment, l'expressió del gen de ckMT és regulada pels mateixos agents que MT1 (metalls, estrès oxidatiu, glucocorticoides, etc).[45] Tot i aquestes similituds, ckMT i MT1 presenten algunes diferències que cal comentar. Per una banda, ckMT té un residu d'His al final de la seva seqüència (C-terminal) que MT1 no té i que d'acord amb la bibliografia pot contribuir a la coordinació metàl·lica.[46,47] Per altra part, en pollastre només s'ha descrit un únic gen que codifica per MT,[44,48] mentre que en mamífer s'han detectat fins a 4 isoformes de MT, les quals poden presentar diferents funcionalitats (apartat 1.5.1).

Pel que fa al coneixement que es té dels agregats metàl·lics als quals dóna lloc ckMT, cal esmentar que els únics treballs existents en la literatura proposen una relació de 7-9 M/proteïna (M = Zn i Cd) pels agregats Cd,Zn-MT obtinguts a partir d'òrgans de pollastres alimentats amb Cd.[49,50] Així mateix, aquests autors també descriuen que l'addició *in vitro* de 15 equivalents de Cu(I) als complexos anteriors provoca la substitució total del Zn i Cd inicialment coordinats per a generar una espècie Cu_{15}-ckMT.[50]

1.5.3 MTs de llevat

Llevat és el nom comú emprat per a denominar certs fongs unicel·lulars (eucariotes). Un dels llevats més coneguts és *Saccharomyces cerevisiae*, que té la facultat de créixer de forma anaeròbica, realitzant la fermentació alcohòlica.

Al contrari del que s'ha comentat en l'apartat anterior (ckMT, una sola MT descrita), s'ha identificat duplicitat dels gens que codifiquen per MT en dos llevats, *Saccharomyces cerevisiae* i *Candida glabrata*. D'acord amb les dades de la Taula 1.2, les isoformes MTI i MTII de *C.glabrata*, regulades transcripcionalment pel Cu i que no presenten homologia de seqüència, donen lloc, respectivament, a agregats Cu_{11-12}-MTI i Cu_{10}-MTII.[51] Si bé ambdues isoformes s'han relacionat amb la destoxificació enfront del coure, es creu que MTII presentaria un paper dominant en la resistència cel·lular al coure, mentre que MTI probablement podria presentar altres funcions.[51,52]

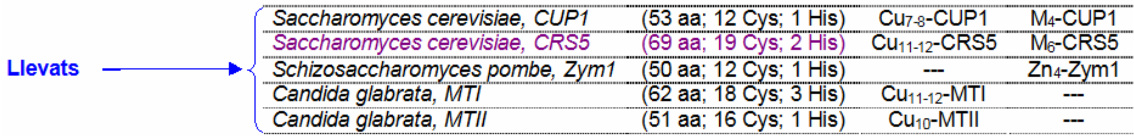

Llevats				
	Saccharomyces cerevisiae, CUP1	(53 aa; 12 Cys; 1 His)	Cu_{7-8}-CUP1	M_4-CUP1
	Saccharomyces cerevisiae, CRS5	(69 aa; 19 Cys; 2 His)	Cu_{11-12}-CRS5	M_6-CRS5
	Schizosaccharomyces pombe, Zym1	(50 aa; 12 Cys; 1 His)	---	Zn_4-Zym1
	Candida glabrata, MTI	(62 aa; 18 Cys; 3 His)	Cu_{11-12}-MTI	---
	Candida glabrata, MTII	(51 aa; 16 Cys; 1 His)	Cu_{10}-MTII	---

Taula 1.2.- Característiques de l'estructura primària i dels complexos amb metalls divalents i/o monovalents de diverses MTs de llevat.

Addicionalment, en presència de Cd(II), *C.glabrata* expressa un pèptid (γ-Glu-Cys)$_n$Gly de la família de les fitoquelatines i cadistines que seria el responsable de la destoxificació envers el Cd.[53] Per *S.pombe* únicament s'havien descrit fitoquelatines,

però recentment s'ha caracteritzat una MT, Zym1, la qual no presenta les propietats de les altres MTs de llevats, que s'indueixen i segresten Cu.[54]

Els gens que codifiquen les MTs de *Saccharomyces cerevisiae*, Cup1 i Crs5, també es troben regulats transcripcionalment per Cu, la qual cosa va portar, inicialment, a relacionar-les amb la destoxificació d'aquest metall. De fet, Cup1 ha estat tradicionalment considerada la Cu-tioneïna de referència. Des que va ser aïllada i caracteritzada l'any 1975,[55] el seu estudi ha donat lloc a un nombre important de treballs. Cal destacar que Cu-Cup1 ha estat la primera i única MT de Cu de la qual s'ha resolt l'estructura i que això s'ha fet tant per RMN[56] com per difracció de raigs X,[25] (Figura 1.2.A). Aquest extens estudi ha permès conèixer amb detall aquesta MT, que *in vivo* enllaça entre 7[56] i 8[25] ions Cu(I) mitjançant 10 de les seves 12 Cys (Taula 1.2). Experiments amb agents quelatants específics de Cu(I) van demostrar la presència de dos ions molt làbils,[57] cosa que explica les diferents relacions Cu/MT trobades. Aquesta labilitat diferencial dels ions Cu(I) enllaçats a Cup1 s'ha atribuït als diferents entorns de coordinació (6 Cu trigonals i 2 de digonals) que presenta el Cu(I) en la proteïna.[25] Estudis *in vitro* han demostrat que aquesta proteïna també pot enllaçar Cd i Zn en una relació de 4 metalls per MT.[58]

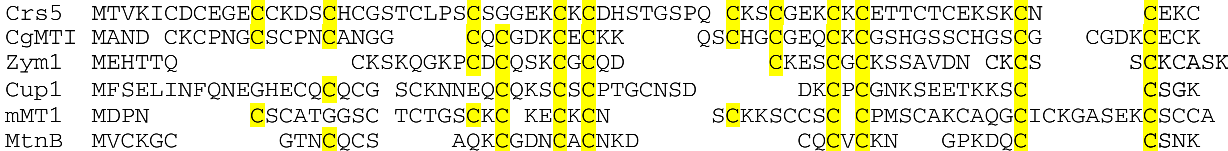

Figura 1.5.- Comparació de la seqüència aminoacídica de diverses MTs entre les quals s'inclouen les de *S.cerevisiae*, Cup1 i Crs5. S'han assenyalat en groc les Cys conservades en les diferents isoformes. (CgMTI = MTI de *C.glabrata*, mMT1 = MT1 de ratolí, MtnB = MTO de *D.melanogaster*)

El gen que codifica per Crs5 no es va descobrir fins l'any 1994,[59] intentant identificar sistemes addicionals de llevat que contribuïssin a l'homeòstasi i destoxificació del Cu. Curiosament, aquesta proteïna presenta similituds amb nombroses MTs de mamífer i d'invertebrats, mentre que comparteix poca semblança (28%) amb l'altra MT de *S.cerevisiae* (Cup1). Així, tant la llargada de la cadena polipeptídica com el número de residus de Cys de Crs5 s'assemblen més a les de les MTs de mamífer que no pas a les de Cup1 (Taula 1.1 i Figura 1.5).[59] La diferència en el número de Cys entre les dues MTs de *S.cerevisiae* comporta també diferents capacitats de coordinació metàl·lica, major en el cas de Crs5 que enllaça entre 11 i 12 ions Cu(I) i 6 ions Cd(II) (Taula 1.2).[60] Aquest alt contingut metàl·lic juntament amb la presència d'un segment dins la seqüència de Crs5 de 8 residus aminoacídics deficients en Cys, suggereix l'organització de la proteïna en dos dominis,[60] tal i com es descriu per a les MTs de mamífer, mentre que Cup1 mostra una disposició

monodominal.[56] Cal destacar també les grans similituds entre les dues MTs de *S.cerevisiae* i les dues de *C.glabrata* (Taula 1.2 i Figura 1.5), tant per la llargada dels polipèptids com pel número de residus de Cys i His i, fins i tot, per les possibles funcions en llevat.

Com ja s'ha dit, el gen *CRS5* es veu regulat positivament per la presència de Cu en el medi i, per tant, la funció de Crs5 també ha estat inicialment relacionada amb els processos d'homeòstasi i destoxificació del Cu.[59] Posteriorment, i donat que els ions Cu(I) enllaçats a Cup1 són cinèticament i, probablement, termodinàmica més estables que els units a Crs5, s'ha proposat que el principal responsable de la tolerància envers el Cu(I) en *S.cerevisiae* seria Cup1. Així doncs, Crs5 semblaria més aviat tenir una funció tamponadora de Cu(I) degut a la seva labilitat d'enllaç. Cal afegir, no obstant, que també s'ha relacionat Crs5 amb l'homeòstasi del Zn.[60]

Un altre fet a destacar és la regulació negativa tant de Crs5 com de Cup1 per l'oxigen.[61] La repressió aeròbica dels gens d'aquestes dues MTs de llevat és ràpida i involucra l'acció dels ions coure sobre l'expressió gènica de Crs5 i Cup1. Així doncs, s'ha vist que els cultius anaeròbics acumulen nivells de Cu majors que els aeròbics i que aquest Cu es perd ràpidament quan les cèl·lules són exposades a l'aire. Conseqüentment, sembla que serien els nivells de Cu(I) en llevat (modulats per l'aerobiosi/anaerobiosi del sistema) els que regularien l'expressió dels gens *CRS5* i *CUP1*.

1.5.4 Altres MTs

No es pot acabar aquesta descripció de les MTs sense comentar alguns dels resultats obtinguts per aquest grup de recerca en l'estudi de MTs d'altres organismes. S'ha considerat oportú incloure aquí aquesta informació ja que algunes dades sobre altres MTs, aparentment no relacionades amb aquest treball, seran força útils a l'hora de considerar els resultats de l'estudi que aquí es presenta.

El grup d'investigació en el sí del qual s'ha realitzat aquesta Tesi ha estudiat algunes MTs de la família dels artròpodes (invertebrats). Més concretament, s'ha treballat amb MTH d'*Homarus americanus* (llamàntol) i els seus dominis constitutius, i les quatre isoformes (MtnA, MtnB, MtnC i MtnD, Taula 1.1) de *Drosophila melanogaster* (mosca del vinagre). Així, s'ha determinat que la MT de llamàntol presenta preferència per als metalls divalents, Zn(II) i Cd(II), enllaçant fins a 6 metalls per MT, mentre que quan s'expressa en presència de Cu dóna lloc a una barreja d'espècies heterometàl·liques Zn,Cu-MTH, la qual cosa ha portat a classificar MTH com una Zn-tioneïna.[10] De les quatre isoformes de MT de mosca, les més conegudes

són MtnA (MTN)[31] i MtnB (MTO)[32] i, contràriament al descrit per MTH, totes presenten major preferència per al Cu(I) que per al Zn(II), generant *in vivo* i en presència de Cu les espècies Cu_8-MtnA, Cu_9-MtnB, Cu_5-MtnC i Cu_5-MtnD.[33] Això, juntament amb les dades obtingudes *in vitro,* ha portat a classificar aquestes quatre MTs com a Cu-tioneïnes.

Curiosament, han estat aquestes MTs de mosca les primeres per a les quals s'ha proposat la presència de lligands addicionals no proteics en els seus complexos metàl·lics. Així, per MtnB s'ha descrit la participació de lligands clorur en les espècies Zn- i Cd-MtnB,[32] i per MtnA s'ha suggerit la presència de lligands sulfur (S^{2-}) en els complexos Cd-MtnA.[31] Aquesta darrera assignació es va fer en base a unes absorcions de DC que apareixien al voltant de 280 nm en afegir ions Cd(II) a l'espècie Zn-MtnA. Absorcions anàlogues a aquestes havien estat descrites prèviament[62,63,64] per als complexos de Cd dels polipèptids (γ-Glu-Cys)$_n$Gly de síntesi enzimàtica anomenats fitoquelatines i cadistines (apartat 1.4). Aquests polipèptids, en presència de Cd(II), generen oligòmers amb un número variable d'unitats (γ-Glu-Cys)$_n$Gly que incorporen sulfur inorgànic (S^{2-}) com a lligands addicionals donant lloc a partícules anomenades *crystallites,*[65] mitjançant un procés de biomineralització (Figura 1.6). Aquests *crystallites* generen absorcions entre 270 i 320 nm, tot depenent de la mida de la partícula, de tal manera que com més gran és la relació S^{2-}:M (M = Zn o Cd) de l'agregat més gran és la longitud d'ona d'absorció.[66]

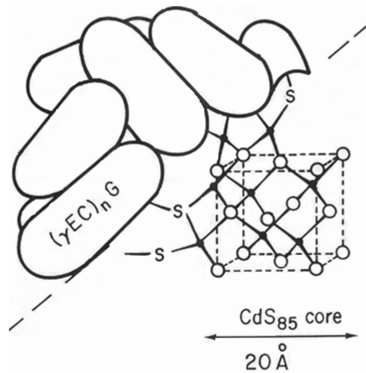

Figura 1.6.- Model hipotètic dels *crystallites* mostrant els pèptids (γ-Glu-Cys)$_n$Gly embolcallant la superfície de la xarxa cristal·lina, que aquí s'ha representat com una blenda de zinc però que en les partícules natives sembla ser molt més policristal·lina.

Pel que fa a MtnB, els espectres de DC de la proteïna recombinant expressada en medis rics en Zn mostren, juntament amb la banda en forma d'*exciton coupling* centrada a 240 nm característica dels cromòfors Zn-tiolat, una banda en forma de gaussiana centrada a 230(+) nm que es desplaça i es fa més estreta en eliminar els clorurs del medi. Per altra banda, els complexos Cd-MtnB obtinguts *in vitro* i en presència d'ions clorur presenten absorcions a 240(+) nm en els espectres de

diferència d'UV-Vis les quals desapareixen quan s'eliminen els clorurs del medi. Aquest fet va portar a proposar la participació dels anions clorur com a lligands en els complexos Zn- i Cd-MtnB.[32] En la literatura es troben altres treballs que també postulen la participació dels lligands clorur en l'estructura i estabilitat del agregats metall-MT.[67]

1.6 Reactivitat i funció fisiològica

La diversitat de metalls que poden coordinar les MTs, la ubiqüitat d'aquestes proteïnes i l'elevat grau de conservació que presenten les seves seqüències aminoacídiques, especialment els residus de Cys, en organismes diferents del mateix ordre fa creure que les MTs són proteïnes d'una gran importància biològica. Tanmateix, gairebé 50 anys després del seu descobriment, la funció o funcions fisiològiques de les MTs resten encara per determinar, de manera que bona part dels treballs actuals apunten cap a l'estudi d'aquets darrer aspecte.

Una de les característiques més rellevants de les MTs, que estableix una clara diferenciació amb la resta de proteïnes, és la seva capacitat per a formar complexos metàl·lics d'elevada nuclearitat. Aquests presenten una gran estabilitat termodinàmica, però l'elevada plasticitat i flexibilitat de l'estructura proteica provoca que presentin alhora una elevada labilitat cinètica, fet que facilita, tant *in vivo* com *in vitro*, el bescanvi relativament ràpid dels ions metàl·lics que contenen quan les condicions del medi ho forcen. Així mateix, el fet que la síntesi de moltes MTs es vegi induïda per metalls suggereix que aquestes proteïnes tenen un paper important en la regulació i destoxificació de metalls en els éssers vius.[68] Així, se'ls han atribuït diverses funcions estretament relacionades les unes amb les altres com a conseqüència de les característiques fisicoquímiques dels seus agregats metàl·lics.[2] Aquestes funcions s'han relacionat amb:

a) l'homeòstasi de Zn i Cu

b) el segrestament de metalls tòxics

c) un paper antioxidant i antiapoptòtic

d) el control metabòlic de producció d'energia

1.7 *Objectius*

Aquesta Tesi Doctoral té com a objectiu principal l'aprofundiment en la relació estructura/funció de les metal·lotioneïnes. Per a poder assolir aquesta fita s'han plantejat tres objectius més concrets, que es descriuen a continuació:

1. **Ampliar els coneixements sobre el comportament coordinant de les MTs de mamífer mitjançant l'estudi d'una nova isoforma, MT4.** Amb aquesta finalitat, s'ha realitzat un estudi de la capacitat enllaçant de MT4 i dels seus dominis per separat en presència de metalls divalents (Zn i Cd) i monovalents (Cu), i els resultats s'han comparat amb els obtinguts, per aquest mateix grup de recerca, amb MT1 de mamífer.

2. **Determinar la participació de lligands no proteics en els agregats M-MT i precisar com afecten en l'estructura d'aquests complexos.** En la literatura es poden trobar treballs on es descriu la participació de certs lligands no-proteics en la coordinació metàl·lica de les MTs. Aquesta participació no només pot afectar l'estructura del complex M-MT sinó que pot determinar funcions específiques per a aquestes proteïnes. Així, s'ha plantejat estudiar la possible implicació dels lligands clorur (Cl^-) i sulfur (S^{2-}) en els complexos metall-MT formats quan la proteïna enllaça Zn(II), Cd(II) i/o Cu(I).

3. **Estudiar les MTs de diferents organismes amb la intenció de validar la proposta de classificació presentada per aquest grup de recerca i, a més, aprofundir en els diferents patrons de diferenciació i especialització de les MTs.** Així, s'ha analitzat el comportament coordinant de les MTs de dos organismes diferents. Per una banda s'ha caracteritzat una MT d'ocell, més concretament de pollastre, organisme evolutivament molt proper als mamífers i que també es troba dins del grup dels vertebrats. D'altra banda, s'ha estudiat la MT d'un organisme menys evolucionat com és el llevat, fong unicel·lular.

2. Resultats i discussió

2. RESULTATS I DISCUSSIÓ

En aquest capítol es dóna una visió global del treball exposant de manera resumida els resultats obtinguts i fent-ne una discussió general.

Cal destacar que la recent demostració d'aquest grup de recerca (article 3) de la presència d'un tercer component fins ara desconegut, els lligands sulfur (S^{2-}), en les espècies metall-MT obtingudes mitjançant enginyeria genètica té implicacions importants en l'anàlisi de les habilitats coordinants de totes les MTs conegudes fins ara. Degut a aquest descobriment i amb l'ànim de facilitar l'exposició i discussió dels resultats d'aquest treball, aquest capítol s'inicia amb l'estudi de les característiques coordinants de la isoforma MT4 de mamífer (apartat 2.1; article 1). Quan es van publicar els resultats de MT4 el grup desconeixia encara la presència d'aquest tercer component en els agregats metall-MT4, per la qual cosa no se'n fa cap esment en l'article 1. Posteriorment, l'elucidació de les implicacions de la presència de lligands sulfur i/o clorur en aquests agregats (apartat 2.2; articles 2 i 3) ha permès fer una nova interpretació d'alguna de les dades de l'article 1 i altres articles anteriors d'aquest grup de recerca, que no es troben publicades i que es recullen en l'apartat 2.2.3. Finalment, els estudis de les habilitats coordinants de ckMT1 (apartat 2.3; article 4) i Crs5 (apartat 2.4; article 5) ja tenen en compte la presència d'aquests lligands addicionals i, com a conseqüència, la seva publicació s'ha vist retardada en espera de la publicació de l'article 3.

En tots els casos les proteïnes recombinants estudiades han estat sintetitzades pel grup de recerca dirigit per la Dra. Sílvia Atrian, Catedràtica del Departament de Genètica de la Facultat de Biologia de la Universitat de Barcelona.

2.1 Capacitat coordinant de la isoforma MT4 de mamífer

El coneixement detallat del comportament de MT1 enfront de metalls divalents i monovalents,[9,30,40,41,69,70,71] juntament amb la manca absoluta de dades sobre la capacitat coordinant de MT4, per a la qual s'ha postulat una funció diferent a la de les altres MTs de mamífer (vegi's apartat 1.5.1), ha incitat que es considerés interessant estudiar la isoforma MT4 de mamífer enfront dels ions Zn(II), Cd(II) i Cu(I). D'aquesta forma aquest treball constitueix el primer estudi sobre el comportament coordinant de MT4 envers diferents ions metàl·lics.

El procediment seguit per a l'estudi de la capacitat coordinant de MT4 envers Zn(II), Cd(II) i Cu(I) ha consistit en una primera etapa de síntesi de la MT4 recombinant de ratolí sencera i dels seus fragments constitutius en medis rics en Zn, Cd o Cu. Aquestes síntesis han portat a l'obtenció de complexos metall-MT4 que s'han caracteritzat mitjançant les tècniques espectroscòpiques i espetromètriques habituals (Mètode d'Ellman, ICP-AES, DC, UV-Vis i ESI-MS). Un cop analitzades les espècies Zn-MT4, s'ha procedit a valorar-les amb Cd(II) i Cu(I) a pH 7 i a temperatura ambient (estudis *in vitro*). Els complexos metàl·lics formats al llarg de les valoracions s'han caracteritzat, tot determinant el seu grau d'estructuració i el seu contingut metàl·lic mitjançant les tècniques de DC, UV-Vis i ESI-MS. Posteriorment, s'han comparat les espècies obtingudes *in vivo* i *in vitro* i s'ha pogut establir el caràcter de Cu-tioneïna de la MT4 sencera així com dels seus dominis αMT4 i βMT4. Finalment, i per a completar l'estudi de la capacitat coordinant d'aquesta proteïna, s'ha comparat el seu comportament amb el de MT1. A diferència del fragment βMT1,[40] ni MT1 ni αMT1 no s'havien expressat amb anterioritat en medis rics en Cd i, per tant, es desconeixien les característiques de les espècies Cd-MT que podien formar aquestes dues proteïnes en aquestes condicions. Per tant, per tal de poder comparar els resultats obtinguts per MT4 amb els de MT1, part d'aquest treball ha consistit en la biosíntesi i caracterització dels complexos Cd-MT1 i Cd-αMT1 de mamífer.

A continuació es donen i comenten els resultats obtinguts.

2.1.1 Propietats coordinants de MT4 envers Zn(II)

La capacitat coordinant de MT4 envers Zn s'apropa bastant a la descrita per a MT1 ja que totes dues proteïnes generen espècies úniques en solució d'estequiometria idèntica, Zn_7-MT, Zn_4-αMT i Zn_3-βMT (Taula 2.1), que presenten espectres de DC propers (Figura 2.1), si bé en el cas de MT4 els tres pèptids estudiats mostren en solució una menor quiralitat que els de MT1. Així doncs, es proposa que la coordinació del Zn confereix un menor grau de replegament a MT4 que a MT1.

Zn	Zn-MT4	Zn-αMT4	Zn-βMT4
[proteïna] (M)	0.63×10^{-4}	2.70×10^{-4}	2.10×10^{-4}
ICP-AES	6.7 Zn	3.6 Zn	2.5 Zn
% Oxidació (Ellman)	5 %	11 %	15 %
ESI-MS	Zn_7-MT4	Zn_4-αMT4	Zn_3-βMT4
Espectre DC			

Taula 2.1.- Resultats de la caracterització dels complexos de MT4 sencera i dels seus fragments constitutius obtinguts per enginyeria genètica mitjançant la seva expressió en medis rics en Zn.

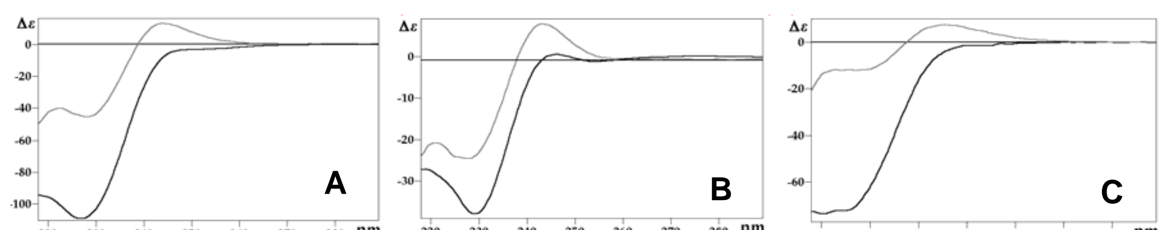

Figura 2.1.- Comparació dels espectres de DC de les espècies Zn_7-MT (**A**), Zn_4-αMT (**B**), i Zn_3-βMT (**C**) de MT1 (gris) i de MT4 (negre).

2.1.2 Propietats coordinants de MT4 envers Cd(II)

Quan la MT4 es sintetitza en medis rics en Cd únicament el fragment αMT4 s'expressa com una única espècie d'estequiometria Cd_4-αMT4, mentre que la proteïna sencera i βMT4 s'expressen com una barreja d'espècies entre les quals es troben els complexos homometàl·lics de Cd esperats, Cd_7-MT4 i Cd_3-βMT4, juntament amb diversos complexos heterometàl·lics Zn,Cd-MT (Taula 2.2).

Cd	Cd-MT4	Cd-αMT4	Cd-βMT4
[proteïna] (M)	$5.0x10^{-5}$	$2.08x10^{-4}$	$2.13x10^{-4}$
ICP-AES	3.6 Zn 2.0 Cd	3.5 Cd	2.0 Cd
% Oxidació (Ellman)	36 %	13 %	34 %
ESI-MS*	Zn_4Cd_3-MT4 (M) Zn_5Cd_2- = Zn_3Cd_4-MT4 Zn_2Cd_5- = Zn_6Cd_1-MT4 Zn_1Cd_6-MT4 Zn_7- = Cd_7-MT4 (m)	Cd_4-αMT4	Cd_3-βMT4 (M) Zn_1Cd_2-βMT4 Zn_2Cd_1-βMT4 (m)
Espectre DC			

Cd	Cd-MT1	Cd-αMT1
[proteïna] (M)	$0.60x10^{-4}$	$1.10x10^{-4}$
ICP-AES	6.2 Cd	4.2 Cd
ESI-MS	Cd_7-MT1	Cd_4-αMT1
Espectre DC		

∗ Les espècies estan ordenades d'acord amb la seva abundància en solució. (M) representa l'espècie majoritària i (m) la minoritària.

Taula 2.2.- Resultats de la caracterització dels complexos de MT4 i MT1 senceres i dels seus fragments constitutius obtinguts per enginyeria genètica mitjançant la seva expressió en medis rics en Cd. L'expressió de βMT1 en medis rics en Cd va ser objecte de treballs previs d'aquest grup.[40]

En el cas de βMT4, Cd_3-βMT4 és l'espècie majoritària en solució; en canvi, el complex Cd_7-MT4 esperat en la síntesi de la proteïna sencera és minoritari, essent Zn_4Cd_3-MT4 l'espècie majoritària. Aquest fet, juntament amb la baixa afinitat de la proteïna sencera envers el Cd en comparació amb la dels seus fragments, denota que αMT4 i βMT4 es comporten de manera diferent quan es troben aïllats que quan es troben formant part de la proteïna sencera. Per tant, es proposa que els dominis αMT4 i βMT4 presenten un comportament dependent enfront de l'ió Cd(II).

Els estudis realitzats *in vitro* sobre la capacitat coordinant de MT4 envers Cd(II) corroboren aquesta baixa afinitat de MT4 envers aquest metall divalent. Així, en valorar les espècies Zn_7-MT4, Zn_4-αMT4 i Zn_3-βMT4 amb Cd(II) s'observa que, tot i arribar a obtenir les corresponents espècies homometàl·liques Cd-MT, és necessari un excés considerable de Cd(II) per a obtenir-les com a espècies úniques en solució. Les dificultats de MT4 i βMT4 per a donar complexos homometàl·lics de Cd també es fan patents *in vitro*, ja que a 15 i 7 equivalents de Cd(II) afegits, respectivament, sobre les corresponents espècies Zn-MT encara es detecten en solució petites quantitats de les espècies heterometàl·liques Zn_1Cd_6-MT4 i Zn_1Cd_2-βMT4. Això ha portat a plantejar un possible paper estructural del Zn(II) en MT4 i βMT4. La necessitat de la presència d'ions Zn(II) per tal que la proteïna pugui replegar-se en solució ja havia estat descrita amb anterioritat per a MT1.[30,69]

Contràriament, MT1 mostra una major afinitat per al Cd(II). Així ho demostra el fet que en expressar la proteïna i els seus fragments constitutius en medis rics en Cd, s'obtinguin únicament les espècies homometàl·liques esperades, Cd_4-αMT1, Cd_7-MT1 (Taula 2.2) i Cd_3-βMT1.[40]

Els agregats Cd_4-αMT4 (obtinguts tant *in vivo* com *in vitro*) i Cd_7-MT4 (obtingut únicament *in vitro*) s'estructuren de manera propera a com ho fan els corresponents agregats de MT1, mentre que l'estructuració de l'espècie Cd_3-βMT4 (obtinguda únicament *in vitro*) en solució és força diferent a la de Cd_3-βMT1 (Figura 4.B, article 1).

Així doncs, segons les capacitats coordinants de MT4 i dels seus fragments constitutius i les característiques estructurals abans esmentades, es proposa que la diferència observada entre MT4 i MT1 respecte la coordinació a Cd(II) s'origina en els respectius fragments βMT, ja que els fragments αMT4 i αMT1 presenten comportaments paral·lels.

2.1.3 Propietats coordinants de MT4 envers Cu(I)

A diferència del que succeeix en el cas del Cd(II), la similitud de pes atòmic entre el Zn (65.38 uma) i el Cu (63.55 uma) i l'amplitud relativa de l'interval de confiança obtingut en les mesures de ESI-MS fan que, mitjançant aquesta tècnica, no sigui possible determinar la relació Zn:Cu:MT de les espècies obtingudes *in vivo* i/o *in vitro* en presència de Cu. Així, en tots els casos, les espècies detectades per ESI-MS es denoten com a M_n-MT4 on M pot ser únicament Cu(I), únicament Zn(II) o una barreja d'ambdós ions metàl·lics.

La MT4 s'ha sintetitzat diverses vegades en medis rics en Cu. Aquestes síntesis recombinants han donat lloc a dos tipus de resultats: les anomenades produccions de Tipus 1 i les de Tipus 2 (Taula 2.3). La síntesi de Tipus 1 ha donat lloc a una barreja d'espècies homometàl·liques Cu-MT on Cu_{10}-MT4 és l'espècie majoritària, la qual cosa es correspon amb la relació metall/MT mesurada per ICP-AES. Altrament, la síntesi de Tipus 2 dóna lloc a una barreja d'espècies heterometàl·liques Zn,Cu-MT, on d'acord amb les dades d'ICP, l'espècie Zn_3Cu_7-MT4 és la majoritària (Taula 2.3). Malgrat aquestes diferències, ambdues síntesis es troben relacionades ja que es pot passar de les espècies obtingudes en la síntesi de Tipus 2 a les de la de Tipus 1 afegint únicament 2 equivalents de Cu(I) (Figura S7.A, article 1).

Cu	Cu-MT4 (Tipus 1)	Cu-MT4 (Tipus 2)
[proteïna] (M)	0.63×10^{-4}	0.17×10^{-4}
ICP-AES	0.0 Zn 9.4 Cu	2.7 Zn 7.3 Cu
ESI-MS*	Cu_{10}-MT4 (M) Cu_{13}-MT4 Cu_{15}-MT4 (m)	M_{10}-MT4 (M) M_8-MT4 (m)
Espectre DC		

Taula 2.3.- Resultats de la caracterització dels complexos de les dues produccions de MT4 obtinguts per enginyeria genètica mitjançant la seva expressió en medis rics en Cu.

* Les espècies estan ordenades d'acord amb la seva abundància en solució. (M) representa l'espècie majoritària i (m) la minoritària.

En la producció de Tipus 2 la MT4 mostra una capacitat coordinant comparable a la de MT1 (Zn_3Cu_7-MT1) i una estructuració propera (Figura S7.C, article 1), mentre que en la de Tipus 1 la MT4 té un comportament envers Cu(I) que s'allunya bastant del

de MT1 (Figura S7.B, article 1). Cal afegir, a més, que és possible reproduir *in vitro* aquests dos comportaments de MT tot valorant Zn_7-MT4 amb Cu(I).

Contràriament al que fa la proteïna sencera, els dos fragments s'han sintetitzat diferents vegades i sempre han donat lloc a una barreja d'espècies homometàl·liques Cu-MT, essent Cu_5-αMT4 i Cu_7-βMT4 les espècies majoritàries (Taula 2.4). Així, βMT4 presenta una capacitat coordinant envers Cu(I) molt propera a βMT1 (espècie majoritària Cu_7-βMT1)[40] mentre que el comportament de αMT4 (Cu-tioneïna) envers Cu(I) és bastant diferent al de αMT1 (Zn-tioneïna),[30] la qual s'expressa com una barreja d'espècies heterometàl·liques Zn,Cu-αMT1. Per tant, sembla que la diferència de comportaments entre MT4 i MT1 envers Cu(I) radica en els seus fragments αMT.

Cu	**Cu-αMT4**	**Cu-βMT4**
[proteïna] (M)	0.20×10^{-5}	1.46×10^{-4}
ICP-AES	0.0 Zn 3.6 Cu	0.0 Zn 5.8 Cu
ESI-MS*	Cu_5-αMT4 (M) Cu_4-αMT4 Cu_6-αMT4 Cu_7-αMT4 (m)	Cu_7-βMT4 (M) Cu_6-βMT4 Cu_4-βMT4 (m)
Espectre DC		

Taula 2.4.- Resultats de la caracterització de αMT4 i βMT4 obtingudes per enginyeria genètica mitjançant la seva expressió en medis rics en Cu.

* Les espècies estan ordenades d'acord amb la seva abundància en solució. (M) representa l'espècie majoritària i (m) la minoritària.

En valorar Zn_4-αMT4 i Zn_4-αMT1 amb Cu(I) s'observen evolucions molt properes mentre hi ha Zn(II) enllaçat a les proteïnes. En canvi, quan el Cu(I) ha substituït tot el Zn comencen a fer-se paleses les diferències entre aquestes dues proteïnes. Contràriament, βMT4 i βMT1 mostren comportaments *in vitro* molt propers, amb una major afinitat envers el Cu per part de βMT4, de manera que només amb 4 equivalents de Cu(I) afegits sobre Zn_3-βMT4 l'espècie majoritària és ja Cu_6-βMT4. Per a 6 equivalents de Cu(I) afegits, l'espècie que predomina en l'espectre de DC és Cu_7-βMT4.

Les diferències detectades en els comportaments *in vitro* de Zn_7-MT4 i Zn_7-MT1 en ser valorades amb Cu(I) radiquen per una part en els diferents espectres de DC de partida, però també en les petites contribucions vora 350(+) nm, característiques del domini βMT4, i en l'absència de processos cooperatius. Tal i com passava per a αMT4, les diferències més importants en les evolucions de les valoracions amb Cu(I) de Zn_7-MT4 i Zn_7-MT1 s'observen quan s'han substituït tots els Zn enllaçats a la proteïna. Al llarg de tota la valoració de Zn_7-MT4 es detecten unes absorcions característiques a *ca.* 350(+) nm, no observades en el cas de MT1, que s'intensifiquen amb la formació de Cu_{10}-MT4, que revelen que MT4 és capaç d'enllaçar el Cu(I) mitjançant un entorn de coordinació que MT1 probablement no pot oferir.

Aquest conjunt de resultats ha portat a classificar MT4 i els seus dominis com a Cu-tioneïnes, mentre MT1 s'ha classificat com una Zn-tioneïna amb un domini αMT1 amb caràcter de Zn-tioneïna i un domini βMT1 amb caràcter de Cu-tioneïna. Així doncs, MT1 presenta una major afinitat per als metalls divalents (Zn i Cd) mentre que MT4 mostra una clara preferència per a enllaçar metalls monovalents (Cu). Així, la millor capacitat coordinant de MT4 respecte a MT1 envers Cu(I) radica en els seus fragments α, ja que αMT1 és una Zn-tioneïna i per tant necessita Zn per a replegar-se, mentre que αMT4 és una Cu-tioneïna. Contràriament, la resistència de MT4 respecte de MT1 a enllaçar Cd(II) s'ha d'atribuir a les dificultats de βMT4, respecte de βMT1, per a formar complexos Cd-MT.

Estudis *in silico*, duts a terme mitjançant el programa ClustalW (versió 1.75), corroboren aquests resultats, de manera que l'anàlisi comparativa de seqüències de diferents organismes mostren que MT4 es trobaria dins del grup de les Cu-tioneïnes mentre que MT1 es trobaria més propera al grup de les Zn-tioneïnes.

Aquesta diferent capacitat coordinant de MT4 respecte MT1 i el fet que MT4 es sintetitzi únicament en el teixit estratificat escamós ha portat a concloure que probablement MT4 desenvolupa funcions diferents a les que desenvolupa MT1 i que aquestes funcions poden estar relacionades amb el rol fisiològic concret del Cu dins d'aquest tipus cel·lular.

2.2 Influència dels lligands no proteics en l'estructura de les espècies metall-MT.

Habitualment, i tret de casos especials com el de SmtA de cianobacteri, on els nitrògens histidínics participen en la coordinació metàl·lica,[22] l'habilitat coordinant de les MTs envers els ions metàl·lics ha estat exclusivament atribuïda als residus de Cys. Tot i així, aquest mateix grup de recerca va postular fa uns anys[31] l'existència de lligands sulfur (S^{2-}) en els complexos Cd-MtnA de *Drosophila melanogaster* i ha descrit recentment[32] la presència de lligands clorur (Cl^{-}) en les espècies Zn- i Cd-MtnB del mateix organisme (apartat 1.5.4). Conseqüentment, en la bibliografia es poden trobar referències sobre la participació de lligands no proteics en l'estructura i estabilitat dels complexos metall-MT. Cal destacar, però, que mentre altres autors també descriuen la participació dels ions clorur en les espècies metall-MT,[67] els lligands sulfur únicament s'han relacionat amb les fitoquelatines i no es troben treballs que considerin la participació d'aquests darrers lligands en la coordinació metàl·lica en MTs.

A l'inici d'aquesta tesi doctoral ja es van detectar indicis de la participació d'altres lligands no proteics en la constitució de les espècies metall-MT, de tal manera que es va fer necessari estudiar la influència dels ions clorur i sulfur en els complexos metàl·lics formats per diferents MTs per tal d'avançar en el seu coneixement. Amb la finalitat de detallar els resultats d'aquest estudi, aquest apartat es divideix en dos. En el primer (apartat 2.2.1) s'exposen els resultats obtinguts en la caracterització dels agregats metall-MT de MT4 i MT1 en presència i en absència d'ions clorur. En el segon (apartat 2.2.2) es recullen les dades que evidencien la participació dels ions sulfur en la pràctica totalitat dels complexos Zn-MT i Cd-MT dels diversos organismes considerats.

El descobriment de la participació dels lligands clorur i sulfur en els complexos metall-MT ens ha obligat a revisar i reconsiderar tots aquells resultats publicats amb anterioritat sobre les MTs. Si bé això no és l'objecte d'aquest estudi, en l'apartat 2.2.3 es recullen totes aquelles consideracions que afecten directament els resultats presentats en aquesta memòria o que han de ser tinguts en compte a l'hora d'analitzar els resultats que aquí es presenten.

2.2.1 Participació dels ions clorur (Cl^{-}) en els complexos metall-MT

L'anàlisi dels espectres de diferència d'UV-Vis enregistrats al llarg de les valoracions de Zn_4-αMT4 i Zn_7-MT4 de mamífer amb Cd(II), corresponents a l'estudi de la capacitat coordinant *in vitro* d'aquestes proteïnes envers Cd(II) (apartat 2.1.2) ha revelat l'aparició d'unes absorcions al voltant de 240 nm quan a les Zn-MT

esmentades se'ls havien afegit 4 i 7 equivalents de Cd(II), respectivament (Figures S1.A i S3.A, article 1). Paral·lelament, la revisió de les dades ja publicades de MT1 ha portat a detectar aquestes mateixes absorcions en els mateixos punts de les valoracions de Zn_4-αMT1 i Zn_7-MT1. Donat que absorcions anàlogues a aquestes s'havien relacionat prèviament amb la participació d'ions clorur en la constitució dels complexos Cd-MtnB de *D.melanogaster,*[32] s'ha considerat adient analitzar la possible participació dels lligands clorur en les espècies metall-MT de MT1 i MT4 i dels seus fragments α. En cap moment s'ha contemplat la realització d'un estudi anàleg per als seus fragments β ja que aquests no donen lloc a les esmentades absorcions.

Aquests estudis s'han dut a terme mitjançant una metodologia similar a l'emprada per a MtnB de *D.melanogaster*. Així, MT1, MT4, αMT1 i αMT4 s'han sintetitzat en medis rics en Zn i les espècies Zn-MT obtingudes s'han eluït per cromatografia de FPLC en tampó Tris-HCl o Tris-$HClO_4$. Posteriorment, aquestes solucions de Zn-MT dels 4 polipèptids s'han valorat amb $CdCl_2$ o $Cd(ClO_4)_2$, respectivament. Aquestes valoracions s'han seguit per tècniques espectroscòpiques (DC i UV-Vis) i les espècies obtingudes *in vivo* i en alguns punts de les valoracions *in vitro* s'han analitzat per espectrometria de masses (ESI-MS).

La comparació de les dades analítiques i espectroscòpiques de les espècies Zn_4-αMT i Zn_7-MT de MT1 i de MT4 obtingudes bé en Tris-HCl bé en Tris-$HClO_4$ ha demostrat que la presència d'ions clorur no afecta l'estequiometria, l'estructura ni la quiralitat d'aquestes espècies. Addicionalment, s'ha comprovat que les diferències estructurals existents entre les espècies Zn-MT1 i Zn-MT4 es mantenen independentment dels ions presents en solució. Conseqüentment, s'estableix que el major grau de replegament de les espècies Zn_4-αMT1 i Zn_7-MT1 respecte les espècies isoestequiomètriques Zn_4-αMT4 i Zn_7-MT4 no pot atribuir-se a la contribució dels lligands clorur en la formació/estabilització dels complexos Zn-MT.

Un cop determinat que la presència/absència d'ions clorur no té cap influència en la naturalesa dels complexos Zn-MT de MT1 i MT4, aquests s'han valorat amb Cd(II), en presència i en absència d'ions clorur. Segons les dades d'ESI-MS enregistrades, la presència de clorurs no afecta la distribució molecular de les diferents espècies presents al llarg de les valoracions d'aquests quatre polipèptids. Addicionalment, les dades de DC mostren que no hi ha cap diferència significativa en les evolucions de les valoracions de Zn-αMT4 ni de Zn-MT4 en presència o absència d'ions clorur. Contràriament, els espectres de DC de les valoracions de Zn-αMT1 i Zn-MT1 mostren lleugeres diferències en les seves etapes finals en funció de la presència/absència de clorurs en solució. En concret, únicament els espectres de DC

dels complexos Cd_7-MT1 mostren lleugeres diferències si aquests es generen en solucions riques en clorurs o en perclorats, mentre que Cd_4-αMT1, Cd_4-αMT4 i Cd_7-MT4 presenten espectres de DC pràcticament idèntics sigui quin sigui el contraió utilitzat. Així, s'estableix que la participació dels anions clorur provoca petits canvis estructurals en les espècies Cd-MT1, molt més rellevants en la proteïna sencera que no pas en el seu fragment α.

Una altra contribució important d'aquest estudi radica en haver determinat que la millor indicació de la participació de lligands clorur en els complexos Cd-MT s'obté dels espectres de diferència d'UV-Vis. En aquest i a diferència del que s'ha proposat per Cd-MtnB,[32] la presència de clorurs provoca un desplaçament global de l'espectre cap a longituds d'ona menors, i no precisament un colze a 240 nm també observable en el cas de MT4 i αMT4 en absència de clorurs en el medi.

2.2.2 Participació dels ions sulfur (S^{2-}) en els complexos metall-MT

El grup de recerca en el qual s'ha desenvolupat aquesta tesi doctoral va iniciar els seus estudis de MTs a principis dels anys 90 i des de llavors s'han estudiat i caracteritzat diverses MTs de diferents organismes. Inicialment, els esforços es van centrar en MTs de mamífer (MT1 i MT4) i artròpodes (crustaci, MTH, i *D.melanogaster*, MtnA-MtnD) però més endavant s'han anat diversificant i en l'actualitat s'està estudiant un gran ventall de proteïnes que inclouen MTs d'aus, plantes, nematodes, mol·luscs, equinoderms, llevats i fins i tot protozous.

Mentre es va treballar amb MTs de Classe I (apartat 1.4) les dades de la literatura obtingudes per a MTs natives concordaven amb les obtingudes en el grup per a les proteïnes recombinants, però tan aviat com es van iniciar els estudis de MTs menys conegudes des del punt de vista bibliogràfic, varen començar a obtenir-se resultats inesperats i que en molts casos mostraven incoherències (Taula 1, article 3). En primer lloc, molt sovint les estequiometries dels complexos Cd-MT eren massa baixes per a les relacions Zn:MT obtingudes per a la mateixa proteïna i el número de residus de Cys disponibles per a la coordinació metàl·lica. Aquestes relacions metall:MT es calculen a partir dels continguts totals en sofre i metalls determinats per ICP-AES, assumint que el sofre total de la mostra prové exclusivament dels residus de Cys i Met dels polipèptids. Així, les baixes relacions Cd:MT feien pensar en l'oxidació dels grups tiol de les MTs i per tant en la pèrdua de les seves capacitats coordinants. Malauradament, la quantificació del grau d'oxidació d'aquests grups tiol mitjançant la reacció d'Ellman[72] no sols no corroborava aquesta predicció sinó que en alguns casos fins i tot proporcionava graus d'oxidació negatius. Addicionalment, els resultats

d'ESI-MS obtinguts en l'anàlisi de la gran majoria de complexos Cd-MT revelaven la coexistència de les espècies metall-MT esperades juntament amb espècies la massa de les quals no s'ajustava a cap complex Cd-MT possible. El fet que, en aquests casos, el Cd fos l'únic metall detectat per ICP-AES feia descartar la participació d'altres metalls en aquestes espècies desconegudes. Finalment, els espectres de DC d'aquestes mostres presentaven, a més a més de les absorcions característiques dels cromòfors $Cd(S_{Cys})_4$ a *ca.* 250 nm, unes altres absorcions entre 260 i 280 nm de difícil assignació (Figura 1, article 3).

Totes aquestes observacions suggerien la presència de lligands no proteics addicionals en aquests complexos metall-MT i la informació de que disposàvem (apartat 2.2.1) indicava que aquest cop no es tractava de lligands clorur. Per altra part, les dades espectroscòpiques suggerien que podia tractar-se de lligands sulfur (S^{2-}) ja que és conegut que els anions sulfur presents en les Cd-fitoquelatines donen lloc a absorcions entre 260 i 300 nm.[62,65] Aquesta suposició era en certa manera atractiva ja que la possible presència de lligands sulfur en els complexos Zn- i Cd-MT donava explicació a tots els resultats anòmals obtinguts amb anterioritat: la desviació de les relacions metall:MT, els graus d'oxidació negatius,[63] i fins i tot la massa de les espècies desconegudes que incloïen múltiples de la massa atòmica del sofre.

Mitjançant una anàlisi qualitativa de presència de sulfurs làbils en medi àcid (Figura 2.2) es va determinar la seva presència en la majoria de les mostres Zn- i Cd-MT estudiades, però en canvi no en les Cu-MT corresponents.

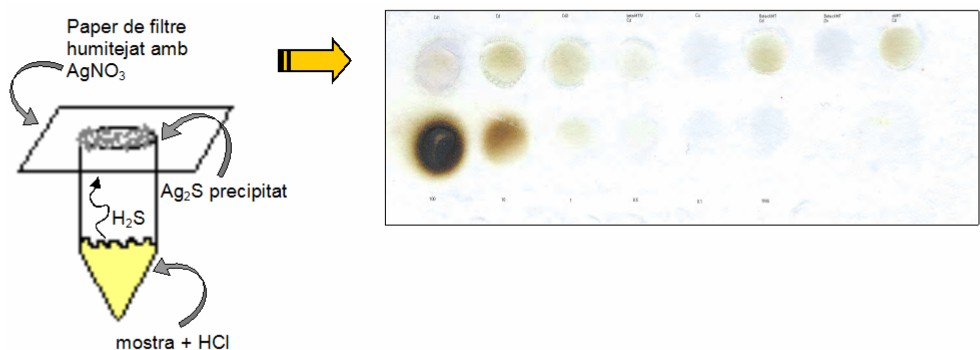

Figura 2.2.- Anàlisi qualitativa de presència de ions S^{2-} làbils en les mostres metall-MT per precipitació de sulfur de plata.

La determinació qualitativa de la presència d'anions sulfur va portar a la modificació del mètode d'ICP-AES *convencional* emprat,[73] ja que amb ions sulfur presents ja no es podia continuar considerant que el contingut en sofre de la mostra era exclusivament degut als residus de Cys i Met de les MTs. Així, a partir d'aquell moment per a la quantificació de la concentració de proteïna es va utilitzar l'anàlisi

d'aminoàcids i el valor obtingut es va corroborar amb un ICP-AES *àcid* que, a més a més, proporcionava relacions metall:MT molt més acurades (Taula 1, article 3).

Per a la determinació quantitativa de la presència d'anions sulfur, Figura 2.3, s'ha utilitzat el mètode del Blau de Metilè,[74] tal i com està descrit en la bibliografia per a les Cd-fitoquelatines.[62] Aquest mètode presenta, però, dos inconvenients: a) interferències per cadmi,[75] i b) la insolubilitat del sulfur de coure el fa inadequat per a mesurar sulfur en mostres que contenen aquest metall. Per aquesta rao, també es va adaptar un altre mètode ja descrit en la bibliografia (GC-FPD)[76] a les característiques de les nostres mostres. Ambdós mètodes han donat resultats coincidents i han permès mesurar el contingut de S^{2-} de totes les MTs considerades (Taula 1, article 3).

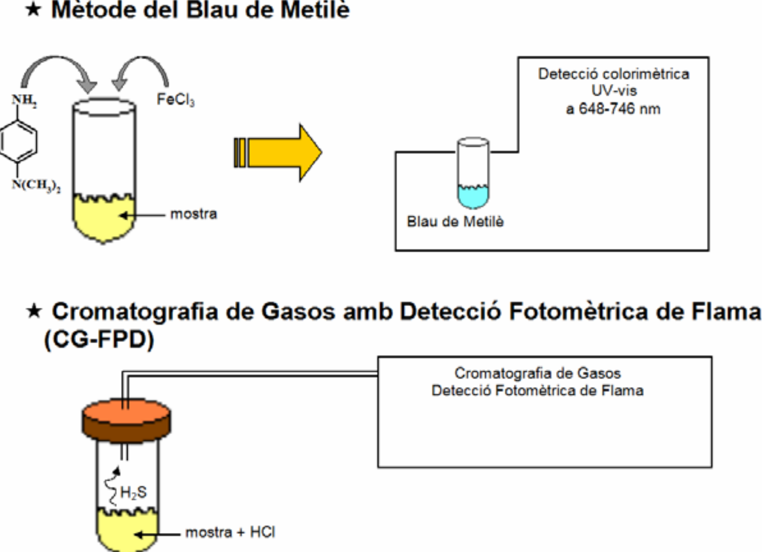

Figura 2.3.- Representació esquemàtica de la quantificació del S^{2-} present en les mostres metall-MT segons el mètode del Blau de Metilè o per GC-FPD.

La confirmació que la participació dels anions sulfur en la coordinació al Cd(II) provoca absorcions en la regió 260-300 nm s'ha aconseguit mitjançant un experiment d'acidificació-reneutralització d'una mostra de Cd-MtnA de *D.melanogaster* (Figura S1, article 3) per comparació dels espectres d'UV-Vis de la mostra abans i després del tractament, Figura 2.4.

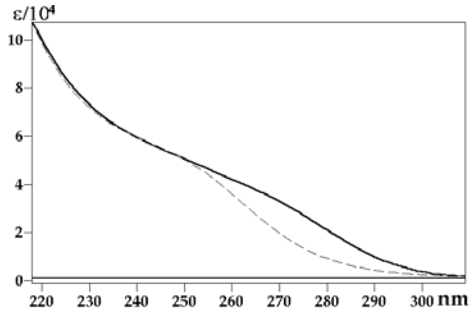

Figura 2.4.- Superposició dels espectres d'UV-Vis de l'espècie Cd-MtnA abans (traç negre) i després (traç discontinu) del tractament d'acidificació-reneutralització.

El conjunt de resultats obtinguts en aquesta part del treball no sols ha demostrat la presència de lligands sulfur en la gran majoria de mostres de MTs recombinants que contenen Zn i/o Cd (cap de les Cu-MT considerades ha donat evidències de presència de sulfur en els seus complexos), sinó que també ha posat de manifest que en una mateixa mostra hi ha un equilibri entre espècies de la mateixa estequiometria metall:MT que contenen sulfur i que no en contenen (Figura 2, article 3). Resta ara continuar treballant en aquesta línia per tal de demostrar si les mostres metall:MT natives també contenen lligands sulfur i si és així esbrinar quines implicacions té aquest descobriment en l'estructura i funció d'aquestes particulars metal·loproteïnes.

2.2.3 Revisió dels resultats publicats sobre MT4 i MT1

En l'apartat 2.1 d'aquesta memòria s'han descrit els resultats publicats respecte la capacitat coordinant de MT4 de mamífer i la seva comparació amb els resultats obtinguts prèviament per a MT1. No obstant això, el recent descobriment descrit en l'apartat anterior sobre la presència d'ions sulfur (S^{2-}) en la majoria de les espècies recombinants Zn- i Cd-MT analitzades exigeix la reconsideració de les dades de MT1 i MT4 publicades amb anterioritat. Així, en aquest apartat, es reconsideren aquestes dades tenint en compte la possible participació dels lligands sulfur en la coordinació metàl·lica de les MTs.

Malauradament, la síntesi i caracterització dels complexos recombinants Zn-MT1, Zn-αMT1 i Zn-βMT1 es va dur a terme en el si d'aquest grup de recerca fa ja uns 10 anys. Des de llavors, tant les tècniques com la metodologia emprada pel grup han anat millorant i ara és difícil accedir i tornar a analitzar els resultats obtinguts en aquells moments. Per això, ha estat necessari tornar a sintetitzar i caracteritzar alguns d'aquests complexos. En tots els casos s'ha determinat la presència d'ions sulfur com a lligands dels agregats de Zn (Taula 1, article 3), però el contingut mitjà de S^{2-}/MT és en tots els casos relativament baix (al voltant de 1 S^{2-}/MT), de manera que els seus espectres de DC no reflecteixen aquesta contribució.

Aquest no és el cas, però, de les expressions d'aquestes mateixes proteïnes en medis rics en Cd(II) per a obtenir les corresponents espècies Cd-MT1, Cd-αMT1 i Cd-βMT1. En primer lloc cal esmentar que únicament la síntesi de Cd-βMT1 correspon a un treball previ d'aquest grup.[40] En aquest treball es va observar clarament que la síntesi a petita escala (0.5 litres) donava lloc a espècies Cd-MT de naturalesa diferent de les que s'obtenien en síntesis a gran escala (30 litres) en base als espectres de DC d'ambdós tipus de produccions (Figura 2.5), les quals en ambdós casos donaven relacions Cd/MT de 1.4.

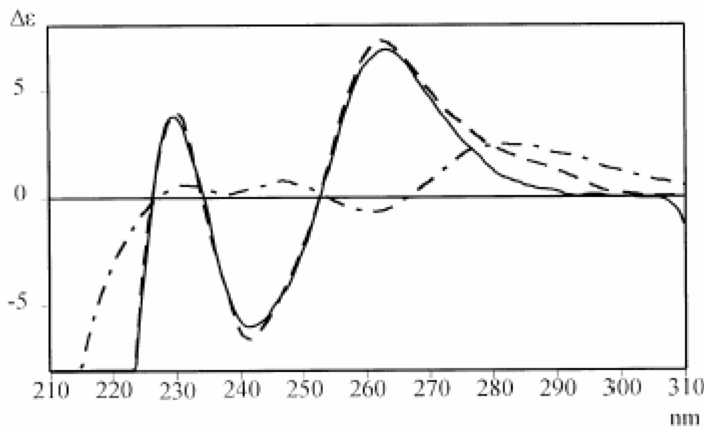

Figura 2.5.- Comparació dels espectres de DC de les solucions de Cd_3-βMT1 obtinguda *in vitro* (traç negre), Cd-βMT1 produïda a petita escala (– – –) i Cd-βMT1 produïda a gran escala (– ▪ – ▪ –). Figura extreta de la referència bibliogràfica número 40.

Amb el coneixement de la possible presència de sulfurs en els agregats metall-MT, ara podem fer una anàlisi alternativa d'aquests resultats. Donat que l'espècie Zn_3-βMT1 conté sulfurs en els seus agregats metàl·lics, en valorar-la amb Cd(II) aquests persisteixen donant lloc a espècies Cd_3-βMT1 que també contenen sulfurs, però pocs, i que per tant donen lloc a espectres de DC del tipus A (Figura 1, article 3). Aquest mateix tipus d'espècies, i per tant d'espectres de DC, s'obtenen en les produccions a petita escala, mentre que les fetes a gran escala provoquen una major participació dels sulfurs en la constitució dels agregats metàl·lics dels complexos Cd-βMT1. Això afavoreix que siguin força més importants les absorcions entre 280 i 300 nm i que les de 250 nm, característiques dels cromòfors $Cd(S_{Cys})_4$, esdevinguin cada cop proporcionalment menys intenses. En aquest cas el que s'observa és un espectre de DC del tipus C (Figura 1, article 3), en el qual s'evidencia clarament un canvi en la quiralitat dels cromòfors $Cd(S_{Cys})_4$, generant un *exciton coupling* de signe contrari al de les produccions a petita escala.

La síntesi i caracterització de Cd_4-αMT1 i de Cd_7-MT1 s'ha descrit en l'apartat 2.1.2 d'aquest treball (Taula 2.2) i només resta per afegir que, d'acord amb les mesures de GC-FPD (Taula 1, article 3), ambdós complexos contenen uns 3 S^{2-} per MT, si bé això no modifica substancialment els seus espectres de DC, que també són del tipus A.

Pel que fa als complexos Zn- i Cd-MT4, ja caracteritzats en l'apartat 2.1 d'aquesta memòria, cal afegir que les mesures d'ICP àcid dels complexos de Zn han permès millorar les relacions Zn/MT publicades, ara més properes a les estequiometries detectades per ESI-MS. Així mateix, la GC-FPD ha confirmat la presència d'entre 1 i 3 S^{2-} per proteïna, els quals no són observables per DC.

Respecte els complexos de Cd, les mesures d'ICP àcid també han permès millorar les relacions M/MT publicades per als tres polipèptids MT4, αMT4 i βMT4. En tots tres casos s'ha detectat presència d'ions S^{2-}, tot i que tant per a MT4 com per a αMT4 aquests no afecten significativament els espectres de DC de les corresponents Cd-proteïnes, obtenint-se en ambdós casos espectres del tipus A. Pel que fa a βMT4, la consideració de la presència de sulfurs en els seus complexos de Cd permet explicar els resultats publicats, ja que per ICP només es va detectar Cd enllaçat a la proteïna (2.0 Cd, 0.0 Zn, Taula 1, article 1) tot i que s'havia proposat que la mescla obtinguda en la bioproducció contenia les espècies Cd_3-βMT4, Cd_2Zn_1-βMT4 i Cd_1Zn_2-βMT4 (Taula 1, article 1). Així, les mesures de GC-FPD, que indiquen uns 4.6 S^{2-}/MT, suggereixen que realment la mescla correspon a una barreja Cd_3-βMT4, Cd_2S_2-βMT4 i Cd_1S_4-βMT4. Aquesta important presència de lligands sulfur en Cd-βMT4 també explica el seu espectre de DC "atípic" que presenta una gaussiana a 250(-) nm (Taula 2.2) i que de fet no correspon a cap dels espectres de DC proposats en l'article 3 d'aquesta memòria.

2.3 Capacitat coordinant de la MT de pollastre, ckMT1

Una part del treball que aquí es presenta s'ha dedicat a l'estudi de ckMT1, l'única MT coneguda de pollastre, que és l'organisme model en el grup de les aus. Tal com s'ha comentat en la introducció (apartat 1.5.2), la proximitat evolutiva de les MTs d'aus i mamífers fan suposar que ambdues provenen d'un ancestre comú. Tenint en compte el coneixement que actualment té el nostre grup de recerca sobre les propietats coordinants de les isoformes MT1 i MT4 de mamífer, serà de gran interès estudiar el comportament coordinant de ckMT1 i comparar-lo amb el de les primeres. D'aquesta manera es pretenen determinar les similituds i diferències de coordinació metàl·lica entre aquestes proteïnes. Això ha de contribuir a ampliar el coneixement de les característiques funcionals que aparentment van determinar els diferents camins evolutius seguits per les MTs d'aus i mamífers en la branca superior de l'evolució dels vertebrats. Per tal de fer possible la comparació entre ckMT1, MT1 i MT4, l'anàlisi del comportament de ckMT1 enfront de Zn(II), Cd(II) i Cu(I) s'ha dut a terme mitjançant metodologies anàlogues a les descrites per a MT4 (apartat 2.1) però incorporant les tècniques necessàries per tal d'estudiar la presència de lligands sulfur en els seus agregats.

Si bé l'anàlisi del genoma de pollastre no ha estat objecte d'aquest treball, cal destacar que membres d'aquest grup de recerca han identificat un segon gen en pollastre que codifica per MT, ckMT2, trencant així un dels principis bàsics acceptats fins al moment que establia que en pollastre només existia una única MT (apartat 1.5.2).

2.3.1 Propietats coordinants de ckMT1 envers Zn(II) i Cd(II)

Les espècies majoritàries obtingudes en la biosíntesi de la proteïna sencera, ckMT1, i dels seus fragments, αckMT1 i βckMT1, en medis rics en Zn(II) o Cd(II) presenten l'estequiometria dels agregats canònics esperats, *i.e.* M_7-ckMT1, M_4-αckMT1 i M_3-βckMT1 (M = Zn o Cd) (Taules 2.5 i 2.6), evidenciant un comportament de ckMT1 més proper al de MT1[9,40,41] que al de MT4 (seccions 2.1.1 i 2.1.2). Tot i això, l'ESI-MS mostra com les espècies M_7-ckMT1, M_3-βckMT1 i Cd_4-αckMT1 (M = Zn o Cd) coexisteixen amb espècies minoritàries que contenen ions sulfur (Taules 2.5 i 2.6). La biosíntesi de Zn_4-αckMT1 és l'única que ha donat lloc a una única espècie en solució.

Pel que fa a la informació estructural que s'obté a partir dels espectres de DC, cal dir que tant M_7-ckMT1 com M_4-αckMT1 presenten l'empremta característica dels agregats Zn-MT i Cd-MT descrits fins ara (Figures 2.6.A i 2.6.B, i Figura 3.B, article 4).

D'altra banda, s'observa que les espècies Zn-ckMT1 presenten un grau d'estructuració més proper al de les de MT1 que al de les de MT4 (Figures 2.6.A i 2.6.B).

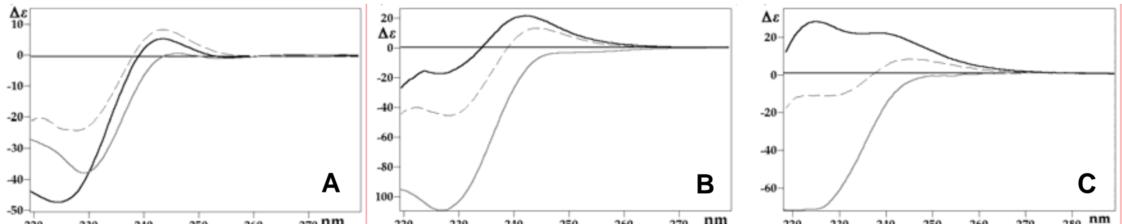

Figura 2.6.- Comparació dels espectres de DC de les solucions recombinants de: (A) Zn_4-αckMT1 (traç negre), Zn_4-αMT4 (traç gris) i Zn_4-αMT1 (traç discontinu); (B) Zn-ckMT1 (traç negre), Zn_7-MT4 (traç gris) i Zn_7-MT1(traç discontinu) i (C) Zn-βckMT1 (traç negre), Zn_3-βMT4 (traç gris) i Zn_3-βMT1 (traç discontinu).

Zn		Zn-ckMT1	Zn-αckMT1	Zn-βckMT1
ICP-AES	[prot.] (M)	$1.51x10^{-4}$	$1.09x10^{-4}$	$4.04x10^{-4}$
	M/MT	6.2 Zn	3.9 Zn	2.4 Zn
ICP-AES àcid	[prot.] (M)	$1.09x10^{-4}$	$1.04x10^{-4}$	$2.23x10^{-4}$
	M/MT	7.0 Zn	4.0 Zn	3.3 Zn
S^{2-}/MT		2.56	1.15	3.10
ESI-MS*		Zn_7-ckMT1 (M) Zn_7S_1-ckMT1 (m)	Zn_4-αckMT1	Zn_3-βckMT1 (M) Zn_3S_3-βckMT1 (m)
Espectre DC				

Taula 2.5.- Resultats de la caracterització dels complexos de ckMT1 sencera i dels seus fragments constitutius obtinguts per enginyeria genètica mitjançant la seva expressió en medis rics en Zn.

* Les espècies estan ordenades d'acord amb la seva abundància en solució. (M) representa l'espècie majoritària i (m) la minoritària.

Contràriament, les espècies M_3-βckMT1 (M = Zn o Cd) presenten espectres de DC que difereixen força dels de M_3-βMT de mamífer (Figura 2.6.C, i Figura 3.D, article 4). Amb la intenció de determinar quins cromòfors provoquen aquestes inesperades empremtes de DC, s'han dut a terme un seguit d'experiments. Així, s'han realitzat en paral·lel dues síntesis recombinants de Zn-βckMT1, una s'ha eluït en presència d'ions clorur (Tris-HCl com a tampó) i l'altra en absència d'aquests ions (Tris-$HClO_4$ com a tampó), d'acord amb la metodologia descrita en l'apartat 2.2.1 (article 2). Aquestes solucions de proteïna s'han valorat respectivament amb $CdCl_2$ o bé $Cd(ClO_4)_2$ i les

espècies M^{II}-βckMT1 generades al llarg de les valoracions s'han caracteritzat mitjançant les tècniques espectroscòpiques i espectromètriques habituals. L'anàlisi dels resultats obtinguts permet afirmar que les solucions que contenen Zn_3-βckMT1 o Cd_3-βckMT1 mostren, en presència i absència de clorurs, els mateixos espectres de DC i que, per tant, els inesperats espectres de DC obtinguts en la biosíntesi d'aquestes espècies no poden ser atribuïts a cromòfors en què hi intervinguin els lligands clorur.

Cd		**Cd-ckMT1**	**Cd-αckMT1**	**Cd-βckMT1**
ICP-AES	[prot.] (M)	2.29×10^{-4}	0.89×10^{-4}	1.75×10^{-4}
	M/MT	3.7 Cd	3.4 Cd	1.6 Cd
ICP-AES àcid	[prot.] (M)	0.63×10^{-4}	0.62×10^{-4}	0.57×10^{-4}
	M/MT	8.8 Cd	4.4 Cd	4.3 Cd
S^{2-}/MT		4.70	2.90	5.60
ESI-MS*		Cd_7-ckMT1 (M) Cd_6S_2-ckMT1 Cd_5S_4-ckMT1 (m)	Cd_4-αckMT1 (M) Cd_3S_2-αckMT1 (m)	Cd_3-βckMT1 (M) Cd_2S_2-βckMT1 (m)
Espectre DC				

Taula 2.6.- Resultats de la caracterització dels complexos de ckMT1 sencera i dels seus fragments constitutius obtinguts per enginyeria genètica mitjançant la seva expressió en medis rics en Cd.

* Les espècies estan ordenades d'acord amb la seva abundància en solució. (M) representa l'espècie majoritària i (m) la minoritària.

Un cop descartats els ions clorur com a responsables dels espectres de DC de les espècies M-βckMT1, i tenint en compte els resultats d'ESI-MS, ICP-AES i GC-FPD que revelen la presència d'ions sulfur tant per M = Zn com per M = Cd, s'ha procedit a l'acidificació d'ambdues solucions des de pH 7.2 fins a pH 1.5 amb HCl 0.05 M, tot esperant provocar l'alliberament dels sulfurs en forma de H_2S gas. La Figura 2.7 mostra els espectres de DC i d'UV-Vis enregistrats al llarg de l'acidificació d'una mostra de Zn-βckMT1. Un cop desmetal·lada la proteïna (Figura 2.7.A), el pH de la solució s'ha portat de nou a pH 7.6 per addició de NaOH 0.05M (Figura 2.7.B). Així, s'observa que l'acidificació provoca una disminució generalitzada de l'absorció, d'acord amb la pèrdua de metalls per part de la proteïna, mentre que amb la reneutralització la forma apo-MT torna a enllaçar els ions metàl·lics, recuperant les absorcions inicials

(Figura 2.7.C). Així, es pot concloure que tampoc els ions sulfur semblen presentar contribucions espectroscòpiques fàcilment observables per DC en el cas de les espècies Zn-βckMT1 i Cd-βckMT1. Conseqüentment, les absorcions dels espectres de DC obtinguts per a les mostres de Zn-βckMT1 i Cd-βckMT1 s'atribueixen exclusivament als respectius cromòfors $Zn(S_{Cys})_4$ (*ca.* 240 nm) i $Cd(S_{Cys})_4$ (*ca.* 250 nm) amb contribucions a baixes longituds d'ona (*ca.* 225 nm) de la conformació de la proteïna.[77]

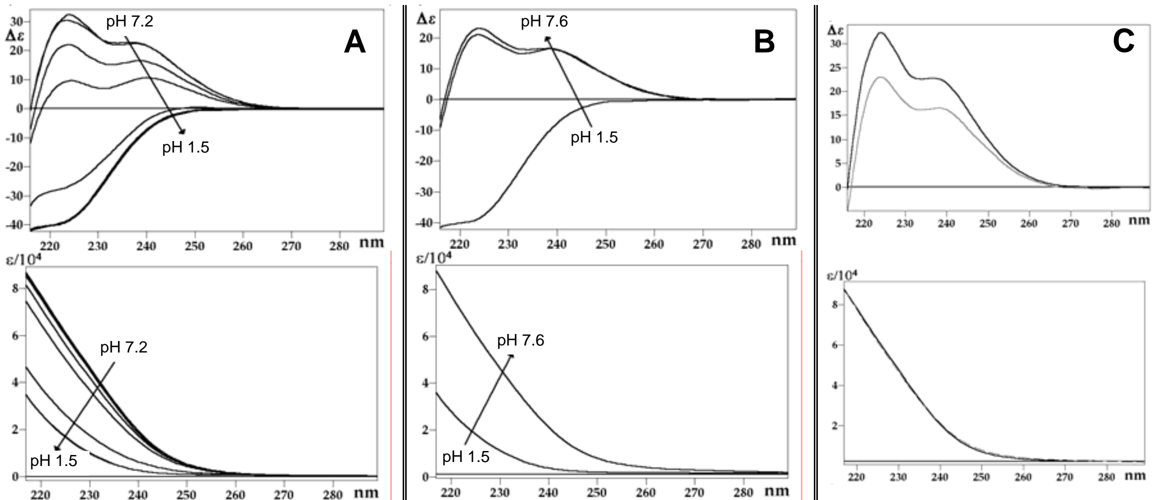

Figura 2.7.- A una solució 25×10^{-6} M de Zn_3-βckMT1: (A) s'afegeix HCl 0.05M i s'enregistren els canvis produïts per la baixada de pH en els espectres de DC i UV-Vis i (B) seguidament s'afegeix NaOH 0.05M fins a pH 7.6. (C) Comparació dels espectres de DC i UV-Vis de la solució inicial (traç negre) i la solució després de ser acidificada i reneutralitzada (traç gris).

Tot i els particulars espectres de DC de les espècies M-βckMT1 (M= Zn o Cd), l'anàlisi comparativa dels resultats obtinguts en la caracterització espectroscòpica de les espècies M_4-αckMT1, M-βckMT1 i M-ckMT1 biosintetitzades permet deduir que en medis rics en Zn(II) i Cd(II) els fragments de ckMT1 aïllats s'estructuren de manera anàloga a com ho fan quan formen part de la MT sencera. Per tant, es proposa que ambdós dominis es comporten de manera independent ja que la suma dels seus espectres de DC pràcticament reprodueix el de la proteïna sencera en presència de metalls divalents (Figura 3.A i 3.B, article 4).

Els experiments realitzats *in vitro* han permès reproduir l'espectre de DC de la mostra Cd-βckMT1 obtinguda *in vivo*. Així, els resultats obtinguts en afegir 3 equivalents de Cd(II) a una solució de Zn_3-βckMT1 a pH 7 evidencien, tant per ESI-MS com per DC, que la mostra així aconseguida presenta unes característiques molt properes a les de la Cd-βckMT1 biosintetitzada. Tot i així, no és fins a 7 eq de Cd(II) afegits que s'obté l'espectre representatiu de l'espècie Cd_3-βckMT1 (amb una petita

contribució del complex Cd_3S_2-βckMT1), el qual és més proper al de Cd_3-βMT1 que al de Cd_3-βMT4 (Figura 4.D, article 4).

Les valoracions amb Cd(II) de les espècies Zn_4-αckMT1 i Zn_7-ckMT1 biosintetitzades han donat lloc a resultats molt interessants. Fins a 4 i 7 equivalents de Cd(II) afegits, respectivament, les evolucions espectroscòpiques han estat comparables a les dels corresponents pèptids de MT1[9,41] i MT4 (apartat 2.1.2 i article 1). Però és a partir d'aquests punts de les valoracions que en afegir més equivalents de Cd(II) comença a fer-se visible una absorció positiva a 250 nm en els espectres de DC. En un estudi anterior d'aquest mateix grup fet amb mutants de MT1 que intercanviaven un residu de Cys per His[47] ja s'havia observat una absorció anàloga, la qual es va relacionar amb la participació de la His en l'enllaç metàl·lic. En base a aquests resultats i per corroborar aquesta participació en el cas de l'enllaç de ckMT1 a Cd(II), s'ha procedit a acidificar amb HCl 0.011 M les solucions finals de les valoracions de Zn_4-αckMT1 i Zn_7-ckMT1 amb Cd(II) des de pH 7 fins a pH 4. Els espectres de DC enregistrats al llarg d'aquests experiments mostren com a mesura que el pH disminueix desapareixen les absorcions a 250 nm, mentre que la resta de senyals del DC es mantenen constants. Aquests resultats indiquen que les diferències entre els espectres de DC a pH 7 i 4 es deuen, molt probablement, a la coordinació del nitrogen imidazólic de la His al Cd(II) donat que es protona a un pH entre 4-5, mentre que per sota d'aquest pH comenca a protonar-se el grup tiolat de la Cys.

En els espectres de DC, s'ha observat juntament amb l'aparició de l'absorció vora 250 nm, una baixada gradual en la intensitat de totes les bandes, més evident en el cas d'αckMT1. En la bibliografia aquesta variació en els espectres de DC s'ha relacionat amb processos de dimerització.[78] Així mateix, un estudi exhaustiu dels resultats d'ESI-MS mostra la presència del dímer Cd_8-2αckMT1 el qual es detecta des de pràcticament els primers punts de la valoració de Zn_4-αckMT1 i l'abundància del qual augmenta amb el nombre d'equivalents de Cd(II) afegits. Tot i que en la valoració de ckMT1 l'evolució espectroscòpica (DC i UV-Vis) és comparable a la de αckMT1, la tècnica d'ESI-MS no ha permès proposar la formació de dímers en el cas de la proteïna sencera. En la bibliografia es descriuen dos tipus de dímers en MT, els que es formen per oxidació dels grups -SH, generant així ponts disulfur entre dos monòmers,[79] i els que es formen via metall.[80] Amb les condicions de treball aquí utilitzades (baixes concentracions de proteïna i atmosfera d'argó) no sembla probable la formació d'un dímer per oxidació. D'altra banda, el fet que els espectres de diferència d'UV-Vis d'ambdues valoracions no mostrin la formació de nous cromòfors a partir de 4 i de 7 eq de Cd(II) respectivament afegits a Zn_4-αckMT1 i Zn_7-ckMT1 i que

per ESI-MS es detecti la coexistència de Cd_4- i Cd_8-2αckMT1, porta a suposar que la formació de dímers tampoc no té lloc via la interacció de dos monòmers que s'enllacen mitjançant un metall que fa de pont. En conseqüència, es proposa un tercer procés de dimerització en MTs en què intervindrien els dos nitrògens dels residus d'His (article 4).

El conjunt de resultats recollits i discutits en aquest apartat han permès concloure que ckMT1 presenta un comportament coordinant enfront dels metalls divalents més proper al de MT1 que al de MT4, i que probablement l'afinitat d'aquesta proteïna per aquests ions metàl·lics es troba entremig de la de MT1 i MT4.

2.3.2 Propietats coordinants de ckMT1 envers Cu(I)

En medis rics en Cu el fragment βckMT1 s'expressa com a barreja d'espècies homometàl·liques Cu-βckMT1 amb una composició similar però diferent abundància a les presentades per βMT1 i βMT4. Així, es detecta Cu_6-βckMT1 com a espècie majoritària enfront de Cu_7-βMT1 i Cu_7-βMT4 (Taula 2.7). D'acord amb les dades de DC les estructures de les tres proteïnes en solució són comparables, tot i que només βckMT1 i βMT4 presenten absorcions en el rang 340-380 nm (Figura 6.C, article 4), la qual cosa suggereix que aquests pèptids són capaços de proporcionar un tipus de coordinació per al Cu(I) que βMT1 no pot oferir. Així doncs, segons aquests resultats, βckMT1 es comporta com una Cu-tioneïna de manera equivalent a com ho fan βMT1 i βMT4.

Cu		Cu-ckMT1	Cu-αckMT1	Cu-βckMT1
ICP-AES	[prot.] (M)	0.39×10^{-4}	0.26×10^{-4}	1.66×10^{-4}
	M/MT	2.5 Zn 7.4 Cu	0.5 Zn 5.7 Cu	0.0 Zn 6.0 Cu
ESI-MS*		M_{10}-ckMT1 (M) M_{12}-ckMT1 M_{11}-ckMT1 (m)	M_6-αckMT1 (M) M_7-αckMT1 M_5-αckMT1 (m)	Cu_6-βckMT1 (M) Cu_7-βckMT1 Cu_5-βckMT1 (m)
Espectre DC				

Taula 2.7.- Resultats de la caracterització de ckMT1 sencera i dels seus fragments constitutius obtinguts per enginyeria genètica mitjançant la seva expressió en medis rics en Cu.

* Les espècies estan ordenades d'acord amb la seva abundància en solució. (M) representa l'espècie majoritària i (m) la minoritària.

Contràriament, ckMT1 i αckMT1 es consideren Zn-tioneïnes ja que en medis rics en Cu donen lloc a barreges d'espècies heterometàl·liques Zn,Cu-MT (Taula 2.7), anàlogament a com ho feien MT1 i el seu fragment αMT1. Per a la proteïna sencera, les similituds amb MT1 són força significatives ja que M_{10}-ckMT1 és l'espècie majoritària (on M = Zn i/o Cu), amb una estequiometria Zn_3Cu_7-ckMT1 (segons dades d'ICP-AES) i un espectre de DC comparable als proposats per a MT1 i MT4 (Tipus 2) (Figura 6.A, article 4), tot i que les absorcions entre 340-380 nm característiques dels fragments βckMT1 i βMT4 en aquests cas només es detecten en l'espectre de Zn_3Cu_7-MT4. Per altra banda, αckMT1 presenta com a espècie majoritària M_6-αckMT1, que contrasta amb la biosintetitzada M_5-αMT1 i, si comparem els resultats obtinguts per ICP-AES (0.5 Zn i 5.7 Cu per αckMT1 enfront de 0.5 Zn i 4.5 Cu per αMT1), sembla evident que la diferència en la relació M/MT entre aquests dos polipèptids és deguda a un Cu(I) addicional en αckMT1. La comparació dels espectres de DC revela que tot i la seva diferent naturalesa, Zn-tioneïna *vs.* Cu-tioneïna, αckMT1 es replega en solució de manera més propera a αMT4 que a αMT1 (Figura 6.B, article 4), la qual cosa fa pensar que la presència de Zn(II) en αckMT1 no té rellevància estructural.

Per aprofundir més en el coneixement de les propietats coordinants de ckMT1 envers Cu(I) s'han dut a terme experiments de substitució Zn/Cu per als tres polipèptids. Tal i com es descriu en el cas de les espècies Cu-βckMT1, Cu-βMT1 i Cu-βMT4 biosintetitzades, les tres Zn-proteïnes mostren *in vitro* comportaments molt propers envers Cu(I). Així, tot i les diferències estructurals de les espècies de partida (Zn_3-βckMT1, Zn_3-βMT1 i Zn_3-βMT4), els tres pèptids donen lloc a reaccions de substitució Zn/Cu anàlogues, amb l'excepció del número d'equivalents de Cu(I) necessaris per assolir determinades etapes de les valoracions. Utilitzant la metodologia definida per aquest grup d'investigació per a identificar empremtes de DC de les espècies metall-MT formades al llarg de les valoracions[81] (article 1, apartat 2.1.3), s'ha observat que amb 5 eq de Cu(I) afegits a Zn_3-βckMT1 ja s'obté l'espectre del complex Cu_7-βckMT1, mentre que per a formar els agregats Cu_7-βMT1[40] i Cu_7-βMT4 (article 1 i apartat 2.1.3), d'estructures comparables a Cu_7-βckMT1, cal afegir 7 i 6 eq de Cu(I), respectivament. El conjunt d'aquestes dades suggereix que βckMT1 presenta *in vitro* una major afinitat per al Cu(I) que βMT1 i βMT4.

Pel que fa al fragment αckMT1, la reacció de substitució Zn/Cu en Zn_4-αckMT1 és més similar a la de Zn_4-αMT1 que no pas a la de Zn_4-αMT4, tot i que les tres valoracions presenten evolucions molt paral·leles fins 5 eq de Cu(I) afegits. L'addició del 6è equivalent de Cu(I) a Zn_4-αMT4 provoca un canvi en la quiralitat de la proteïna

el qual s'observa també en els casos de αckMT1 i αMT1 però després de l'addició de 7 i 8 eq de Cu(I), respectivament. Aquests resultats permeten proposar que la capacitat coordinant de αckMT1 envers el Cu(I) es troba entre les de αMT1 i αMT4.

Les tres proteïnes senceres, Zn-ckMT1, Zn-MT1 i Zn-MT4, evolucionen de manera similar fins a 7 eq de Cu(I) afegits, punt on es detecta la formació d'espècies anàlogues d'estequiometria Zn_3Cu_7-MT, equivalents a les obtingudes en la síntesi recombinant de les tres proteïnes en medis rics en Cu. Les diferències observades en aquest primer estadi de les valoracions s'han d'atribuir a les diferències en els espectres de DC de partida i en el cas de MT4 a una contribució en la zona de 350 nm relacionada amb la coordinació de Cu(I) per part del domini βMT4 (article 1 i apartat 2.1.3). Aquesta absorció present en MT4, que s'intensifica amb la formació de Cu_{10}-MT4, no apareix mai en el cas de la valoració de MT1, mentre que en el cas Zn-ckMT1 es detecta en afegir 12 eq de Cu(I), la qual cosa denota que aquesta última proteïna presenta la capacitat, tal i com ho feia MT4 (article 1 i apartat 2.1.3), d'enllaçar Cu(I) mitjançant un entorn de coordinació especial quan s'han afegit quantitats importants de Cu(I).

Contràriament a la independència de comportament de αckMT1 i βckMT1 envers Zn(II) i Cd(II), els dos dominis de ckMT1 interaccionen *in vivo* amb Cu(I) de manera diferent quan es troben lliures o quan formen part de la proteïna sencera, és a dir, mostren un comportament dependent. Aquest fet s'evidencia clarament per les estequiometries de les espècies biosintetitzades en medis rics en Cu. Així, per a la proteïna sencera s'obté com a complex majoritari M_{10}-ckMT1, en contraposició a l'espècie M_6,Cu_6-ckMT1 que caldria esperar tenint en compte les estequiometries dels agregats majoritaris obtinguts en les biosíntesis dels fragments, M_6-αckMT1 i Cu_6-βckMT1. Aquests resultats denoten, tal i com es va observar en el cas de MT1 i de MT4, una major capacitat coordinant *in vivo* envers Cu(I) dels fragments per separat que de la proteïna sencera. L'elevat nombre d'espècies que coexisteixen en les diferents etapes de les valoracions *in vitro* dificulta la determinació del comportament dependent/independent dels dominis de ckMT1 *in vitro.*

El conjunt de resultats recollits en aquest apartat porta a concloure que, anàlogament a com s'ha proposat en el cas dels metalls divalents, les habilitats coordinants dels pèptids de ckMT1 enfront del Cu(I) es situarien entre les de MT1 i les de MT4, de manera que l'esquema d'afinitat d'aquestes proteïnes envers el Cu(I) seria: MT4 > ckMT1 > MT1.

2.4 *Capacitat coordinant d'una MT de llevat, Crs5*

Tal i com s'ha comentat en l'apartat 1.5.3, s'han descrit dues MTs en el llevat *S.cerevisiae*, Cup1 i Crs5, molt diferents entre si. La primera, àmpliament estudiada, ha estat relacionada amb la destoxificació i homeòstasi del Cu no només perquè l'expressió del seu gen és induïda per la presència de Cu, sinó també perquè en purificar-la s'obté com una espècie homometàl·lica de Cu. Per altra banda, Crs5, amb una estructura primària que la fa més propera a les MTs de mamífer que a Cup1, també es veu regulada positivament per la presència de Cu en el medi però a uns nivells molt més baixos que Cup1. Tot i això, s'ha proposat que aquesta MT podria tenir un paper en la destoxificació i homeòstasi del Zn.[60] Amb la intenció d'aprofundir en l'estudi de Crs5 i de les seves possibles funcions, i establir el seu caràcter de Zn- o Cu-tioneïna, s'ha estudiat el comportament coordinant d'aquesta MT de llevat. En aquest apartat es recullen els resultats i la discussió de l'estudi de caracterització d'aquesta MT obtinguts mitjançant la metodologia habitual emprada per aquest grup de recerca.

Cal esmentar que, en el procés de clonació del gen de Crs5 (equip del Departament de Genètica), s'han obtingut dues metal·lotioneïnes lleugerament diferents, Crs5 i Crs5*, que difereixen únicament en un aminoàcid (una Lys de Crs5 que és un Glu a Crs5*). La seva caracterització s'ha dut a terme en paral·lel i ha revelat que la mutació no té pràcticament cap influència en les propietats de coordinació metàl·lica de Crs5 (en la Taula 2.8 es mostren els resultats de la caracterització de Zn-Crs5 i Zn-Crs5*). Per tant, a continuació es comenten únicament els resultats obtinguts per a Crs5.

2.4.1 *Propietats coordinants de Crs5 envers Zn(II) i Cd(II)*

Crs5 s'expressa en medis rics en Zn(II) com una barreja d'espècies homometàl·liques amb Zn_6- i Zn_7-Crs5 com a espècies majoritàries (Taula 2.8). L'espectre de DC de Zn-Crs5 presenta una absorció en forma de gaussiana a *ca.* 240 nm, representativa dels cromòfors $Zn(S_{Cys})_4$. Cal destacar que la intensitat dels espectres de DC d'aquesta mostra hi denoten un alt grau de quiralitat en comparació amb el d'altres Zn-MTs.

Anàlogament a les altres MTs estudiades en aquest treball, els complexos Zn-Crs5 contenen lligands sulfur en els seus agregats, si bé en aquest cas el nombre de S^{2-} per molècula de MT és relativament baix (0.4 - 0.7 S^{2-}/MT), cosa que fa que pràcticament no hi hagi discrepàncies entre les mesures d'ICP-AES convencional i àcid i en les relacions Zn/proteïna calculades a partir d'aquestes.

Zn		Zn-Crs5	Zn-Crs5*
ICP-AES	[prot.] (M)	1.72×10^{-4}	4.30×10^{-4}
	M/MT	5.8 Zn	5.6 Zn
ICP-AES àcid	[prot.] (M)	1.67×10^{-4}	4.09×10^{-4}
	M/MT	5.7 Zn	5.7 Zn
Blau de Metilè		0.35 S/prot.	0.58 S/prot.
GC-FPD		0.44 S/prot.	0.77 S/prot:
ESI-MS*		Zn_7- ≈ Zn_6-Crs5 (M) Zn_5-Crs5 Zn_7S_2- ≈ Zn_4-Crs5 (m)	Zn_6-Crs5 (M) Zn_7-Crs5 Zn_5-Crs5 Zn_4- = Zn_3-Crs5 (m)
Espectre DC			

Taula 2.8.- Resultats de la caracterització dels complexos de Crs5 i Crs5* obtinguts per enginyeria genètica mitjançant la seva expressió en medis rics en Zn.

* Les espècies estan ordenades d'acord amb la seva abundància en solució. (M) representa l'espècie majoritària i (m) la minoritària.

L'expressió de Crs5 en medis rics en Cd(II) ha donat lloc a preparacions de més difícil caracterització ja que la FPLC dels últims estadis del procés de purificació de les mostres dóna lloc a dos pics, els quals s'han separat i analitzat independentment. Ambdues mostres contenen complexos Cd-Crs5 de composició i, per tant, també de característiques diferents. Tanmateix, els seus espectres de DC i les seves dades analítiques presenten algunes característiques comunes (Taula 2.9), que són:

- absorció de DC al voltant de 250 nm, atribuïble als cromòfors $Cd(S_{Cys})_4$
- absorció de DC entre 280 i 300 nm, atribuïble a la presència de lligands sulfur en els complexos Cd-Crs5

La intensitat relativa de les absorcions de DC a 250 i 280-300 nm està d'acord amb el contingut en lligands sulfur de cadascuna de les mostres (Figura 4 A, article 5) detectat per ESI-MS i CG-FPD. D'aquesta forma, el primer pic que es separa per FPLC (Pic 1) conté complexos Cd-Crs5 amb un major contingut en S^{2-} que aquells presents en el Pic 2, cosa que està d'acord amb les respectives característiques espectroscòpiques i analítiques. Cal destacar també que si es recullen els dos pics

conjuntament (Pic 1+2) es pot veure que els complexos amb elevat contingut en sulfur no són majoritaris en la bioproducció de Cd-Crs5.

Cd		**Cd-Crs5** 1ª síntesi	**Cd-Crs5** 2ª síntesi	
		Pic 1+2	Pic 1	Pic 2
ICP-AES	[prot.] (M)	$2.25x10^{-4}$	$0.47x10^{-4}$	$1.04x10^{-4}$
	M/MT	0.1 Zn, 3.2 Cd	0.0 Zn, 1.8 Cd	0.0 Zn, 3.1 Cd
ICP-AES àcid	[prot.] (M)	----	$0.1x10^{-4}$	$0.38x10^{-4}$
	M/MT	----	9.0 Cd	0.1 Zn, 7.4 Cd
GC-FPD		2.03	----	1.81
ESI-MS*		Cd_7-Crs5 (M) Cd_6S_2-Crs5 Cd_6- = Cd_7S_2-Crs5 Cd_8- = Cd_5S_2-Crs5 (m)	Cd_7S_2-Crs5 (M) Cd_8-Crs5 (m)	Cd_7-Crs5 (M) Cd_7S_2-Crs5 Cd_8-Crs5 Cd_6S_2-Crs5 Cd_5S_4-Crs5 (m)
Espectre DC				

Taula 2.9.- Resultats de la caracterització dels complexos de Crs5 obtinguts per enginyeria genètica mitjançant la seva expressió en medis rics en Cd.

* Les espècies estan ordenades d'acord amb la seva abundància en solució. (M) representa l'espècie majoritària i (m) la minoritària.

La valoració de la forma Zn-Crs5 amb Cd(II) (Figures 5 i S1, article 5) ha revelat que, d'acord amb el baix contingut en lligands sulfur de Zn-Crs5, la substitució del Zn(II) pel Cd(II) permet generar *in vitro* mescles d'espècies Cd-Crs5 anàlogues a les obtingudes *in vivo* i eluïdes per FPLC en l'anomenat Pic 2 (Figura 4C, article 5). En canvi, en cap moment de les valoracions es detecten absorcions anàlogues a les enregistrades per a les mostres Cd-Crs5 del Pic 1.

Cal destacar que, a diferència del cas descrit per a ckMT1 (apartat 2.3.1), en Crs5 (que conté 2 residus d'His) no s'ha observat cap evidència de la participació dels residus d'His en la coordinació a Zn(II) o a Cd(II).

2.4.2 Propietats coordinants de Crs5 envers Cu(I)

Tal com és habitual, Crs5 s'ha expressat múltiples vegades en medis rics en Cu i s'han fet cultius tant a petita com a gran escala. Així, en les produccions a petita escala s'utilitzen erlenmeyers de 2 litres amb 1.5 litres de cultiu que s'agiten a 250

rpm, mentre que els cultius a gran escala es fan en fermentadors de 10 litres amb agitació important i oxigenació constant (més d'un 70-80% de saturació). A diferència del que s'havia observat fins ara, la caracterització de les preparacions fetes a petita i a gran escala ha revelat que la naturalesa dels complexos Cu-Crs5 depèn de com s'ha dut a terme la seva biosíntesi. Així mateix, i a diferència de quan la proteïna es produïa en presència de Cd(II), en aquest cas els pics de MT separats per FPLC mostren composicions anàlogues, de manera que s'han caracteritzat conjuntament.

Els resultats obtinguts en les diferents produccions de Cu-Crs5 (Taula 2.10) mostren que en les de petita escala s'obtenen espècies homometàl·liques de Cu, mentre que les de gran escala donen lloc a espècies heterometàl·liques Zn,Cu-Crs5.

Cu		**Cu-Crs5** (gran escala)	**Cu-Crs5** (petita escala)
ICP-AES	[proteïna] (M)	1.72×10^{-4}	3.22×10^{-4}
	Relació M/MT	1.7 Zn 0.0 Cd 5.0 Cu	0.2 Zn 0.0 Cd 11.0 Cu
ESI-MS*		M_9-Crs5 ≈ M_8-Crs5 (M) M_{10}-Crs5 M_{11}-Crs5 ≈ M_{12}-Crs5 M_6-Crs5 ≈ M_7-Crs5 (m)	Cu_{10}-Crs5 Cu_9-Crs5 Cu_{11}-Crs5 Cu_{12}-Crs5 Cu_{13}-Crs5 Cu_8-Crs5
Espectre DC			

Taula 2.10.- Resultats de la caracterització dels complexos Cu-Crs5 obtinguts mitjançant l'expressió recombinant del gen *CRS5* en cultius en medis rics en Cu.

* Les espècies estan ordenades d'acord amb la seva abundància en solució. (M) representa l'espècie majoritària i (m) la minoritària.

Les mesures de presència d'anions sulfur com a lligands en els complexos Cu-Crs5 (article 3) han indicat, una vegada més, la seva absència en ambdós tipus de produccions. Així, a petita escala trobem com a espècie majoritària Cu_{10}-Crs5, que estaria bastant d'acord amb les dades d'ICP que mostren un contingut d'11 Cu, mentre que a gran escala les espècies majoritàries són M_8- i M_9-Crs5, quan els valors d'ICP sumen 7 com a molt. Els espectres de DC d'una i altra produccions són també

característics. Els de gran escala (Zn,Cu-Crs5) són força més intensos que els de petita escala (Cu-Crs5) però ni els primers s'assemblen gaire als de les espècies heteronuclears de les MTs de mamífer (Zn_3Cu_7-MT1 o Zn_3Cu_7-MT4) (Figura 6.C, article 5) ni els segons als de les homonuclears de Cu de MT4 (Cu_{10}-MT4) (Figura 6.A, article 5).

Els resultats aquí exposats suggereixen que la major/menor presència d'oxigen en les biosíntesis de Crs5 en *E.coli* fetes a gran/petita escala és la que determina la naturalesa homo o heteronuclear dels complexos metall-MT que s'obtenen. Per tal de demostrar la relació entre la presència/absència d'oxigen i la naturalesa hetero/homonuclear dels complexos metall-Crs5 obtinguts es varen fer dues noves produccions de proteïna a petita escala però en condicions de major oxigenació. La primera es va dur a terme emprant dos erlenmeyers de 2 litres amb 0.75 litres de cultiu cadascun, als quals s'hi van adaptar uns bombollejadors d'aire domèstics. La segona biosíntesi es va realitzar de manera anàloga a la primera però en el moment de la inducció per IPTG es van ajuntar els dos volums en un sol erlenmeyer i es va retirar el bombollejador, igualant així el volum (1.5 L) i condicions habituals de síntesi a petita escala. En totes dues produccions la velocitat d'agitació va ser lleugerament superior a l'habitual (260-270 rpm). Les dades obtingudes en ambdues produccions, que es recullen a la Taula 2.11, mostren que en tots dos casos s'obtenen espècies heteronuclears Zn,Cu-Crs5 i que, per tant, és efectivament l'oxigenació elevada la que determina que no es formin complexos homonuclears de Cu.

Addicionalment, els resultats obtinguts permeten aprofundir una mica més en l'efecte de l'oxigen en les produccions de Cu-Crs5 a partir de l'anàlisi dels espectres de DC i de les dades analítiques d'aquestes dues darreres produccions respecte als de les primeres. De fet, els continguts de Zn i Cu de les espècies bioproduïdes a gran escala, la seva estequiometria i els seus espectres de DC són més semblants als de la producció en la qual s'ha forçat la presència d'un excés d'oxigen només abans de la inducció que als d'aquella en què l'oxigenació s'ha mantingut al llarg de tota la producció (Figura 7, article 5). Pel que fa a l'espectre de DC dels complexos metall-Crs5 obtinguts quan es dóna la màxima oxigenació al medi, cal dir que aquest difereix de l'enregistrat per a les espècies heterometàl·liques obtingudes a gran escala però que és força proper als obtinguts *in vitro* en els primers estadis de les valoracions amb Cu(I) de Zn-Crs5. De fet, ambdós espectres de DC d'aquestes darreres síntesis poden ser reproduïts *in vitro* valorant Zn-Crs5 amb Cu(I) (vegi's més avall).

Cu		**Cu-Crs5** (oxigenació important al llarg de tota la producció)	**Cu-Crs5** (oxigenació important abans de la inducció)
ICP-AES	[prot.] (M)	0.35×10^{-4}	2.05×10^{-4}
	M/MT	2.6 Zn 0.0 Cd 2.8 Cu	1.7 Zn 0.0 Cd 5.5 Cu
ESI-MS*		M_8-Crs5 ≈ M_4-Crs5 (M) M_5-Crs5 M_6-Crs5 ≈ M_9-Crs5 M_7-Crs5 M_{10}-Crs5 (m)	M_8-Crs5 ≈ M_9-Crs5 (M) M_{10}-Crs5 M_{11}-Crs5 M_{12}- ≈ M_5- ≈ M_7-Crs5 M_6-Crs5 (m)
Espectre DC			

Taula 2.11.- Resultats de la caracterització dels complexos Cu-Crs5 obtinguts mitjançant l'expressió recombinant del gen *CRS5* en cultius a petita escala en medis rics en Cu.

* Les espècies estan ordenades d'acord amb la seva abundància en solució. (M) representa l'espècie majoritària i (m) la minoritària.

Aquests experiments s'han completat amb proves de quantificació de metall total (Cu i Zn) en la cèl·lula en medis aeròbics i anaeròbics, de manera que s'ha pogut observar que la quantitat de Zn(II) en la cèl·lula és independent del grau d'oxigenació mentre que la del Cu total disminueix significativament quan s'ha oxigenat el medi. Així doncs, i d'acord amb les dades de la bibliografia, una possible explicació als fets observats podria ser que Crs5 es sintetitzés com una Zn-Crs5 i que posteriorment intercanviés els ions Zn(II) per ions Cu(I). Donat que una major oxigenació del medi (cultius a gran escala) implica una menor quantitat de Cu en la cèl·lula, és més probable l'obtenció d'espècies heteronuclears Zn,Cu-Crs5. En canvi, si no es força l'oxigenació del medi (cultius a petita escala), hi ha més Cu a la cèl·lula i més efectivament pot ser substituït el Zn inicialment coordinat, donant lloc a espècies homonuclears de Cu.

La comprovació del fet que les espècies heterometàl·liques Zn,Cu-Crs5 obtingudes en medis força oxigenats podien donar lloc a les homometàl·liques Cu-Crs5 es va aconseguir *in vitro* tot addicionant Cu(I) a les primeres, per tal de generar les segones. En aquest experiment es va poder veure clarament que el Cu(I) afegit a una de les Zn,Cu-Crs5 bioproduïdes a gran escala s'enllaçava lentament a la

proteïna, ja que va ser necessari addicionar 1 eq de Cu(I) cada 24 h per tal de poder enregistrar espectres que no fluctuessin amb el temps. Així, els espectres de DC (Figura 9.A i 9.B, article 5) mostren que cada addició provoca una lleugera variació dels espectres, fins que per al 6è equivalent ja s'observa l'empremta característica de les espècies homonuclears Cu-Crs5 (Figura 9.C, article 5).

També s'ha valorat amb Cu(I) la Zn-Crs5 bioproduïda per tal de comparar les espècies formades *in vitro* per desplaçament del Zn inicialment coordinat amb les sintetitzades *in vivo* en medis enriquits en Cu. Així, s'ha pogut determinar que, en els primers estadis de la valoració, el Zn(II) és fàcilment substituït pel Cu(I) (Figura S2, article 5) per tal de donar lloc, per a 7 eq de Cu(I) afegits, a una mescla d'espècies de característiques espectropolarimètriques molt properes a les de les espècies heterometàl·liques Zn,Cu-Crs5 obtingudes *in vivo* en les produccions a gran escala (fermentador). Un detall interessant és que abans d'arribar a aquest estadi de la valoració, per a 6 eq de Cu(I) afegits, quan Crs5 encara té molt Zn(II) i poc Cu(I) enllaçats, l'espectre de DC de la mescla és molt semblant al de la producció feta a petita escala en la que s'ha mantingut una oxigenació important durant tota la producció (Figura 8, article 5). De 7 a 11 eq de Cu(I) els espectres de DC pràcticament no canvien, però és en aquest rang d'equivalents de Cu(I) afegits quan es reprodueixen els espectres de DC d'aquelles mostres Zn,Cu-Crs5 biosintetitzades amb una oxigenació parcial. A partir d'11 eq de Cu(I) es comencen a obtenir espectres de DC semblants als de les espècies homonuclears Cu-Crs5 obtingudes *in vivo* si bé no és fins a 13 eq de Cu(I) afegits que es reprodueixen del tot aquests espectres.

Els resultats presentats aquí suggereixen que Crs5 podria comportar-se bé com una Zn-tioneïna bé com una Cu-tioneïna, tot depenent de les concentracions intracel·lulars de Cu que a la vegada estan relacionades amb l'estat d'oxigenació cel·lular. Així, en presència d'elevades concentracions de Cu podria col·laborar amb Cup1 en l'homeòstasi del Cu, mentre que per a concentracions de Cu convencionals seria Cup1 la que desenvoluparia aquesta funció i Crs5 es comportaria com una Zn-tioneïna, realitzant hipotèticament altres funcions. Aquests resultats concorden amb els obtinguts *in silico* (Figura 1, article 5), on Crs5 presenta una situació intermèdia entre aquelles MTs considerades típicament Cu-tioneïnes i les considerades Zn-tioneïnes, si bé amb una proximitat lleugerament superior a les tioneïnes de Zn que a les de Cu.

3. Conclusions

3. CONCLUSIONS

El treball realitzat en el marc d'aquesta tesi doctoral ha permès arribar a un conjunt de conclusions que s'exposen a continuació agrupades d'acord amb els diferents objectius proposats.

3.1 Comportament coordinant d'una nova isoforma de MT de mamífer, MT4

- MT4 és la primera Cu-tioneïna descrita en organismes superiors (MT1 havia estat prèviament classificada com una Zn-tioneïna). Aquest fet, i donada la conservació dels residus de cisteïna d'ambdues proteïnes, demostra la influència dels residus no cisteínics en la preferència metàl·lica.
- Les diferències entre MT1 i MT4 en la coordinació a Cd(II) han d'atribuir-se als respectius fragments β (βMT1 i βMT4), mentre que les seves diferències a l'enllaçar Cu(I) es deuen als seus fragments α (αMT1 i αMT4)
- MT4 és capaç de formar agregats homometàl·lics de Cu(I) estables en medis fisiològics en els quals la proteïna proporciona un entorn de coordinació "particular" per al Cu(I). Cap d'aquestes dues característiques es troba en la isoforma MT1.
- Les característiques de MT4 suggereixen una possible funció biològica per aquesta MT diferent a la/les de MT1.

3.2 Estudi de la participació de lligands no proteics en els complexos M-MT

- Els ions clorur tenen una petita participació en l'estabilització de l'estructura dels complexos Cd-MT1 però no en la dels complexos Cd-MT4.
- Totes les espècies recombinants Zn- i Cd-MT estudiades, pertanyents a una àmplia varietat d'organismes, contenen lligands sulfur (S^{2-}). Això obre noves perspectives, tant estructurals com funcionals, en el camp de les MTs.

3.3 Capacitat coordinant de la MT de pollastre, ckMT1

- CkMT1 es classifica com una Zn-tioneïna, si bé sembla que pot haver-hi una gradació entre el caràcter de Zn- o Cu-tioneïna de les MTs.
- CkMT1 presenta una capacitat coordinant envers Zn(II), Cd(II) i Cu(I) intermèdia entre les descrites per a MT1 i MT4, amb un comportament envers metalls divalents més proper al de MT1, però més similar al de MT4 quan enllaça Cu(I).

- La presència d'una His en l'extrem C-terminal del fragment αckMT1 confereix a la proteïna certes capacitats coordinants especials enfront de Cd(II) que la diferencien de MT1 i MT4. Aquesta His no només coordina Cd(II) sinó que és la responsable de la formació de dímers mitjançant un procés, fins ara no descrit, de dimerització de MTs.

3.4 Capacitat coordinant d'una MT de llevat, Crs5

- En la síntesi recombinant de Crs5 el grau d'oxigenació dels medis de cultiu enriquits en Cu afecta la naturalesa homo- o heteronuclear dels agregats M-Crs5, M = Zn(II) i/o Cu(I), que se'n recuperen, obtenint-se espècies homometàl·liques Cu-Crs5 si no s'oxigena el medi i complexos heterometàl·lics Zn,Cu-Crs5 en presència d'una oxigenació elevada.
- Crs5 presenta un comportament intermedi entre una Zn-tioneïna i una Cu-tioneïna, de manera que podria comportar-se com una Zn-tioneïna en situacions de baixa concentració de Cu intracel·lular, mentre que actuaria com una Cu-tioneïna en presència de concentracions de Cu significatives.

4. Bibliografia

4. BIBLIOGRAFIA

1.- M. Margoshes, B. Vallee, *J. Am. Chem. Soc.* (1957) **79**, 4813
2.- P. Gonzàlez-Duarte, “Metallothioneins”. Dins: J.A. McCleverty and T.J. Meyer, (eds.). *Comprehensive Coordination Chemistry II*. Oxford: Elsevier (2003) Secció 8.9, pag. 213
3.- M.J. Stillman, *Coordination Chemistry Reviews* (1995) **144**, 461
4.- J.F. Riordan, B.L. Vallee, eds. *Methods Enzymol.*, **205**, Academic Press, San Diego, (1991)
5.- F.J. Kull, M.F. Reed, T.E. Elgren, T.L. Ciardelli, D.E. Wilcox, *J. Am. Chem. Soc.* (1990) **112**, 2291
6.- A. Muñoz, D.H. Petering, C.F. Shaw III, *Inorg. Chem.* (2000) **39**, 6114
7.- Y. Nishiyama, S. Nakayama, Y. Okada, K.S. Min, S. Onosaka, K. Tanaka. *Chem. Pharm. Bull.* (1990) **38**, 2112
8.- a) Y. Okada, N. Ohta, S. Iguchi, Y. Tsuda, H. Sasaki, T. Kitagawa, M. Yagyu, K.S. Min, S. Onosaka, K. Tanaka, *Chem. Pharm. Bull.* (1986) **34**, 986. b) H.J. Hartmann, Y.J. Li, U. Weser, *Biometals* (1992) **5**, 187. c) Y.J. Li, U. Weser, *Inorg. Chem.* (1992) **31**, 5526. d) A.K. Sewell, L.T. Jensen, J.C. Erikson, R.D. Palmiter, D.R. Winge, *Biochemistry* (1995) **34**, 4740
9.- M. Capdevila, N. Cols, N. Romero-Isart, R. González-Duarte, S. Atrian, P. Gonzáles-Duarte, *Cell. Mol. Life Sci.* (1997) **53**, 681
10.- M. Valls, R. Bofill, R. González-Duarte, P. González-Duarte, M. Capdevila, S. Atrian, *J. Biol. Chem.*(2001) **276**, 32835
11.- P.A. Cobine, R.T. McKay, K. Zangger, C.T. Dameron, I.M. Armitage, *Eur. J. Biochem.* (2004) **271**, 4213
12.- N. Romero-Isart, M. Vašák, *J. Inorg. Biochem.* (2002) **88**, 388
13.- P. Schultze, E. Worgotter, W. Braun, G. Wagner, M. Vašák, J.H.R. Kägi, K. Wüthrich, *J. Mol. Biol.* (1988) **203**, 251
14.- A. Aseniev, P. Schultze, E. Wörgötter, W. Braun, G. Wagner, M. Vašák, J.H.R. Kägi, K. Wüthrich, *J. Mol. Biol.* (1988) **201**, 637
15.- B.A. Messerle, A. Schäffer, M. Vašák, J.H.R. Kägi, K. Wüthrich, *J. Mol. Biol.* (1990) **214**, 765
16.- K. Zangger, G. Öz, J.D. Otvos, I.M. Armitage, *Protein Sci.* (1999) 8, 2630
17.- G. Öz, K. Zangger, I.M. Armitage, *Biochemistry* (2001) **40**, 11433
18.- C. Capasso, V. Carginale, O. Crescenzi, D. Di Maro, E. Parisi, R. Spadaccini, P.A. Temussi, *Structure* (2003) **11**, 435
19.- S.S. Narula, M. Brouwer, Y. Hua, I.M. Armitage, *Biochemistry* (1995) **34**, 620
20.- A. Muñoz, F.H. Försterling, C.F. Shaw III, D.H. Petering, *J. Biol. Inorg. Chem.* (2002) **7**, 713
21.- R. Riek, B. Prêcheur, Y. Wang, E.A. Mackay, G. Wider, P. Güntert, A. Liu, J.H.R. Kägi, K. Wüthrich, *J. Mol. Biol.* (1999) **291**, 417
22.- C.A. Blindauer, M.D. Harrison, J.A. Parkinson, A.K. Robinson, J.S. Cavet, N.J. Robinson, P.J. Sadler, *Proc. Natl. Acad. Sci. USA* (2001) **98**, 9593
23.- Y.L. Li, U. Weser, *Inorg. Chem.* (1992) **31**, 5526
24.- I. Bertini, H. -J. Hartmann, T. Klein, G. Liu, C. Luchinat, U. Weser, *Eur. J. Biochem.* (2000) **267**, 1008
25.- V. Calderone, B. Dolderer, H.J. Hartmann, H. Echner, C. Luchinat, C. Del Bianco, S. Mangani, U. Weser, *Proc. Natl. Acad. Sci. USA* (2005) **102**, 51
26.- T.A. Smith, K. Lerch, K.O. Hodgson, *Inorg. Chem.* (1986) **25**, 4677
27.- B.A. Fowler, C.E. Hildebrand, Y. Kojima, M. Webb, Nomenclature of Metallothionein. A: *Metallothionein II*. J.H.R. Kägi, Y. Kojima, Eds., Birkhäuser Verlag, Basel (1987) **52**, 19
28.- P.A. Binz, J.H.R. Kägi, In: *Metallothionein IV*, Birkhäuser Verlag, Basel (1999) **7**
29.- http://www.unizh.ch/~mtpage/classif.html
30.- R. Bofill, M. Capdevila, N. Cols, S. Atrian, P. González-Duarte, *J. Biol. Inorg. Chem.* (2001) **6**, 408
31.- M. Valls, R. Bofill, N. Romero-Isart, R. González-Duarte, J. Abián, M. Carrascal, P. González-Duarte, M. Capdevila, S. Atrian, *FEBS Lett.* (2000) **467**, 189
32.- J. Domenech, O. Palacios, L. Villarreal, P. González-Duarte, M. Capdevila, S. Atrian, *FEBS Lett.* (2003) **533**, 72
33.- D. Egli, J. Domenech, K. Balamurugan, H. Hua, A. Selvaraj, H. Yepiskoposyan, A. Vardanyan, M. Capdevila, S. Atrian, O. Georgiev, W. Schaffner, *J. Biol. Chem.* (2005), 000
34.- http://www.expasy.org/cgi-bin/lists?/metallo.txt
35.- C.J. Quaife, S.D. Findley, J.C. Erikson, G.J. Froelick, E.J. Kelly, B.P. Zambrowicz, R.D. Palmiter, *Biochemistry* (1994) **33**, 7250

36.- L. Liang, K. Fu, D.K. Lee, R.J. Sobieski, T. Dalton, G.K. Andrews, *Molecular Reproduction and Development* (1996) **43**, 25
37.- M. Vašák, D.W. Hasler, *Curr. Opin. Chem. Biol.* (2000) ***4***, 177
38.- B. Roschitzki, M. Vašák, *J. Biol. Inorg. Chem.* (2002) ***7***, 611
39.- J. Hidalgo, M. Aschner, P. Zatta, M. Vašák, *Brain Res. Bull.* (2001) **55**, 133
40.- N. Cols, N. Romero-Isart, R. Bofill, M. Capdevila, P. González-Duarte, R. González-Duarte, S. Atrian, *Protein Eng.* (1999) **12**, 265
41.- N. Cols, N. Romero-Isart, M. Capdevila, B. Oliva, P. Gonzàlez-Duarte, R. Gonzàlez-Duarte, S. Atrian, *J. Inorg. Biochem.* (1997) **68**, 157
42.- International Chicken Genome Sequencing Consortion, *Nature* (2004) **432**, 695
43.- http://www.biochem.unizh.ch/mtpage/poster/posterevol.html
44.- C.C. McCormick, C.S. Fullmer, J.S. Garvey, *Proc. Natl. Acad. Sci.* USA (1988) **85**, 309
45.- D. Wei, G.K. Andrews, Med. *Cent., Univ. Kansas City, KS, USA, Nuc. Acids Res.* (1988) **16**, 537
46.- M.J. Daniels, J.S. Turner-Cavet, R. Selkirk, H. Sun, J.A. Parkinson, P.J. Sadler, N.J. Robinson, *J. Biol. Chem.* (1998) **273**, 22957
47.- N. Romero-Isart, N. Cols, M.K. Termansen, J.L. Gelpí, R. González-Duarte, S. Atrian, M. Capdevila, P. González-Duarte, *Eur. J. Biochem.* (1999) **259**, 519
48.- D. Wei, G.K. Andrews, *Nuc. Acids Res.* (1988) **16**, 537
49.- U. Weser, F. Donay, H. Rupp, *FEBS Lett.* (1973) **32**, 171
50.- H. Rupp, W. Voelter, U. Weser, *Hoppe-Seyler's Z. Physiol. Chem.* (1975) **356**, 755
51.- R.K. Mehra, J.R. Garey, T.R. Butt, W.R. Gray, D.R. Winge, *J. Biol. Chem.* (1989) **264**, 19747
52.- J.L. Thorvaldsen, R.K. Mehra, W. Yu, A.K. Sewell, D. R. Winge, *Yeast* (1995) **11**, 1501
53.- R.K. Mehra, E.B. Tarbet, W.R. Gray, D.R. Winge, *Proc. Natl. Acad. Sci. USA* (1988) **85**, 8815
54.- G.P.M. Borrelly, M.D. Harrison, A.K. Robinson, S.G. Cox, N.J. Robinson, S.K. Whitehall, *J. Biol. Chem.* (2002) **277**, 30394
55.- R. Prinz and U. Weser, *Hoppe-Seyler's Z. Physiol. Chem.* (1975) **356**, 767
56.- C. Luchinat, B. Dolderer, C. Del Bianco, H. Echner, H.J. Hartmann, W. Voelter, U. Weser, *J. Biol. Inorg. Chem.* (2003) **8**, 353
57.- U. Weser, H.J. Hartmann, *Biochim. Biophys. Acta* (1988) **953**, 1
58.- D.R. Winge, K.B. Nielson, W.R. Gray, D.H. Hamer, *J. Biol. Chem.* (1985) **260**, 14464
59.- V.C. Culotta, W.R. Howard, X.F. Liu, *J. Biol. Chem.* (1994) **269**, 25295
60.- L.T. Jensen, W.R. Howards, J.J. Strain, D.R. Winge, V.C. Culotta, *J. Biol. Chem.* (1996) **271**, 18514
61.- J. Strain, V.C. Culotta, *Mol. Gen. Genet.* (1996) **251**, 139
62.- R.N. Reese, D.R. Winge, *J. Biol. Chem.* (1988) **263**, 12832
63.- D.N. Weber, F. Shaw III, D.H. Petering, *J. Biol. Chem.* (1987) **262**, 6962
64.- R.N. Reese, R.M Mehra, E.B. Tarbet, D.R. Winge, *J. Biol. Chem.* (1988) **263**, 4186
65.- D. Winge, C.T. Dameron, R.K. Mehra in *Metallothioneins* (Eds. M.J. Stillman, F.C. Shaw III, K.T. Suzuki), VCH Publishers Inc., New York (1992) **ch 11**, 257
66.- C.T. Dameron, D.R. Winge, *Inorg. Chem.* (1990) 29, 1343
67.- W. Maret, G. Heffron, H.A. Hill, D. Djuricic, L.J. Jiang, B.L. Vallee, *Biochemistry* (2002) **41**, 1689
68.- D. H. Hamer, *Ann. Rev. Biochem.* (1986) **55**, 913
69.- K. Polec, O. Palacios, M. Capdevila, P. González-Duarte, R. Lobinski, *Talanta* (2002) **57(5)**, 1011
70.- R. Bofill, O. Palacios, M. Capdevila, N. Cols, R. González-Duarte, S. Atrian, P. González-Duarte, *J. Inorg. Biochem.* (1999) **73**, 57
71.- K. Polec, J. Szpunar, O. Palacios, P. González-Duarte, S. Atrian, R. Lobinski, *J. Anal. At. Spectrom.* (2001) **16**, 567
72.- W. Birchmeier, P. Christen, *FEBS Lett.* (1971) **18**, 209
73.- J. Bongers, C.D. Walton, D.E. Richardson, J.U. Bell, *Anal. Chem.* (1988) **60**, 2683
74.- In *Standard Methods for the Examination of Water and Wastewater* (Eds. L.S. Clesceri, A.E. Greenberg, A.D. Eaton), American Public Health Association, Washington D.C., (1998)
75.- T.E. King, R.O. Morris, *Methods Enzymol.* (1967) **10**, 634
76.- A. Marcó, R. Compañó, R. Rubio, I. Casals, L. Krotz, L. Ragaglia, G. Giazzi, *Analyst* (2001) **126**, 1820

77.- H. Rupp, U. Weser, *Biochim. Biophys Acta* (1978) **533**, 209
78.- P. Palumaa, E.A. Mackay, M. Vasák, *Biochemistry* (1992) **31**, 2181
79.- Y. Hathout, K.J. Reynolds, Z. Szilagyi, C. Fenselau, *J. Inorg. Biochem.* (2002) **88**, 119
80.- K. Zangger, I.M Armitage, *J. Inorg. Biochem.* (2002) **88**, 135
81.- O. Palacios, K. Polec-Pawlak, R. Lobinski, M. Capdevila, P. Gonzàlez-Duarte, *J. Biol. Inorg. Chem.* (2003) **8**, 831

5. Articles publicats

Acceptats per la Comissió de Doctorat a 15 de Juny del 2005

Article 1

Functional Differentiation in the Mammalian Metallothionein Gene Family
Metal binding features of mouse MT4 and comparison with its paralog MT1

Journal of Biological Chemistry, 2004, **279**, 24403-24413

THE JOURNAL OF BIOLOGICAL CHEMISTRY
Vol. 279, No. 23, Issue of June 4, pp. 24403–24413, 2004
Printed in U.S.A.
© 2004 by The American Society for Biochemistry and Molecular Biology, Inc.

Functional Differentiation in the Mammalian Metallothionein Gene Family

METAL BINDING FEATURES OF MOUSE MT4 AND COMPARISON WITH ITS PARALOG MT1* [S]

Received for publication, February 6, 2004, and in revised form, March 17, 2004
Published, JBC Papers in Press, March 19, 2004, DOI 10.1074/jbc.M401346200

Laura Tío‡§¶, Laura Villarreal¶‖, Sílvia Atrian‡ ‡‡, and Mercè Capdevila‖**

From the ‡Departament de Genètica, Facultat de Biologia, Universitat de Barcelona, Avd. Diagonal 645, 08028 Barcelona, Spain and ‖Departament de Química, Facultat de Ciències, Universitat Autònoma de Barcelona, 08193 Bellaterra, Barcelona, Spain

This paper reports on the characterization of the metal binding abilities of mammalian MT4 and their comparison with those of the well known MT1. Heterologous *Escherichia coli* expression in cultures supplemented with zinc, cadmium, or copper was achieved for MT4 and for its separate αMT4 and βMT4 domains as well as for MT1 and its αMT1 domain in cadmium-enriched medium. The *in vivo* conformed metal complexes and the *in vitro* substituted zinc/cadmium and zinc/copper MT4 aggregates were characterized. Biosynthesis of MT4 and βMT4 in Cd(II)-supplemented medium revealed that these peptides failed to form the same homometallic species as MT1, thus appearing less effective for cadmium coordination. Conversely, the entire MT4 and both of its domains showed better Cu(I) binding properties than MT1, affording Cu_{10}-MT4, Cu_5-αMT4 and Cu_7-βMT4, stoichiometries that make the domain dependence toward Cu(I) clear. Overall results allow consideration of MT4 as a novel copper-thionein, made up of two copper-thionein domains, the first of this class reported in mammals, and by extension in vertebrates. Furthermore, the *in silico* protein sequence analyses corroborated the copper-thionein nature of the MT4 peptides. As a consequence, there is the suggestion of a possible physiological role played by MT4 related with copper requirements in epithelial differentiating tissues, where *MT4* is expressed.

Postgenomic molecular biology is facing up to the quest for function as its major challenge and possibly the most important bottleneck for its current progression. For some decades, data on new genes/proteins have slowly been accumulated, as a product of classical molecular genetics approaches. Nowadays, the massive outburst of genome projects is dramatically providing long registers of putative gene products without a concomitant development of biochemical and/or physiological role assignment. In particular, function differentiation within gene families deserves special attention 1) because gene duplication plus function differentiation is commonly accepted as the source/driving force of molecular evolution, from the unicellular eukaryota and first metazoa (1, 2) to the chordate/vertebrate (3) world, and 2) because in this case the widely applied homology-based function prediction is worthless unless paralogous members have achieved large differentiation. Wet *in vivo* and *in vitro* approaches thus remain the only alternative, not only in ascertaining the function profile for each protein but also in tracing the evolutionary pattern of function acquisition associated with gene duplication.

Mammalian metallothioneins (MTs)[1] clearly illustrate the state of the art in incomplete knowledge of functional differentiation within gene families, even nearly 50 years after the isolation of the first member, MT1, as the kidney response to Cd intoxication in horses (4). MT are metal-chelating peptides reported in all animals, most plants, and some prokaryotes but only related among different taxonomical groups through their high cysteine content and low molecular weight (classifications available on the World Wide Web at http://www.unizh.ch/~mtpage/classif.html). In vertebrates, MT constitute a family of homology, with gene multiplicity present in birds and mammals. In the latter, tandem duplications originated four MT isoforms, *MT1–MT4* (Fig. 1), and in humans MT1 was further amplified up to 13-fold, a situation not described in rodents or sheep.

Mammalian MT1 and MT2 ability to form stable aggregates either with physiological or xenobiotic metals, as well as the ubiquitous, metal-induced expression of their genes, led to the proposal of homeostasis, transport, and detoxification of metals as main biological roles, although this is still a matter of intense debate and may have a nonunique answer (6, 7). Isolation of the third family member, MT3, and its identification as a neuronal growth-inhibitory factor (8), synthesized in neural tissues and down-regulated in patients of Alzheimer's disease (9), immediately brought about a high commitment to biomedical research. MT3 exclusive function was attributed to its most dissimilar amino acid sequence (70% identity *versus* MT1/MT2) (Fig. 1). Unexpectedly, in 1994, MT4 was identified in human and mouse DNA (10) as a fourth, transcriptionally active, family member. Although MT4 is more similar to MT1/MT2 than MT3, hints of a differential biological function were readily contributed by its unique tissular and developmental specific expression pattern (10). Mouse *MT4* transcription seemed re-

* This work was supported by Spanish Ministerio de Ciencia y Tecnología Projects BIO2000-0910, BIO2003-03892, and BQU2001-1976. The costs of publication of this article were defrayed in part by the payment of page charges. This article must therefore be hereby marked "*advertisement*" in accordance with 18 U.S.C. Section 1734 solely to indicate this fact.

[S] The on-line version of this article (available at http://www.jbc.org) contains 10 additional figures and a table.

§ Supported by a predoctoral scholarship from the Spanish Ministerio de Ciencia y Tecnología.

¶ These two authors contributed equally to this work.

** Supported by a predoctoral scholarship from the Departament de Química of the Universitat Autònoma de Barcelona.

‡‡ To whom correspondence should be addressed. Tel.: 34-934-02-1501; Fax: 34-934-11-0969; E-mail: satrian@ub.edu.

[1] The abbreviations used are: MT, metallothionein(s); ESI-MS, electrospray ionization mass spectrometry; ICP-AES, inductively coupled plasma-atomic emission spectroscopy.

```
MT 4  MDPGECTCMSGGICICGDNCKCTTCSCKTCRKSCCPCCPPGCAKCARGCICK       GGSDKCSCCP
MT 1  MDP NCSCSTGGSCTCTSSCACKNCKCTSCKKSCCSCCPVGCSKCAQGCVCK       GAADKCTCCA
MT 2  MDP NCSCASDGSCSCAGACKCKQCKCTSCKKSCCSCCPVGCAKCSQGCICK       EASDKCSCCA
MT 3  MDPETCPCPTGGSCTCSDKCKCKGCKCTNCKKSCCSCCPAGCEKCAKDCVCKGEEGAKAEAEKCSCCQ
      <------------ ß domain ------------><-------------- α domain -------------->
```

FIG. 1. **Amino acid sequences of the four mouse MT isoforms, shown according to their ClustalW alignment and with the conserved Cys residues highlighted.** Limits of the β and α domains, as reported for MT1, are indicated.

stricted to the stratified squamous epithelia of the upper digestive tract, tail, footpads, and vagina, all in cornified layers acting as protective surfaces, plus the maternal deciduum and neonatal skin (10, 11). Furthermore, classic MT1 inducers such as divalent metal ions or bacterial endotoxins (lipopolysaccharide) had a reduced effect on *MT4* (11). Evolutionary studies locate MT4 as the most ancient mammalian form in the maximum parsimony tree calculated with the 55 available vertebrate MT cDNA sequences (available on the World Wide Web at http://www.unizh.ch/~mtpage/trees.html), whereas *MT1* would have emerged late in evolution. Paradoxically, although older, MT4 peptides are most similar among themselves (93.4% identity for mouse MT4 *versus* human MT4) rather than in comparison with the different isoforms within the same organism (55.7% identity for mouse MT4 *versus* mouse MT1), indicating a stronger functional constraint for MT4 than for MT1. Unfortunately, at this point, the lack of isolation and functional characterization of any MT4 protein precluded any further understanding of mammalian MT differentiation and evolution. When considering the huge amount of molecular, structural, and functional information accumulated for MT1/MT2 and MT3, and the large number of cellular and physiological events (normal and/or pathological) to which they have been related, there is a dire lack of information available for MT4.

Since first described (4), MT1 has been the paradigm for MT. Studies with either synthetic peptides or *in vitro* reconstituted native metal aggregates provided insights into the structure/function relationship in MT1, which culminated with the report of the three-dimensional structure of Zn_2Cd_5-MT1 (13, 14). Overall data revealed that this 61-residue peptide, which includes 20 cysteines, folds into two domains when coordinating divalent metal ions, the N-terminal segment (β domain) giving rise to an $M^{II}_3(S\text{-}Cys)_9$ complex and the C-terminal segment (α domain) giving rise to an $M^{II}_4(S\text{-}Cys)_{11}$ aggregate. Subsequent analyses of the *in vitro* affinity of the MT1 fragments to physiological ions (zinc and copper) showed that monovalent metal ions preferentially bind to the βMT1 domain, whereas divalent ions prefer to occupy the αMT1 counterpart (15–19). Further characterization of the metal aggregates obtained by recombinant synthesis of several MTs provided knowledge on their *in vivo* metal binding preferences, which allowed us to set up a new comprehensive frame for MT classification and evolution (20). Thus, on the basis of structure/function relationships, we identified MT1 and αMT1 as Zn-thioneins (21–23) and the independent βMT1 as a Cu-thionein (24, 25). Currently known Cu-thioneins belong to arthropoda (*Drosophila* (26, 27) and crustacea (28)) and unicellular eukaryota (yeasts (29) and ciliate protozoa (30)).

This work aims at evaluating the character of Zn- or Cu-thionein of MT4 through the spectroscopic and spectrometric characterization of the zinc, cadmium, and copper aggregates rendered by full-length recombinant mouse MT4 and its separate β and α domains as well as of the metal species obtained by Zn/Cd or Zn/Cu *in vitro* replacement. Comparison of these data with those of the paralogous metal-MT1 clusters (this work) (21–25) will shed light on the functional differentiation of MT4 *versus* MT1 and on the possible MT4 biological roles. Both insights will significantly contribute to the understanding of the duplication and differentiation evolutionary pattern of metallothioneins.

EXPERIMENTAL PROCEDURES

Cloning of the Mouse MT4 Coding Region and Its Independent α and β Domains in an E. coli Expression System—The murine MT4 coding sequence was amplified by PCR, using as a template the MT4 cDNA inserted in a pSP64 plasmid, kindly provided by Dr. Palmiter of the University of Washington. The following oligonucleotides were used as PCR primers: MT4-BamHI (5′-GCCGGATCCATGGACCCTGGGGA-3′, upstream) and MT4-SalI (5′-GCGCGCGTCGACTCAGGGACAGCA-3′, downstream). Through this reaction, a BamHI restriction site was introduced before the ATG initiation codon and a SalI site immediately after the stop codon. A 35-cycle PCR amplification (30 s at 94 °C (denaturing), 30 s at 55 °C (annealing), and 30 s at 72 °C (extension)) was carried out in a total reaction volume of 100 µl, comprising 2 µl of 25 mM dNTP mixture, 2 µl of 20 µM primer solution, 1 unit of DeepVent (New England Biolabs) thermoresistent DNA polymerase, and 100 ng of the template DNA. The DNA fragments encoding the independent MT4 domains were obtained by mutagenic PCR on the pSP64 template. To amplify the αMT4 fragment, which extends from the 32nd MT4 residue (Lys) to the C terminus (Fig. 1), a PCR was performed with the αMT4-BamHI primer (5′-CCCGGATCCATGAAAAGCTGCTGTCC-3′, upstream) and the MT4-SalI primer (downstream). The βMT4 fragment extends from the ATG initiation codon to the 31st residue (Arg) (Fig. 1). The primers used for its PCR synthesis were MT4-BamHI (upstream) and βMT4-SalI (5′-CCGCGCGTCGACCTAACGACAGGTTTTACACG-3′, downstream). The conditions for both PCRs were the same as for the entire MT4 cDNA. The construction of MT1 expression vectors has previously been described (21, 22).

In all cases, the PCR products were isolated from 2% agarose gels, digested with BamHI-SalI and subsequently cloned into the corresponding sites of the pGEX-4T-1 expression vector (Amersham Biosciences). Previous to protein synthesis assays, all of the DNA constructs were confirmed by automatic DNA sequencing (ABI 370; PerkinElmer Life Sciences), using the Amersham Dye Terminator Cycle Kit. JM105 was the *E. coli* recipient strain for cloning and sequencing purposes, and thereafter, the expression plasmids were transformed into the *E. coli* protease-deficient strain BL21 for recombinant overexpression.

Recombinant Synthesis and Purification of the Zn-MT4, Cd-MT4, and Cu-MT4 Aggregates—For the characterization of M(II)-MT4 aggregates, recombinant bacteria were grown according to two kinds of conditions. Small scale cultures (1.5 liters, performed in Erlenmeyer flasks) were used for analytical purposes, whereas large scale volumes (at least 10 liters, grown in a Microferm fermentor (New Brunswich), coupled to a Westfalia CSA-1-06-475 centrifuge and controlled by a TVE-OP 76/0 programmer (Braun Biotech)) were used for preparative purposes. In both cases, the transformed *E. coli* cells were grown as described in Ref. 20, supplementing the medium either with $ZnCl_2$ or $CdCl_2$ to a final concentration of 300 µM. In order to characterize the MT4 copper coordination behavior, and due to the special significance of these data, synthesis of MT4 and its independent domains in copper-supplemented medium were assayed in different culture conditions. In short, induction times assayed were 3 h for αMT4 and βMT4 and 2 and 3 h for the entire MT4; isopropyl-1-thio-β-D-galactopyranoside final concentration assayed was 100 mM for βMT4 and 100 and 200 mM for αMT4 and the entire MT4; culture volumes were 1.5 and 5 liters for αMT4 and βMT4 and 1, 1.5, and 5 liters for the entire MT4. Only the 5-liter assays were performed in the fermentor, the smaller volumes corresponding to Erlenmeyer flask cultures. Purification of all of the recovered metal-MT complexes was performed as described for MT1 (21, 25). Aliquots of the MT-containing fast performance liquid chromatography fractions in 50 mM Tris-HCl buffer, pH 7.0, were analyzed in 15% SDS-PAGE Coomassie Blue-stained gels. Samples were pooled, aliquoted, and kept at −80 °C under argon atmosphere until further analysis.

TABLE I
Molecular masses and zinc- or cadmium-to-protein ratios found for the in vivo synthesized MT4, MT1, αMT4, βMT4, and αMT1 metal aggregates

MT isoform (metal supplemented in culture media)	Protein	M_{exp}[a]	M_{calc}[b]	M/MT[c]	M/MT[d]	Oxidation degree[e]
		Da	*Da*			
MT4 (M = Zn)	MT4	6864.2 ± 0.9	6864.29	Zn_7-MT	6.7 Zn	5
	αMT4	3598.6 ± 1.3	3598.56	Zn_4-αMT	3.6 Zn	11
	βMT4	3558.6 ± 0.5	3559.03	Zn_3-βMT	2.5 Zn	15
MT4 (M = Cd)	MT4	7004.2 ± 1.8	7005.35	Zn_4Cd_3-MT (S)	3.6 Zn, 2 Cd	36
		7052.9 ± 1.3	7052.37	Zn_3Cd_4-MT (e)		
		6958.9 ± 0.5	6958.33	Zn_5Cd_2-MT (e)		
		7099.8 ± 1.3	7099.39	Zn_2Cd_5-MT (ee)		
		6914.9 ± 0.0	6911.31	Zn_6Cd_1-MT (ee)		
		6863.6 ± 1.1	6864.29	Zn_7-MT (s,e)		
		7194.0 ± 0.7	7193.43	Cd_7-MT (s,e)		
	αMT4	3787.0 ± 0.6	3786.64	Cd_4-αMT	0 Zn, 3.5 Cd	13
	βMT4	3700.0 ± 1.5	3700.10	Cd_3-βMT (S)	0 Zn, 2.0 Cd	34
		3654.9 ± 0.4	3653.07	Zn_1Cd_2-βMT		
		3605.5 ± 1.6	3606.05	Zn_2Cd_1-βMT (s)		
MT1 (M = Cd)	MT1	6937.3 ± 1.5	6935.93	Cd_7-MT	0 Zn, 6.2 Cd	
	αMT1	3738.2 ± 1.1	3738.54	Cd_4-αMT	0 Zn, 4.2 Cd	
	βMT1[25]	3489.7 ± 1.1	3789.74	Cd_3-βMT		

[a] Experimental molecular masses for the Zn- and Cd-MT complexes.
[b] Calculated molecular mass for neutral species with loss of two protons/zinc or cadmium bound (34).
[c] Zinc or cadmium per MT molar ratio calculated from the mass difference between holo- and apoprotein. S, major species; s, minor species; e and ee, equimolarity.
[d] Zinc or cadmium per MT molar ratio calculated from the zinc, cadmium, and sulfur content (ICP-AES).
[e] Percentage of thiol groups (Ellman's method) over total sulfur (ICP-AES).

Inductively coupled plasma-atomic emission spectroscopy (ICP-AES) was used to determine the amount of protein present in the different preparations and the metal/protein ratios, as described in Ref. 31, measuring sulfur at 182.04 nm, zinc at 213.85 nm, cadmium at 228.80 nm, and copper at 324.75 nm. Additionally, Ellman's method (32) facilitated determining the percentage of thiol groups over total sulfur in the samples by reaction with 5,5′-dithiobis(nitrobenzoic acid), except for those aggregates containing copper, since the presence of this metal in MT prevents the applicability of the procedure (33).

Spectroscopic Characterization of the Metalated MT4 and MT1 Species—Spectroscopic (UV-visible electronic absorption) and spectropolarimetric (CD) analysis of the metal-MT4 clusters and of the species formed *in vitro* during the zinc/cadmium and zinc/copper displacement studies at pH 7.0 was carried out and processed as described in Refs. 21, 23, and 24. Electronic absorption measurements were performed on an HP-8453 diode array UV-visible electronic absorption spectrophotometer. A Jasco spectropolarimeter (model J-715) interfaced to a computer (GRAMS 32 Software) was used for CD determinations. All assays were performed under argon atmosphere, and titrations were carried out at least in duplicate to assure reproducibility. The pH for all experiments remained constant throughout, without the addition of buffers, and the temperature was kept at 25 °C by means of a Peltier PTC-351S apparatus.

Spectrometric Characterization of the Metalated MT4 and MT1 Species—The molecular mass of the Zn-, Cd-, and Cu-MT species obtained *in vivo* and *in vitro* was determined by electrospray ionization mass spectrometry (ESI-MS) on a Fisons Platform II instrument, equipped with MassLynx software and calibrated with horse heart myoglobin (0.1 mg/ml). The assay conditions for the zinc- and cadmium-containing species were as follows: 20 μl of protein solution injected at 40 μl/min; the use of a high performance liquid chromatography Uptisphere C_4 33 mm × 2 mm × 5 μm column to separate analytes; capillary counter-electrode voltage, 4.5 kV; lens counterelectrode voltage, 1.0 kV; cone potential, 60 V; source temperature, 120 °C; *m/z* range, 850–1950; scanning rate, 3 s/scan; interscan delay, 0.3 s. The assay conditions for the copper-containing species were as follows: 20 μl of protein solution injected at 30 μl/min; capillary counterelectrode voltage, 3.5 kV; lens counterelectrode voltage, 1.0 kV; cone potential, 35 V; source temperature, 160 °C; *m/z* range, 850–1950; scanning rate, 3 s/scan; interscan delay, 0.3 s. In all cases, the running buffer was an appropriate mixture of acetonitrile and 5 mM ammonium acetate/ammonia, pH 7.5. The molecular mass of the apo-forms was determined as for the copper-containing species, except that the carrier was a 1:1 mixture of acetonitrile and trifluoroacetic acid, pH 1.5. Masses for the holo-species were calculated as described in Ref. 34.

In Silico Analysis of DNA and Protein Sequences—Protein sequences were aligned by ClustalW (version 1.75), using the Blosum62 as a distance matrix, and a gap penalty of 10/100, a gap extension value of 0.05/100, and a 40% delay between divergent sequences (35). The ClustalW alignments were the input for calculating protein distances and constructing the corresponding bootstrap neighbor-joining trees, through the Fitch-Margoliash tree-building algorithm (36). In this case, 1000 unrooted trees were examined for each bootstrap trial with a random generator seed of 111/1000. The protein distance and tree-building applications are included in the *Phylip* software package (37). The protein sequence similarity analyses were performed using the clusters of zinc-thionein and copper-thionein MT sequences previously characterized (20, 27).

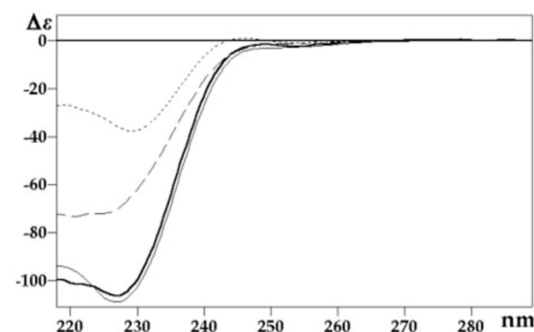

FIG. 2. **Comparison of the circular dichroism spectra of Zn_7-MT4 (*solid gray line*), Zn_4-αMT4 (*dotted line*) and Zn_3-βMT4 (*dashed line*).** The spectra depicted as a *solid black line* represents the sum of the circular dichroism spectra of Zn_4-αMT4 and Zn_3-βMT4.

RESULTS AND DISCUSSION

Cloning and Expression of the MT4-, αMT4-, and βMT4-cDNA Constructs—**DNA sequencing confirmed that the three amplified PCR products corresponded to the entire MT4, αMT4, and βMT4 coding regions, without the introduction of any undesired nucleotide substitution. The SDS-PAGE analysis of the M-MT4, M-αMT4, and M-βMT4 aggregates (where M represents Zn(II), Cd(II), or Cu(I)) synthesized in the corresponding metal supplemented cultures as well as of the Cd-MT1 and Cd-αMT1 species recovered from Cd-supplemented medium revealed homogeneous preparations at a concentration range of 0.5–7.0 × 10^{-4} M. The identity and integrity of all**

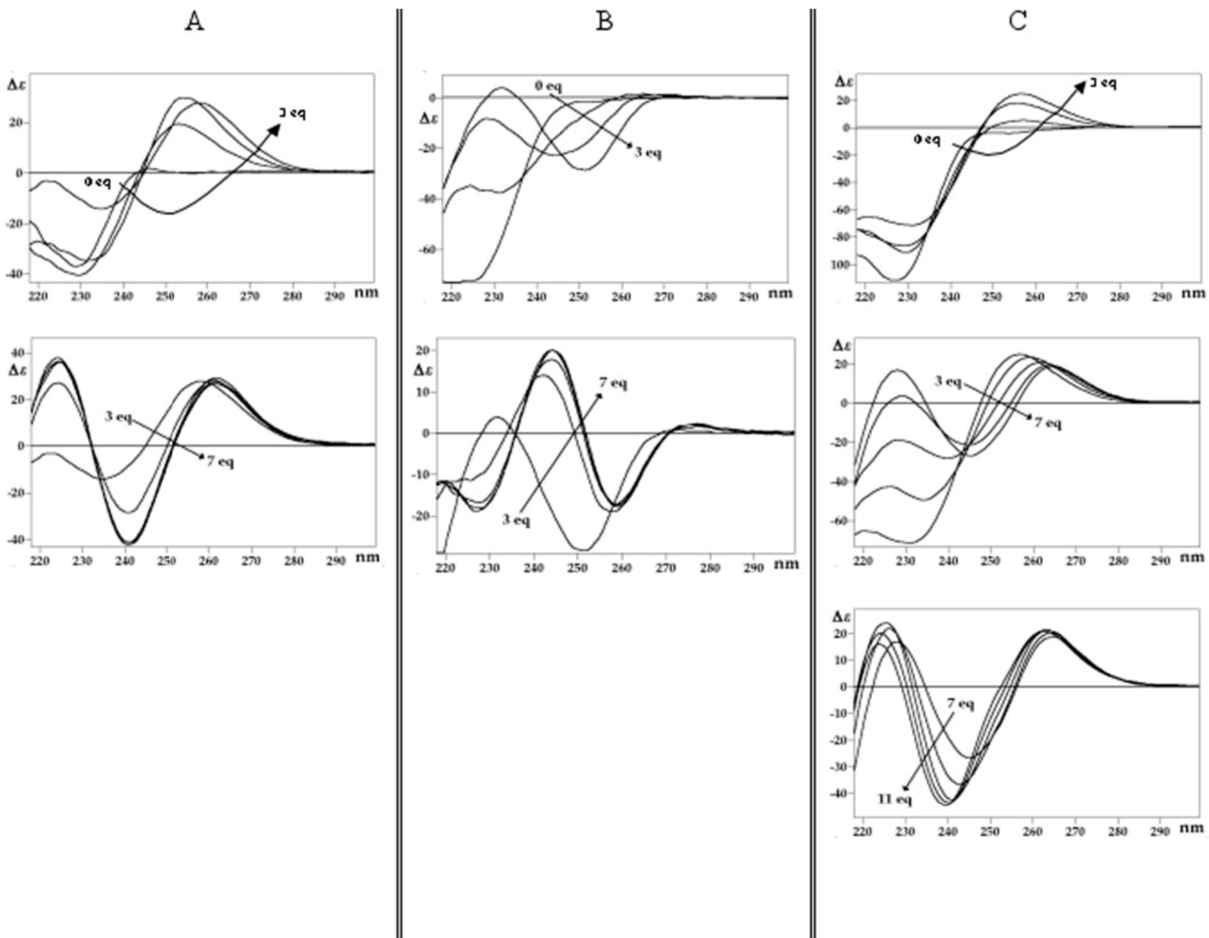

αMT4: Zn_4-αMT ⟶ Zn_3Cd_1-αMT ⟶ Zn_2Cd_2-αMT ⟶ Zn_1Cd_3-αMT ⟶ Cd_4-αMT

βMT4: Zn_3-βMT ⟶ Zn_2Cd_1-βMT ⟶ Zn_1Cd_2-βMT ⟶ Cd_3-βMT

MT4: Zn_7-MT → Zn_6Cd_1-MT → Zn_5Cd_2-MT → Zn_4Cd_3-MT → Zn_3Cd_4-MT → Zn_2Cd_5-MT → Zn_1Cd_6-MT → Cd_7-MT

FIG. 3. **Circular dichroism spectra corresponding to the titrations of Zn_4-αMT4 (*A*), Zn_3-βMT4 (*B*), and Zn_7-MT4 (*C*) with Cd(II) at pH 7.** The *arrows* show the evolution of the spectra when the indicated number of Cd(II) equivalents was added. Corresponding reaction pathways are shown.

recombinant peptides were confirmed by the molecular masses of their apo-forms obtained by acidification (pH 1.5) of the corresponding zinc aggregates. ESI-MS measurements yielded the following values: 6419.66 ± 0.6 Da (calculated molecular mass, 6420.56 Da) for MT4; 3344.52 ± 0.6 Da (calculated molecular mass, 3345.00 Da) for αMT4; and 3369.45 ± 0.8 Da (calculated molecular mass, 3368.89 Da) for βMT4.

Metal Binding Abilities of MT4—Analysis of the monovalent and divalent metal binding capabilities of MT4 was attained through a two-step strategy. First, the *in vivo* synthesized M-MT4, M-αMT4, and M-βMT4 (where M represents zinc, cadmium, and copper) aggregates and the recombinant Cd-MT1 and Cd-αMT1 species, not previously studied, were characterized. Second, the reaction pathways of the *in vitro* zinc/cadmium and zinc/copper replacement processes undergone by the three Zn-MT4 peptides at pH 7 were determined using the rationale previously applied for MT1 (21–24). Detailed analysis of the spectroscopic (CD and UV-visible electronic absorption) sets of data recorded during these titrations provided information on the number of metal-MT species generated, their stoichiometry, and their degree of folding. Additionally, the spectrometric (ESI-MS) measurements revealed the molecular distribution (38, 39) of the various complex species present at each point of the titrations, and the absence of cooperativeness during the zinc/metal replacements in the three MT4 peptides. However, although it was possible to determine the zinc/cadmium/MT ratios in the heterometallic species formed in the zinc/cadmium replacements, the proximity between the atomic weights of zinc and copper, together with the ESI-MS experimental error range, prevented determination of the zinc/copper/MT ratios for the zinc/copper reactions. When the addition of Chelex-100 did not alter the optical spectra of the solutions, the exact stoichiometry of the heterometallic Cu,Zn-MT species was determined through chelation experiments (23). Other-

TABLE II

Distribution of the metal aggregates present in solution, according to ESI-MS data, during the titration of Zn_4-αMT4 (top left), Zn_3-βMT4 (top right), and Zn_7-MT4 (bottom) with $CdCl_2$ at pH 7 as a function of the number of Cd(II) equivalents added

√, the major species; x, species of intermediate abundance; ◆, the minor species present in solution.

	Cd(II) equivalents added				
	1	3	4	5	9
Zn_4-αMT4	✓				
Zn_3Cd_1-αMT4	✓	◆			
Zn_2Cd_2-αMT4	x	x			
Zn_1Cd_3-αMT4	◆	✓	◆		
Cd_4-αMT4		x	✓	✓	✓

	Cd(II) equivalents added					
	1	2	3	4	5	7
Zn_3-βMT4	◆	◆				
Zn_2Cd_1-βMT4	x	x	◆			
Zn_1Cd_2-βMT4	✓	✓	x	◆	◆	◆
Cd_3-βMT4	◆	x	✓	✓	✓	✓

	Cd(II) equivalents added								
	1	3	4	5	6	7	8	11	15
Zn_7-MT4	✓	◆							
Zn_6Cd_1-MT4	x	x							
Zn_5Cd_2-MT4	x	x	◆						
Zn_4Cd_3-MT4	x	✓	x	◆					
Zn_3Cd_4-MT4	x	x	✓	x	◆				
Zn_2Cd_5-MT4	◆	x	✓	✓	x	◆			
Zn_1Cd_6-MT4			x	x	✓	x	◆	◆	◆
Cd_7-MT4			◆	x	x	✓	✓	✓	✓

wise, it was either inferred from the remaining spectroscopic data or denoted as undetermined (Zn_x,Cu_n-MT).

In Vivo Zn(II) Binding Abilities of Mouse MT4 and MT1— The biosynthesis of Zn_7-MT4, Zn_4-αMT4, and Zn_3-βMT4 as unique metal aggregates in zinc-supplemented cultures (Table I) confirmed the same binding capacity for each MT4 fragment either alone or when linked together. This independent behavior could be extended to the folding of each domain in Zn_7-MT, since comparison of the CD fingerprint of Zn_7-MT4 with that of the sum of Zn_4-αMT4 and Zn_3-βMT4 revealed only minor differences (Fig. 2), even less significant than those reported for MT1 (21) or *Homarus americanus* metallothionein (20). Thus far, MT4 Zn(II) binding behavior fully mimics that of MT1, although comparison of the CD spectra revealed lower chiralities for the Zn-MT4 peptides with respect to the paralogous Zn-MT1 forms. This suggests that Zn(II) coordination induces a poorer degree of MT4 folding than for that of MT1 and constitutes an initial result for calling into question the Zn-thionein nature of MT4.

In Vivo Cd(II) Binding Abilities of Mouse MT4 and MT1— The results of the protein syntheses in cadmium-enriched cultures enhanced the above mentioned hypothesis that MT4 was not optimal for divalent metal chelation. Of the three MT4 forms, only the αMT4 fragment was synthesized as a unique species, Cd_4-αMT4, whereas MT4 and βMT4 rendered mixtures of the expected homometallic complexes with several heterometallic Zn,Cd-MT aggregates (Table I). Furthermore, whereas homometallic Cd_3-βMT4 aggregate was the major product recovered, the entire MT4 afforded a mixture of species in which Zn_4Cd_3-MT was the major form, and Cd_7-MT, together with Zn_7-MT, were the minor products. These results show not only the low MT4 ability for Cd(II) coordination *in vivo* but also the highly dissimilar behavior of its domains. The paralogous MT1 form exhibited a distinct cadmium binding behavior, since all MT1 peptides were synthesized as unique, homometallic cadmium aggregates (*i.e.* Cd_7-MT1, Cd_4-αMT1 (Table I), and Cd_3-βMT1) (25). According to the composition of the recombinant samples reported here, only the CD spectra of the Cd_4-αMT4, Cd_7-MT1, and Cd_4-αMT1 solutions can be considered representative of the CD fingerprints of these species (data included in Fig. 4), all showing the characteristic derivative-shaped band at ~250 nm of the Cd-MT aggregates (21, 22). In contrast, the CD spectra of the recombinant Cd-MT4 and Cd-βMT4 samples (data included in Fig. 4) only provided an average of the optical features of the coexisting species. Interestingly, recombinant Cd-MT4 and Cd-βMT4 were the samples with the highest oxidation degrees found among all the biosynthesized proteins (Table I).

In Vitro Cd(II) Binding Abilities of Mouse MT4 and MT1— For the sake of brevity, only the CD spectra of the titrations of Zn_7-MT4, Zn_4-αMT4, and Zn_3-βMT4 at pH 7 with $CdCl_2$ (Fig. 3) and the corresponding ESI-MS results (Table II) are shown, whereas the full set of spectroscopic data and some representative MS spectra are provided as supplementary material (Figs. S1–S6). Analysis of the overall results led to the proposal of the zinc/cadmium replacement pathways shown in Fig. 3.

The *in vitro* data provide further evidence of the Cd binding reluctance of the Zn-MT4 peptides. First, although the three expected fully cadmium-loaded species could indeed be generated by zinc/cadmium replacement, this only occurred after the addition of a number of Cd(II) equivalents higher than those stoichiometrically required (Table II). The ESI-MS analysis also showed that for 4, 3, and 7 eq of Cd(II) added to Zn_4-αMT4, Zn_3-βMT4, and Zn_7-MT4, respectively, there was a coexistence of Cd_4-αMT4, Cd_3-βMT4, and Cd_7-MT4 with cadmium-underloaded Zn,Cd-MT4 species. As a consequence, the CD fingerprints of the canonical Cd-MT4 forms are only available upon saturation of the spectral signals (*i.e.* after the addition of 5, 6, and 11 eq of Cd(II) to the respective zinc aggregates). Second, only the Zn_4-αMT4 titration ended with a unique species, Cd_4-

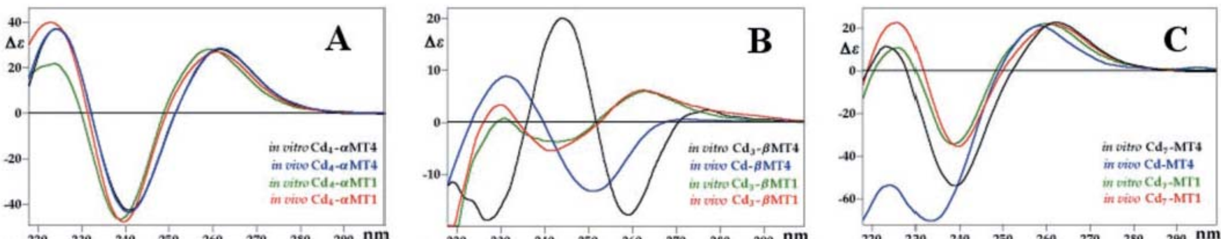

FIG. 4. **Comparison of the circular dichroism spectra of the recombinant mouse Cd_4-αMT4 and Cd_4-αMT1 (*A*), Cd-βMT4 and Cd_3-βMT1 (*B*), and Cd-MT4 and Cd_7-MT1 (*C*) with those of the species of the same stoichiometry obtained *in vitro* by zinc/cadmium replacement studies on the corresponding zinc aggregates.** Data corresponding to MT1 are from Refs. 21, 22, and 25.

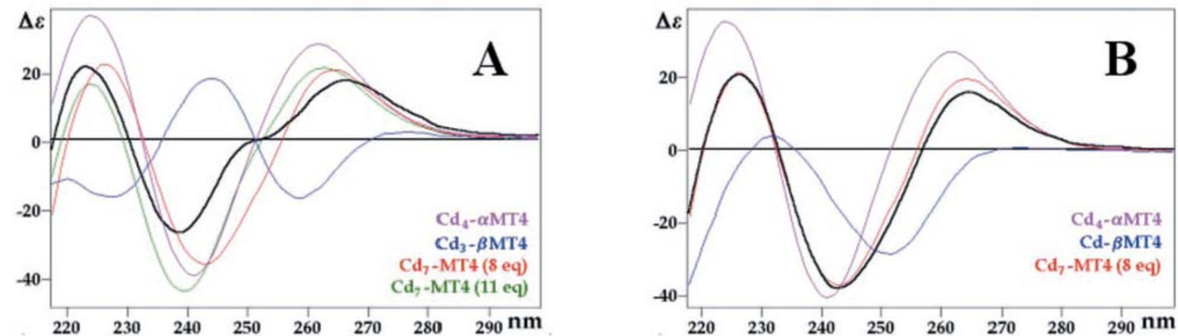

FIG. 5. **Circular dichroism spectra of Cd_4-αMT4, Cd_3-βMT4, Cd_7-MT4 and that corresponding to the addition of 8 eq of Cd(II) to Zn_7-MT4 (*A*) and of Cd_4-αMT4 and those corresponding to the addition of 3 and 8 eq of Cd(II) to Zn_3-βMT4 and Zn_7-MT4, respectively (*B*).** In *both panels*, the spectrum depicted in *black* represents the sum of the circular dichroism spectra of the Cd_4-αMT4 and Cd-βMT4 corresponding species.

TABLE III

Molecular masses and Zn- or Cu-to-protein ratios found for the in vivo synthesized MT4 and its αMT4 and βMT4 domains

Metal supplemented in culture media	Protein	M_{exp}[a]	M_{calc}[b]	M/MT[c]	M/MT[d]
		Da	*Da*		
M = Cu	MT4 (Type 1)	7039.7 ± 6.5	7046.06	Cu_{10}-MT (S)	0 Zn, 9.4 Cu
		7220.1 ± 18.0	7233.71	Cu_{13}-MT (s)	
		7353.7 ± 7.7	7358.81	Cu_{15}-MT (s)	
	MT4 (Type 2)	7043.7 ± 3.2	7046.06	M_{10}-MT (S)	2.7 Zn, 7.3 Cu
		6920.2 ± 0.0	6920.96	M_8-MT (s)	
	αMT4	3655.9 ± 0.0	3657.50	Cu_5-αMT (S)	0 Zn, 3.6 Cu
		3594.7 ± 0.4	3595.00	Cu_4-αMT	
		3717.6 ± 1.0	3720.00	Cu_6-αMT	
		3779.6 ± 0.0	3782.50	Cu_7-αMT (s)	
	βMT4	3807.2 ± 1.2	3806.39	Cu_7-βMT (S)	0 Zn, 5.8 Cu
		3743.7 ± 0.8	3743.89	Cu_6-βMT	
		3619.4 ± 3.8	3618.89	Cu_4-βMT (s)	

[a] Experimental molecular masses for the Cu-MT complexes.
[b] Calculated molecular mass for neutral species with loss of one proton/copper bound (34).
[c] Zinc or copper per MT molar ratio calculated from the mass difference between holo- and apoprotein. S, major species; s, minor species.
[d] Zinc or copper per MT molar ratio calculated from the zinc, copper, and sulfur content (ICP-AES).

αMT4, whereas in the other cases, the Cd_3-βMT4 and Cd_7-MT4 aggregates coexisted with cadmium-underloaded zinc-containing species, Zn_1Cd_2-βMT4 and Zn_1Cd_6-MT4, even for an important excess of Cd(II) (Table II, top right and bottom). In light of these results, it makes sense to locate the Zn(II) ion remaining in Zn_1Cd_6-MT4 within the βMT4 domain. Although reluctance in exchanging the last Zn(II) ion in the M3 position of the βMT1 aggregate has already been described (40, 41), the need for an excess of Cd(II) to generate the canonical Cd-MT1 species was never observed (21, 22).

Comparable Cd(II) binding abilities for αMT4 and αMT1 can be proposed on the basis of similar zinc/cadmium replacement pathways (Fig. S1) and on the match between the CD spectra of the *in vitro* and *in vivo* generated Cd_4-αMT species (Fig. 4*A*), which shows the isostructurality of the four metal aggregates. Isoforms uniquely differ in the higher number of Cd(II) ions required to generate Cd_4-αMT4 than to generate Cd_4-αMT1. This scenario cannot be extended to βMT4. On the one hand, the CD spectrum of the *in vivo* Cd-βMT4 sample (Fig. 4*B*) was reproduced by the addition of 3 eq of Cd(II) to Zn_3-βMT4 (Fig. 3*B*), confirming a comparable mixture of species in both situations (Table I and Table II, top right). On the other, the CD fingerprint of Cd_3-βMT4 did not resemble those of the isostructural Zn_3-βMT4, Zn_3-βMT1 and Cd_3-βMT1 (Figs. 4*B* and S2), indicating that Cd_3-βMT4 represents a novel complex. Moreover, this species, unlike Cd_3-βMT1 that renders Cd_4 and Cd_9 aggregates (22), does not give rise to any overmetalated species. Finally, when analyzing the entire MT4 folding, the resemblance between the CD spectra of Cd_7-MT4, Cd_7-MT1 (Fig. 4*C*), Zn_7-MT4, and Zn_7-MT1 and the closeness of the Cd(II) titrations of Zn_7-MT4 and Zn_7-MT1 (Fig. S3, Table II) (38), led us to propose that both Cd_7-MT species present similar three-

αMT4: Zn_4-αMT → Zn_xCu_3-αMT → Zn_yCu_4-αMT → Cu_6-αMT → Cu_7-αMT → Cu_8-αMT

βMT4: Zn_3-βMT → Zn_1Cu_3-βMT → Zn_1Cu_4-βMT → Cu_6-βMT → Cu_7-βMT → $Cu_{x,y}$-βMT

MT4: Zn_7-MT → Zn_xCu_3-MT → $Zn_yCu_{4,5}$-MT → Zn_3Cu_7-MT → Cu_{10}-MT → Cu_{11}-MT → Cu_{12}-MT → Cu_{13}-MT → Cu_{14}-MT

FIG. 6. **Circular dichroism spectra corresponding to the titrations of Zn_4-αMT4 (*A*), Zn_3-βMT4 (*B*), and Zn_7-MT4 (*C*) with Cu(I) at pH 7.** The *arrows* show the evolution of the spectra when the indicated number of Cu(I) equivalents were added. Corresponding reaction pathways are shown.

dimensional structures and are formed through isostructural zinc/cadmium replacement reactions that only differ in their saturation points.

Unlike MT1 (21) (this work), the MT4 fragments do not interact with Cd(II) in the same way when alone or linked together, neither *in vivo* nor *in vitro*. Whereas Cd_3-βMT4 and Cd_4-αMT4 were the major species synthesized, Cd_7-MT4 was almost absent when the MT4 was expressed in Cd-rich medium. The dependent behavior of both MT4 fragments is also patent *in vitro*, since the sum of the CD fingerprints of Cd_3-βMT4 and Cd_4-αMT4 did not compare well with that of Cd_7-MT4 (Fig. 5*A*). However, CD data (Fig. 5*B*) revealed an independent behavior of both MT4 fragments up to Zn_7-MT4 plus 8 eq of Cd(II), since at this point the CD spectrum nicely matches the sum of the CD spectra of Cd_4-αMT4 and of Zn_3-βMT4 + 3 eq of Cd(II) (equivalent to the *in vivo* Cd-βMT4). Thus, dependence between domains appeared after the 8th eq of Cd(II) added to Zn_7-MT4, when the α domain had already achieved a Cd_4-αMT4 composition, and the β domain was expected to evolve to Cd_3-βMT4 by replacing the last Zn(II) bound. This suggests that linkage of the β domain to its α counterpart hinders the polypeptide rearrangement needed to achieve the

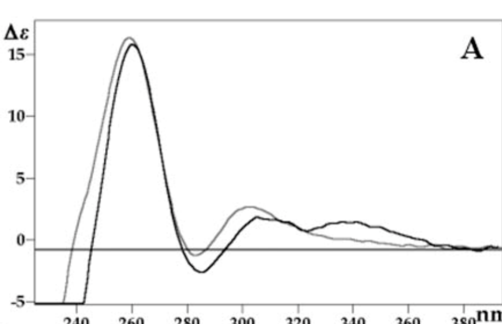
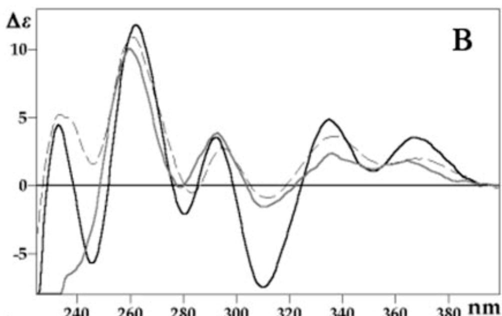

FIG. 7. **Comparison of the circular dichroism fingerprints of the *in vitro* obtained Cu_6-βMT4 (Zn_3-βMT4 + 4 eq of Cu(I)) (*solid black line*) with that of Cu_6-βMT1 (Zn_3-βMT1 + 6 eq of Cu(I)) (*solid gray line*) (*A*) and of the *in vitro* obtained Cu_7-βMT4 (Zn_3-βMT4 + 6 Cu(I) eq) (*solid black line*) with that of the *in vivo* synthesized Cu-βMT4 species (*solid gray line*) and that of *in vitro* Cu_7-βMT1 (Zn_3-βMT1 + 7 Cu(I) eq) (*dashed line*) (*B*).** Data regarding the Cu-MT1 forms are from Refs. 24 and 25.

novel Cd_3-βMT4 folding. This βMT4 restriction on structurally behaving as it would if alone could account for the poor capacity of the full-length MT4 to form *in vivo*-stable Cd_7-MT4 aggregates.

In Vivo Cu(I) Binding Abilities of Mouse MT4 and MT1—Multiple recombinant syntheses of the entire MT4 in copper-supplemented medium yielded two kinds of results, Type 1 and Type 2, with no evident relationship to any of the assayed culture parameters. Type 1 was a mixture of homometallic copper aggregates, Cu_{10}-MT4 being the major species, whereas Type 2 was a mixture of heterometallic M_{10}-MT4 (major) and M_8-MT4 (minor) aggregates (where M represents zinc and copper), with Zn_3Cu_7-MT4 as the most abundant species (Table III). The CD spectrum of the Type 1 sample could be readily reproduced by the *in vitro* addition of 2 eq of Cu(I) to Type 2 (Fig. S7A), providing evidence for the close relationship between both Cu-MT4 preparations. Thus, an M_{10}/MT4 ratio appears the most favored stoichiometry in copper-rich biological medium, M_{10} being either Cu_{10} or Zn_3Cu_7, in an equilibrium depending on biological parameters that, unfortunately, could not be determined. It is worth recalling that MT1 biosynthesis in Cu-rich medium yielded only the Zn_3Cu_7-MT1 species (23).

Contrary to the full-length MT4, several syntheses of recombinant Cu-αMT4 and Cu-βMT4 invariantly yielded mixtures of homometallic copper aggregates, Cu_5-αMT4 and Cu_7-βMT4 being the major respective forms (Table III), with minor species corresponding to aggregates of lower and exceptionally higher (Cu_7-αMT4) stoichiometry. Unfortunately, the CD fingerprints of the biosynthesized Cu_5-αMT4 and Cu_7-βMT4 species are not available due to the significant abundance of the other coexisting species. βMT4 and βMT1 show comparable *in vivo* copper binding behaviors, since they are both produced as mixtures of homometallic, isostoichiometric Cu-βMT species: Cu_7- and Cu_6-βMT (Table III) (25). Conversely, the biosynthesis of homometallic Cu-αMT4 aggregates constitutes an important difference with its αMT1 counterpart (23), suggesting that differences in Cu(I) coordination between MT4 and MT1 can be attributed to their α-domains.

In Vitro Cu(I) Binding Abilities of Mouse MT4 and MT1—The CD spectra of the Zn_4-αMT4, Zn_3-βMT4, and Zn_7-MT4 titrations with $[Cu(CH_3CN)_4]ClO_4$ at pH 7 are shown in Fig. 6, whereas the full set of optical and spectrometric data is given as supplementary material (Figs. S8–S10 and Table S1). Overall results allowed the proposal of the zinc/copper replacement reaction pathways of the three Zn-MT species, also shown in Fig. 6.

Despite slight initial structural dissimilarities, Zn_4-αMT4 and Zn_4-αMT1 endeavored parallel zinc/copper replacement reactions while there were Zn(II) ions bound. Their behavior diverged after the addition of the 5th or 6th eq of Cu(I), which caused the formation of metal aggregates of different stoichiometry and probably of distinct three-dimensional structure. Finally, the saturation of both peptides rendered species of comparable three-dimensional arrangement (Fig. S8), although of different copper contents (Cu_8-αMT4 and Cu_9-αMT1). βMT4 and βMT1 exhibit a similar *in vitro* copper-binding behavior, since both *in vitro* zinc/copper replacements proceeded analogously (Fig. S9), but with βMT4 showing a higher Cu(I) affinity than βMT1; only 4 eq of Cu(I) added to Zn_3-βMT4 were needed to form a Cu_6-βMT4 species, practically unique in solution (Table S1), and the addition of up to 6 Cu(I) eq gave rise to a very characteristic CD spectra that could be assigned to the fingerprint of the Cu_7-βMT4 aggregate (Fig. 6*B*). Species of the same Cu(I)/MT ratio and close three-dimensional structure (Fig. 7) are formed by Cu(I) addition to Zn_3-βMT1, but only after 6 and 7 eq of Cu(I), respectively (24). Furthermore, the unraveling associated with the transition of Cu_7-βMT to species of higher stoichiometry is faster for βMT4 than for βMT1 (*i.e.* it requires fewer Cu(I) ions, as suggested by the evolution of the respective CD spectra) (Fig. S9).

Although a first glance at the optical data of the Cu(I) titrations of Zn_7-MT4 and Zn_7-MT1 (Fig. S10) suggests marked differences, both isoforms evolved similarly until 7 eq of Cu(I) were added, rendering equivalent Zn_3Cu_7-MT aggregates, also analogous to the biosynthesized complexes (Fig. S7*C*). The apparent dissimilarities in this first stage of the titrations are attributable to the different CD spectra of the starting species; to a small contribution at ~350(+) nm characteristic of the βMT4 domain (Fig. 6*B*) and to the lack of cooperative processes in Cu(I) binding to Zn_4-MT4. As described for the α domain, the main isoform differences appeared concomitantly with the displacement of the last zinc ions bound, now between 6 and 10 eq of Cu(I) added. Then Zn_3Cu_7-MT4 gave rise to Cu_{10}-MT4, both species clearly different in three-dimensional structure, whereas Zn_3Cu_7-MT1 evolved to Zn_1Cu_{10}-MT1, both species sharing a similar three-dimensional structure. According to the CD data, the structures of the *in vivo* and *in vitro* Cu_{10}-MT4 forms are very close and clearly different from that of $Cu_{10}Zn_1$-MT1 (Fig. S7*B*). Only after displacing the last Zn(II) bound to MT1 do both proteins once more show comparable behavior. Nevertheless, the characteristic ~350(+) nm absorption, which intensifies with the formation of Cu_{10}-MT4, remained absent in MT1, thus revealing that Cu(I) is bound by MT4 through a coordination environment that MT1 cannot offer and which provides enough stability to the Cu_{10}-MT4 aggregates to last in physiological medium. It is also worth noting that for αMT4 and the entire MT4, the differences with MT1 are only found in

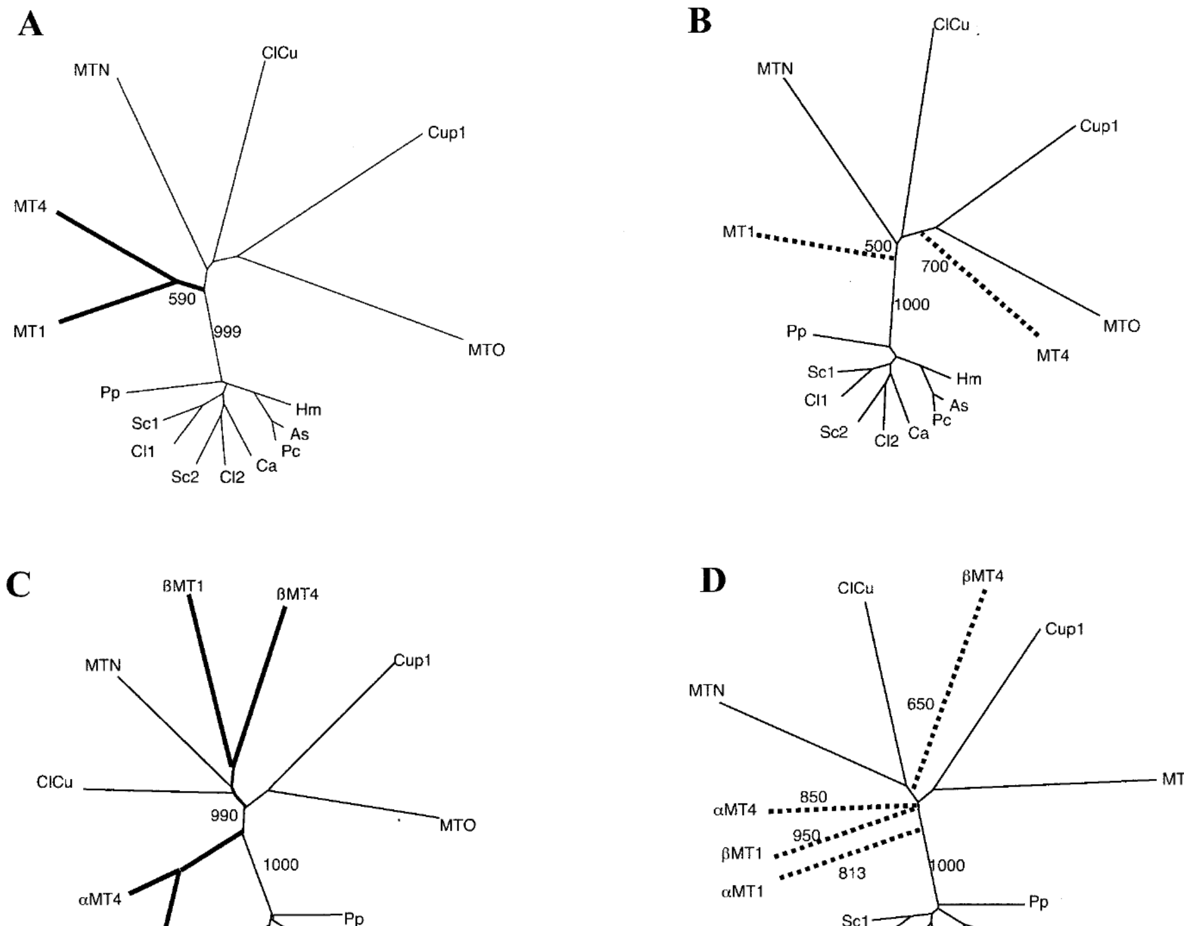

FIG. 8. **Protein distance trees of MT4, MT1 and their separate β and α domains.** *A*, neighbor-joining trees constructed with the entire MT4 and MT1 mouse polypeptides; *B*, joint representation of the positions of the branches of MT4 and MT1 when their sequences were analyzed separately; *C*, tree constructed with the βMT4, βMT1, αMT4 and αMT1 separate domains; *D*, joint representation of the positions of the branches of the four MT domains when their sequences were analyzed separately. *Cl, Callinectes sapidus* isoforms 1 and 2 and Cu-thionein; *Sc, Scylla serrata* isoforms 1 and 2; *Ca, Carcinus maenas*; *As, Astacus astacus*; *Pc, Pacifastacus leniusculus*; *Hm, Homarus americanus*; *Pp, Potamon potamios*; *Cup1, Saccharomyces cerevisiae* Cup1; *MTN, Drosophila melanogaster* MtA; *MTO, Drosophila melanogaster* MtB.

those zinc/copper displacement reaction stages that yield *in vitro* formation of biologically relevant species, which can be identified by consideration of the *in vivo* results.

αMT4 and βMT4 do not exhibit an *in vivo* independent copper binding behavior. As described for MT1 (23), the *in vivo* Cu(I) binding capacity is higher for the MT4 separate fragments (Cu_5-αMT4 and Cu_7-βMT4 as major species) than for the entire protein, since neither Type 1 nor, obviously, Type 2 biosyntheses rendered Cu_{12}-MT4 aggregates, as would correspond to the sum of domains, but instead yielded Cu_{10}-MT4. Unfortunately, the elucidation of the *in vitro* dependent/independent behavior of αMT4 and βMT4 and the proposal of a detailed metal distribution between domains, comparable with that reported for MT1 (23), are prevented, since the coexistence of species in almost all of the titration points hampers the identification of the CD fingerprints for each species proposed in the reaction pathways of Fig. 6.

MT4 Structure/Function Relationship—The thorough analysis of the *in vivo* and *in vitro* metal binding features of MT4 and MT1 revealed significant differences between isoforms, which can be summarized as improved copper binding and hindered cadmium binding abilities for the MT4 isoform. This, together with the following observations, led us to propose MT4 as a Cu-thionein composed of two Cu-thionein domains, whereas MT1 was previously classified as a Zn-thionein formed by a Cu-thionein (βMT1) and a Zn-thionein (αMT1) domain (20). First, recombinant syntheses in copper-enriched medium afforded homometallic Cu-MT4 species, in contrast to heterometallic Zn_3Cu_7-MT1 and Zn_1Cu_4-αMT1 (23). Second, the three zinc-MT4 complexes showed a patent low chirality. Third, the biosynthesis in cadmium-enriched medium revealed MT4 inability for Cd(II) binding, given that a mixture of cadmium-zinc aggregates was the major product instead of the expected Cd_7-MT4. Further consideration of the *in vitro* results corroborated the Cu-thionein character of MT4 and allowed us to ascertain fuller details of its metal binding features. In summary, it was concluded that the better MT4 *versus* MT1 copper binding ability relies on a different behavior of their αMT domains, whereas βMT4 exhibits a behavior parallel to, but faster than, βMT1. In contrast to this, MT4 cadmium binding reluctance

can be attributed to the extreme difficulty of βMT4 in forming cadmium-fully loaded aggregates, whereas αMT4 shows a cadmium binding behavior analogous to, but slower than, αMT1. Thus, to summarize, the differences in Cd(II) coordination between MT4 and MT1 should be assigned to their β domains, the α domains only contributing to these, whereas the opposite situation is found for Cu(I) coordination, the α domains being responsible for the differences, with the β domain harboring an enhancing effect.

Protein sequence distance trees proved powerful enough to discriminate the different metal preferences experimentally determined for MT4 and MT1, thus validating the methodology previously applied for *Arthropoda* MTs (20, 27). The full-length MT4 and MT1 and their corresponding fragments were considered separately to avoid distortions caused by the artifactual alignment between an entire polypeptide and one of its halves. MT4 and MT1 shared the closest sequence similarity, as otherwise expected for the comparison between *Arthropoda* and mammalian sequences, with a branch emerging closer to Cu-thioneins than to Zn-thioneins (Fig. 8*A*). The results of the study repeated individually for each isoform agreed with their experimental characterization; whereas the MT1 position almost coincided with that of the MT4/MT1 couple, MT4 alone branched from an internal point to the Cu-thionein family (Fig. 8*B*). When the MT domains were analyzed, the results remained in close agreement with the wet science data. The tree including the four domains (Fig. 8*C*) showed association of both βMT, clearly inside the Cu-thionein cluster, with both αMT in an intermediate position between Zn- and Cu-thioneins, as was the case for the entire MTs. However, both β peptides were situated far apart when individually analyzed (Fig. 8*D*), since βMT4, but not βMT1, moved inside the Cu-thionein group.

Sequence similarity between MT4 and MT1 is almost entirely due to their fully conserved cysteines, since intercalating residues are highly dissimilar. Therefore, these should be made responsible for the differential MT4 and MT1 metal binding behavior. Furthermore, the residue replacement ratios differ substantially between domains. The β domains have considerably diverged during evolution, with up to 62% of their non-Cys residues nonconserved, which is almost twice the ratio in the α domain (35%). βMT4 has a −2 charge with respect to βMT1 and contains considerably bulkier amino acids, as shown by a volume increment of +252 (βMT4 *versus* βMT1) as opposed to +21.2 (αMT4 *versus* αMT1), calculated according to Ref. 42. This could entail a severe steric hindrance for the allocation of Cd(II), imposing the particular fold described here for Cd_3-βMT4 with respect to Cd_3-βMT1 and even to Zn_3-βMT4. The diminished Cd(II) binding ability of αMT4 *versus* αMT1 could be attributed to its high Pro content, interestingly in Cys-Pro doublets, in agreement with the association of these motifs to structural perturbations interfering with the geometrical requirements of Cd-S clusters recently suggested for MT3 (43). Non-Cys residues seem to be less determinant for copper interaction, and the βMT4 enhanced Cu(I) binding ability may be related to its more negative charge and also to the previously mentioned Pro content, assuming that the turns imposed by the prolyl bonds would yield a polypeptide chain architecture, somehow favoring Cu(I) coordination.

Considerations on MT4 Biological Function—Hypotheses about the MT4 biological function should combine its Cu-thionein character (reported here) and its developmentally controlled, tissue-specific expression pattern (10). Recent DNA microarray analyses of genes involved in mouse-epidermis differentiation identified *MT4* as a target of the transcriptional activator *Whn*, detecting its expression not only in the squamous epidermis but in all epithelial developing tissues, including hair follicles and the back skin (44). Therefore, functional genomics not only corroborates but also extends the physiological role of MT4 in mammalian epithelia differentiation. Since the MT1/MT4 transcriptional switch has been reported as coincident with that of k4/k13 keratin subtypes associated to the generation of the outermost epidermic structures (10), it is tempting to suggest that MT4 would better suit the keratinocyte specific requirements in this specific stage than would MT1. Although an MT4 physiological role involving zinc transport or exchange had been postulated (44), consideration of the copper requirement of several enzymes involved in the S–S bond formation during keratin biosynthesis would be consistent with MT4 being more optimal in this context due to its Cu-thionein character. Metal analyses of copper smelter workers have also shown that hair and nails are the sites of maximum copper accumulation (12). This distinctive copper metabolism and avidity in epithelial structures would require the presence of a specific MT form, MT4, whereas essential copper homeostasis and detoxification roles in the organisms would still be carried out by MT1 and MT2 (5).

In an enlightening review (6), it was stated that "the evolutionary forces that led to the initial appearance, gene duplications, and nearly ubiquitous expression of MTs remain enigmatic." In this work, we are confident of providing evidence that supports a significant functional divergence between the MT4 and MT1 paralogs. This may contribute to the unveiling of further structure/function molecular bases underlying the duplication events that generated the MT family in mammalian genomes.

Acknowledgments—We acknowledge the Serveis Científico-Tècnics, Universitat de Barcelona (DNA sequencing, ICP-AES, and ESI-MS) and the Servei d'Anàlisi Química, Universitat Autònoma de Barcelona (Atomic Absorption Spectrometry, CD, and UV-visible electronic absorption) for allocating instrument time.

REFERENCES

1. Wolfe, K. H., and Shields, D. C. (1997) *Nature* **387,** 708–713
2. Lundin, L. G. (1999) *Semin. Cell Dev. Biol.* **10,** 523–530
3. Holland, P. W., Garcia-Fernandez, J., Williams, N. A., and Sidow, A. (1994) *Dev. Suppl.* **43,** 125–133
4. Kägi, J. H. R., and Vallee, B. L. (1960) *J. Biol. Chem.* **235,** 3460–3465
5. Suzuki, K. T., Someya, A., Komada, Y., and Ogra, Y. (2002) *J. Inorg. Biochem.* **88,** 173–182
6. Palmiter, R. D. (1998) *Proc. Natl. Acad. Sci. U. S. A.* **95,** 8428–8430
7. Vasak, M., and Hasler, D. W. (2000) *Cur. Opin. Chem. Biol.* **4,** 177–183
8. Uchida, Y., Takio, K., Titani, K., Ihara, Y., and Tomonaga, M. (1991) *Neuron* **7,** 337–347
9. Tsuji, S., Kobayashi, H., Uchida, Y., Ihara, Y., and Miyatake, T. (1992) *EMBO J.* **11,** 4843–4850
10. Quaife, C. J., Findley, S. D., Erickson, J. C., Froelick, G. J., Kelly, E. J., Zambrowicz, B. P., and Palmiter, R. D. (1994) *Biochemistry* **33,** 7250–7259
11. Liang, L., Fu, K., Lee, D. K., Sobieski, R. J., Dalton, T., and Andrews, G. K. (1996) *Mol. Reprod. Dev.* **43,** 25–37
12. Gerhardsson, L., Englyst, V., Lundström, N., Sandberg, S., and Nordberg, G. (2002) *J. Trace Elem. Med. Biol.* **16,** 261–266
13. Otvos, J. D., and Armitage, I. M. (1980) *Proc. Natl. Acad. Sci. U. S. A.* **77,** 7094–7098
14. Robbins, A. H., McRee, D. E., Williamson, M., Collett, S. A., Xuong, N. H., Furey, W. F., Wang, B. C., and Stout, C. D. (1991) *J. Mol. Biol.* **221,** 1269–1293
15. Nielson, K. B., and Winge, D. R. (1984) *J. Biol. Chem.* **259,** 4941–4946
16. Nielson, K. B., and Winge, D. R. (1985) *J. Biol. Chem.* **260,** 8698–8701
17. Okada, Y., Ohta, N., Yagyu, M., Min, K.-S., Onosaka, S., and Tanaka, K. (1985) *FEBS Lett.* **183,** 375–378
18. Okada, Y., Ohta, N., Iguchi, S., Tsuda, Y., Sasaki, H., Kitagawa, T., Yagyu, M., Min, K.-S., Onosaka, S., and Tanaka, K. (1986) *Chem. Pharm. Bull.* **34,** 986–998
19. Li, H., and Otvos, J. D. *Biochemistry* (1996) **35,** 13929–13936
20. Valls, M., Bofill, R., González-Duarte, R., González-Duarte, P., Capdevila, M., and Atrian, S. (2001) *J. Biol. Chem.* **276,** 32835–32843
21. Cols, N., Romero-Isart, N., Capdevila, M., Oliva, B., Gonzàlez-Duarte, P., Gonzàlez-Duarte, R., and Atrian, S. (1997) *J. Inorg. Biochem.* **68,** 157–166
22. Capdevila, M., Cols, N., Romero-Isart, N., González-Duarte, R., Atrian, S., and González-Duarte, P. (1997) *Cell. Mol. Life Sci.* **53,** 681–688
23. Bofill, R., Capdevila, M., Cols, N., Atrian, S., and González-Duarte, P. (2001) *J. Biol. Inorg. Chem.* **6,** 405–417
24. Bofill, R., Palacios, O., Capdevila, M., Cols, N., Gonzàlez-Duarte, R., Atrian, S., and Gonzàlez-Duarte, P. (1999) *J. Inorg. Biochem.* **73,** 57–64
25. Cols, N., Romero-Isart, N., Bofill, R., Capdevila, M., Gonzàlez-Duarte, P., Gonzàlez-Duarte, R., and Atrian, S. (1999) *Prot. Eng.* **12,** 265–269

26. Valls, M., Bofill, R., Romero-Isart, N., Gonzàlez-Duarte, R., Abián, J., Carrascal, M., Gonzàlez-Duarte, P., Capdevila, M., and Atrian, S. (2000) *FEBS Lett.* **467,** 189–194
27. Domenech, J., Palacios, O., Villarreal, L., Gonzàlez-Duarte, P., Capdevila, M., and Atrian, S. (2003) *FEBS Lett.* **533,** 72–78
28. Syring, R. A., Hoexum-Brouwer, T., and Brouwer, M. (2000) *Comp. Biochem. Physiol. C.* **125,** 325–332
29. Bertini, I., Hartman, H.-J., Klein, T., Liu, G., Luchinat, C., and Weser, U. (2000) *Eur. J. Biochem.* **267,** 1008–1018
30. Santovito, G., Irato, P., Palermo, S., Boldrin, F., Sack, R., Hunziker, P., and Piccinni, E. (2001) *Protist* **152,** 219–229
31. Bongers, J., Walton, C. D., Richardson, D. E., and Bell, J. U. (1988) *Anal. Chem.* **60,** 2683–2686
32. Birchmeier, W., and Christen, P. (1971) *FEBS Lett.* **18,** 209–213
33. Winge, D. R. (1991) *Methods Enzymol.* **205,** 458–469
34. Fabris, D., Zaia, J., Hathout, Y., and Fenselau, C. (1996) *J. Am. Chem. Soc.* **118,** 12242–12243
35. Thompson, J. D., Higgins, D. G., and Gibson, T. J. (1994) *Nucleic Acids Res.* **22,** 4673–4680
36. Fitch, W. M., and Margoliash, E. (1967) *Science* **155,** 279–284
37. Felsenstein, J. (1989) *Cladistics* **5,** 164–166
38. Polec, K., Palacios, O., Capdevila, M., González-Duarte, P., and Lobinski, R. (2002) *Talanta* **57,** 1011–1017
39. Palacios, O., Polec-Pawlak, K., Lobinski, R., Capdevila, M., and González-Duarte, P. (2003) *J. Biol. Inog. Chem.* **8,** 831–842
40. Chang, C.-C., and Huang, P. C. (1996) *Prot. Eng.* **9,** 1165–1172
41. Chang, C.-C., Liao, W.-F., and Huang, P. C. (1998) *Prot. Eng.* **11,** 41–46
42. Zamyatin, A. A. (1972) *Prog. Biophys. Mol. Biol.* **24,** 107–123
43. Romero-Isart, N., Jensen, L. T., Zerbe, O., Winge, D. R., and Vasak, M. (2002) *J. Biol. Chem.* **277,** 37023–37028
44. Schlake, T., and Boehm, T. (2001) *Mech. Dev.* **109,** 419–422

SUPPLEMENTARY MATERIAL

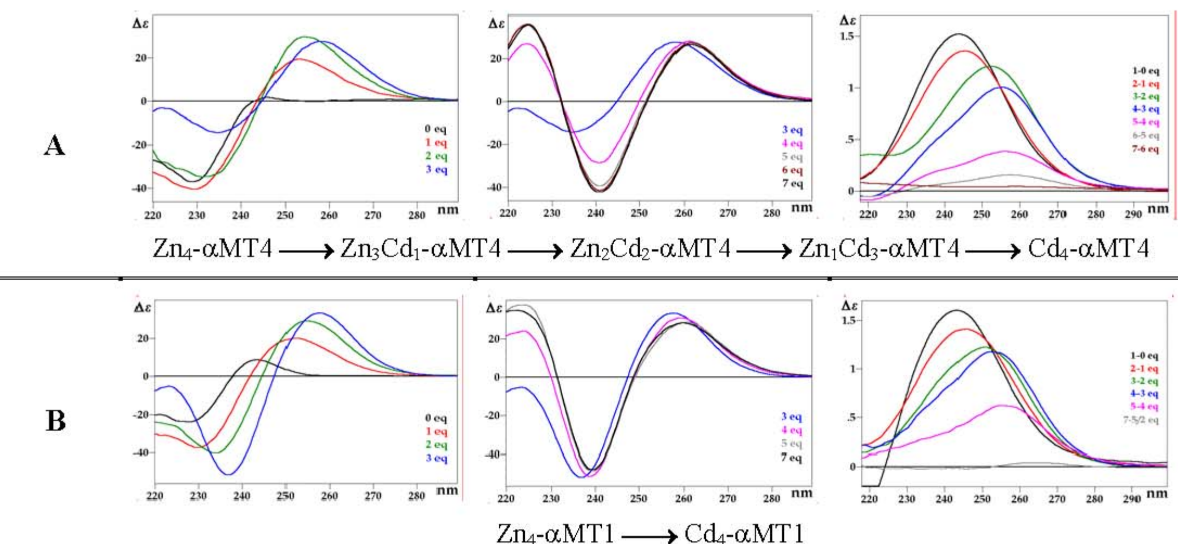

Fig. S1.-Comparison of the behavior of Zn_4-αMT4 (**A**) and Zn_4-αMT1 (**B**) towards Cd(II) through the circular dichroism and UV-vis difference spectra recorded during their titration with $CdCl_2$ at pH 7 and the corresponding reaction pathways. Data regarding Zn_4-αMT1 are from (22).

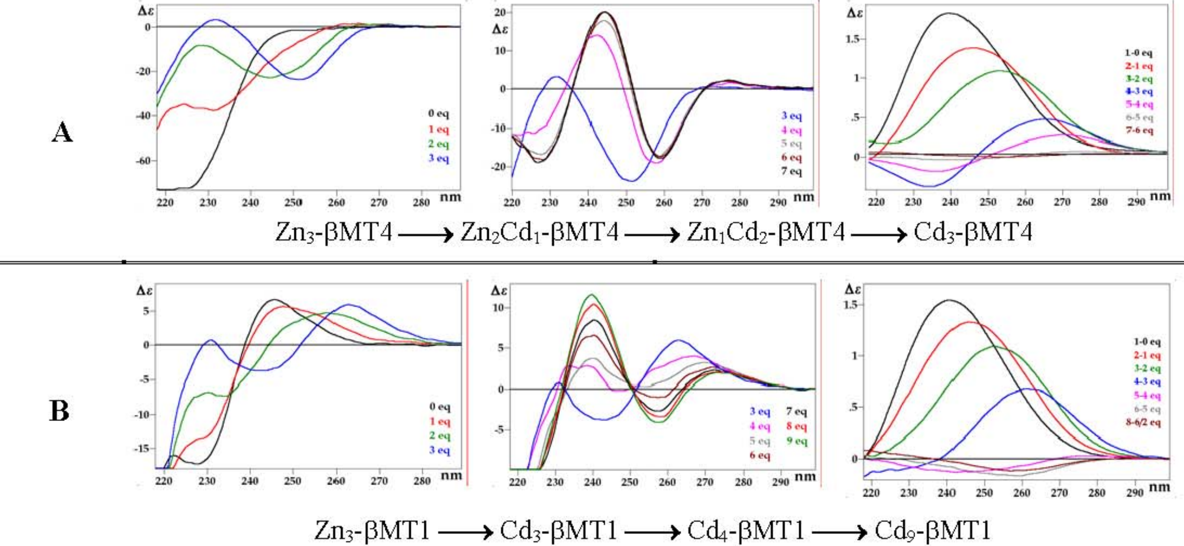

Fig. S2.-Comparison of the behavior of Zn_3-βMT4 (**A**) and Zn_3-βMT1 (**B**) towards Cd(II) through the circular dichroism and UV-vis difference spectra recorded during their titration with $CdCl_2$ at pH 7 and the corresponding reaction pathways. Data regarding Zn_3-βMT1 are from (22).

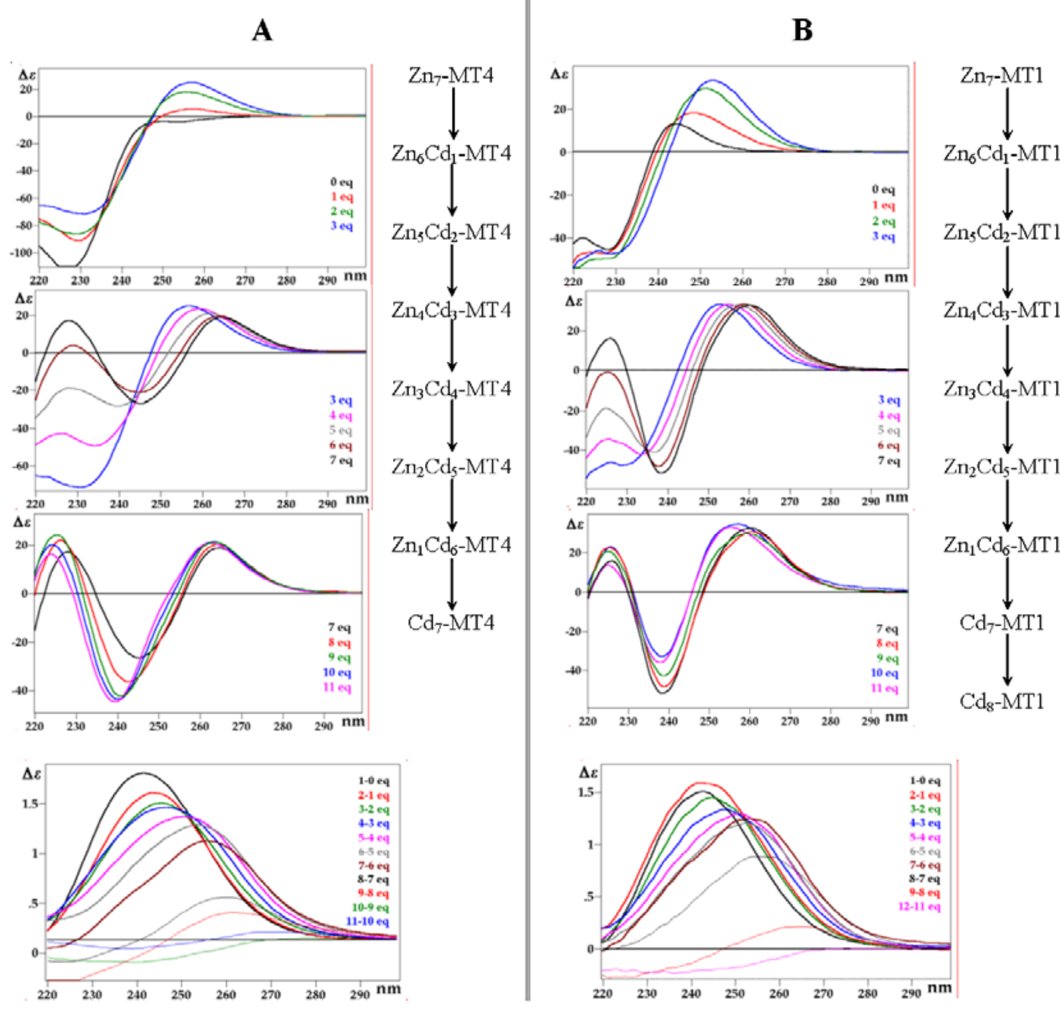

Fig. S3.- Comparison of the behavior of Zn_7-MT4 (**A**) and Zn_7-MT1 (**B**) towards Cd(II) through the circular dichroism and UV-vis difference spectra recorded during their titration with $CdCl_2$ at pH 7 and the corresponding reaction pathways. Data regarding Zn_7-MT1 are from (21, 38).

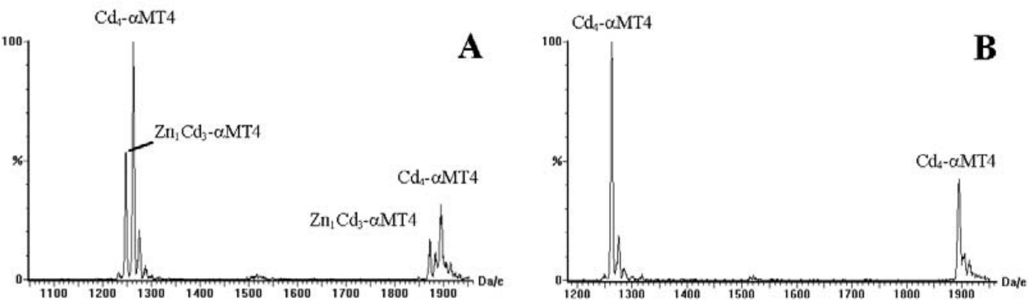

Fig. S4.- ESI-MS mass spectra recorded for the addition of (A) 4 and (B) 5 Cd(II) equivalents, during the Cd(II) titration of Zn_4-αMT4.

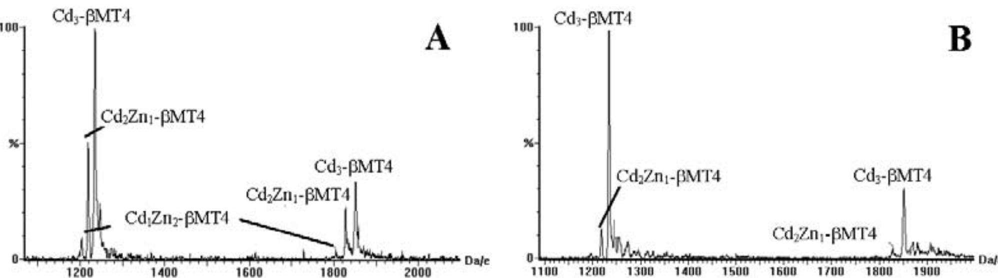

Fig. S5.- ESI-MS mass spectra recorded for the addition of (A) 3 and (B) 5 Cd(II) equivalents, during the Cd(II) titration of Zn_3-βMT4.

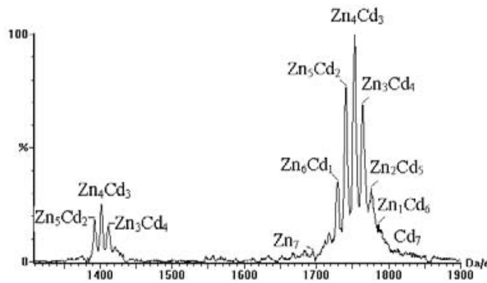

Fig. S6.- ESI-MS mass spectra of the *in vivo* synthesized Cd-MT4 species.

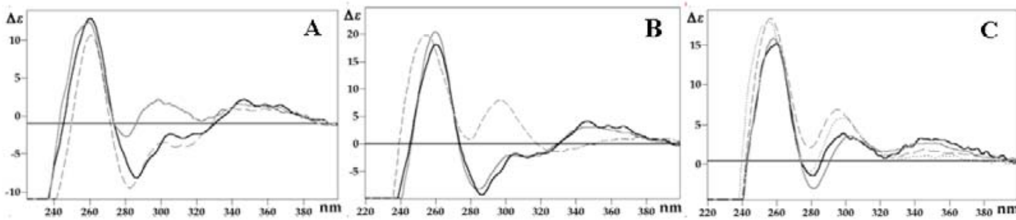

Fig. S7.- Comparison of the circular dichroism spectra of: (A) Type 1 Cu_{10}-MT4 (solid black line) and Type 2 Zn_3Cu_7-MT4 (solid gray line). The spectrum depicted as a dotted line corresponds to that recorded after the addition of 2 Cu(I) equivalents to Type 2 Zn_3Cu_7-MT4; (B) *in vivo* Cu_{10}-MT4 (solid black line), Zn_7-MT4 + 10 Cu(I) (solid grey line) and Zn_1Cu_{10}-MT1 (dashed line); and (C) *in vivo* Zn_3Cu_7-MT4 (solid black line), Zn_7-MT4 + 7 Cu(I) (solid grey line), and *in vivo* (dashed line) and *in vitro* (dotted line) Zn_3Cu_7-MT1. Data regarding the Cu-MT1 proteins are from (23).

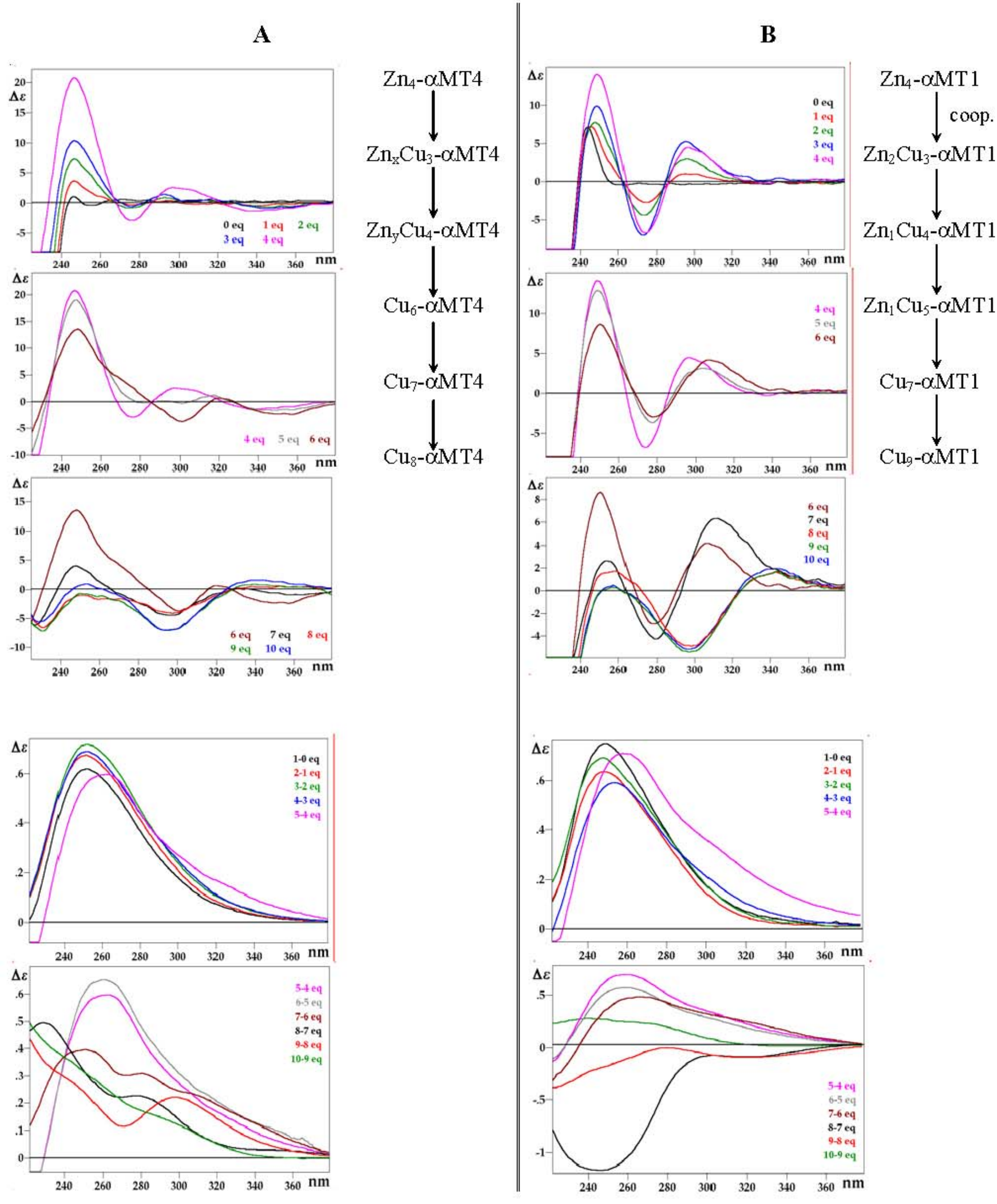

Fig. S8.- Comparison of the behavior of Zn_4-αMT4 (**A**) and Zn_4-αMT1 (**B**) towards Cu(I) through the circular dichroism and UV-vis difference spectra recorded during their titration with $[Cu(CH_3CN)_4]ClO_4$ at pH 7 and the corresponding reaction pathways. Data regarding Zn_4-αMT1 are from (23).

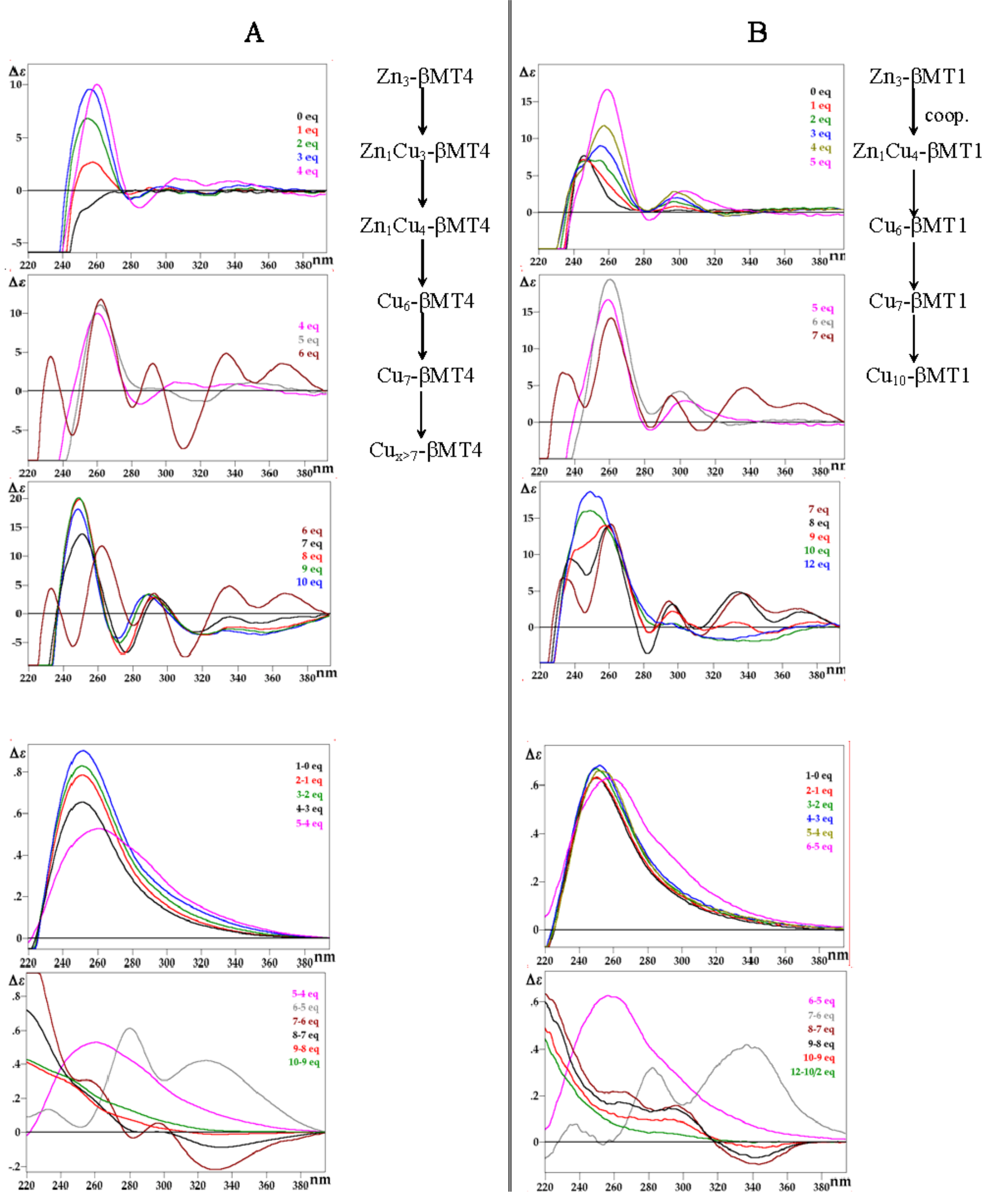

Fig. S9.-Comparison of the behavior of Zn_3-βMT4 (**A**) and Zn_3-βMT1 (**B**) towards Cu(I) through the circular dichroism and UV-vis difference spectra recorded during their titration with $[Cu(CH_3CN)_4]ClO_4$ at pH 7 and the corresponding reaction pathways. Data regarding Zn_3-βMT1 are from (24).

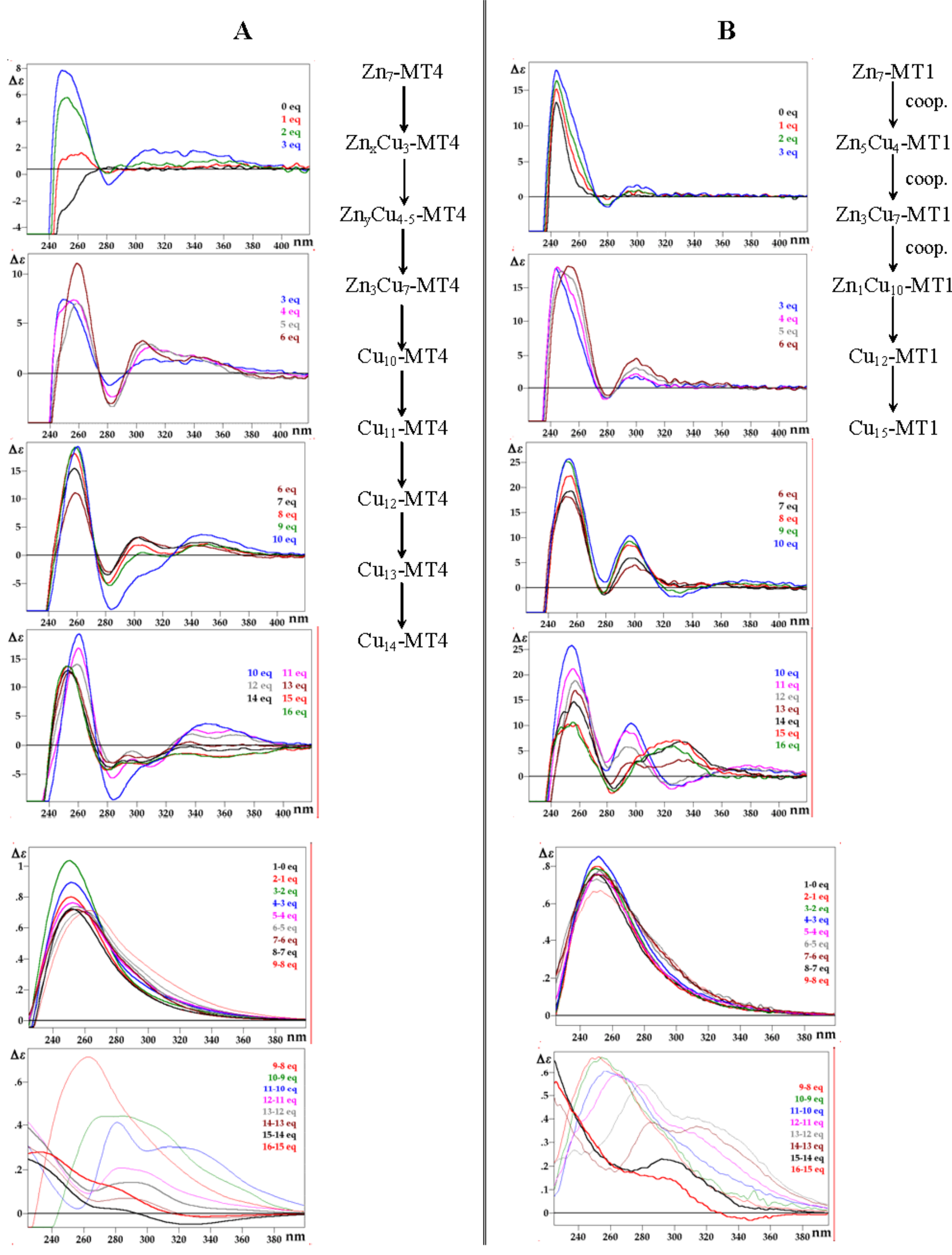

Fig. S10.-Comparison of the behavior of Zn_7-MT4 (**A**) and Zn_7-MT1 (**B**) towards Cu(I) through the circular dichroism and UV-vis difference spectra recorded during their titration with $[Cu(CH_3CN)_4]ClO_4$ at pH 7 and the corresponding reaction pathways. Data regarding Zn_7-MT1 are from (23).

TABLE S1

Distribution of the metal aggregates present in solution, according to ESI-MS data, during the titration of Zn_4-αMT4 (**A**), Zn_3-βMT4 (**B**) and Zn_7-MT4 (**C**) with $[Cu(CH_3CN)_4]ClO_4$ at pH 7 as a function of the number of Cu(I) equivalents added*

A	Cu(I) equivalents added				
	1	3	4	6	10
M_4-αMT4	✓	✓	✓	◆	
M_5-αMT4	x	x	x	x	
M_6-αMT4	◆	x	◆	✓	
M_7-αMT4		◆	◆	x	
M_8-αMT4				x	✓

B	Cu(I) equivalents added					
	1	3	4	6	7	10
M_3-βMT4	✓	◆				
M_4-βMT4	x	x	◆	◆		
M_5-βMT4	x	✓	◆	x	◆	
M_6-βMT4	◆	x	✓	✓	✓	✓
M_7-βMT4				x	✓	✓

C	Cu(I) equivalents added						
	3	4	6	7	8	9	10
M_7-MT4	x						
M_8-MT4	✓	x	◆	◆			◆
M_9-MT4	x	✓	x	x	x	x	x
M_{10}-MT4	◆	✓	✓	✓	✓	✓	x
M_{11}-MT4		◆	x	x	✓	✓	✓
M_{12}-MT4			x	x	x	x	✓
M_{13}-MT4					◆	x	x
M_{14}-MT4						◆	◆

✓, denotes the major species; x, species of intermediate abundance and ◆, the minor species present in solution.

* The species detected by ESI-MS spectrometry during the three titrations are denoted as M_n-MT4 (M= solely Cu(I), exclusively Zn(II) or a mixture of both metal ions) due to the ESI-MS experimental error range and the proximity between the atomic weights of Zn (65.38) and Cu (63.55).

Article 2

Influence of chloride ligands on the structure of Zn- and Cd-metallothionein species

Archives of Biochemistry and Biophysics, 2005, **435**, 331-335

ELSEVIER

Available online at www.sciencedirect.com
SCIENCE DIRECT®

Archives of Biochemistry and Biophysics 435 (2005) 331–335

www.elsevier.com/locate/yabbi

Influence of chloride ligands on the structure of Zn– and Cd–metallothionein species

Laura Villarreal[a,1], Laura Tío[b,1], Sílvia Atrian[b], Mercè Capdevila[a,*]

[a] *Departament de Química, Facultat de Ciències, Universitat Autònoma de Barcelona, E-08193 Bellaterra, Barcelona, Spain*
[b] *Departament de Genètica, Facultat de Biologia, Av. Diagonal 645, Universitat de Barcelona, E-08028, Barcelona, Spain*

Received 19 November 2004, and in revised form 15 December 2004
Available online 7 January 2005

Abstract

It is now commonly accepted that non-proteic ligands contribute to the structure and stability of metal–metallothionein (M–MT) species, although this contribution may differ substantially depending on the MT and the metal ions involved. Conversely, literature data are unconnected, lacking correlation studies between the contribution of inorganic ligands to the M–MT complexes and the corresponding CD and UV–vis fingerprints. To contribute towards filling this gap, we have analyzed the influence of chloride anions in the Zn– and Cd–MT complexes of mammalian MT1 and MT4 isoforms. Starting from the initial hypothesis that the shoulders appearing at 240 nm in the UV–vis difference spectra during the Cd(II) titrations of Zn–MTs would be indicative of chloride participation in these metal–MT complexes, we can now propose that, while their absence definitely rules out these ligands being involved in metal coordination, their presence should not necessarily be attributed to the formation of metal–Cl bonds. Instead, we identified a global blue shift for the UV–vis difference spectral envelope as the most liable indication of chloride participation in the binding sites of the M–MT species. Following this criterion, we determined that chloride anions are bound to the Cd_7–MT1 and Cd_4–αMT1 complexes but not in the isostoichiometric Zn complexes, nor in the Zn- or Cd-complexes of the homologous MT4 peptides.
© 2004 Elsevier Inc. All rights reserved.

Keywords: Cd–metallothionein; Zn–metallothionein; Chloride ligands; Zn–MT; Cd–MT

The metallothionein (MTs)[2] superfamily comprises a wide range of low molecular weight and high cysteine content polypeptides present in almost all living organisms (q.v. http://www.unizh.ch/~mtpage/classif.html). Although MTs' ability to coordinate heavy metal ions has related these peptides to metal homeostasis and detoxification processes, their definite physiological function, or functions, is still a matter of debate and prompts most of the research within this field. One of the goals of our research work is to contribute to the elucidation of MT function through the determination of those structural features that could provide information on their physiological role and behavior. In contrast with the number of MT sequences reported up to date, knowledge on 3D structures comes down to a small number of metal–MT complexes. These include mammalian, invertebrate, and bacterial forms exclusively containing Zn(II) and/or Cd(II) ions, while only limited structural data is available for copper-containing MTs [1]. Vertebrate MTs are composed of two domains, the α-domain (C-terminal) enfolding a $M(II)_4(SCys)_{11}$ aggregate and the β-domain (N-terminal) harboring a $M(II)_3(SCys)_9$ cluster. Differing from the bacterial SmtA MT, whose His residues contribute to metal coordination [2], all structurally known metal–MT species

* Corresponding author. Fax: + 34 935 813 101.
E-mail address: merce.capdevila@uab.es (M. Capdevila).
[1] Both authors contributed equally to this work.
[2] *Abbreviations used:* AAS, atomic absorption spectrometry; CD, circular dichroism; ESI–MS, electrospray ionization mass spectrometry; ICP–AES, inductively coupled plasma–atomic emission spectroscopy; GST, glutathione-*S*-transferase; MT, metallothionein; MTO, *Drosophila melanogaster* metallothionein; UV–vis, ultraviolet–visible electronic absorption.

0003-9861/$ - see front matter © 2004 Elsevier Inc. All rights reserved.
doi:10.1016/j.abb.2004.12.024

contain divalent metal ions tetrahedrally coordinated only to Cys residues, which can act either as terminal or bridging ligands. This notwithstanding, participation of non-proteic ligands in metal–MT complexes has been extensively postulated in the literature. Thus, while Vaher et al. [3] suggested the participation of non-sulfur ligands in rabbit Cd_3, Cu_5–MT2 metal coordination on the basis of ^{113}Cd NMR measurements, Maret et al. [4] identified chloride as a ligand in Cd_7–MT2 by employing ^{35}Cl and ^{1}H NMR spectroscopy and associated this feature to putative ATP binding regulation, which implies a great biological significance. The observation of a characteristic UV–vis difference fingerprint, with an unprecedented absorption at ca. 240 nm, led us to propose the possible binding of chloride anions also in certain metal–*Drosophila* MTO species [5]. Interestingly, our recent studies on the metal binding features of the mammalian MT4 isoform [6] revealed the presence of shoulders at 240 nm, equivalent to those reported for MTO, in the UV–vis difference absorption spectra of the Cd(II) titrations of Zn_7–MT4 and Zn_4–αMT4, but not in those of the Zn_3–βMT4 fragment. In view of the interest of determining variations in the contribution of chloride in different metal–MT complexes, and taking into account the lack of information about which electronic absorption features the non-proteic metal–MT ligands are associated with, this work aims at determining the influence of the chloride anions in the structure of mammalian metal–MT complexes. To this end, Zn_7–MT4, Zn_4–αMT4, and the paradigmatic Zn_7–MT1 and Zn_4–αMT1 forms have been obtained from recombinant synthesis and eluted both in the presence and absence of chloride ions. Subsequently, the eight Zn–MT preparations have been, respectively, titrated with either Cd(II) chloride or Cd(II) perchlorate solutions, and the M–MT species formed have been characterized by means of spectroscopic and spectrometric techniques. Our data are consistent with the presence of chloride ligands in the Cd–MT1 species, but not in the homologous Cd–MT4 forms. Furthermore, we identified a definite global blue shift associated to chloride involvement in the metal–MT complexes in the CD and UV–vis difference spectra of the corresponding species.

Materials and methods

Protein preparation and characterization

As previously described [6–8], fermentator-scale cultures, recovery of the GST–MT fusion constructs and purification of the metal–MT species led to preparations of recombinant mouse Zn_7–MT4, Zn_7–MT1, Zn_4–αMT1, and Zn_4–αMT4 in 50 mM Tris–HCl buffer (pH 7). Alternatively, these Zn-peptides were purified using 50 mM Tris–$HClO_4$ buffer (pH 7) in the final HPLC elution step [5]. In all eight cases, the identity and integrity of the Zn-peptides was established by measurement of their molecular mass and metal-to-protein ratio by electrospray ionization mass spectrometry (ESI–MS) on a Fisons Platform II Instrument (VG Biotech) calibrated using horse heart myoglobin (0.1 mg/ml) [6–8]. Inductively coupled plasma–atomic emission spectrometry (ICP–AES) [9] was used to determine the total sulfur content of the different preparations and to corroborate their zinc/protein ratios, using a Thermo Jarrell Ash, Polyscan 61E and measuring at 182.0 nm (S) or 213.9 nm (Zn). Additionally, Ellman's method [10] was used to measure the thiol groups over total sulfur, that means the oxidation degrees of the different preparations, by using the reagent DTNB (5,5′-dithiobis(nitrobenzoic acid)). The protein solutions obtained from the purification processes were diluted to a final concentration of ca. 10 μM (entire MT) or 20 μM (α fragments) with Milli Q-purified and Ar-degassed water before being titrated with the corresponding Cd^{2+} solution at 25 °C.

Metal solutions and metal ion binding reactions

All solutions used in Cd^{2+} titrations were prepared with Milli-Q purified water and were either argon saturated or vacuum degassed prior to use. Glassware was cleaned with 10% (v/v) nitric acid and repeatedly rinsed with ultrapure water. The in vitro cadmium binding ability of the four Zn–MT peptides was tested in either Tris–HCl or Tris–$HClO_4$ buffer, using either $CdCl_2$ or $Cd(ClO_4)_2$ as titrating agent, respectively. The $CdCl_2$ solution was a Merck AAS Cd^{2+} standard of 1000 ppm, while preparation of that of $Cd(ClO_4)_2$ required determination of the Cd^{2+} concentration by AAS, using a Perkin–Elmer 2100 apparatus.

Zinc/cadmium displacement studies at pH 7.0 were carried out and processed as previously described [6–8]. Electronic absorption measurements were performed on an HP-8453 diode array UV–visible electronic absorption spectrophotometer and a Jasco spectropolarimeter (Model J-715) interfaced to a computer (GRAMS 32 Software) was used for CD determinations. All assays were performed under argon atmosphere, and titrations were carried out at least in duplicate to assure their reproducibility. The pH for all experiments remained constant throughout, without the addition of buffers, and temperature was maintained at 25 °C by means of a Peltier PTC-351S equipment.

Results and discussion

Characterization of the initial recombinant Zn-peptides

The purification of Zn_7–MT1, Zn_7–MT4, Zn_4–αMT1, and Zn_4–αMT4 as unique complexes of identical stoichi-

Table 1
Molecular masses of the Zn- and apo-forms and zinc-to-protein ratios of the in vivo synthesized MT1, MT4, αMT1, and αMT4 metal complexes

Protein	Elution buffer	Molecular mass (Da)				Zn/MT[a]	Zn/MT[b]	Oxid[c]
		Apo form		Zn form				
		Expected	Observed	Expected	Observed			
MT1	Tris–HCl	6162.13	6163.0	6605.90	6605.5	7	7.3	0
	Tris–$HClO_4$	6162.13	6157.2	6605.90	6603.6	7	5.7	23
MT4	Tris–HCl	6420.56	6420.8	6864.29	6864.2	7	6.7	5
	Tris–$HClO_4$	6420.56	6419.8	6864.29	6862.9	7	6.8	9
αMT1	Tris–HCl	3296.94	3297.0	3550.80	3550.8	4	4.1	0
	Tris–$HClO_4$	3296.94	3295.5	3550.80	3549.5	4	3.8	1
αMT4	Tris–HCl	3345.00	3344.5	3598.56	3598.6	4	3.6	11
	Tris–$HClO_4$	3345.00	3344.8	3598.56	3597.1	4	4.0	4

[a] Zinc per MT molar ratio calculated from the mass difference between holo- and apo-protein.
[b] Zinc per MT molar ratio calculated from the zinc and sulfur content (ICP–AES).
[c] Percentage of thiol groups (Ellman's method) over total sulfur (ICP–AES).

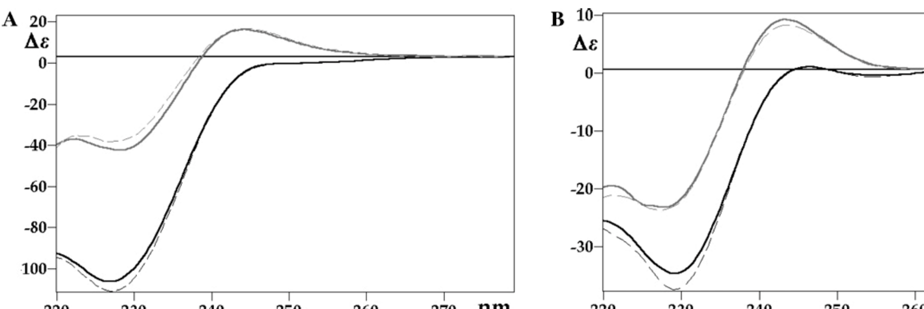

Fig. 1. Circular dichroism spectra of recombinant (A) Zn_7–MT4 eluted in Tris–HCl (solid black line) and in Tris–$HClO_4$ (dashed black line) and Zn_7–MT1 eluted in Tris–HCl (solid gray line) and in Tris–$HClO_4$ (dashed gray line) and (B) Zn_4–αMT4 eluted in Tris–HCl (solid black line) and in Tris–$HClO_4$ (dashed black line) and Zn_4–αMT1 eluted in Tris–HCl (solid gray line) and in Tris–$HClO_4$ (dashed gray line).

ometry using either chloride- or perchlorate-equilibrated buffers confirmed that the availability of additional chloride ligands does not alter the binding capacity of these MT forms (Table 1). Furthermore, the comparison of the CD fingerprints of the Zn_7–MT and Zn_4–αMT species eluted either in Tris–HCl or in Tris–$HClO_4$ (Fig. 1) reveals that, at the concentrations assayed (ca. 50 mM), the presence of chloride anions has no spectroscopically detectable influence either on their structure or on their chirality. It is worth noting that the reported differences between the 3D structures of Zn–MT1 and Zn–MT4 [6] are maintained independently of the anions present in the solution. This leads to the immediate conclusion that the higher folding degree of Zn_7–MT1 and Zn_4–αMT1 vs. the isostoichiometric Zn_7–MT4 and Zn_4–αMT4 species is not ascribable to the contribution of chloride ligands to Zn binding.

In vitro Cd(II) binding studies

Once it had been established that, at our experimental conditions, the features of the Zn–MT species remained unaltered by the presence/absence of chloride ligands, the eight Zn–MT preparations were titrated with increasing amounts of either cadmium chloride or cadmium perchlorate, and the corresponding CD and UV spectra recorded for all Cd(II) addition steps. ESI–MS spectrometry measurements allowed determination of the number and stoichiometry of the coexisting species from aliquots withdrawn at some titration points. Detailed analysis of these spectroscopic and spectrometric data, provided as Supplementary data (Figs. S1–S4 and Tables S1–S4) for the sake of brevity, gave rise to interesting results, which we now discuss.

According to ESI–MS results, the molecular distributions at each point of the Cd(II) titrations are not affected by the presence of chloride anions, as analogous results are found for each MT form independently of the counterion accompanying the Cd(II) cations (Tables S1–S4). However, comparison of the evolution of the CD data shows slight but definite differences at the end of the titrations of both MT1 and αMT1, depending on the presence of chloride or perchlorate in the solution (Figs. S2 and S4), while divergences for the MT4 peptides are negligible (Figs. S1 and S3). These results lead to the conclusion that, although not detected by ESI–MS, chloride anions participate in the last stages of the formation of the Cd_7–MT1 and Cd_4–αMT1 species and not

in those of the homologous MT4 cadmium complexes. Interestingly, only Cd_7–MT1 shows slightly different CD spectra if generated in a chloride or perchlorate rich solution, the other three canonical Cd–MT species basically showing the same CD spectra regardless of the counterion used (Fig. 2). As a consequence, it could be deduced that only minor structural changes are introduced by the participation of chloride anions in the Cd–MT1 species, those of the entire protein being more relevant than those of its α fragment.

The clearest evidence of chloride binding in Cd–MT1 complexes comes from the UV–vis difference spectra where, though in opposition to what was previously proposed for the Cd–MTO species [5], the *chloride signal* appears to be related to a blue shift of the global spectral envelope instead of being related to a 240 nm shoulder. As shown in Fig. 3, these shoulders, which are observed in the UV–vis difference spectra for 7–6 and 4–3 Cd(II) equivalents added, respectively, to Zn_7–MT4 or Zn_4–αMT4 in the presence of chloride ions [6], are surprisingly also detected when these anions are not in solution (Figs. S1 and S3). Thus, the contribution of other chromophores to the final spectral envelope probably gives rise to these particular fingerprints, which we had initially associated with chloride binding. An opposite situation arises when considering the UV–vis difference spectra corresponding to the same Cd(II) equivalents added to the homologous MT1 peptides. Thus, both Zn_7–MT1 (Fig. S2) and Zn_4–αMT1 (Fig. S4) give rise to the expected absorptions at 240 nm in the presence of chloride anions but not when perchlorate ions are in solution, in accordance with the proposed participation of the former in both Cd–MT1 complexes. Furthermore, a clear blue shift of the whole UV–vis difference spectral pattern (absorption maxima from 258 to 252 nm) is observed in Fig. 3 in those cases where the chloride ions contribute to the final Cd–MT species (i.e., Cd_7–MT1 and Cd_4–αMT1). The fact that the spectral signals associated in this work to chloride ligands in the Cd–MT1 complexes differ from those previously published for *Drosophila* MTO should therefore be attributed to the high amino acid divergence between the non-homolo-

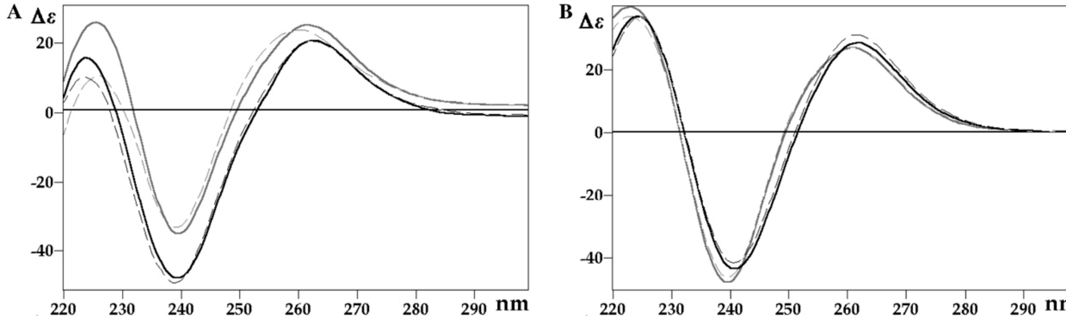

Fig. 2. Superimposition of the CD spectra of (A) Cd_7–MT4 in Tris–HCl (solid black line) and in Tris–$HClO_4$ (dashed black line) and of Cd_7–MT1 in Tris–HCl (solid gray line) and in Tris–$HClO_4$ (dashed gray line) and of (B) Cd_4–αMT4 in Tris–HCl (solid black line) and in Tris–$HClO_4$ (dashed black line) and of Cd_4–αMT1 in Tris–HCl (solid gray line) and in Tris–$HClO_4$ (dashed gray line). The CD spectra corresponding to a major presence of the Cd_7–MT and Cd_4–αMT species in chloride and perchlorate media have been chosen taking into account the information retrieved from ESI–MS data [6,8,11].

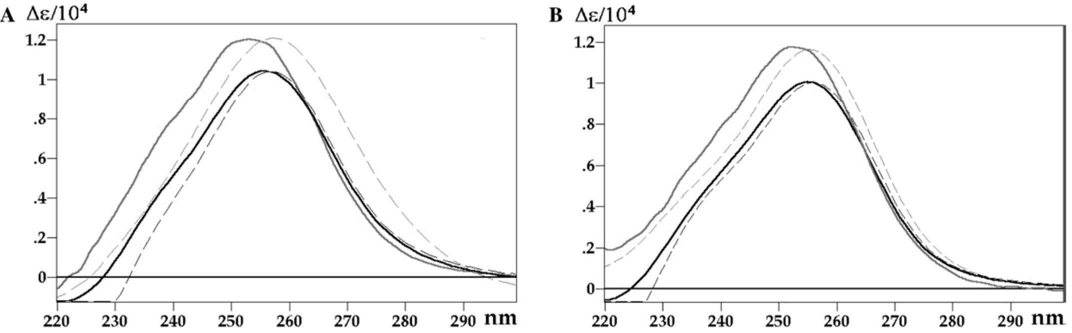

Fig. 3. Superimposition of the UV–vis difference spectra recorded during the Cd(II) titrations of (A) Zn_7–MT4 in Tris–HCl (solid black line) and in Tris–$HClO_4$ (dashed black line) and of Zn_7–MT1 in Tris–HCl (solid gray line) and in Tris–$HClO_4$ (dashed gray line) for 7–6 Cd(II) eq added and (B) Zn_4–αMT4 in Tris–HCl (solid black line) and in Tris–$HClO_4$ (dashed black line) and of Zn_4–αMT1 in Tris–HCl (solid gray line) and in Tris–$HClO_4$ (dashed gray line) for 4–3 Cd(II) eq added.

gous mammalian and diptera MT polypeptides [5], the latter showing far more pronounced 240 nm shoulders than the former.

In our opinion, these results highlight two relevant conclusions to be considered when undertaking new metal–MT structural characterization studies. First, the contribution of inorganic ligands to conformational features may be particularly dependent on a given MT polypeptide, as we have shown that two paralogous mammalian MTs (MT1 and MT4) behave differently in this respect. Since chloride, especially, has been related to ATP–MT1 interaction [4], the capacity of an MT to establish this association, or not, may be of crucial biological relevance. Second, the conformational features of certain M–MT complexes are indeed dissimilar if chloride anions are or are not present when they are *assembled*, and thus consideration of the physiological environments in which this assembly takes place may be of great significance.

Acknowledgments

This work was supported by the Spanish *Ministerio de Ciencia y Tecnología* (Projects BQU2001-1976 and BIO2003-03892). L.V. and L.T. are indebted to the *Departament de Química* of the *Universitat Autònoma de Barcelona* and to the Spanish *Ministerio de Ciencia y Tecnología*, respectively, for pre-doctoral scholarships. We are also indebted to Dr. Joan Sola for fruitful data and manuscript discussion. We acknowledge the *Servei d'Anàlisi Química, Universitat Autònoma de Barcelona* (AAS, CD, UV–vis) and the *Serveis Científico-Tècnics, Universitat de Barcelona* (ICP–AES and ESI–MS), for allocating instrument time.

Appendix A. Supplementary data

Supplementary data associated with this article can be found, in the online version, at doi:10.1016/j.abb.2004.12.024.

References

[1] P. González-Duarte, in: J.A. McCleverty, T.J. Meyer (Eds.), Comprehensive Coordination Chemistry II, Metallothioneins, vol. 8, Elsevier-Pergamon, Amsterdam, 2003, pp. 213–228.
[2] C.A. Blindauer, M.D. Harrison, J.A. Parkinson, A.K. Robinson, J.S. Cavet, N.J. Robinson, P.J. Sadler, Proc. Natl. Acad. Sci. USA 98 (2001) 9593–9598.
[3] M. Vaher, N. Romero-Isart, M. Vasák, P. Palumaa, J. Inorg. Biochem. 83 (2001) 1–6.
[4] W. Maret, G. Heffron, H.A. Hill, D. Djuricic, L.J. Jiang, B.L. Vallee, Biochemistry 41 (2002) 1689–1694.
[5] J. Domenech, O. Palacios, L. Villarreal, P. González-Duarte, M. Capdevila, S. Atrian, FEBS Lett. 533 (2003) 72–78.
[6] L. Tío, L. Villarreal, S. Atrian, M. Capdevila, J. Biol. Chem. 279 (2004) 24404–24413.
[7] N. Cols, N. Romero-Isart, M. Capdevila, B. Oliva, P. González-Duarte, R. González-Duarte, S. Atrian, J. Inorg. Biochem. 68 (1997) 157–166.
[8] M. Capdevila, N. Cols, N. Romero-Isart, R. González-Duarte, S. Atrian, P. González-Duarte, Cell. Mol. Life Sci. 53 (1997) 681–688.
[9] J. Bongers, C.D. Walton, D.E. Richardson, J.U. Bell, Anal. Chem. 60 (1988) 2683–2686.
[10] W. Birchmeier, P. Christen, FEBS Lett. 18 (1971) 208–213.
[11] K. Polec-Pawlak, Ò. Palacios, M. Capdevilla, P. Gonzalez-Duarte, R. Lobinski, Talanta 57 (2002) 1011–1017.

Supplementary Material

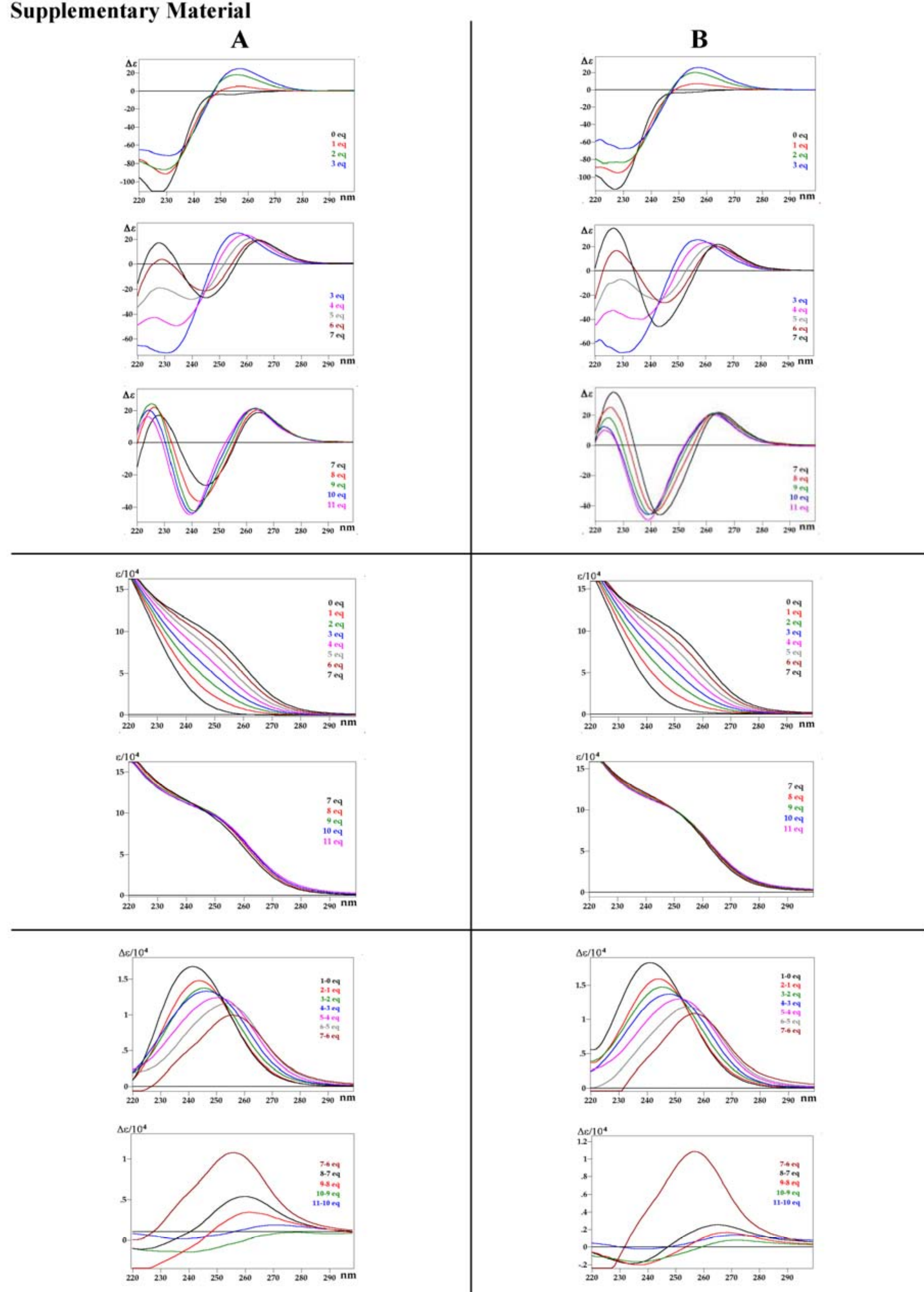

Figure S1.- Comparison of the behavior of (**A**) Zn_7-MT4/Tris-HCl and (**B**) Zn_7-MT4/Tris-$HClO_4$ toward Cd(II) through the CD, UV-vis, and UV-vis difference spectra recorded during their respective titrations with $CdCl_2$ or $Cd(ClO_4)_2$ at pH 7. Data regarding Zn_7-MT4/Tris-HCl are from [6].

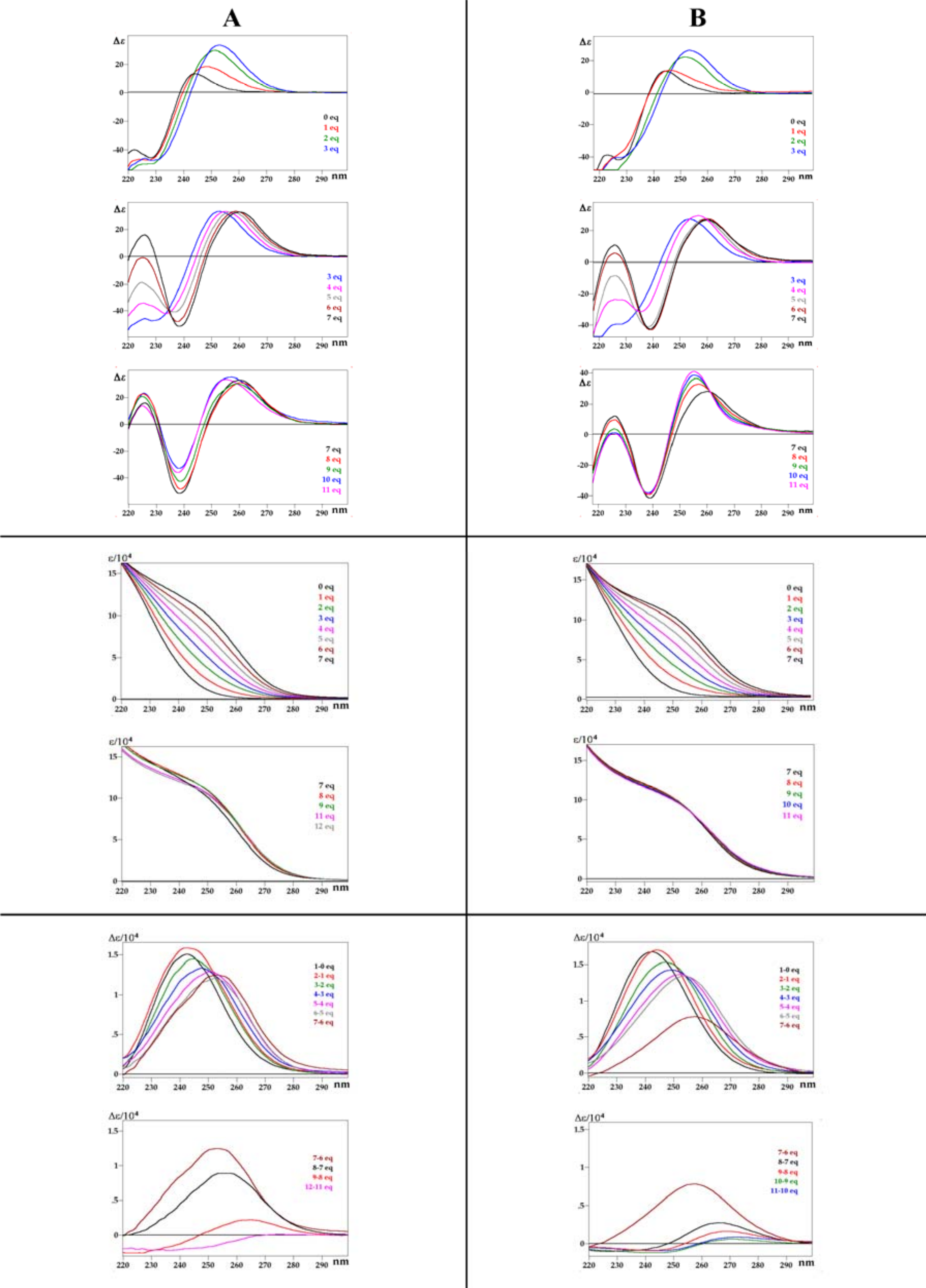

Figure S2.- Comparison of the behavior of (**A**) Zn_7-MT1/Tris-HCl and (**B**) Zn_7-MT1/Tris-$HClO_4$ toward Cd(II) through the CD, UV-vis, and UV-vis difference spectra recorded during their respective titrations with $CdCl_2$ or $Cd(ClO_4)_2$ at pH 7. Data regarding Zn_7-MT1/Tris-HCl are from [7,11].

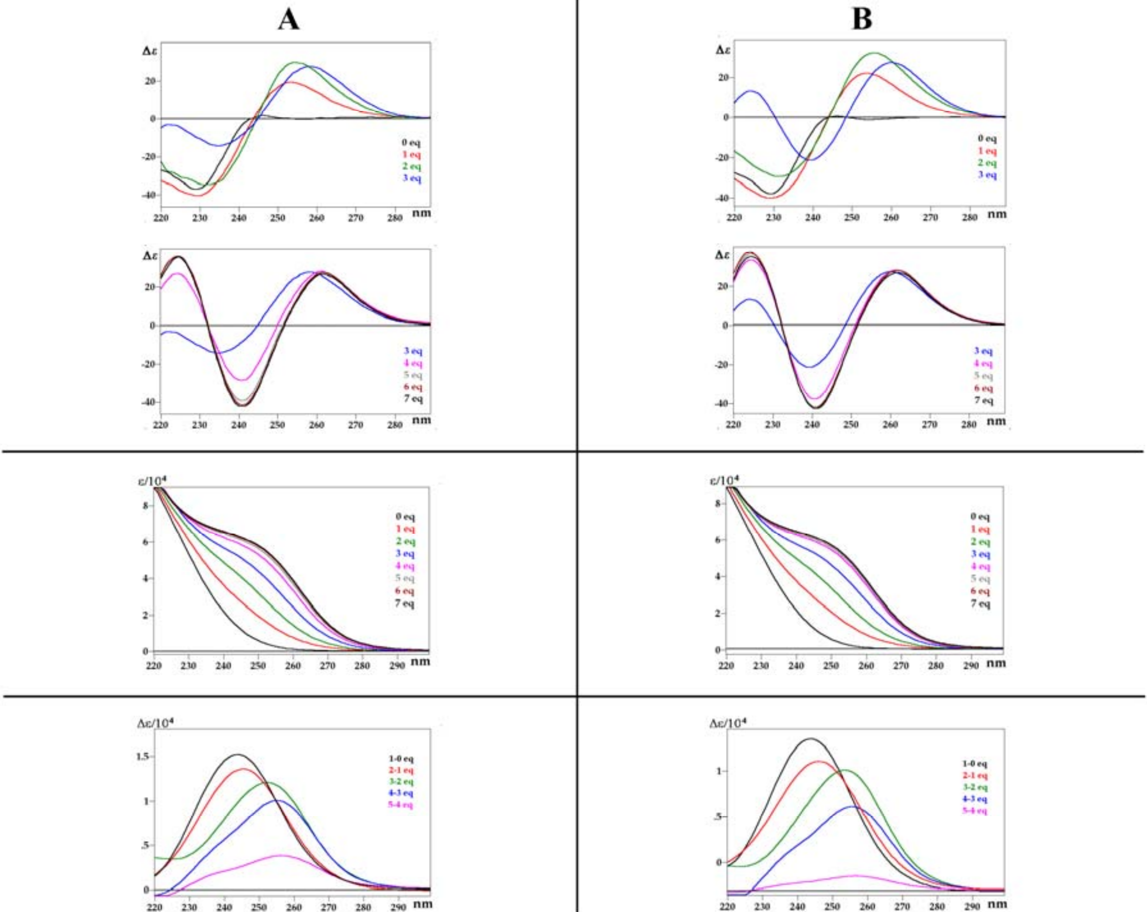

Figure S3.- Comparison of the behavior of (**A**) Zn_4-αMT4/Tris-HCl and (**B**) Zn_4-αMT4/Tris-$HClO_4$ toward Cd(II) through the CD, UV-vis, and UV-vis difference spectra recorded during their respective titrations with $CdCl_2$ or $Cd(ClO_4)_2$ at pH 7. Data regarding Zn_4-αMT4/Tris-HCl are from [6].

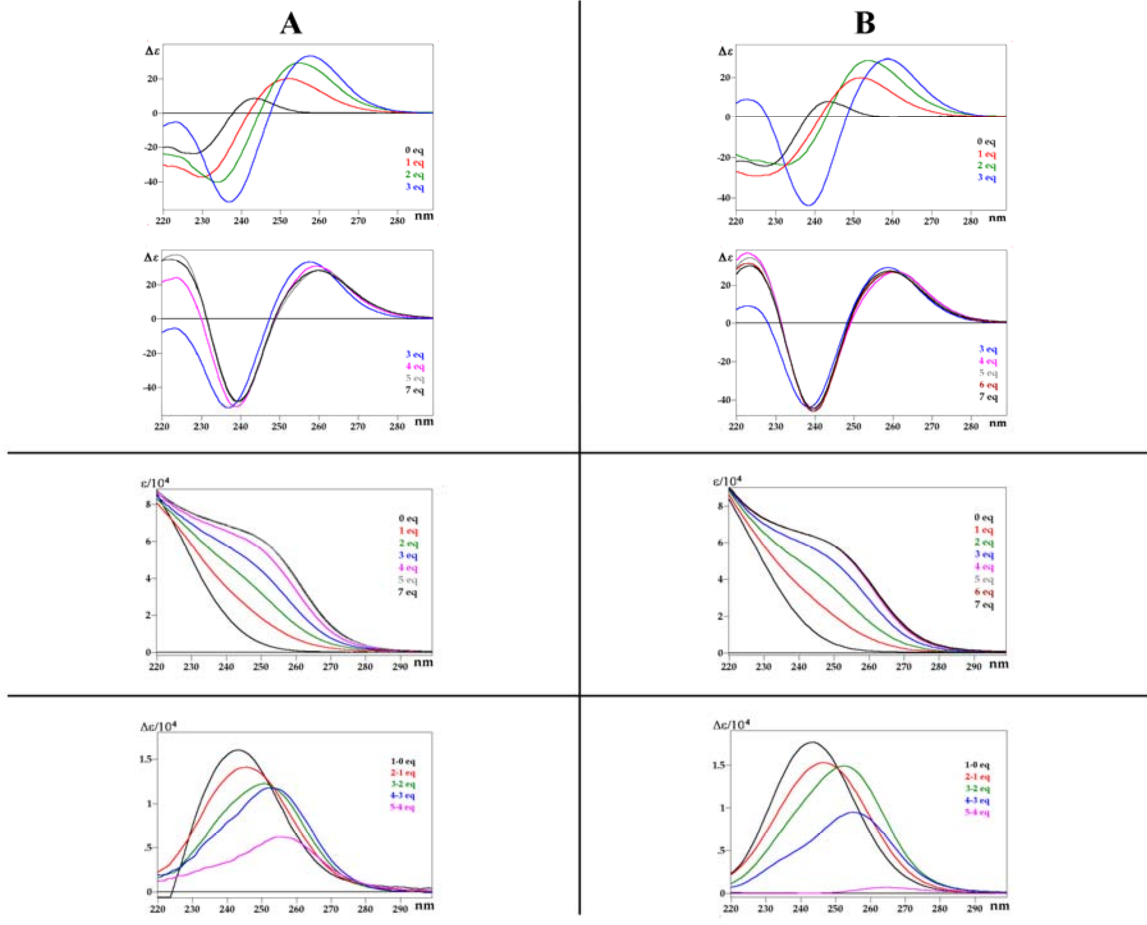

Figure S4.- *Comparison of the behavior of (**A**) Zn_4-αMT1/Tris-HCl and (**B**) Zn_4-αMT1/Tris-$HClO_4$ toward Cd(II) through the CD, UV-vis, and UV-vis difference spectra recorded during their respective titrations with $CdCl_2$ or $Cd(ClO_4)_2$ at pH 7. Data regarding Zn_4-αMT4/Tris-HCl are from [8].*

	Cd(II) equivalents added																	
	1		3		4		5		6		7		8		11		15	
	Cl^-	ClO_4^-	Cl^-	ClO_4^-	Cl^-	ClO_4^-	Cl^-	ClO_4^-	Cl^-	ClO_4^-	Cl^-	ClO_4^-	Cl^-	ClO_4^-	Cl^-	ClO_4^-	Cl^-	ClO_4^-
Zn_7-MT4	✓	--	◆															
Zn_6Cd_1-MT4	x	--	x															
Zn_5Cd_2-MT4	x	--	x	--	◆													
Zn_4Cd_3-MT4	x	--	✓	--	x	--	◆											
Zn_3Cd_4-MT4	x	--	x	--	✓	--	x	--	◆	◆								
Zn_2Cd_5-MT4	◆	--	x	--	✓	--	✓	--	x	x	◆	◆		◆		◆		
Zn_1Cd_6-MT4					x	--	x	--	✓	x	x	x	◆	x	◆	x	◆	◆
Cd_7-MT4					◆	--	x	--	x	✓	✓	✓	✓	✓	✓	✓	✓	✓

Table S1.- Distribution of the metal aggregates present in solution, according to ESI-MS data, during the titration of Zn_7-MT4/Tris-HCl and Zn_7-MT4/Tris-$HClO_4$ toward Cd(I) with $CdCl_2$ or $Cd(ClO_4)_2$, respectively, at pH 7 as a function of the number of Cd(II) equivalents added. Data regarding Zn_7-MT4/Tris-HCl + $CdCl_2$ are from [6]. ✓ denotes the major species; x, species of intermediate abundance and ◆, the minor species present in solution

	Cd(II) equivalents added									
	2		4		7		9		11	
	Cl^-	ClO_4^-	Cl^-	ClO_4^-	Cl^-	ClO_4^-	Cl^-	ClO_4^-	Cl^-	ClO_4^-
Zn_7-MT1										
Zn_6Cd_1-MT1	x	◆								
Zn_5Cd_2-MT1	x	x	x							
Zn_4Cd_3-MT1	✓	✓	x	x						
Zn_3Cd_4-MT1	x	x	✓	✓						
Zn_2Cd_5-MT1	◆	x	✓	✓	◆	◆	◆		◆	
Zn_1Cd_6-MT1		◆	x	x	◆	x	x	x	x	◆
Cd_7-MT1			◆	◆	✓	✓	✓	✓	✓	✓
Zn_2Cd_6-MT1							x		x	
Zn_1Cd_7-MT1						◆	x	◆	x	x
Cd_8-MT1						x	◆	x	◆	x

Table S2.- Distribution of the metal aggregates present in solution, according to ESI-MS data, during the titration of Zn_7-MT1/Tris-HCl and Zn_7-MT1/Tris-$HClO_4$ toward Cd(I) with $CdCl_2$ or $Cd(ClO_4)_2$, respectively, at pH 7 as a function of the number of Cd(II) equivalents added. Data regarding Zn_7-MT1/Tris-HCl + $CdCl_2$ are from [11]. ✓ denotes the major species; x, species of intermediate abundance and ◆, the minor species present in solution

	Cd(II) equivalents added									
	1		3		4		5		9	
	Cl^-	ClO_4^-	Cl^-	ClO_4^-	Cl^-	ClO_4^-	Cl^-	ClO_4^-	Cl^-	ClO_4^-
Zn_4-αMT4	✓	--								
Zn_3Cd_1-αMT4	✓	--	◆							
Zn_2Cd_2-αMT4	x	--	x	◆						
Zn_1Cd_3-αMT4	◆	--	✓	✓	◆	◆				
Cd_4-αMT4		--	x	x	✓	✓	✓	✓	✓	--

Table S3.- Distribution of the metal aggregates present in solution, according to ESI-MS data, during the titration of Zn_4-αMT4/Tris-HCl and Zn_4-αMT4/Tris-$HClO_4$ toward Cd(I) with $CdCl_2$ or $Cd(ClO_4)_2$, respectively, at pH 7 as a function of the number of Cd(II) equivalents added. Data regarding Zn_4-αMT4/Tris-HCl + $CdCl_2$ are from [6]. ✓ denotes the major species; x, species of intermediate abundance and ◆, the minor species present in solution

	Cd(II) equivalents added							
	2		3		4		7	
	Cl^-	ClO_4^-	Cl^-	ClO_4^-	Cl^-	ClO_4^-	Cl^-	ClO_4^-
Zn_4-αMT1		◆						
Zn_3Cd_1-αMT1	x	x		x				
Zn_2Cd_2-αMT1	✓	✓	◆	x				
Zn_1Cd_3-αMT1	x	x	✓	✓	◆	◆	◆	◆
Cd_4-αMT1	◆	x	◆	✓	✓	✓	✓	✓

Table S4.- Distribution of the metal aggregates present in solution, according to ESI-MS data, during the titration of Zn_4-αMT1/Tris-HCl and Zn_4-αMT1/Tris-$HClO_4$ toward Cd(I) with $CdCl_2$ or $Cd(ClO_4)_2$, respectively, at pH 7 as a function of the number of Cd(II) equivalents added. Data regarding Zn_4-αMT1/Tris-HCl + $CdCl_2$ are from [8]. ✓ denotes the major species; x, species of intermediate abundance and ◆, the minor species present in solution

Article 3

Zn- and Cd-Metallothionein Recombinant Species from Most Diverse Phyla May Contain Sulfide (S^{2-}) Ligands

Angewandte Chemie International Edition, 2005, **44**, 4618-4622

Bioinorganic Chemistry

Zn– and Cd–Metallothionein Recombinant Species from the Most Diverse Phyla May Contain Sulfide (S^{2-}) Ligands**

Mercè Capdevila, Jordi Domènech, Ayelén Pagani, Laura Tío, Laura Villarreal, and Sílvia Atrian*

After much multidisciplinary research into metallothioneins (MTs), the ubiquitous metal-binding proteins first described by Vallee and Margoshes[1] in 1957, there is still little information on the structures and functions[2,3] of the biological metal–MT complexes. There are two main obstacles to studying the physiological features of MTs. First, although MTs are present in all living organisms except Eubacteria, most of the existing data refers to mammalian MTs, which precludes any homology-driven structural, functional, or evolutionary inference because of the extreme sequence heterogeneity of this family of metalloproteins (see http://www.biochem.unizh.ch/mtpage/MT.html). Second, the difficulties encountered when trying to obtain homogeneous native preparations have led to the common utilization of in vitro reconstituted metal–MT complexes, based on the assumption that they represent genuine structural and functional native MT species. Thus, most of the data available to date, especially referring to MT structure, comes from nonbiological characterization of metal–MT complexes.[4] Following the MT discovery, another class of eukaryote metal-coordinating molecules was reported in plants and fungi: the enzymatically synthesized γ-glutamyl (γ-EC) peptides, also called phytochelatins and cadystins, which have always been considered as providing a very different mechanism of metal detoxification compared to the gene-encoded MTs, sharing few, if any, structural and functional features with them. From the chemical point of view, MTs bind a variety of metal ions giving rise to individual polynuclear clusters that are linked exclusively to cysteine residues through thiolate bonds. In contrast, γ-EC peptides create oligomeric clusters with a variable number of units that, most significantly, include acid-labile sulfide (S^{2-}) ions as additional ligands which induce the clusters to evolve to peptide-coated particles, so-called crystallites.[5]

Herein, we report the first definite evidence that sulfide ions are also present in nearly all the recovered Zn^{II}–MT and Cd^{II}–MT complexes, but never in the Cu^{I}–MT species of a wide range of recombinant metal–MT aggregates, thus sulfide ions are found in species formed in vivo, that is, in a physiological, although heterologous, environment. We have determined the presence of the acid-labile S^{2-} ligands both qualitatively and quantitatively by analytical, spectroscopic, and spectrometric techniques, and it is clear that the features of the recovered Zn^{II}–MT and Cd^{II}–MT complexes correlate well with those reported for plant and yeast Zn– or Cd–γ-glutamyl peptides,[5] therefore bridging the behavior gap between both types of metal-binding molecules.

Recombinant expression in *E. coli* has permitted the routine synthesis of a large number of proteins that are difficult or even impossible to obtain in their native forms. MTs stand out among them because of their extreme complexity and heterogeneity. Nearly ten years ago we developed an *E. coli* expression system that allows the biosynthesis of intact Zn^{II}–, Cd^{II}–, and Cu^{I}–MT complexes, isolated domains, and mutant variants, in sufficient quantity and purity for analytical, spectrometric, and spectroscopic characterization. As a first characterization on the mouse Zn–MT1 system[6,7] fully validated the correspondence between native and recombinant complexes, research was expanded to mammalian MT isoforms (MT1[8–10] and MT4[11]), the crustacean MTH,[12] *Drosophila* MTs (MTN[13] and MTO[14]), and the plant *Quercus suber* QsMT.[15]

We are now focused on studying MT species from the most diverse taxa (Table 1) and in the course of this work we found that many experimental results from analyzing Zn–MT, and particularly Cd–MT complexes, made little sense, as shown in Table 1. First, the stoichiometry of the Cd–MT complexes determined by inductively coupled plasma atomic emission spectroscopy (ICP-AES) was unusually low in comparison with the values expected from the corresponding Zn–MT complexes and the number of cysteine residues available for metal coordination. The metal-binding stoichiometries are assessed directly from the total sulfur and metal content of the sample provided by ICP-AES,[16] assuming that the total sulfur in the preparation arises from the summation of cysteine and methionine residues within the polypeptide. The unusually low stoichiometries calculated first suggested a partial oxidation of thiol groups and consequent loss of MT metal-binding capacity, but the Ellman reaction[17] quantification of the thiol groups in the samples did not support this prediction. Furthermore, ESI-MS analyses of most of the Cd–MT isolates revealed, besides the expected species, the presence of complexes whose mass did not match any

[*] Dr. M. Capdevila, L. Villarreal+
Departament de Química
Facultat de Ciències
Universitat Autònoma de Barcelona
08193 Bellaterra, Barcelona (Spain)
Fax: (+34) 93-581-3101
E-mail: merce.capdevila@uab.es

J. Domènech,+ A. Pagani,+ L. Tío,+ Prof. S. Atrian
Departament de Genètica
Facultat de Biologia
Universitat de Barcelona
Av. Diagonal 645, 08028 Barcelona (Spain)

[+] These authors contributed equally to this work.

[**] This work was financially supported by the Spanish Ministerio de Educación y Ciencia (grants BIO2003-03892 to S.A. and CTQ2004-00359/BQU to M.C.). We thank the Serveis Científico-Tècnics de la Universitat de Barcelona and the Servei d'Anàlisi Química de la Universitat Autònoma de Barcelona for allocating instrument time. We thank Dr. I. Casals for his help in setting up the GC-FPD assay, and Dr. R. Bofill for manuscript comments. The cDNA clone of *S. purpuratus* MT (SpMTA), for which full characterization is in progress, was kindly provided by J. Kägi (Zürich, Switzerland). Finally, we are indebted to D. Winge (Utah, USA) for an invigorating exchange of ideas.

Supporting information for this article is available on the WWW under http://www.angewandte.org or from the author.

 © 2005 Wiley-VCH Verlag GmbH & Co. KGaA, Weinheim DOI: 10.1002/anie.200501183 Angew. Chem. Int. Ed. 2005, 44, 4618–4622

Table 1: Analytical characterization of several purified metal–MT aggregates, corresponding to organisms of the most diverse taxa.[a]

Metal–MT	[MT][b] [×10^{-4} M]	[MT][c] [×10^{-4} M]	Metal/MT[d]	Metal/MT[e]	$AgNO_3$ test	S^{2-}/MT[f] (GC-FPD)	ESI-MS major species
Zn-QsMT	2.62	2.18	2.3	3.9	+	1.90	Zn_4-QsMT[15]
Cd-QsMT	1.49	0.58	2.5	6.5	+	3.44	Cd_6S_5-QsMT[15]
Cu-QsMT	0.29	0.26	5.8[g]	7.2[g]	–	n.d.	M_8-QsMT[15]
Zn-CRS5	1.72	1.67	5.7	5.8	–	0.44	Zn_6-CRS5[h]
Cd-CRS5	6.01	0.92	3.4	8.5	+	1.85	Cd_8-CRS5[h]
Cu-CRS5	3.22	3.16	11.3	11.4	–	n.d.	Cu_{11}-CRS5[h]
Zn-MTN	0.40		3.5				Zn_4-MTN[13]
Cd-MTN	1.80	0.80	1.7	3.8	+	2.34	Cd_4-MTN[h]
Cu-MTN	0.42		7.0		–		Cu_8-MTN[13]
Zn-MTO	0.78	0.63	3.2	3.7		0.90	Zn_4-MTO[14]
Cd-MTO	0.50	0.30	3.2	4.1	+	2.63	Cd_4-MTO[h]
Cu-MTO	0.37		8.9		–		Cu_9-MTO[14]
Zn-SpMTA	1.40	1.22	5.2	5.6	+	2.33	Zn_8/Zn_7S_2-SpMTA[h]
Cd-SpMTA	0.81	0.62	6.3	7.2	+	3.62	Cd_7-SpMTA[h]
Cu-SpMTA	0.41	0.39	7.1[g]	7.1[g]	–	n.d.	M_8-SpMTA[h]
Zn-ckMT	1.51	1.09	5.5	7.5		3.75	Zn_7-ckMT[h]
Cd-ckMT	2.29	0.63	3.7	8.8	+	4.70	Cd_7-ckMT[h]
Cu-ckMT	0.39		9.9[g]		–	n.d.	M_{10}-ckMT[h]
Zn-MT1	1.38	1.13	6.0	7.3		1.50	Zn_7-MT1[7]
Cd-MT1	1.90	1.13	3.7	6.4	+	3.17	Cd_7-MT1[11]
Cu-MT1	0.13		9.6[g]		–	n.d.	M_{10}-MT1[10]
Zn-MT4	2.18	1.18	6.7	7.0		3.5	Zn_7-MT4[11]
Cd-MT4	0.19	0.11	5.5[g]	6.9[g]	+	14	M_7-MT4[11]
Cu-MT4	0.36		9.4		–	n.d.	Cu_{10}-MT4[11]

[a] QsMT = *Quercus suber* MT; CRS5 = a *S. cerevisiae* MT; MTN and MTO are *Drosophila* MT forms; SpMTA = *S. purpuratus* type A MT; ckMT = chicken MT; MT1 = mammalian isoform 1 MT; MT4 = mammalian isoform 4 MT. Equivalent analyses with *T. pyriformis* MT1, *C. elegans* MT2, and *M. edulis* MT10IV yielded comparable results with regard to the presence of sulfide in their metal–MT complexes (data not shown). [b] Protein concentration calculated from conventional ICP-AES results. [c] Protein concentration calculated from acid ICP-AES results. Amino acid analysis led to identical values ±0.01. [d] Metal/MT ratio deduced from the metal content measured by conventional ICP-AES and results in (b). [e] Metal/MT ratio deduced from the metal content measured by ICP-AES and the acid ICP-AES and the results in (c). [f] n.d. = not detectable. [g] In this case, the metal/MT ratio represents the mean metal content per MT of preparations which had heterometallic composition (Zn and Cu or Zn and Cd). [h] This work. The corresponding manuscripts including the full MT characterization are in preparation.

possible Cd^{II} metallated complexes. These unknown mass peaks did not arise from the presence of other metal ions in putative heterometallic MT species, as Cd was the only metal detected by ICP-AES. Finally, circular dichroism (CD) spectroscopy of the Cd–MT samples showed features in the 260–280 nm range that clearly were not attributable to the known tetrahedral $Cd(SCys)_4$ chromophores that absorb at approximately 250 nm, which were also present in the spectra (Figure 1).

At this stage, the most likely explanation for our observations was the presence of an additional ligand in the purified Zn–MT and Cd–MT species, but none of the reported possibilities (chloride participation,[18] phosphate-driven dimerization[19]) were consistent with the analytical and spectral features of the samples. However, transitions between 260 and 300 nm have been reported in the CD spectra of Cd-phytochelatins containing sulfide anions[5,20] and we have already suggested that these ligands could be present in *Drosophila* Cd–MTN species.[13] The presence of extra sulfur in our samples as sulfide ligands would provide a sound explanation for all the bizarre results mentioned above as well as the negative oxidation degrees measured by reactions with the 3,3′-dithiobis(6-nitrobenzoic acid) (DTNB).[21] Therefore, we performed a quick test[22] to assess the presence of S^{2} ions in our panel of recombinant metal–MTs by determining hydrogen sulfide gas generation after acidification of the samples with HCl. Blackening of a filter paper moistened with a solution of $AgNO_3$ which was capping the sample tube, as a consequence of silver sulfide precipitation, unequivocally identified the presence of sulfide in all the Cd–MT and some Zn–MT samples, but not from the control (sample without MT) or any Cu–MT preparations.

Zn–, Cd–, and Cu–MT species from different taxa were analyzed more thoroughly to determine whether sulfide ion binding was common in the diverse metal–MT complexes. If sulfide ions were present, then the ICP-AES approach for global metal–MT ratio calculation was not valid, as the sulfur quantization would not report exclusively on Cys and Met

 © 2005 Wiley-VCH Verlag GmbH & Co. KGaA, Weinheim

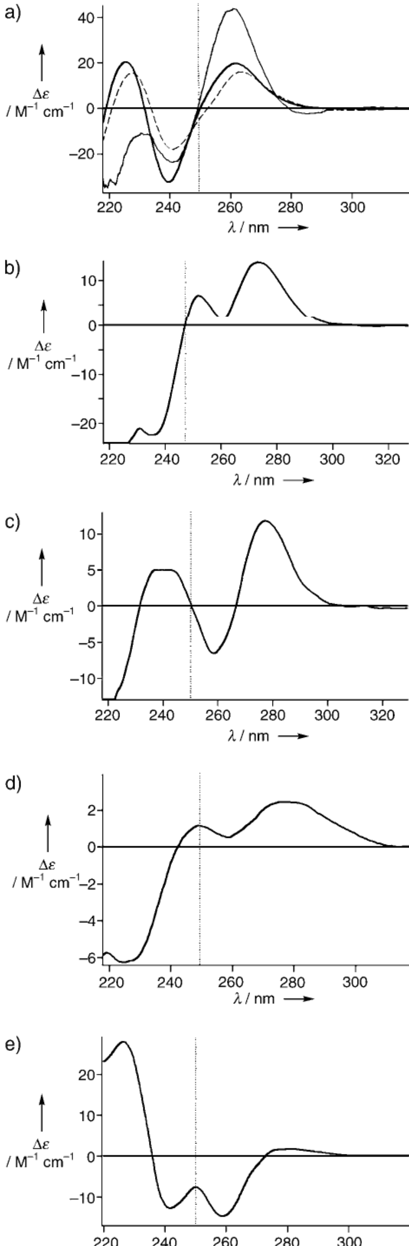

Figure 1. Representative CD spectra of several Cd–MT species from the most diverse taxa. Spectra have been grouped as a) type A (conventional spectra expected for Cd–MT species): Cd–MT1 (solid black line), Cd–SpMTA (solid gray line), and Cd–ckMT (dashed black line); b) type B: Cd–QsMT; c) type C: Cd–MTN; d) type D: Cd-CRS5; e) type E: Cd–MTO. All spectra show the characteristic absorption features of the $Cd(SCys)_4$ chromophores at approximately 250 nm (vertical dotted line) either as derivative shaped signals of different signs (A and B versus C), Gaussian bands (D) or more complex absorptions mixed with chloride participation[18] in Cd binding (E). The most (B, C, D and E) and least (A) intense absorptions at approximately 280 nm could be attributed to the presence of $Cd{-}S^{2-}$ bonds.

concentrations. Protein concentrations were then redetermined simultaneously by two methods: acid ICP-AES and amino acid analysis. Acid ICP-AES involves acidification of the sample with 1 M HCl prior to the conventional method[16] to favor the loss of the acid-labile ligands such as H_2S and thus ensure that all the sulfur remaining in the sample corresponded to Cys and Met. Acid ICP-AES results gave new metal–MT ratios that were now highly consistent with the expected stoichiometries (Table 1). The amino acid analysis was used to quantify protein levels, and these data nicely matched those obtained by acid ICP-AES. Finally, considering single or multiple 32 Dalton (sulfur atomic weight) additions to the value of the mass of the canonical metal–MT species yielded values that were coincident with the unassigned ESI-MS peaks of the sample.

We attempted quantification of the sulfide content in all the samples, initially using a methylene blue method[23] similar to that applied for Cd–phytochelatin analyses.[20] However, this method has serious drawbacks, as some degree of interference with cadmium ions has been reported[24] and it is not suitable for samples containing copper owing to the insolubility of copper sulfide. As a consequence, we adapted a GC-FPD (flame photometric detector) approach initially reported for solid samples.[25] Both methods gave consistent results and permitted the mean S^{2} ion content per MT to be determined (Table 1). These data demonstrated that acid-labile sulfide was present in all the recombinant Cd–MT samples and in many Zn–MT isolates, although always at lower ratios than in the corresponding Cd–MT samples. Furthermore, ESI-MS analyses of the Zn– and Cd–MT preparations not only accounted for the presence of S^{2} ions as additional ligands but also showed coexistence of S^{2}-containing and S^{2}-devoid metal–MT species (Figure 2), indicating an equilibrium between the two forms in the original preparations. None of the MT proteins synthesized in Cu-supplemented media gave any evidence of sulfide ligands in their complexes. All of these findings are consistent with the features reported for the presence/absence of sulfide in Zn– or Cd–, and Cu–phytochelatins, respectively.[5,26] As for the spectroscopic analyses, evidence that sulfide in the Cd–MT complexes is associated with absorptions in the 260–280 nm range came from acidification/reneutralization experiments(see Supporting Information).

The data presented herein support the hypothesis that recombinant synthesis in *E. coli* of diverse MTs results in the recovery of sulfide-containing complexes in addition to the expected non-sulfide-containing canonical species. This is the first demonstration that Zn–MT and Cd–MT species have the capacity to form Zn- and Cd-thiolate complexes in which labile sulfide ligands contribute to the Zn^{II} and Cd^{II} binding.

This situation has major practical and theoretical implications. From a practical point of view, it is important that the ever-growing community of MT researchers using recombinant strategies to produce metal–MT complexes evaluates the presence of S^{2} in their preparations to attain a true interpretation of their analytical, spectroscopic, and spectrometric data. From a theoretical angle, the presence of S^{2} ions in metal–MT aggregates raises significant questions. Because of the observed metal and protein dependency and the

 © 2005 Wiley-VCH Verlag GmbH & Co. KGaA, Weinheim

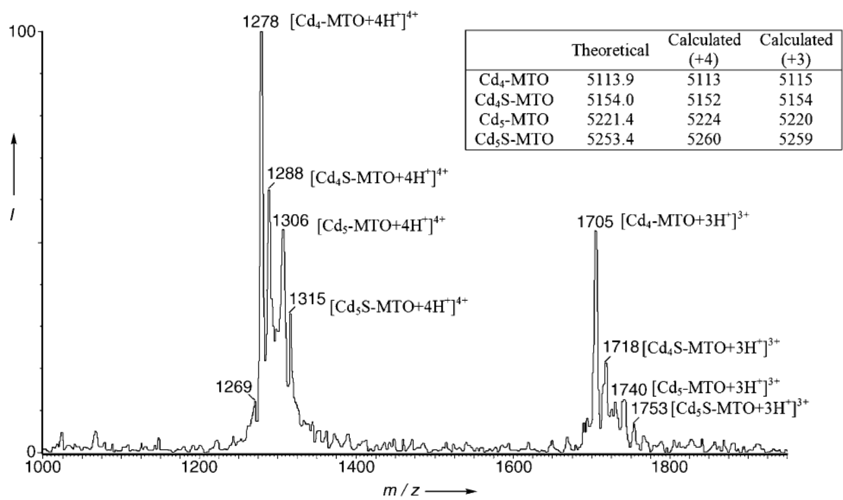

	Theoretical	Calculated (+4)	Calculated (+3)
Cd_4-MTO	5113.9	5113	5115
Cd_4S-MTO	5154.0	5152	5154
Cd_5-MTO	5221.4	5224	5220
Cd_5S-MTO	5253.4	5260	5259

Figure 2. ESI-MS spectrum of the recombinant Cd–MTO preparation. The two sets of peaks corresponding to two charge states (+4 and +3) are shown, to illustrate the coexistence of sulfide-loaded and sulfide-devoid Cd–MTO forms. The table gives the corresponding molecular weights of the species as calculated from the MS data and predicted.

equilibrium between S^2 -containing and S^2 -devoid forms, it is unlikely that S^2 binding is a mere artifact, thus it is pertinent to ask if sulfide incorporation also occurs in endogenous metal–MT complexes, that is, in native forms. Should this be the case, it is intriguing why it has not been previously detected. A likely explanation is that for nearly half a century most of the MT research has been carried out using in vitro reconstituted metal–MT species, which are prepared by adding the corresponding metal ions to apo-MT (metal-devoid MT) polypeptides. These species are obtained after heavy acidification of the purified metal–MT forms and thus, any sulfide ions involved in the initial Zn^{II} or Cd^{II} complexation would be lost. Furthermore, the native isolates of MT complexes from many species contain significant heterogeneity of isoforms and metal compositions.[27,28] Therefore a lot of effort has been devoted to obtaining pure chromatographic fractions, which may involve discarding other minor metal–MT species originally present in the sample and that are assumed to be impurities, mixed-metal species, or simply, non-MT metal-containing aggregates.

The S^2 ion is a species not restricted to *E. coli*, but rather a universal cell component. At present, evidence is being gathered that relates the presence of S^2 ions with physiological events, which have also been proposed for MT function candidates (redox equilibrium,[29] neurotransmission, and neuromodulation[30]). Consequently, evaluation of the sulfide-binding MT capability in endogenous MT forms is worth considering in further studies of native MT forms, especially Zn–MT, as new data could shed light into the physiological significance of this poorly understood protein in view of the recently revised relationship between the biological and inorganic zinc clusters in nature.[31] But, in any case, knowledge of the capability of divalent metal–MTs to include S^2 ions in their aggregates, or in other words, to build metal-MT aggregates that include S^2 ions would be highly significant for structural, nanobiological, biotechnological, and biomedical applications in which MTs are involved. In conclusion, a new attribute must be added to the already long list of peculiar features of these versatile proteins.

Experimental Section

Zn–, Cd–, and Cu–MT complexes were synthesized according to a recombinant fusion-protein strategy (GST-MT) fully reported in references [6,7]. This method is based on cultures of *E. coli* cells transformed with the corresponding expression constructs in LB (Luria Bertini) medium supplemented with Zn^{II}, Cd^{II}, or Cu^{II} (300 µM, 300 µM, and 500 µM, respective final concentrations). After cell sonication, all the steps were performed under argon atmosphere. The total protein extract was only submitted to Glutathione-Sepharose affinity chromatography, thrombin digestion, and FPLC (fast performance liquid chromatography) in 50 mM Tris-HCl (Tris = 2-amino-2-(hydroxymethyl)-1,3-propanediol), pH 7.5 buffer. All MT complexes were synthesized and purified under identical conditions.

The molecular mass of the metal–MT species was determined by electrospray ionization mass spectrometry (ESI-MS) on a Fisons Platform II Instrument, equipped with MassLynx software and calibrated with horse-heart myoglobin (0.1 $mg mL^{-1}$). The assay conditions for the Zn- and Cd-containing species were as follows: 20 µL of protein solution injected at 40 $µL min^{-1}$; the use of an HPLC Uptisphere C_4 33 mm × 2 mm × 5 µm column to separate analytes; capillary counterelectrode voltage, 4.5 kV; lens counterelectrode voltage, 1.0 kV; cone potential, 60 V; source temperature, 120 °C; *m/z* range, 850–1950; scanning rate, 3 $s scan^{-1}$; interscan delay, 0.3 s. The assay conditions for the Cu-containing species were: 20 µL of protein solution injected at 30 $µL min^{-1}$; capillary counterelectrode voltage, 3.5 kV; lens counterelectrode voltage, 1.0 kV; cone potential, 35 V; source temperature, 160 °C; *m/z* range, 850–1950; scanning rate, 3 $s scan^{-1}$; interscan delay, 0.3 s. In all cases, the running buffer was an appropriate mixture of acetonitrile and 5 mM ammonium acetate/ammonia, pH 7.5.

Electronic absorption measurements were performed on an HP-8453 Diode array UV/Vis spectrophotometer. A Jasco spectropolarimeter (J-715) interfaced to a computer (GRAMS 32 Software)

 © 2005 Wiley-VCH Verlag GmbH & Co. KGaA, Weinheim

was used for CD determinations. The temperature for all measurements was kept at 25°C by means of a Peltier PTC-351S apparatus.

ICP-AES, using a Polyscan 61E (Thermo Jarrell Ash) spectropolarimeter, allowed determination of S (182.040 nm), Zn (213.856 nm), Cd (228.802 nm), and Cu (324.803 nm) sample contents. Two alternative methods were used: conventional ICP implied no previous sample treatment,[16] while acid ICP included acid incubation of the sample (1M HCl, 65°C, 5 min) prior to ICP measurements. In both cases, protein concentration was calculated from the S content, assuming it was only contributed to by the Cys and Met residues of the peptides. In addition, protein concentration was assessed by amino acid analysis (hydrolysis in 6M HCl at 110°C for 22 h) on an Alpha Plus Amino Acid Autoanalyzer (Pharmacia LKB). Ser, Lys, and Gly contents were used to extrapolate MT concentrations.

GC-FPD[32] was used as the most suitable methodology for direct (i.e. without sample derivatization) S^{2-} detection at low concentrations, since it presents a quadratic response to compounds including one unique S atom.[25] H_2S was generated by strong acidification (H_2SO_4, pH 0.0) of the sample to ensure disruption of the metal–MT complex and to avoid precipitation of insoluble ZnS and CdS. The calibration curve was determined with dilute standards of S^{2-} at 0, 0.25, 0.5, 1, 1.5, 2.5, and 3 ppm prepared from a stock solution of S^{2-} at 1000 ppm which was obtained by dissolving a single crystal of $Na_2S·9H_2O$ in oxygen-free water and standardized by iodine titration using $NaIO_3$.[22] Sample aliquots, as well as the standard solutions, were transferred to airtight 2-mL vials, acidified to a final volume of 0.5 mL, and immediately sealed. Vials were then incubated at 40°C for 2 h with agitation (250 rpm) to accelerate the evolution of H_2S from the aqueous phase and equilibration of gas phase in the headspace. 500 μL of the head-space gas were subjected to gas chromatography (HP5890 Serie II coupled to a FPD80CE Instruments (Thermo Finnigan) detector). The gaseous mixture was carried by a 6.6 mL min^{-1} flux of He through the GC glass column (SPB608 30 m × 0.25 mm i.d. with 0.5 μm particle size). Both the injection and the detection port were kept at 110°C while the column was operated at a constant temperature of 35°C. The H_2S peak generated from MT samples was readily identified by a retention time coincident with that of the standard solutions. All determinations were performed in duplicate with independent samples.

Received: April 4, 2005

Keywords: bioinorganic chemistry · cadmium · metallothioneins · S ligands · zinc

[1] M. Margoshes, B. Vallee, *J. Am. Chem. Soc.* **1957**, *79*, 4813–4814.
[2] R. Palmiter, *Proc. Natl. Acad. Sci. USA* **1998**, *95*, 8428–8430.
[3] P. Coyle, J. C. Philcox, L. C. Carey, A. M. Rofe, *Cell. Mol. Life Sci.* **2002**, *59*, 62–647.
[4] P. Gonzalez-Duarte in *Comprehensive Coordination Chemistry II, Vol. 8* (Eds.: J. A. McCleverty, T. J. Meyer), Elsevier-Pergamon, Amsterdam, **2003**, pp. 213–228.
[5] D. Winge, C. T. Dameron, R. K. Mehra in *Metallothioneins* (Eds.: M. J. Stillman, F. C. Shaw III, K. T. Suzuki), VCH, New York, **1992**, pp. 257–270.
[6] M. Capdevila, N. Cols, N. Romero-Isart, R. González-Duarte, S. Atrian, P. González-Duarte, *Cell. Mol. Life Sci.* **1997**, *53*, 681–688.
[7] N. Cols, N. Romero-Isart, M. Capdevila, B. Oliva, P. González-Duarte, R. González-Duarte, S. Atrian, *J. Inorg. Biochem.* **1997**, *68*, 157–166.
[8] N. Cols, N. Romero-Isart, R. Bofill, M. Capdevila, P. González-Duarte, R. González-Duarte, S. Atrian, *Protein Eng.* **1999**, *12*, 265–269.
[9] R. Bofill, O. Palacios, M. Capdevila, N. Cols, R. Gonzàlez-Duarte, S. Atrian, P. Gonzàlez-Duarte, *J. Inorg. Biochem.* **1999**, *73*, 57–64.
[10] R. Bofill, M. Capdevila, N. Cols, S. Atrian, P. González-Duarte, *J. Biol. Inorg. Chem.* **2001**, *6*, 405–417.
[11] L. Tío, L. Villarreal, S. Atrian, M. Capdevila, *J. Biol. Chem.* **2004**, *279*, 24404–24413.
[12] M. Valls, R. Bofill, R. González-Duarte, P. González-Duarte, M. Capdevila, S. Atrian, *J. Biol. Chem.* **2001**, *276*, 32835–32843.
[13] M. Valls, R. Bofill, N. Romero-Isart, R. Gonzàlez-Duarte, J. Abián, M. Carrascal, P. Gonzàlez-Duarte, M. Capdevila, S. Atrian, *FEBS Lett.* **2000**, *467*, 189–194.
[14] J. Domenech, O. Palacios, L. Villarreal, P. González-Duarte, M. Capdevila, S. Atrian, *FEBS Lett.* **2003**, *533*, 72–78.
[15] G. Mir, J. Domènech, G. Huguet, W. Guo, P. Goldsbrough, S. Atrian, M. Molinas, *J. Exp. Bot.* **2004**, *55*, 2483–2493.
[16] J. Bongers, C. D. Walton, D. E. Richardson, J. U. Bell, *Anal. Chem.* **1988**, *60*, 2683–2686.
[17] W. Birchmeier, P. Christen, *FEBS Lett.* **1971**, *18*, 209–213.
[18] L. Villarreal, L. Tío, S. Atrian, M. Capdevila, *Arch. Biochem. Biophys.* **2005**, *435*, 331–335.
[19] P. Palumaa, M. Vasak, *Eur. J. Biochem.* **1992**, *205*, 1131–1135.
[20] R. N. Reese, D. R. Winge, *J. Biol. Chem.* **1988**, *263*, 12832–12835.
[21] D. N. Weber, F. Shaw III, D. H. Petering, *J. Biol. Chem.* **1987**, *262*, 6962–6964.
[22] A. I. Vogel in *A Text-Book of Macro and Semimicro Qualitative Inorganic Analysis*, Longmans, **1954**, p. 335.
[23] In *Standard Methods for the Examination of Water and Wastewater* (Eds. L. S. Clesceri, A. E. Greenberg, A. D. Eaton), American Public Health Association, Washington D. C., **1998**.
[24] T. E. King, R. O. Morris, *Methods Enzymol.* **1967**, *10*, 634–637.
[25] A. Marcó, R. Compañó, R. Rubio, I. Casals, L. Krotz, L. Ragaglia, G. Giazzi, *Analyst* **2001**, *126*, 1820–1825.
[26] R. N. Reese, R. K. Mehra, E. B. Tarbet, D. R. Winge, *J. Biol. Chem.* **1988**, *263*, 4186–4192.
[27] J. H. R. Kägi, S. R. Himmelhoch, P. D. Whanger, J. L. Bethune, B. L. Vallee, *J. Biol. Chem.* **1974**, *249*, 3537–3542.
[28] D. R. Winge, R. Premakumar, K. V. Rajagopalan, *Arch. Biochem. Biophys.* **1975**, *170*, 242–252.
[29] W. Maret, *Biochemistry* **2004**, *43*, 3301–3309.
[30] D. E. Barañano, C. D. Ferris, S. H. Snyder, *Trends Neurosc.* **2001**, *24*, 99–106.
[31] C. Blindauer, P. Sadler, *Acc. Chem. Res.* **2005**, *38*, 62–69.
[32] T. Ubuka, *J. Chromatogr. B* **2002**, *781*, 227–249.

Supporting Information

© Wiley-VCH 2005

69451 Weinheim, Germany

Zn- and Cd-Metallothionein Recombinant Species from the Most Diverse Phyla May Contain Sulfide (S^{2-}) Ligands**

Mercè Capdevila, Jordi Domènech,# Ayelén Pagani,# Laura Tío,# Laura Villarreal,# & Sílvia Atrian*

Experimental Procedures.

Expression and purification of the recombinant MT domains: To overexpress MT the recombinant constructs were introduced into the protease deficient strain *E.coli* BL21. Overnight cultures of the transformed host strains in LB supplemented with 100 mg l^{-1} ampicillin at 37 °C were inoculated to a x10 fresh medium volume. After growth at 37 °C to an A600 value of 1.0, the bacteria were induced with 0.1 mM isopropyl-β-D-thiogalactopyranoside (IPTG, final concentration and bacteria growth was allowed for 30 min. The culture was then supplemented with and the corresponding salt metal solution, as mentioned in the main text. After 2.5 h, the cell biomass was harvested, washed in phosphate-buffered saline 1.4 M NaCl, 27 mM KCl, 101 mM Na_2HPO_4, 18 mM KH_2PO_4 (PBS) and pelleted by centrifugation at 7700 x *g* for 10 min. For protein purification, cells were resuspended in 5% of the original volume of ice-cold PBS-0.5% v:v β-mercaptoethanol. To prevent oxidation of the metal-free cysteines, pure grade 5.6 argon was bubbled through all the steps of the purification procedure. Suspended cells were sonicated at 4 °C with 20 s pulses for 5 min, and centrifuged at 12000 x *g* for 15 min. The supernatant was recovered and used to purify the GST-MT and fusion protein by batch affinity chromatography with Gluthatione-Sepharose-4B (Pharmacia) at a volume ratio 1:10 matrix:sample. The mixture was incubated with gentle agitation for 30 min at room temperature. After three washes in PBS, the matrix was packed in a column (15 cm x 3 cm) for subsequent purification steps. The polylinker of the pGEX vector used included a thrombin recognition site, which allowed cleavage of the fusion protein. To that end, a thrombin-PBS solution (10 units of thrombin (Pharmacia)/mg of fusion protein) was poured into the matrix bed, and digestion was carried out overnight at 23–25 °C. The GST portion of the expressed fusion protein remained bound to the gel matrix, whereas the MT portion was eluted together with thrombin. The eluate was then five-fold concentrated using Centriprep Concentrators (Amicon) with a cutoff of 3 kD, and subsequently fractionated using FPLC. A Superdex-75 (Pharmacia) exclusion column was equilibrated with 50 mM Tris-HCl, pH 7.0 and run at 1 ml min^{-1}. 1 ml fractions were collected and analysed for protein content by their absorbance at 254 nm. Aliquots of the protein-containing Superdex-75 fractions were analysed by SDS-PAGE on 15% gels and stained with Coomassie Blue. Positive samples were pooled, and aliquots were stored at -70 °C for further use.

Figure S1. CD and UV-vis spectra associated with the acidification and reneutralization of Cd-MTN. The Cd-MTN preparation (**type C** CD spectra, Fig 1) was acidified with HCl 0.05M from pH 7.2 to 1.4 and afterwards reneutralized to pH 7.5 with NaOH 0.05M in an Ar atmosphere and the CD (a, b and d) and UV-vis (c and e) spectra recorded and corrected for dilution effects. Interestingly, acidification of the initial sample (major species: Cd_4-MTN; minor species Cd_3- and Cd_4S_2-MTN) provokes an increase in quirality that reaches its maximum at pH 3.6 (major species: Cd_4- and Cd_3-MTN; minor species Cd_2- and Cd_4S_2-MTN). Both ESI-MS and UV-vis data indicate the loss of both Cd^{2+} and S^{2-} ions, while CD data suggest a higher degree of folding for Cd_3- than for Cd_4-MTN. As expected, acidification until pH 1.4 results in all CD and UV absorptions being lost (b and c). Reneutralization from pH 1.4 to 7.5 (d and e) allows Cd^{2+} binding (major species: Cd_4- and Cd_3-MTN; no sulfide-containing species detected by ESI-MS) although a lesser degree of folding and a distinct 3D structure (**type D** CD spectra, Fig 1) is achieved (d). Comparison of the UV-vis spectra (g) of the initial (solid line) and final (dashed line) samples clearly reveals that S^{2-} ligands have been lost during the process. Plate f shows the superimposition of the normalized CD spectra of the initial sample, at pH 7.2, (solid black line); the intermediate sample, at pH 3.6, (solid gray line); and the reneutralized sample, at pH 7.5 (dashed line).

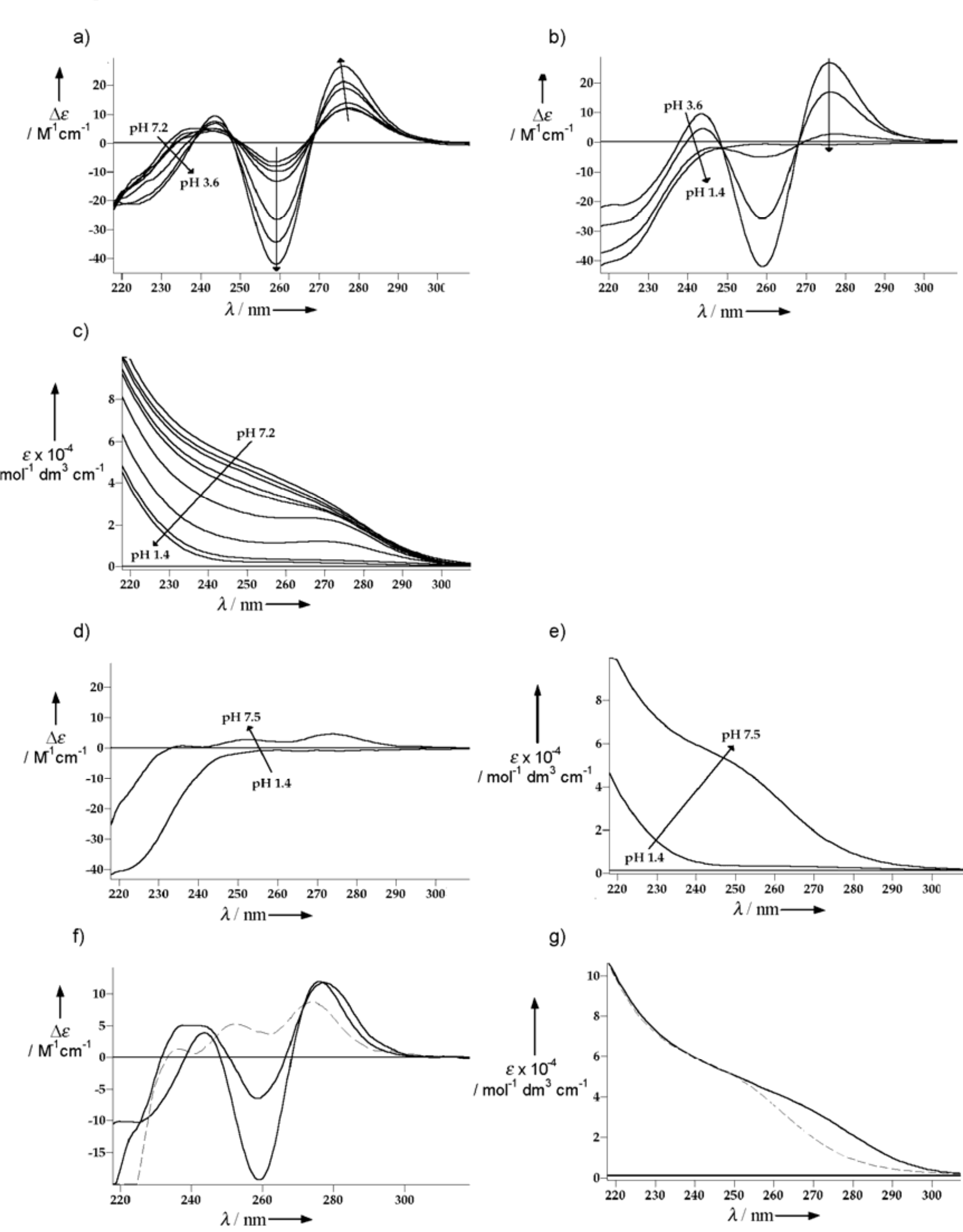
Figure S1.
a)
Δε / M-1cm-1
pH 7.2
pH 3.6
λ / nm
b)
Δε / M-1cm-1
pH 3.6
pH 1.4
λ / nm
c)
ε x 10-4 mol-1 dm3 cm-1
pH 7.2
pH 1.4
λ / nm
d)
Δε / M-1cm-1
pH 7.5
pH 1.4
λ / nm
e)
ε x 10-4 / mol-1 dm3 cm-1
pH 7.5
pH 1.4
λ / nm
f)
Δε / M-1cm-1
λ / nm
g)
ε x 10-4 / mol-1 dm3 cm-1
λ / nm

6. Annex

Articles i manuscrits elaborats amb posterioritat a la Comissió de Doctorat de Juny del 2005

Article 4

Metallothionein (MT) differentiation in warm-blooded Vertebrates.: Comparative Genomics and metal-binding analysis of chicken MT *vs.* mammalian forms.

FEBS Journal, **enviat el 19/07/2005**

Metallothionein (MT) differentiation in warm-blooded Vertebrates. Comparative Genomics and metal-binding analysis of chicken MT *vs.* mammalian forms.

Laura Villarreal[1*], Laura Tío[2*], Mercè Capdevila[1], Sílvia Atrian[2]

1 Departament de Genètica, Facultat de Biologia, Universitat de Barcelona, Barcelona, Spain

2 Departament de Química, Facultat de Ciències, Universitat Autònoma de Barcelona, Bellaterra, Spain

*These two authors contributed equally to this work

Keywords
dimerization; *Gallus gallus*; metal binding; Metallothionein; molecular evolution

Abbreviations
FPD, flame photometric detector; ICP-AES, inductively coupled plasma-atomic emission spectroscopy; MT, Metallothionein.

Correspondence
S. Atrian, Department of Genetics, Faculty of Biology, University of Barcelona, Av. Diagonal 64508028-Barcelona, SpainTel: +34934021501Fax: +34934034420e-mail: satrian@ub.edu

Chicken metallothionein (MT) is the paradigm for the study of these metal-binding proteins in avian vertebrate radiation. The available literature data depicted the ckMT gene/protein system as highly similar to mammalian MT1. The functional differentiation known for the four mammalian MT isoforms suggested it would be interesting to revisit avian MT. In this work, the ckMT metal binding abilities towards Zn(II), Cd(II) and Cu(I) have been determined and compared with those of mammalian MT1 and MT4 isoforms. Furthermore, an exhaustive *in silico* search for MT-like proteins in the chicken genome has enabled a comparative evolutionary study. The joint consideration of functional and genomic data reported here contradicts with the two main dogmas that until now have defined avian MTs. First, the singularity of an MT gene copy is contradicted by the identification of a chicken MT2 sequence showing all the features to be considered an active gene. Second, *in vivo* and *in vitro* metal-binding studies have revealed that the Zn(II), Cd(II) and Cu(I) binding abilities of ckMT1 lay between those of mammalian MT1 and MT4, being closer to those of MT1 for the divalent metal ions but more similar to those of MT4 for Cu(I). This is in agreement with the strong functional constraint of low copy genes having to cope with differentiating functional abilities. Finally, a new mechanism of MT dimerization is proposed, on the basis of the His C-terminal composition of the ckMT1 polypeptide.

Introduction

Metallothioneins (MTs), the ubiquitous metal-binding proteins first described by Vallee in 1957 [1] constitute a large superfamily of small, cysteine-rich peptides present in some prokaryotes and in all eukaryotes (protista and fungi, plants and animals) examined so far (*http://www.expasy.org/cgi-bin/lists?/metallo.txt*). The current limited knowledge of their origin and differentiation patterns can mainly be attributed to the lack of detailed, comparative studies involving MTs other than mammalian isoforms. Besides, it must be stressed that any homology-driven structural, biochemical or functional inference using mammalian MT data makes little sense, due to the extreme sequence heterogeneity among MT family members. Since no definite physiological roles have been assigned to MTs, functional constraints or adaptative trends modulating their evolutionary history are also difficult to envisage.

In this scenario, some attempts at evolutionary characterization have been carried out for Vertebrate MTs, an unquestionable family of homology, through the analysis of the maximum parsimony trees constructed with protein and cDNA MT sequences (http://www.biochem.unizh.ch/mtpage/poster/posterevol.html). These studies not only located fish, amphibian and avian MTs in increasing order of proximity to mammalian MT radiation, but also proposed that all vertebrate MTs originated from a single ancestor. Unfortunately, the level of gene and protein understanding of MTs in all non-mammalian groups is still too scarce to experimentally support this hypothesis. Avian MTs gather patent interest, as they represent a class of warm-blooded vertebrates that evolved in parallel to mammals for nearly 310 million years, after the late Palaeozoic divergence of the Reptilia/Aves and Mammalia lineages [2]. Chicken (*Gallus gallus*) is the model organism for avian molecular studies, and chicken MT (ckMT) has also been the paradigm for the characterization of avian MTs [reviewed in 3]. CkMT was isolated and roughly characterized in the early 70's as not significantly different from the mammalian (mouse) MT1-MT2 system [4,5]. CkMT protein and gene features enhanced the picture of high similarity between bird and mammalian forms, maybe dispiriting a deeper interest in avian MTs. CkMT is a 63-residue long polypeptide, with 68 % sequence similarity and two

amino acid insertions in relation to mouse MT1 [6]. Chicken MT cDNA [7] and gene [8] characterization, again suggested great structural and functional similarity with the mammalian MT system. Indeed, the *ckMT* gene showed the same exon/intron distribution and was apparently regulated by the same kind of *cis* elements, responding to the same stimuli: metal overdose, oxidative stress, glucocorticoids and lipopolysaccharides [9,10]. Only two differences were considered worthy of mention, the ontogenic expression pattern of liver ckMT, which acutely increases after hatching [11] and the apparently solid evidence that MT was a one-copy gene in birds [6,7]. Studies of other avian genera (*Meleagris gallopavo* (turkey), *Phasianus colchicus* (pheasant), *Colinus virginianus* (new world quail) [11]; *Cairina moschata* and *Anas platyrhyncos* (ducks) [12]; and *Coturnix coturnix* (quail) [13]) not only unanimously supported the inexistence of an MT gene family in birds, but also confirmed an exceptional conservation rate for the unique MT form: no amino acid substitution and 97 % identity at cDNA level, which was readily justified by the functional constraint imposed on a single copy gene. Description in *Columba livia* (pigeon) of two MT isoforms, none which were coincident with the previously reported avian MT sequence [14], was the sole evidence of MT multiplicity in an avian genome, and also of sequence diversity among avian MTs. The assumed simplicity of the avian MT system contrasts with the complexity of mammalian MT radiation, in which duplication events originated a four-gene cluster (MT1-MT4), identified in sheep, rodents, primates and humans, the MT1 further 13-fold amplified in the latter. Functional differentiation has been shown for these four isoproteins: the MT1-MT2 ubiquitous, metal-induced forms have been related to homeostasis, transport and detoxification of metals in organisms; MT3, only synthesized in neural tissues, has been related to neuronal growth; and a role for MT4 in the differentiation of stratified squamous epithelia, the only tissue in which it is expressed, has been suggested. Furthermore, and regarding their metal coordination abilities, while MT1 has been characterized as optimum for divalent metals (*Zn-thionein behaviour* [15]), MT4 exhibits a copper-binding preference that correlates well with a *copper-thionein* character [16]. Paradoxically, and although *older* in evolution, mammalian MT4 peptides are most similar among themselves (93.4% identity for mouse MT4 *vs.* human MT4) than in comparison to the MT1 isoform within the same organism (55.7% identity for mouse MT4 *vs.* mouse MT1), thus indicating a stronger functional constraint for MT4 than for MT1, albeit its apparently reduced expression pattern.

In this work, we focused our interest on chicken MT, in an attempt to determine its metal binding behaviour, and compare it with the mammalian MT1 and MT4 isoforms, previously characterized in our group by parallel methodological approaches. This was accomplished by determination of the spectroscopic and spectrometric features of the Zn-, Cd- and Cu-complexes rendered by the recombinant full-length ckMT1 and its separate ß and α domains, as well as of the metal species obtained by Zn/Cd or Zn/Cu *in vitro* replacement. Fortunately, in the course of this research, the annotation of the complete chicken genome was released [2], allowing us to perform an exhaustive *in silico* search for MT-like sequences, as well as the determination of synteny relationships between the MT gene containing regions in the human, rat and mouse genomes. Thus, evaluation of the avian *vs.* mammalian MT functional differentiation trends was completed by comparative genomics analyses. The joint consideration of function and genomic data presented here basically contradicts the two main *dogma* statements that have defined avian MTs until now: the singularity of gene copies and the full equivalence with mammalian MT1. In summary, these results will significantly contribute to the knowledge of the functional features that apparently determined distinct evolutionary pathways for birds and mammals MTs, the uppermost level of Vertebrate evolution.

Results and Discussion

Chicken genome search, Comparative Genomics and Protein Sequence Analysis

At the beginning of this study, a unique chicken MT gene, herein named ckMT1 and whose cDNA [7] was that cloned and heterologously expressed in this work, was known. It encodes an amino acid sequence that is absolutely conserved in all avian MTs, except for the two *Columba* forms, as shown in Fig. 1A. The most significant feature of this sequence is the presence at the C-terminal end of an His residue, absent in the mammalian forms, and highly interesting because this amino acid is a well-known metal ligand. Unexpectedly, when we searched the chicken genome (v.29.1) using this cDNA as a query, homology was detected in two different regions (Fig. 2). One of them (chromosome 11, contig 100.32) contained the ckMT1 gene. Although the sequence included in the Data Bank clones is discontinuous, its exon 3 sequence perfectly match those of the ckMT1 cDNA, and the size of the contiguous non-

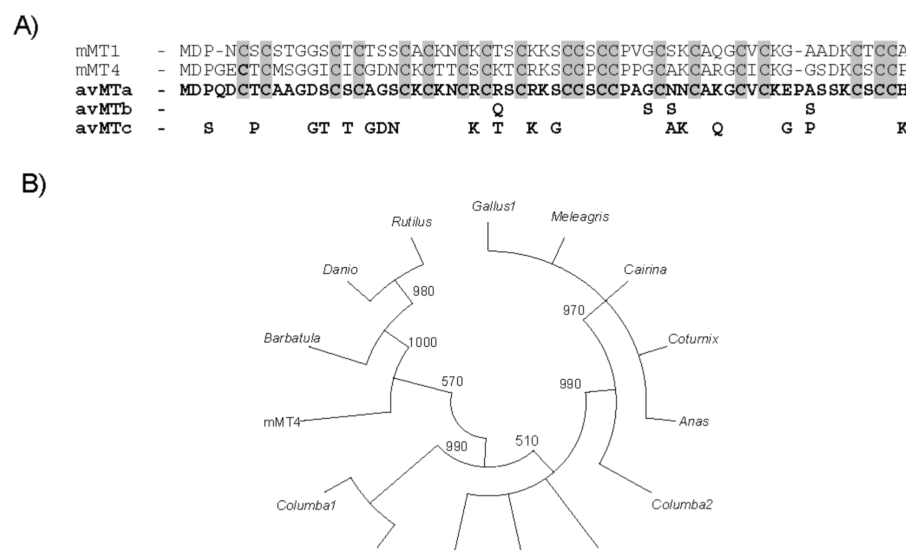

Fig. 1. A) ClustalW alignment of the known avian MT sequences, and the MT1 and MT4 mammalian forms. The shaded boxes indicate the cysteine residues. The **avMTa** sequence corresponds to the MT of *Gallus gallus 1, Cairina moschata, Meleagris gallopavo, Anas platyrhynchos* and *Coturnix japonica.* The **avMTb** is the *Columba livia 2* isoform. The **avMTc** sequence is found in the *Columba livia 1* and *Gallus gallus 2* isoforms. For avMTb and avMTc only the residues differing from avMTa are shown. B) Protein distance tree constructed with the amino acid sequences of the avian MT isoforms, the mammalian MT1, MT2 and MT4 isoforms, the fish MTs of genera *Rutilus*, *Danio* and *Barbatula*, and the amphibian *Ambystoma* MT. The bootstrap values of the branching points are indicated.

sequenced fragments is sufficient to contain the remaining gene regions, due to their small size [3], so that misidentification was ruled out. The other sequence includes a second MT ORF, that we denominate ckMT2, and whose translation fully matches the *Columba livia* form1 MT.

Analysis of the relationships between the ckMT1 and ckMT2 containing regions and the human and mouse genomes clearly identified synteny between the 50-kb ckMT1 genomic environment and the mammalian MT clusters (111 kb in mouse and 200 kb in humans), bordered in both cases by the *Bbs2* and *Nup93* genes, which we used as flanking markers (Fig. 2). Thus, the initial idea of a unique chicken MT gene instead of an MT gene cluster remains valid only if considering the corresponding syntenic region, but not for the whole genome, as further MT genes are found outside this location. Whether this only applies to the chicken genome or can be extended to other avian forms remains to be elucidated. Although at present there is no experimental data to guarantee that ckMT2 is a real gene, indirect evidence highly favours this possibility: the sequence identity that the putative ckMT2 protein would share with the reported *Columba* MT1 form [14], the integrity of the ckMT2 gene structural elements, the scarcity of retrogenes in the chicken genome [2], the identification of this region as a chicken EST in the corresponding database, and the identification in the 5’ ckMT2 gene region of putative regulatory elements, including three metal-response-elements (MREs) at positions -269, -130 and -96. A low and/or time- and tissue-restricted ckMT2 expression pattern would plausibly be the reason why its cDNA has never been detected and thus the corresponding gene has gone unnoticed. In fact, the expression levels of the ortologous *Columba* MT1 are reported five-fold lower than those of the main avian MT form [14].

The features of the three currently known avian MT protein sequences (Fig. 1A) were analysed and compared, on the one hand to those of mammalian MT1 and MT4, and on the other hand, to the representatives of lower Vertebrates. From the protein distance relationships, (Fig. 1B) it is

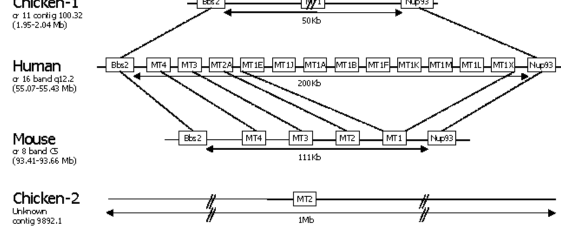

Fig. 2. Structure and synteny of the chicken, mouse and human genomic regions containing the MT genes. The chromosome number and bands enclosing the MT cluster are indicated for the mammalian genomes. For the chicken genome, the name of the corresponding contig is shown, as well as of the known chromosome. Two genes external to the MT cluster have been used as flanking synteny markers.

reasonable to consider *Columba* MT2 (avMTb in Fig. 1A) to be a slight variant of the predominant avMTa avian MT form. Then, an early duplication would have arisen in the avian lineage, generating one MT form (~ ckMT1) closer to the amphibian and mammalian MT1-MT2 system, with a syntenic chromosomal localization for the latter; and another MT form (~ ckMT2), more similar to the supposedly primeval mammalian MT4, in a non-related chromosomal localization. What can no longer be assumed is the general rule of the alleged single-copy composition for the avian MT system, although, and in reflection of the general avian *vs.* mammalian genomic features, the MT gene family has been largely expanded in mammals if compared with birds [2].

Analysis of the monovalent and divalent metal binding ability of ckMT1, αckMT1 and βckMT1

Analysis of the metal binding capabilities of ckMT1 was performed through a two-step strategy. First, the *in vivo* synthesized M-ckMT1, M-αckMT1, and M-βckMT1 (M= Zn^{II}, Cd^{II} and Cu^{I}) complexes were characterized. Second, the reaction pathways of the *in vitro* Zn/Cd and Zn/Cu replacement processes of the three Zn-ckMT1 peptides at pH 7 were determined using the rationale previously followed for MT1 and MT4 [16-20]. Detailed analysis of the spectroscopic (CD and UV-visible electronic absorption) sets of data provided information on the number of metal-MT *in vivo* and *in vitro* generated species, their stoichiometry, and their degree of folding. Additionally, the spectrometric (ESI-MS) measurements revealed the composition of the recombinant preparations and the molecular distribution [21,22] of the various complex species present at each point of the titrations. Although it was possible to determine the Zn:Cd:MT ratio in the heterometallic Zn,Cd-ckMT1 species, the proximity between the atomic weights of zinc and copper, together with the ESI-MS experimental error range, prevented determination of the ratio of these metal ions in the heterometallic Zn,Cu-ckMT1 species.

Zn(II) and Cd(II) binding abilities of ckMT1 and their separate domains—Analytical data (Table 1) provides evidence that the synthesis of ckMT1, αckMT1 and βckMT1 either in Zn- or in Cd-

Table 1. Molecular masses and metal (Zn, Cd or Cu) to protein ratios found for the *in vivo* synthesized ckMT1, αckMT1 and βckMT aggregates

Metal supplemented in culture media	Protein	MW_{exp} [a]	MW_{calc} [b]	M/MT[c]	M/MT[d]	M/MT[e]	S^{2-}/MT[f]
		Da	*Da*				
M = Zn	ckMT1	7050.9 ± 0.8 7083.5 ± 1.4	7049.20 7081.26	Zn_7-ckMT1 (S) Zn_7S_1-ckMT1 (s)	6.2 Zn	7.0 Zn	2.5
	αckMT1	3744.5 ± 0.7	3744.63	Zn_4-αckMT1	3.9 Zn	4.0 Zn	1.1
	βckMT1	3597.7 ± 0.8 3692.6 ± 1.7	3597.98 3694.16	Zn_3-βckMT1 (S) Zn_3S_3-βckMT1 (s)	2.4 Zn	3.3 Zn	3.1
M = Cd	ckMT1	7378.9 ± 2.4 7332.4 ± 2.5 7284.4 ± 5.5	7378.34 7332.13 7285.92	Cd_7-ckMT1 (S) Cd_6S_2-ckMT1 Cd_5S_4-ckMT1 (s)	0.0 Zn 3.7 Cd	0.0 Zn 8.8 Cd	4.7
	αckMT1	3932.5 ± 0.9 3884.7 ± 0.0	3932.71 3885.69	Cd_4-αckMT1 (S) Cd_3S_2-αckMT1(s)	0.0 Zn 3.4 Cd	0.0 Zn 4.4 Cd	2.9
	βckMT1	3738.6 ± 0.3 3692.7 ± 0.6	3739.00 3692.40	Cd_3-βckMT1 (S) Cd_2S_2-βckMT1 (s)	0.0 Zn 1.6 Cd	0.0 Zn 4.3 Cd	5.6
M = Cu	ckMT1	7231.7 ± 2.1 7292.0 ± 3.5 7358.3 ± 1.7	7231.04 7293.59 7356.14	M_{10}-ckMT1 (S) M_{12}-ckMT1 M_{11}-ckMT1	2.5 Zn 7.4 Cu	N/D[g]	N/D
	αckMT1	3862.7 ± 2.6 3925.2 ± 0.0 3807.4 ± 0.0	3866.37 3928.92 3803.82	M_6-αckMT1 (S) M_7-αckMT1 M_5-αckMT1 (s)	0.5 Zn 5.7 Cu	N/D	N/D
	βckMT1	3783.6 ± 1.0 3845.3 ± 0.9 3719.9 ± 1.0	3783.11 3845.66 3720.56	Cu_6-βckMT1 (S) Cu_7-βckMT1 Cu_5-βckMT1	0.0 Zn 6.0 Cu	N/D	N/D

[a] Experimental molecular masses for the Zn-, Cd- and Cu-MT complexes.
[b] Calculated molecular weight for neutral species with loss of two protons/zinc or cadmium bound and one proton/copper bound [8].
[c] Metal per MT molar ratio calculated from the mass difference between holo- and apo-protein. (S) denotes a major species; (s) denotes a minor species.
[d] Metal to MT ratio deduced from the metal content measured by *conventional* ICP-AES.
[e] Metal to MT molar ratio deduced from the Zn, Cd, Cu and S content measured by acid ICP-AES.
[f] S^{2-} to MT ratio measured by GC-FPD.
[g] N/D means non detectable.

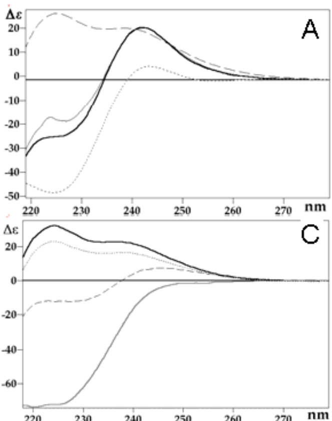

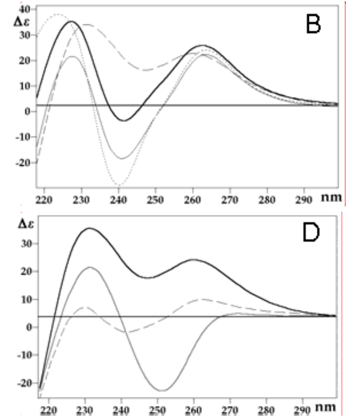

Fig. 3. Comparison of the CD spectra of the biosynthesised (A) Zn-ckMT1 (solid grey line), Zn_4-αckMT1 (dotted line) and Zn-ßckMT1 (dashed line); (B) Cd-ckMT1 (solid grey line), Cd-αckMT1 (dotted line) and Cd-ßckMT1 (dashed line). The spectra depicted in a solid black line in (A) and (B) represent the sum of the CD spectra of M-αckMT1 and M-ßckMT1; (C) Zn-ßckMT1 (solid black line), Zn-ßMT4 (solid grey line), Zn_3-ßMT1 (dashed line) and Zn-ßckMT1 reneutralized (dotted line); (D) Cd-ßckMT1 (solid black line), Cd-ßMT4 (solid grey line) and Cd_3-ßMT1 (dashed line).

supplemented media yields the expected canonical complexes as major species, *i.e.* M_7-ckMT1, M_4-αckMT1 and M_3-βckMT1 (M = Zn or Cd). This behaviour coincides with that of mammalian MT1. However, ESI-MS data also shows the presence of minor sulfide-containing species in all preparations except that of Zn_4-αckMT1. As previously shown [23], the presence of these acid-labile ligands partially invalidates the conventional ICP analyses, and therefore acid ICP measurements were performed, obtaining more consistent M/MT stoichiometric results (Table 1). Finally, the GC-FPD data for evaluation of the S^{2-}/MT content suggests a more significant role of the S^{2-} ligands in the Cd- than in the Zn-complexes, in agreement with the ESI-MS detected species and with the differences between the conventional and acid ICP-AES results.

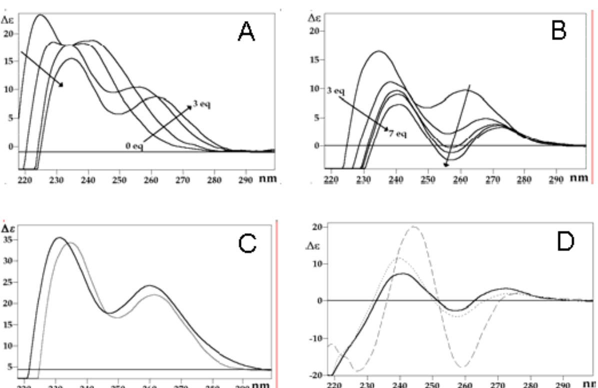

Fig. 4. (A) and (B) CD spectra corresponding to the titration of Zn-ßckMT1 with Cd(II) at pH 7. The arrows show the evolution of the spectra when the indicated number of Cd(II) equivalents were added. (C) Superimposition of the spectra recorded after 3 Cd(II) eq added to Zn-ßckMT1 (solid grey line) and the spectra of the biosynthesized Cd-ßckMT1 (solid black line). (D) Comparison of the *in vitro* constituted Cd_3-ßMT complexes of ßckMT1 (solid black line), ßMT4 (dashed line, [16]) and ßMT1 (dotted line [18] and note 2 in supplementary material).

The CD spectra of the biosynthesised M-ckMT1 and M-αckMT1 (M=Zn, Fig. 3A; M=Cd, Fig. 3B) closely resemble those of the corresponding MT1 complexes [17,18] and provide evidence that the degree of folding of ckMT1 when coordinating Zn(II) is more similar to that of MT1 than to that of MT4 [16]. In spite of the experimental evidence of the presence of S^{2-} ligands in the Zn-ckMT1, Cd-ckMT1 and Cd-αckMT1 samples (Table 1), the absorptions of the corresponding metal-sulfide chromophores are of such a low intensity that the *in vivo* preparations show Type A CD spectra, in accordance to the classification proposed in [23]. Conversely, the CD spectra of the *in vivo* M^{II}-βckMT1 samples differ significantly from those expected after the results obtained for mammalian βMT1 and βMT4 (M=Zn, Fig. 3C; M=Cd, Fig. 3D). To determine the chromophores that may contribute to these interesting new CD fingerprints, recombinant Zn-βckMT1 was purified both in the presence or absence of chloride ions [24]. Subsequently, the two Zn-βckMT1 preparations were titrated with either Cd(II) chloride or Cd(II) perchlorate, respectively, and all the M^{II}-βckMT1 (M^{II} = Zn or/and Cd) species formed characterized. From the comparison of the CD fingerprints of the Zn-βckMT1 and Cd-βckMT1 species either in Tris-HCl or in Tris-$HClO_4$ (data not shown) we concluded that, at the assayed concentrations, the presence of chloride anions has no spectroscopically detectable contribution either to the metal-cluster structure or to its chirality. Once the participation of chloride anions in the CD fingerprints had been discarded, and taking into account the fact that the

ESI-MS, ICP-AES and GC-FPD data suggested the participation of sulfide ligands in the Zn-βckMT1 and Cd-βckMT1 *in vivo* samples, both preparations were acidified to pH 1.5 and reneutralized to pH 7.5. As there was no significant difference between the initial and the final CD spectra (shown in Fig. 3C for Zn-βckMT1) we assumed that there was no detectable contribution of the S^{2-} ligands to the spectroscopic features of the samples. Consequently, the characteristic CD fingerprint of Zn- and Cd-βckMT1 should only be attributed to the peculiarities of the $M(SCys)_4$ chromophores, with perhaps some contributions of protein conformation at the lowest wavelengths [25]. Full comparison of the spectroscopic Cd-ßMT1, Cd-ßMT4 and Cd-ßckMT1 features is provided in Fig. 3D and in note 1 of the supplementary material. A further corroboration of the CD fingerprint of *in vivo* Cd-βckMT1 was achieved by titration of Zn-βckMT1 with $CdCl_2$ at pH 7 (Fig. 4A and 4B, Table 2). The results obtained indicate that the addition of 3 Cd(II) eq to Zn-βckMT1 renders a mixture of the same composition (Table 2B) and accordingly equivalent CD spectra (Fig. 4C) to that of the biosynthesized Cd-βckMT1, showing that the Cd-βckMT1 sample is generated at that stage of the *in vitro* zinc/cadmium replacement reaction. Addition of further Cd(II) to this solution causes a red shift and a decrease in the intensity of the main CD signals (Fig. 4B), giving rise to a CD spectrum that could be considered characteristic of the Cd_3-βckMT1 species (with a contribution of the Cd_3S_2-βckMT1 complex, Table 2B) and that is clearly related to that of the Cd_3-βMT1 and Cd_3-βMT4 species (Fig. 4D).

Finally, and in spite of the unusual CD fingerprint obtained for the *in vivo* preparations of Zn- and Cd-βckMT1, summation of the CD spectra of *in vivo* M-βckMT1 and M-αckMT1 affords spectra that closely resemble those of the full length M-ckMT1 (M = Zn, Cd) (Fig. 3A and 3B), suggesting that both ckMT1 fragments behave independently when binding Zn(II) and Cd(II), as was the case for MT1 [18]. This independent behaviour can be extended to the binding capacity of each domain not only for the major (Zn_3- or Cd_3-βckMT1 + Zn_4- or Cd_4-αckMT1= Zn_7- or Cd_7-ckMT1) but also for the minor species (*i.e.* Cd_2S_2-βckMT1+ Cd_3S_2-αckMT1= Cd_5S_4-ckMT1) (Table 1).

Titration of Zn-ckMT1 and Zn_4-αckMT1 with Cd(II) produced some remarkably unexpected results. Until 7 and 4 Cd(II) eq were added, respectively, the evolutions of the CD spectra (Fig. 5A) were comparable to those observed for the

Table 2. Distribution of the metal aggregates present in solution, according to ESI-MS data, during the titration of Zn_4-αckMT1 (**A**), Zn_3-βckMT1 (**B**) and Zn_7-ckMT1 (**C**) with $CdCl_2$ at pH 7 as a function of the number of Cd(II) equivalents added

A)

	Cd(II) equivalents added				
	3	4	7	13	15
Zn_2Cd_2-αckMT1	x				
Zn_1Cd_3-αckMT1	✓	x			
Cd_4-αckMT1	x	✓	✓	✓	✓
Cd_8-2αckMT1	◆	◆	◆	◆	◆

B)

	Cd(II) equivalents added				
	1	2	3	4	7
Zn_3-βckMT1	x	◆			
Zn_2Cd_1-βckMT1	✓	x	◆		
Zn_1Cd_2-βckMT1	x	✓	x	x	
Cd_3-βckMT1	◆	x	✓	✓	✓
Cd_3S_2-βckMT1			x	◆	◆

C)

	Cd(II) equivalents added							
	3	5	7	9	12	16	18	20
Zn_6Cd_1-ckMT1	◆							
Zn_5Cd_2-ckMT1	x							
Zn_4Cd_3-ckMT1	x	◆						
Zn_3Cd_4-ckMT1	✓	x						
Zn_2Cd_5-ckMT1	x	x	x					
Zn_1Cd_6-ckMT1	x	✓	x	x	x	◆		
Cd_7-ckMT1	◆	x	✓	✓	✓	✓	✓	✓
Cd_7S_1-ckMT1		x	x	x	x	x	◆	◆
Cd_8-ckMT1		x	◆	◆	◆			

✓, denotes the major species; x, species of intermediate abundance and ◆, the minor species present in solution

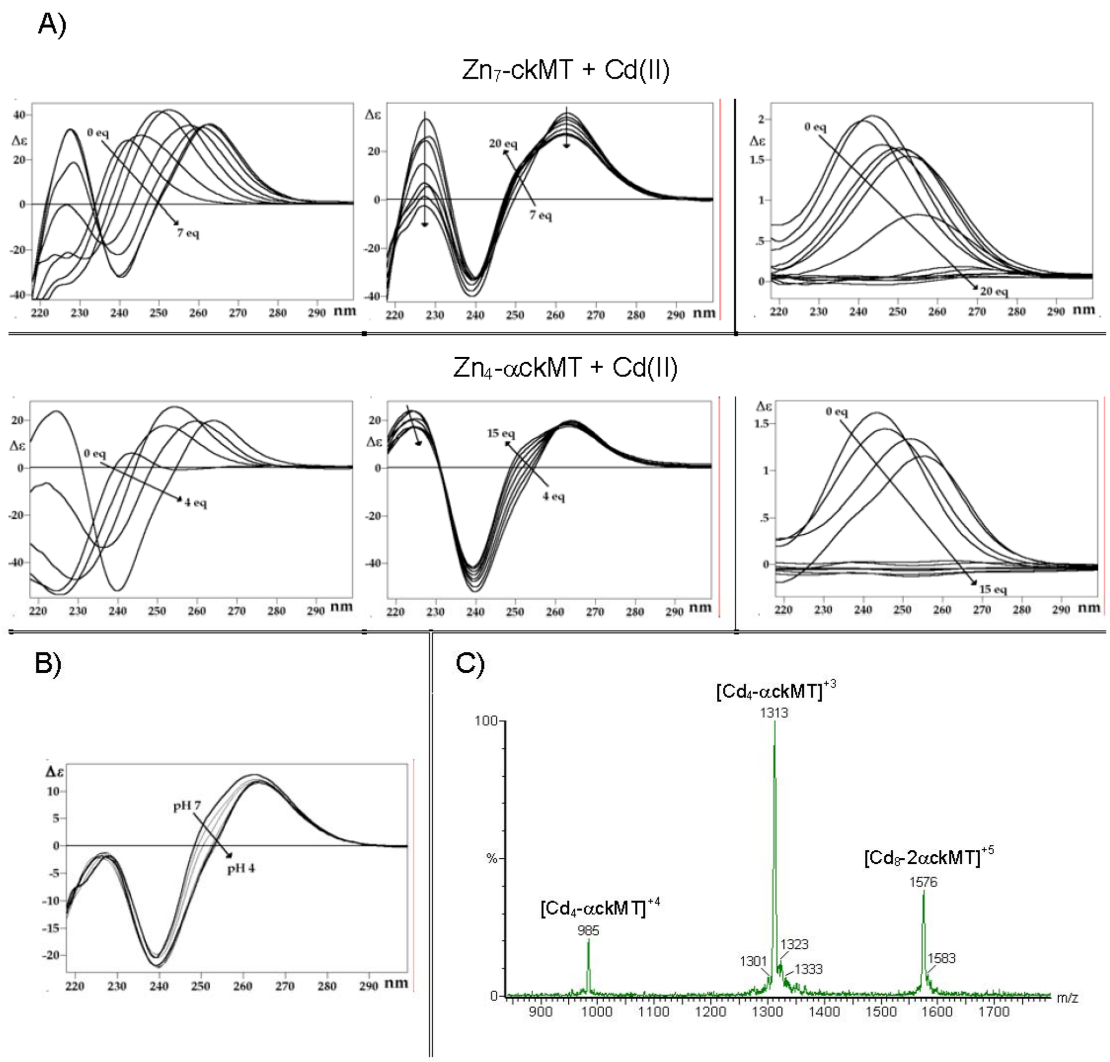

Fig. 5 (A) CD and UV-vis difference spectra corresponding to the titrations of Zn-ckMT1 and Zn_4-αckMT1 with Cd(II) at pH 7. Arrows show the evolution of the spectra when the indicated number of Cd(II) eq was added. (B) CD spectrum of the acidification of the final solution of the Cd(II) titration of Zn-ckMT1, the arrow shows the evolution from pH 7 to 4. (C) ESI-MS spectra of an aliquot of the solution obtained after adding 7 Cd(II) eq to Zn_4-αckMT1.

corresponding MT1 [17,18] and MT4 peptides [16]. However in both cases, the addition of further Cd(II) eq led to a marked increase in the intensity of a positive shoulder at *ca.* 250 nm. Previous studies of this group with Cys-to-His site-directed MT1 mutants [26] related this absorption to NHis coordination to Cd(II), and it was therefore reasonable to hypothesize that there is participation of the terminal ckMT1 His residue of the entire protein and its α fragment in metal coordination. To corroborate this, the final solutions of the Cd(II) titrations of Zn_4-αckMT1 and Zn_7-ckMT1 were acidified from pH 7 to 4 (Fig. 5B), and in both cases, this implied the disappearance of the CD signals at 250 nm, while all other were maintained. This result is consistent with Cd-His coordination being responsible for the 250 nm shoulder, since this amino acid protonates at a 4-5 pH range, while the lower pK_a of the cysteine thiolates still allows for maintenance of the Cd-SCys bonds at this pH. Interestingly, the appearance of this 250 nm absorption in the final stages of the titrations is accompanied by a gradual decrease in the intensity of all CD envelopes, more significant for the full length ckMT1 than for the αckMT1. This variation has been related to MT dimerization events [27], and a detailed study of the ESI-MS data of these samples (Table 2A, Fig. 5C) revealed the presence of dimeric Cd_8-$(\alpha ckMT1)_2$ species, even at the initial points of the titration, whose abundance increased as more Cd(II) was added to Zn_4-αckMT1. Unfortunately, dimers corresponding to the full-length protein could not be detected in our ESI-MS conditions (Table 2C). Literature data

refers to two types of dimerization processes in MTs: oxidative dimerization, mediated by disulfide bridge formation [28] and metal-mediated [29] dimer formation, but neither is consistent with our analytical and spectroscopic data. On the other hand, ESI-MS data for the final steps of the Cd(II) titration of Zn_4-αckMT1 showed disappearance of the Cd_8-$(\alpha ckMT1)_2$ species after acidification, this suggesting that a third type of MT dimerization, mediated by the terminal His residues can occur. As shown in the CD and UV-vis difference spectra (Fig. 5A), once the dimerization starts being spectroscopically detectable, the formation of new chromophores stops and consequently, we propose a dimerization mechanism that involves a simultaneous intermolecular formation ($N_{\alpha1}$-$Cd_{\alpha2}$ and $N_{\alpha2}$-$Cd_{\alpha1}$) and intramolecular loss ($N_{\alpha1}$-$Cd_{\alpha1}$ and $N_{\alpha2}$-$Cd_{\alpha2}$) of two Cd-NHis bonds, via the second nitrogen donor atom of two His residues (Scheme 1). Therefore, in the dimeric species, two His residues would bridge two α fragments in a similar way to that described for the active centre of the superoxide dismutase (SOD) protein [30].

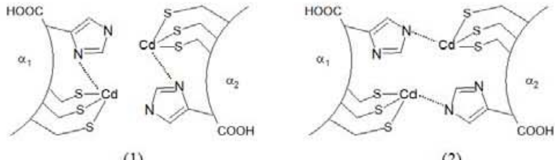

Scheme 1. Possible mechanism of dimerization. The Cd-NHis dashed bonds in (1) are broken when those of (2) are formed.

Cu(I) binding abilities of ckMT1 and their separate domains— Table 1 shows the analytical data obtained in the characterization of ckMT1 proteins biosynthesized in Cu-supplemented media. As expected [23], none of the Cu-ckMT1 preparations show evidence of sulfide ligands in their complexes. In copper-supplemented media, βckMT1 renders a mixture of homometallic Cu-species analogous to that obtained for βMT1 [20,31] and βMT4 [16] and therefore should be considered Cu-thionein. However, in this case Cu_6-βckMT1 is the major species, contrasting with the Cu_7-βMT major stoichiometry reported for βMT1 and βMT4. Consequently, the CD spectra of these three preparations are comparable but non-identical (Fig. 6C). βckMT1 and not βMT1 shows absorptions at the 330-400 nm range, which suggests that only the former would be capable of offering the previously reported particular binding site for Cu(I) in for ßMT4 [16].

Conversely, the recombinant syntheses of ckMT1 and αckMT1 in Cu(I)-supplemented media yield mixtures of heterometallic Zn,Cu-ckMT1 species, as typical Zn-thioneins. This behaviour is coincident with that of the MT1 peptides [20], but differs from the Cu-thionein character of the MT4 counterparts [16]. The entire ckMT1 yields a major M_{10}-ckMT1 cluster (M= Zn and/or Cu) with a Zn_3Cu_7-ckMT1 stoichiometry according to ICP-AES results (Table 1), as reported for the MT1 [20] and Type 2 MT4 [16]. Coincidently, the three Cu-biosynthesized proteins afford comparable CD spectra (Fig. 6A). The αckMT1 peptide renders M_6-αckMT1 as the most abundant species, contrasting with the biosynthesized major M_5-αMT1 complex [20]. On the basis of the ICP-AES data (0.5 Zn and 5.7 Cu for αckMT1 towards 0.5 Zn and 4.5 Cu for αMT1) this different M/αMT stoichiometric ratio could be interpreted by the presence of one additional Cu(I) ion in αckMT1. Comparison of CD spectra (Fig. 6B) reveals that the folding of αckMT1 in the presence of Cu(I) is closer to that of αMT4

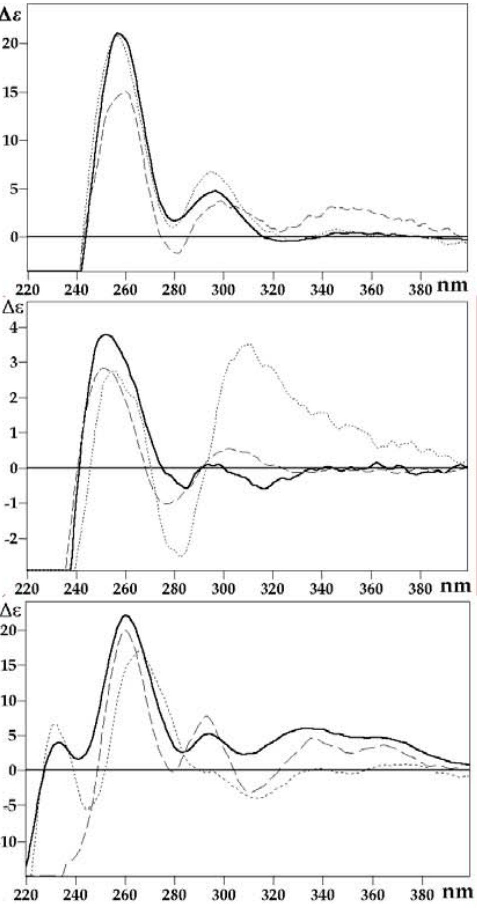

Fig. 6.- CD spectra of the recombinant (A) Zn_3Cu_7-ckMT1 (black solid line), Zn_3Cu_7-MT4 (dashed line) and Zn_3Cu_7-MT1 (dotted line); (B) Cu-αckMT1 (black solid line), Cu-αMT4 (dashed line) and Cu-αMT1 (dotted line); and (C) Cu-ßckMT1 (black solid line), Cu-ßMT4 (dashed line) and Cu-ßMT1 (dotted line).

than to that of αMT1, in spite of their hetero- *vs.* homometallic nature. This suggests that the presence of Zn(II) in αckMT1 would not have a relevant structural role.

To allow for further insight into the ckMT1 Cu(I) coordination properties and how they compare with those of mammalian MT1 and MT4, the three Zn-ckMT1 preparations were titrated with Cu(I) solutions and the corresponding *in vitro* Zn/Cu displacement reactions analyzed (full set of spectroscopic data shown in Fig. 7; spectrometric data recorded for some aliquots of the three titrations included in Table S1). In spite of the structural dissimilarities between Zn-βckMT1, Zn-βMT1 and Zn-βMT4 (Fig. 3C) and as otherwise expected from their similar *in vivo* Cu(I) binding behaviour, all three peptides give rise to analogous Zn/Cu replacement reactions, with only a slight difference in the number of Cu(I) eq needed to achieve some particular titration stages. The experimental data recorded during the Cu(I) titration of Zn-βckMT1 indicates that the Cu_7-βckMT1 species is formed after the addition of only 5 Cu(I) eq. Species of the same Cu(I):MT ratio and near 3D structure (Fig. 7B) are obtained *in vitro* by the addition of 6 or 7 Cu(I) eq to Zn_3-βMT4 [16] and Zn_3-βMT1 [20], respectively. All this data suggests a higher *in vitro* affinity of βckMT1 for Cu(I) than βMT1 or βMT4. Contrasted with the behaviour of the βMT peptides, Zn/Cu replacement on Zn-αckMT1 shares more similarities with that on Zn-αMT1 than with that on Zn-αMT4, although parallel evolutions until 5 Cu(I) eq are observed in the three cases. For 6 Cu(I) eq added, Zn-αMT4 suffers a change in chirality that αckMT1 and αMT1 also show but after the addition of 7 or 8 Cu(I) eq, respectively. This data led us to postulate a Cu(I) binding ability of αckMT1 lying between αMT1 and αMT4. Full length Zn-ckMT1, Zn-MT1 and Zn-MT4 also evolve similarly until 7 Cu(I) eq added, a step that leads in all cases to the formation of Zn_3Cu_7-MT complexes, which are also equivalent to the corresponding *in vivo*-conformed Zn_3Cu_7-MT species (Fig. 6A). The differences observed at this stage of the three titrations should be attributed to the dissimilarity of the starting species CD spectra,

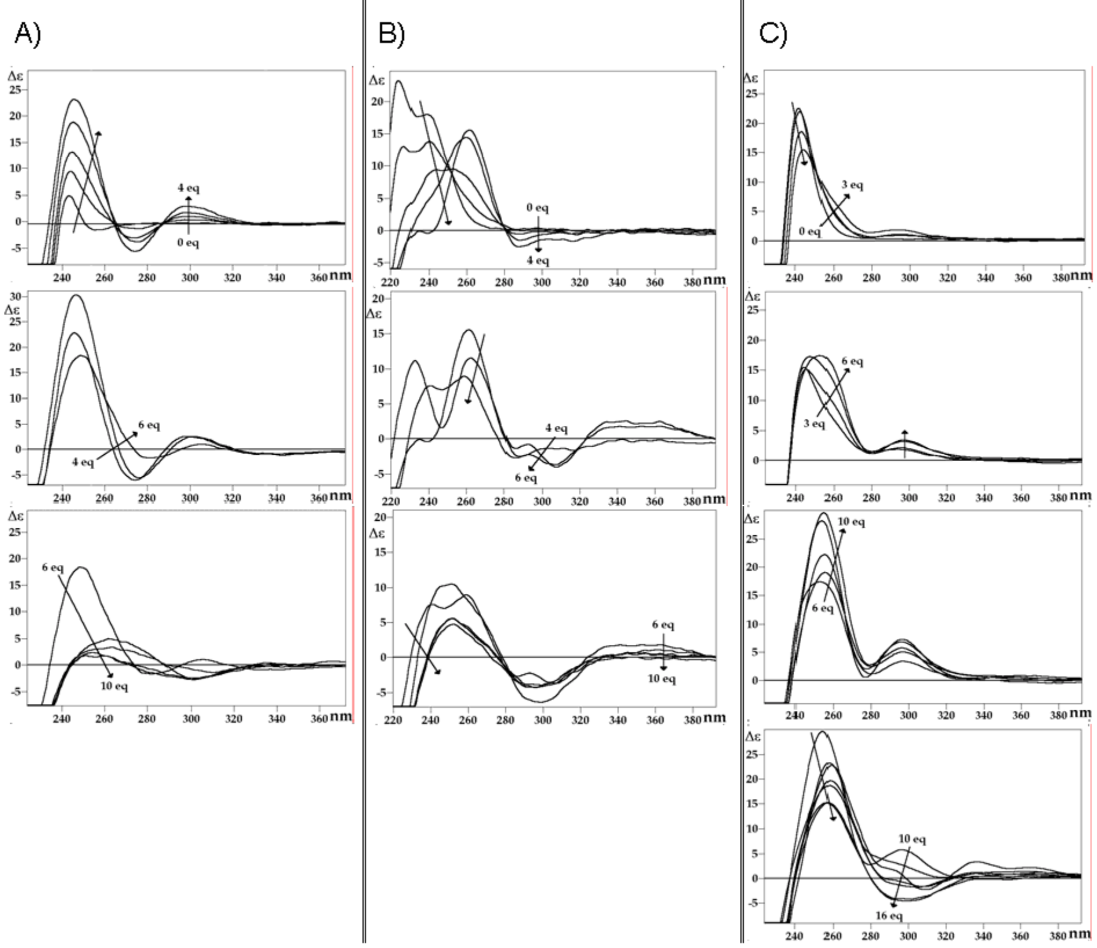

Fig. 7.- CD spectra corresponding to the titrations of (A) Zn_4-αckMT1, (B) Zn_3-βckMT1, and (C) Zn_7-ckMT1 with Cu(I) at pH 7. The arrows show the evolution of the spectra when the indicated number of Cu(I) equivalents were added.

and in the case of MT4, to the minor contribution at *ca.* 350(+) nm assigned to the binding of Cu(I) to the βMT4 domain [16]. This particular MT4 absorption, which intensifies with the formation of Cu_{10}-MT4, remains absent during the entire Cu(I) titration of Zn-MT1, but develops after the addition of 12 Cu(I) eq to Zn-ckMT1, thus revealing that ckMT1 can also provide this special coordination environment when large amounts of Cu(I) are present in the solution.

Differing from the independent behaviour of αckMT1 and βckMT1 towards divalent metal ions, both independent domains do not interact with Cu(I) in the same way as they do when linked together, therefore exhibiting a dependent Cu-binding behaviour. This observation becomes obvious from the results of the biosynthesis of ckMT1, αckMT1 and βckMT1 in Cu-rich media, as instead of the expected M_{12}-ckMT1 complex that would result from the addition of the major M_6-αckMT1 and Cu_6-βckMT1 species, Cu-ckMT1 biosynthesis renders M_{10}-ckMT1 complexes. Thus, as in MT1 [20] and MT4 [16], the ckMT1 separate domains are characterized by a higher *in vivo* Cu(I) binding capacity than the entire protein. Unfortunately, the coexistence of several complexes both in the expressions and in almost all the Cu(I) titration points of the three Zn-ckMT1 peptides, hampers the assignation of the CD fingerprints of the species formed in the titrations and, as a consequence, the elucidation of the *in vitro* dependent/independent behaviour of αckMT1 and βckMT1.

Conclusive Remarks

Overall results presented here allowed for deeper insight into the metal binding abilities of MTs and their evolutive relationships in higher vertebrates. For ckMT1, it can be established that its Zn(II), Cd(II) and Cu(I) binding abilities lie between those of MT1 and MT4, with a behaviour towards divalent metal ions closer to that of MT1, but more similar to that of MT4 when binding monovalent ions.

$$\xrightarrow{\hspace{4em}} \text{Cu(I)}$$
MT1 ckMT1 MT4
$$\text{Zn(II), Cd(II)} \xleftarrow{\hspace{4em}}$$

According to protein sequence distances, ckMT1 should share more metal binding abilities with mammalian MT1 than with MT4. This is true for Zn(II) and Cd(II), but not for Cu(I) binding. The intermediate functional behaviour we have shown for ckMT1 could be well understood if considering a strong functional constraint on the chicken form, that preserving the monovalent coordination features of a MT4-like ancestor, has been able to evolve to a MT peptide that is more optimized for divalent metal binding, somehow emulating MT1 functionalities. The lack of multiplicity in the avian gene families fully agrees with these features, although the implications of the existence of the newly identified ckMT2 form has yet to be elucidated.

Experimental procedures

***In silico* analysis of the chicken genome and avian MT protein sequences: Databank searches, sequence comparison and evolu tionary analysis.** The last annotated chicken Genome version (29.1e, the Wellcome Trust Sanger Institute, http://www.ensembl.org/Gallus_gallus/) was used for an *in silico* search of MT-like sequences, through the Blast facility accessible from the same WEB site. The sequence of the chicken MT cDNA cloned for recombinant expression in this work was used as a query. A 500-bp region upstream the putative transcription initiation site of the identified MT genes was analyzed using the MatInspector application in the Genomatix WEB interface (Genomatix v.3.4.1) to search for MRE boxes [32].

MT protein sequences were aligned with ClustalW (v1.81), using the Gonnet series as a distance matrix, and *a gap-penalty* of 10/100, a *gap-extension value* of 0.2/100 and a 30% delay between divergent sequences [33]. The ClustalW alignments were the input for protein distance calculations and construction of the corresponding Neighbor-Joining tree. A bootstrap test was run and 1000 replica trees were examined for each bootstrap. The nodes with a bootstrap number below 500 were collapsed. The protein-distance and tree-building applications are included in the Mega 3 software [34].

Bacterial strains and plasmids

The *E. coli* strains DH5α [35] and JM105 [36] were used for DNA manipulation and sequencing, and *E. coli* BL21 [37] for recombinant protein synthesis. The expression plasmid used was pGEX-4T-1 (GE-Amersham Biosciences), for GST-fusion production. Recombinant *E. coli* strains were grown at 37 ºC in Luria-Bertani media supplemented with ampicillin (final concentration 100 μg.mL^{-1}). Induction of protein synthesis was achieved by the addition of 10 mM IPTG (isopropyl-1-thio-ß-D-galactopyranoside) (final concentration) to the corresponding cultures, and metal ions were added as $ZnCl_2$, $CdCl_2$ or Cu_2SO_4 salts to final concentrations of 300 μM, 300 μM and 500 μM, respectively.

Cloning of the chicken MT cDNA and its independent α and ß domains for recombinant expression

The ckMT1 coding sequence, kindly provided by Dr. G.K. Andrews of the University of Kansas Medical Center [7] as a pSP6 clone, was amplified by PCR using oligonucleotides with the following sequences: upstream primer, ckMT1-*Bam*HI (5' GCCGGATCCATGGACCCTCAGGA 3') and downstream primer, ckMT1-*Sal*I (5' GCGCGCGTCGACTCAGTGGCAGCA 3'). Through this reaction, a *Bam*HI restriction site (underlined) was introduced before the ATG initiation codon and a *Sal*I site (underlined) immediately after the stop codon. A 35-cycle PCR profile -30 s at 94 ºC (denaturing), 30 s at 60 ºC (annealing) and 30 s at 72 ºC (extension)- was carried out in a total reaction volume of 100 μl, comprising 2 μl of 25 mM dNTP mixture, 2 μl of 20 μM primer solution, 1 u of DeepVent DNA polymerase (New England Biolabs) and 100 ng of the template DNA. The cDNAs encoding the independent ckMT1 domains were obtained by mutagenic PCR on the initial Bluescript clone. To amplify the ckMT α fragment, which extends from the thirty-second MT residue (Lys) to the C-terminus, a PCR reaction was performed with the αckMT-*Bam*HI primer (5'CGCGGATCCATG AAGAGCTGCTGCTC 3', upstream) and the ckMT1-*Sal*I primer (downstream). The ckMT1β fragment extends from the ATG initiation codon to the thirty-first residue (Arg). The primers used for its PCR synthesis were: ckMT1-*Bam*HI (upstream) and βckMT-*Sal*I (5'CCGCGCGTCGACCTAGCG GCAGCTCCCG GCAGCGG 3', downstream). The conditions for both PCR reactions were the same as for the entire ckMT1 cDNA.

In all cases, the PCR products were isolated from 2% agarose gels using the Gel Band Purification kit (GE-Amersham Biosciences), digested with *Bam*HI and *Sal*I (Takara) and subsequently ligated into the same sites in pGEX-4T-1 (GE-Amersham Biosciences). Before protein synthesis, all the DNA constructs were confirmed by automatic DNA sequencing (ABI 370, Perkin Elmer), using the Dye Terminator Cycle Kit (GE-Amersham Biosciences), to ensure correct PCR amplification of the desired coding regions and to rule out the presence of PCR induced substitutions.

Synthesis and purification of the ckMT1, αckMT1 and ßckMT1 metal complexes

Recombinant bacteria were grown both in small-scale cultures (1.5 l, performed in Erlenmeyer flasks) and large-scale cultures (at least 10 l in a Microferm Fermentor New Brunswich, coupled to a Westfalia CSA-1-06-475 centrifuge and controlled by a TVE-OP 76/0 programmer, Braun Biotech). In both cases, the transformed *E. coli* cells were grown as described in [16], supplementing the medium either with $ZnCl_2$, $CdCl_2$ or $CuSO_4$ as explained above. Purification of all the metal-MT complexes, starting from the recovered GST-MT fusion peptides, was performed as described for mammalian MT1 [17,18]. Aliquots of the thrombin-digested MT-containing fractions eluted from a FPLC Superdex™75 column (GE-Amersham Biosciences) in 50 mM Tris-HCl buffer, pH 7.0, were analyzed in 15% SDS-PAGE gels. Samples were pooled, aliquoted and kept at -80 ºC under argon until required.

Analysis of the ckMT1, αckMT1 and ßckMT1 metal content

Inductively coupled plasma-atomic emission spectroscopy (ICP-AES) was used to determine the amount of protein present in the different preparations and the global metal-to-protein ratios, measuring sulphur at 182.04 nm, zinc at 213.85 nm, cadmium at 228.80 nm and copper at 324.75 nm. Acid ICP-AES included a sample acidification (incubation in 1 M HCl at 65 ºC for 5 min) before the conventional ICP procedure [23].

Spectroscopic characterization of the ckMT1, αckMT1 and ßckMT1 metal complexes

Spectroscopic (UV-Vis) and spectropolarimetric (CD) analysis of the metal-ckMT1 clusters and of the species formed *in vitro* during the Zn/Cd and Zn/Cu displacement studies at pH 7.0 were carried out and processed as described in [16]. Electronic absorption measurements were performed on an HP-8453 Diode array UV-visible spectrophoto meter. A Jasco spectropolarimeter (Model J-715) interfaced to a computer (GRAMS 32 Software) was used for CD determinations. All assays were performed under Ar atmosphere, and titrations were carried out at least in duplicate to assure reproducibility. The pH for all experiments remained constant throughout, without the addition of buffers, and the temperature was kept at 25 ºC by means of a Peltier PTC-351S apparatus.

Spectrometric characterization (ESI-MS) of the ckMT1, αckMT1 and ßckMT1 metal complexes

The molecular mass of the Zn-, Cd-, and Cu-MT species obtained *in vivo* and *in vitro* was determined by electrospray ionization mass spectrometry (ESI-MS) on a Fisons Platform II Instrument, equipped with MassLynx software and calibrated with horse-heart myoglobin (0.1 mg/ml). The assay conditions for the Zn- and Cd-containing species were as follows: 20 μl of protein solution injected at 60 μl/min; the use of an HPLC Kromasil-100 C_4 (3.5 μm, 5 x 0.21 cm) column to separate analytes;

capillary counter-electrode voltage, 4.5 kV; lens counter-electrode voltage, 1.0 kV; cone potential, 60 V; source temperature, 120 ºC; m/z range, 850-1950; scanning rate, 3 s/scan; interscan delay, 0.3 s. The assay conditions for the Cu-containing species were: 20 μl of protein solution injected at 30 μl/min; capillary counter-electrode voltage, 3.5 kV; lens counter-electrode voltage, 1.0 kV; cone potential, 35 V; source temperature, 160 ºC; m/z range, 850-1950; scanning rate, 3 s/scan; interscan delay, 0.3 s. In all cases, the running buffer was an appropriate mixture of acetonitrile and 5 mM ammonium acetate/ammonia, pH 7.5. The molecular mass of the apo-forms was determined as for the Cu-containing species, except that the carrier was a 1:1 mixture of acetonitrile and trifluoroacetic acid, pH 1.5. Masses for the holo-species were calculated as described in [38].

Gas chromatography determination of the sulfide content in the ckMT1, αckMT1 and ßckMT1 metal complexes

The sulfide presence in the ckMT1, αckMT1 and ßckMT1 metal complexes was quantified by heavy acidification of the MT preparation, followed by gas chromatography and detection of the volatile S^{2-} generated through a flame photometric detector-GC coupled system (FPD-GC). Analysis conditions are detailed in [23].

Acknowledgements

This work was supported by the *Spanish Ministerio de Ciencia y Tecnología* grants BIO2003-03892 to Silvia Atrian and CTQ2004-00359/BQU to Mercè Capdevila. We acknowledge the *Serveis Científico-Tècnics, Universitat de Barcelona* (DNA sequencing, ICP-AES, ESI-MS) and the *Servei d'Anàlisi Química, Universitat Autònoma de Barcelona* (AAS, CD, UV-Vis) for allocating instrument time.

Supplementary material

The following material is available from the corresponding WEB site.

Note S1. Comparison of the CD fingerprints of the three *in vivo* Cd-βMT samples: Cd-βckMT1, Cd_3-βMT1 and Cd_3-βMT4.

Note S2. Assignement of the CD spectrum of the Cd_3-ßMT1 species.

Table S1. Distribution of the metal aggregates present in solution, according to ESI-MS data, during the titration of Zn_4-αckMT1 (A), Zn_3-βckMT1 (B) and Zn_7-ckMT1 (C) with $[Cu(MeCN)_4]ClO_4$ at pH 7 as a function of the number of Cu(I) equivalents added.

References

1 Margoshes M & Vallee BL (1957) A cadmium protein from equine kidney cortex. *J Am Chem Soc* **79**, 4813-4814.
2 International Chicken Genome Sequencing Consortium (2004) Sequence and comparative analysis of the chicken genome provide unique perspectives on vertebrate evolution. *Nature* **432**, 695-716.
3 Andrews GK, Fernando LP, Moore KL, Dalton TP & Sobieski R J (1996) Avian metallothioneins: structure, regulation and evolution. *J Nutr* **126**, 1317S-1332S.
4 Weser U, Donay F & Rupp H (1973) Cadmium-induced synthesis of hepatic metallothionein in chicken and rats. *FEBS Lett* **32**, 171-174.
5 Weser U, Rupp H, Donay F, Linnemann F, Voelter W, Voetsch W & Jung G (1973) Characterization of Cd, Zn-Thionein (Metallothionein) isolated from rat and chicken liver. *Eur J Biochem* **39**, 127-140.
6 McCormick CC, Fullmer CS & Garvey JS (1988) Amino acid sequence and comparative antigenicity of chicken metallothionein. *Proc Natl Acad Sci USA* **85**, 309-313.
7 Wei D & Andrews GK (1988) Molecular cloning of chicken metallothionein. Deduction of the complete amino acid sequence and analysis of expression using cloned cDNA. *Nucleic Acids Res* **16**, 537-553.
8 Fernando LP & Andrews GK (1989) Cloning and expression of an avian metallothionein-encoding gene. *Gene* **81**, 177-183.
9 Fernando LP, Wei D & Andrews GK (1989) Structure and expression of chicken metallothionein. *J Nutr* **119**, 309-318.
10 Dalton T, Paria BC, Fernando LP, Huet-Hudson YM, Dey SK & Andrews GK (1997) Activation of the chicken metallothionein promoter by metals and oxidative stress in cultured cells and transgenic mice. *Comp Biochem Physiol* **116B**, 75-86.
11 Shartzer KL, Kage K, Sobieski RJ & Andrews GK (1993) Evolution of avian metallothionein: DNA sequence analyses of the turkey metallothionein gene and metallothionein cDNAs from pheasant and quail. *J Mol Evol* **36**, 255-262.
12 Lee Y-L, Chen Y-P, Wang S-H, Chow W-Y & Lin L-Y (1996) Structure and expression of metallothionein gene in ducks. *Gene* **176**, 85-92.
13 Maxfield LF, Fraize CD & Coffin JM (2005) Relationship between retroviral DNA-integration-site selection and host cell transcription. *Proc Natl Acad Sci USA* **102**, 1436-1441.
14 Lin L, Lin WC & Huang PC (1990) Pigeon metallothionein consists of two species. *Biochim Biophys Acta* **1037**, 248-255.
15 Valls M, Bofill R, Gonzalez-Duarte R, Gonzalez-Duarte P, Capdevila M, Atrian S (2001) A new insight into metallothionein classification and evolution. The *in vivo* and *in vitro* metal binding features of *Homarus americanus* recombinant MT. *J Biol Chem* **276**, 32835-32843.
16 Tio L, Villarreal L, Atrian S & Capdevila M (2004) Functional differentiation in the mammalian Metallothionein gene family. *J Biol Chem* **279**, 24403-24413.
17 Cols N, Romero-Isart N, Capdevila M, Oliva B, Gonzalez-Duarte P, Gonzalez-Duarte R &Atrian S (1997) Binding of excess Cadmium(II) to Cd7-metallothionein from recombinant mouse Zn_7-metallothionein 1. UV-VIS absorption and circular dichroism studies and theoretical location approach by surface accessibility analysis. *J Inorg Biochem* ***68**, 157-166.*
18 Capdevila M, Cols N, Romero-Isart N, Gonzalez-Duarte R, Atrian S & Gonzalez-Duarte P (1997) Recombinant synthesis of mouse Zn_3-β and Zn_4-α metallothionein 1 domain and characterization of their cadmium (II) binding capacity. *Cel Mol Life Sci* **53**, 681-688.
19 Bofill R, Palacios O, Capdevila M, Cols N, Gonzalez-Duarte R, Atrian S & Gonzalez Duarte P (1999) A new insight into the Ag^+ and Cu^+ binding sites in metallothionein ß domain. *J Inorg Biochem* **73**, 57-64.
20 Bofill R, Capdevila M, Cols N, Atrian S & Gonzalez-Duarte P (2001) Zn(II) is required for the *in vivo* and *in vitro* folding of mouse Cu-metallothionein in two domains. *J Biol Inorg Chem* **6**, 405-417.
21 Polec K, Palacios O, Capdevila M, Gonzalez-Duarte P & Lobinski R (2002) Monitoring of the metal displacement from the recombinant mouse liver metallothionein Zn_7-complex by capillary zone electrophoresis with electrospray MS detection. *Talanta* **57**, 1011-1017.
22 Palacios O, Polec K, Lobinski R, Capdevila M & Gonzalez-Duarte P (2003) Is Ag(I) an adequate probe for Cu(I) in structural copper–metallothionein studies? The binding features of Ag(I) to mammalian metallothionein 1. *J Biol Inorg Chem* **8**, 831-842.

23 Capdevila M, Pagani A, Domenech J, Tio L, Villarreal L & Atrian S (2005) Zn- and Cd-Metallothionein recombinant species from the most diverse phyla may contain sulfide ligands. *Angew Chem Int Ed.* **44**, 4618-4622.
24 Villarreal L, Tio L, Atrian S & Capdevila M (2005) Influence of chloride ligands on the structure of Zn- and Cd-metallothionein species. *Arch Biochem Bioph* **435**, 331-335.
25 Rupp H & Weser U (1978) Circular dichroism of metallothioneins. A structural approach. *Biochim Biophys Acta.* **533**, 209-26.
26 Romero-Isart N, Cols N, Termansen M, Gelpi JL, Gonzalez-Duarte R, Atrian S, Capdevila M & Gonzalez-Duarte P (1999) Replacement of terminal cysteine with histidine in the metallothionein α and ß domain maintains its binding capacity. *Eur J Biochem* **259**, 519-527.
27 Palumaa P, Mackay EA & Vasak M (1992) Nonoxidative cadmium-dependent dimerization of Cd_7-metallothionein from rabbit liver. *Biochemistry* **31**, 2181-6.
28 Hathout Y, Reynolds KJ, Szilagyi Z & Fenselau J (2002) Metallothionein dimers studied by nano-spray mass spectrometry. *J Inorg Biochem* **88**, 119-122.
29 Zangger K & Armitage IM (2002) Dynamics of interdomain and intermolecular interactions in mammalian metallothionein. *J Inorg Biochem* **88**, 135-143.
30 Ferraroni M, Rypniewski W, Wilson KS, Viezzoli MS, Banci L, Bertini I & Mangani S. (1999) The crystal structure of the monomeric human SOD mutant F50E/G51E/E133Q at atomic resolution. The enzyme mechanism revisited. *J Mol Biol* **288**, 413-26.
31 Cols N, Romero-Isart N, Bofill R, Capdevila M, Gonzalez-Duarte P, Gonzalez-Duarte R & Atrian S (1999) *In vivo* copper- and cadmium-binding ability of mammalian metallothionein ß domain. *Protein Eng* **12**, 265-269.
32 Quandt K, Frech K, Karas H, Wingender E. & Werner T (1995) MatInd and MatInspector - New fast and versatile tools for detection of consensus matches in nucleotide sequence data. *Nucleic Acids Res* **23**, 4878-4884.
33 Thompson, JD, Higgins DG & Gibson TJ (1994) CLUSTAL W: improving the sensitivity of progressive multiple sequence alignment through sequence weighting, position specific gap penalties and weight matrix choice. *Nucleic Acids Res* **22**, 4673-4680.
34 Kumar S, Tamura K & Nei M (2004) MEGA3: Integrated Software for Molecular Evolutionary Genetics Analysis and Sequence Alignment. *Brief. Bioinformatics* **5**,150-163.
35 Hanahan D (1983) Studies on transformation of *Escherichia coli* cells with plasmids. *J Mol Biol* **166**, 557-580.
36 Yanish-Perron C, Viera J & Messing J (1985) Improved M13 phage cloning vectors and host strains: nucleotide sequences of the M13mp18 and pUC19 vectors. *Gene* **33**, 103-109.
37 Studier FW & Moffatt BA (1986) Use of bacteriophage T7 RNA polymerase to direct selective high-level expression of cloned genes. *J Mol Biol* **189**, 113-130.
38 Fabris D, Zaia J, Hathout Y & Fenselau C (1996) Retention of Thiol Protons in Two Classes of Protein Zinc Coordination Centers. *J Am Chem Soc* **118**, 12242-12243.

Supplementary material.

Note S1. Interestingly, the comparison of the CD fingerprints of the three *in vivo* Cd-βMT samples reveals some similarities between Cd-βckMT1 and Cd_3-βMT1 [31], which clearly differ from the Cd-βMT4 preparation (Fig. 3D). The revision of the analytical data obtained from the three protein preparations in Cd-supplemented media shows that while Cd_3-βMT1 was obtained as a single species [31], βMT4 and βckMT1 gave rise to mixtures where the corresponding Cd_3-βMT complex was the major species. Our recent findings on the presence of sulfide ligands in recombinant Zn- and Cd-MTs [23] now enable us to propose that the composition of ßMT4 synthesized in Cd-supplemented medium includes Cd_3-βMT4, Cd_2S_2-βMT4 and Cd_1S_4-βMT4, rather than heterometallic Zn,Cd-βMT4 complexes [16]. Furthermore, current results in this paper show that the minor species of the Cd-βckMT1 samples also contain S^{2-} ligands (Table 1). Accordingly, ßMT4 and ßckMT1 preparations should exhibit similar spectroscopic features, which is not the case, those of ßMT1 being closer to ßckMT, and thus corroborating the differential conformational arrangement previously proposed for Cd_3-βMT4 [16].

Note S2. The spectrum depicted in Fig. 4D as representative of the Cd_3-ßMT1 species, was originally attributed to Cd_9-ßMT1 [18]. Currently, a large amount of experimental evidence enables to revise these results. First, it should be noted that the Cd_9-ßMT1 alleged species could never be detected by ESI-MS. Second, we have later proved that no less than 7 Cd(II) eq have to be added to either Zn_3-ßckMT1 (this paper) or Zn_3-ßMT4 [16] to reach the respective Cd_3- complexes as unique species. Therefore, the CD spectrum recorded after 9 Cd(II) eq added to Zn_3-ßMT1 should be considered representative of the Cd_3-ßMT1 complex, while that recorded after 3 Cd(II) eq would consist of a summation of the CD features of the diverse species coexisting at this stage of the titration (probably heterometallic Zn,Cd-ßMT1 complexes and sulfide-containing species).

Table S1. Distribution of the metal aggregates present in solution, according to ESI-MS data, during the titration of Zn_4-αckMT1 (**A**), Zn_3-βckMT1 (**B**) and Zn_7-ckMT1 (**C**) with $[Cu(MeCN)_4]ClO_4$ at pH 7 as a function of the number of Cu(I) equivalents added

A)	Cu(I) equivalents added				
	3	4	5	7	10
M_4-αckMT1	◆	x			
M_5-αckMT1	x	x	x	✓	x
M_6-αckMT1	x	x	x	x	x
M_7-αckMT1	✓	✓	✓	x	x
M_8-αckMT1	x	x	◆	◆	x
M_9-αckMT1	x	◆	◆		

B)	Cu(I) equivalents added		
	3	4	5
M_3-βckMT1	x		
M_4-βckMT1	x		
M_5-βckMT1	✓	✓	◆
M_6-βckMT1	x	x	✓
M_7-βckMT1	◆	◆	x

C)	Cu(I) equivalents added							
	3	4	5	6	7	8	10	16
M_7-ckMT	◆							
M_8-ckMT	◆	x						
M_9-ckMT	✓	✓	x	◆				
M_{10}-ckMT	x	x	✓	✓	✓	◆	◆	x
M_{11}-ckMT		◆	x	x	x	x	x	x
M_{12}-ckMT		◆	◆	x	x	✓	x	x
M_{13}-ckMT					◆	x	✓	✓
M_{14}-ckMT							x	x
M_{15}-ckMT								◆

✓, denotes the major species; x, species of intermediate abundance and ◆, the minor species present in solution

Article 5

Yeast Crs5: a putative ancestor in the Zn-thionein lineage

Manuscrit en preparació

Yeast Crs5: a putative ancestor in the Zn-thionein lineage

Laura Villarreal[1*], Ayelen Pagani[2*], Sílvia Atrian[2], Mercè Capdevila[1]

1 Departament de Química, Facultat de Ciències, Universitat Autònoma de Barcelona, Bellaterra, Spain

2 Departament de Genètica, Facultat de Biologia, Universitat de Barcelona, Barcelona, Spain

Abstract

Two important, partially related, questions about Metallothioneins (MTs)[1] still remain far from a clear answer: their intrinsic biological function and their evolutionary history. Obviously, the main drawback to envisage a sensible differentiation pattern driving MT specialization and natural selection through Evolution is the heterogeneity among all the members of this superfamily of proteins, which gathers under the generic denomination of MTs, a jumbled set of low molecular weight, high cys-content, metal chelating peptides, almost ubiquitously present in all the living organisms except Eubacteria (for reviews see 1 to 3). A quick glance at their sequences, through the web page http://www.expasy.ch/cgi-bin/lists?metallo.txt, immediately evidences a lack of homology that points to a probable polyphyletic origin of this protein superfamily, which would therefore include peptides evolved from different *MT primeval forms*.

Some time ago, and in an attempt to set up a new comprehensive frame for the study of MTs classification and evolution, we proposed a sorting criterion, on the basis of their *in vivo* metal binding preferences, which afforded to two main groups of MTs: zinc-thioneins and copper-thioneins, with more or less explicit protein sequence similarities among their members (4). Two well-known MTs are the paradigm for these two MT families: *S. cerevisiae* Cup1 for copper-thioneins (5), and the mammalian MT1 for zinc-thioneins (6). The crustacean MTH (MT1 from *Homarus americanus*) has also been characterized as a Zn-thionein (4), whereas the *Drosophila* MntA and MtnB proteins are typical copper-thioneins (7, 8). Most interestingly, we have identified some intermediate MTs that exhibit a dual behavior, reflecting either a special evolutionary constraint, as for chicken MT1 (9) or a functionally reminiscent form in case of gene multiplicity, as for mammalian MT4 (10).

When searching for the representatives of the primeval peptides generating each MT type, it is sensible to turn our attention to the fungal/yeast forms, as the most primitive eukaryotic cells. The origin of the "copper-MT" lineage is well identifiable in the short, one-domain Cup1 peptide, only represented among the metazoan organism MTs in *Drosophila*, where it generated the 4-member family of MtnA to MtnD peptides (11). Conversely, the seed of the zinc-MT lineage, the longer, typically bidominial forms predominant in most of the invertebrate and vertebrate actual groups, is not clearly defined. Under these premises, we turned our attention to the second *S. cerevisiae* MT, Crs5, in order to analyze its possible significance as a zinc-MT primeval form.

Crs5 (cooper-resistant suppressor 5) was first identified in 1994 as a protein able to reestablish copper resistance *CUP1*-null yeast cells, and readily characterized as a member of the MT superfamily (12). However, comparison of the Crs5 protein sequence and gene expression pattern with those of Cup1 early revealed a significant structural, and possible functional, divergence. On the one hand, the 69-amino acid long Crs5 polypeptide, containing 19 cysteines, was patently non-homologous to Cup1, with 61 residues –54 in its mature form- and only 12 cysteines, in fact sharing a superior protein similarity with the well-known MTs of higher eukaryotes rather than with its *S.cerevisiae* counterpart (12). On the other hand, although both *CUP1* and *CRS5* were positively

* These two authors contributed equally to this work

[1] The abbreviations used are: CD, circular dichroism, ESI-MS, electrospray ionization mass spectrometry; FPD, flame photometric detector; ICP-AES, inductively coupled plasma-atomic emission spectroscopy; MT, Metallothionein

regulated by high copper concentrations, and through the same copper-sensing transcription factor, Ace1, a relatively important constitutive expression level was reported for the latter, so that copper induction only represents a few fold increment of its normal synthesis rate (13). The situation was the opposite for Cup1, whose levels, insignificant in uninduced conditions, increase far beyond those of Crs5 as a response to high copper. The leader role of *CUP1* in yeast copper detoxification was primarily attributed to this different gene response, caused by the different number of cis-controlling Ace1-binding elements in the *CUP1* and *CRS5* regulatory regions, as neatly shown by a *CRS5*/*CUP1* promoter/coding sequences exchange experiment (13). However, it was also been pointed out that the metal binding abilities of both polypeptides should also be taken into account when trying to understand the secondary role of Crs5 in copper detoxification, and consequently, when trying to find an alternative function for this MT. Comparative copper binding analysis revealed that the Cu(I) ions coordinated to Crs5 are kinetically more labile and more solvent accessible than those in Cup1 (13). Therefore, and also considering the important constitutive presence of Crs5 in yeast cells, an alternative physiological role was suggested more in the line of a housekeeping metal metabolism agent involved in bioavailability, utilization and homeostasis of essential metals, including zinc (13). This hypothesis results highly attractive for the possibility of considering Crs5 as a putative ancestor in the Zn-thionein lineage.

Another interesting yeast MT feature caught our attention: both Cup1 and Crs5 levels depend on culture oxygenation levels: anaerobiosis causes an accumulation of copper inside the cell that is sensed by Ace1, triggering the expression of their target genes, among which CUP1 and CRS5; while aerobiosis induces the loss of the cytoplasmic copper and thus the recovery of normal intracellular levels, and the return of MT genes to their non-induced condition (14). This observation poses another intriguing question upon Crs5: which is the function of the constitutive Crs5 in the absence of copper, and consequently, which is the ability of Crs5 to bind zinc, which is the alternative form that may arise from this synthesis? Finally, it should be noted that a proper Zn-thionein, Zym1, induced by high zinc levels, was recently identified in the fission yeast, *Schizossacharomyces pombe*, (15) this discarding the hypothesis that all the fungal MTs were copper-reactive peptides, and that in the *Mycetae* kingdom divalent metals were only handled by glutathione-derived peptides of the phytochelatin type.

Consequently, we decided to undertake the evaluation of the Zn- or Cu-thionein character of Crs5, through the spectrometric and spectroscopic characterization of the zinc, copper and cadmium species recovered through its recombinant synthesis in *E.coli* cultures grown in metal supplemented media, an in different aeration conditions. The Crs5 *in vitro* metal binding abilities were evaluated by the study of the corresponding Zn/Cu and Zn/Cd replacement reactions. Additionally, the capacity of Crs5 to confer some advantage to transformed yeast cells in front of high zinc levels was evaluated. Finally, we examined our experimental results in the light of protein sequence similarity analysis, including the other known yeast MTs, as well as some paradigmatic MT forms. All our results converge on a conditional Zn-thionein character of Crs5, related to the aerobiosis levels of the producing cultures, which allows the consideration of Crs5 as representative of the primeval Zn-thionein lineage that evolved until the well-characterized mammalian MT family.

EXPERIMENTAL PROCEDURES

PCR Amplification, Cloning, and Sequence Analysis of Saccharomyces cerevisiae CRS5 Metallothionein Coding Region—The *CRS5* coding region (12) was amplified by colony PCR. Briefly, 1.5-2 mm colonies of *S. cerevisiae* strain VC-sp6 (*MATα trp1-1 ura3-52 ade$^-$ his$^-$ CAN^R gal1 leu2-3,112 cup1^S*) (12), microwaved for 1 min, were used as a template. Previously, several attempts using the strains YPH499, 1700, BY4741, DBY746, AH109, L40, Y190 and CG1945 as template failed to render a complete cDNA. All of them are derivatives of the strain S288C (16), which harbours *CRS5* sequence displaying a nonsense mutation in its ninth codon, instead of a Glu encoding triplet (17). In one of these amplifications, a *CRS5* cDNA without the nonsense mutation, but with a single change in codon 34 (rendering a Lys/Glu substitution) was obtained. This sequence was called CRS5* and it was also cloned to pursue expression experiments. The oligonucleotides used in PCR amplifications were: 5' GCCGGATCCATGACTGTAAAGATATGT 3' for the upstream primer and 5' ACTTAAGTCGACCTAACATTTTTCACAATT 3' for the downstream primer. To facilitate the cloning in frame of the cDNAs in the expression vector, a *BamHI* and a *SalI* restriction sites were generated just before the ATG start codon and after the stop signal with the upstream and downstream primers, respectively. Thirty five cycles of PCR amplification were performed in the following conditions: 94 °C for 30 s (denaturation), 55 °C for 30 s (annealing) and 72 °C for 30 s (extension), using Deep Vent (New England Biolabs) thermostable DNA polymerase.

The PCR products were isolated from 2% agarose gels, digested with B*amH*I-*Sal*I and subsequently cloned into the corresponding sites of the pGEX-4T-1 expression vector (GE Healthcare formerly Amersham Biosciences), for glutathione-S-transferase (GST)-MT

fusion protein synthesis (18). Restriction enzymes were from Takara and New England Biolabs. Previous to protein synthesis assays, all the DNA constructs were confirmed by automatic DNA sequencing (ABI 370; PerkinElmer Life Sciences), using the Amersham Dye Terminator Cycle Kit. JM105 was the *E. coli* recipient strain for cloning and sequencing purposes, and thereafter, the expression plasmids were transformed into the *E. coli* protease-deficient strain BL21 for recombinant overexpression.

Recombinant Synthesis and Purification of the Zn-, Cd- and Cu-CRS5 and Zn-, Cd- and Cu-CRS5 Aggregates*—For the characterization of all the CRS5 and CRS5* *in vivo* conformed metal aggregates, recombinant bacteria were grown according to two kinds of conditions. Small scale cultures (1.5 l, performed in 2 l Erlenmeyer flasks) were used for analytical purposes, whereas large scale volumes (10 liters, grown in a Microferm fermentor (New Brunswich), coupled to a Westfalia CSA-1-06-475 centrifuge and controlled by a TVE-OP 76/0 programmer (Braun Biotech) were used for preparative purposes. Transformant *E. coli* cells were grown in LB medium with 100 µg/ml ampicillin and one of the following metal supplements: 300 µM $ZnCl_2$ or $CdCl_2$ for the zinc- or cadmium-rich media, respectively, and 500 µM $CuSO_4$ for the copper-rich medium. Cultures were induced with isopropyl-1-thio-β-D-galactopyranoside at a final concentration of 100 µM 30 min before the addition of the metal solution. After 2.5 h induction, cells were harvested, washed in PBS buffer (1.4 M NaCl, 27 mM KCl, 101 mM Na_2HPO_4, 18 mM KH_2PO_4), and pelleted by centrifugation at 7700 x*g* for 10 min. For protein purification, the cells were resuspended in 5% of the original volume of ice-cold PBS-0.5% v/v ß-mercaptoethanol. To prevent oxidation of the metal-MT aggregates, pure grade argon was bubbled in all the steps of the purification procedure following cell disruption. The suspended cells were sonicated at 4 °C with 20-s pulses for 5 min and centrifuged at 12,000 x *g* for 15 min. The supernatant was recovered and used to purify the GST-MT polypeptides by batch affinity chromatography with gluthatione-Sepharose 4B at a volume ratio of 1:10 matrix/sample. The mixture was incubated with gentle agitation for 60 min at room temperature. After three washes in PBS, the matrix was packed in a column (15 x 3 cm) for subsequent purification steps. Because the GST-MT fusion protein included a thrombin recognition site, a thrombin/PBS solution (10 units per mg of fusion protein) was poured into the matrix bed, and digestion was carried out overnight at 23-25 °C. Subsequently, the GST portion of the expressed fusion protein remained bound to the gel matrix, whereas the MT segment was eluted together with thrombin. The eluate was then 5-fold concentrated using Centriprep Concentrators (Amicon) with a cut-off of 3 kDa and later fractionated using FPLC (a Superdex-75 column (GE Healthcare formerly Amersham Pharmacia Biotech) equilibrated with 50 mM Tris-HCl, pH 7.0, and run at 1 ml/min). 1-ml fractions were collected and analyzed for protein content by their absorbance at 254 nm. Aliquots of the protein-containing FPLC fractions were analyzed by 15% SDS-PAGE and stained by Coomassie Blue. MT-containing samples were pooled and stored at -70 °C until further use.

In order to further characterize the CRS5 copper binding ability, and due to the special significance of the oxygenation of the culture in these results, synthesis of CRS5 in copper supplemented media was assayed in parallel in different aeration conditions. Cultures were grown in four 2 l erlenmeyers flasks with 0,75 l of LB medium and bubbled with air. Before induction, cultures of two flasks were joined and the bubbling was stopped. The rest of the protocol continued as described for the joined erlenmeyer flask and with air bubbling for the other two flasks.

In Silico *Analysis of Protein Sequences*—Protein sequences were aligned by ClustalW (version 1.4), using Blosum62 as a distance matrix, with a gap penalty of 10/100, a gap extension value of 0.05/100, a 40% delay between divergent sequences (19) and finally it was adjusted manually. The ClustalW alignment was the input for calculating protein distances and constructing the corresponding bootstrap trees, through the Fitch-Margoliash tree-building algorithm (20). In this case, 1000 unrooted trees were examined for each bootstrap trial with a random generator seed of 5/1000. The protein distance and tree building applications are included in the *Phylip* software package (20).

Yeast functional complementation assays—An endogenous MT-null strain of *Saccharomyces cerevisiae* strain was used: DTY4 (*MATα, leu2-3, 112his3*$^{\Delta}$*1, trp1-1, ura 3-50, gal1, cup1::URA3*) (22). The yeast vector p424-CRS5 was constructed as follows: the CRS5 coding region was excised from pGEX-CRS5 by digestion with *Bam*HI/*Sal*I and ligated into the yeast vector p424 (23) under the transcriptional control of the yeast GPD (glyceraldehyde-3-phosphate dehydrogenase) constitutive promoter. The p424 vector also contains the CYC1 (cytochrome c oxidase) terminator, the 2µ replication origin and the TRP1 tryptophan marker. Vector p424 and the construct p424-CRS5 were introduced into DTY4 cells using the lithium acetate procedure (24) and transformed cells were selected by their capacity to grow in complete synthetic medium (SC), lacking Trp (SC-Trp).

For the functional complementation experiments, cultures of DTY4 cells carrying either p424 or p424-CRS5 were grown in SC-Trp liquid medium at 30 °C and 250 rpm, to OD_{600}=0.5. Four 10-fold dilutions were performed, and 3 µl of each dilution were spotted on SC plates and on SC supplemented with 10 mM $ZnCl_2$ or 10 mM $ZnCl_2$ + 5 µl $CuSO_4$. Plates were incubated for 3 days at 30 °C and photographed.

Metal binding studies of CRS5— The analysis of the metal binding capabilities of CRS5 towards Zn(II), Cd(II) and Cu(I) was attained through a two-step strategy by following an analogous rationale to that we used in the study of mammalian MT1 (18, 25, 26). First, the in vivo synthesized M-CRS5 complexes (were M represents the above mentioned metal ions) were characterized. Second, the reaction pathways of the in vitro Zn/Cd and Zn/Cu replacement processes undergone by the Zn-CRS5 peptide at pH 7 were determined. The detailed analysis of the spectroscopic (CD and UV-

visible electronic absorption) sets of data recorded during these titrations provided information on the number of metal-CRS5 species generated, their stoichiometry, and their degree of folding. Additionally, the spectrometric (ESI-MS) data revealed the molecular distribution (10, 27) of the various complex species coexisting at each point of the titrations. However, although it was possible to determine the Zn:Cd:CRS5 ratios in the heterometallic complexes formed in the Zn/Cd replacements, the proximity between the atomic weights of Zn and Cu, together with the ESI-MS experimental error range, prevented determination of the Zn:Cu:CRS5 ratios for the Zn/Cu displacement reactions.

Analytical, spectroscopic and spectrometric characterization of the CRS5 metal complexes—Acid ICP-AES (Inductively coupled plasma-atomic emission spectroscopy), which included an acidification of the samples before the conventional ICP procedure (28), was used to determine the amount of protein present in the different preparations and the global metal-to-protein ratios, measuring sulfur at 182.04 nm, zinc at 213.85 nm, cadmium at 228.80 nm and copper at 324.75 nm.

The sulfide presence in the CRS5 metal complexes was quantified by heavy acidification of the preparations, followed by gas chromatography and detection of the volatile H_2S generated through a flame photometric detector-GC coupled system (FPD-GC). Analysis conditions are detailed in (28).

Spectroscopic (UV-Vis) and spectropolarimetric (CD) analysis of the metal-CRS5 clusters and of the species formed *in vitro* during the Zn/Cd and Zn/Cu displacement titrations at pH 7.0 were carried out and processed as described in (10). Electronic absorption measurements were performed on an HP-8453 Diode array UV-visible spectrophotometer. A Jasco spectropolarimeter (Model J-715) interfaced to a computer (GRAMS 32 Software) was used for CD determinations. All assays were performed under Ar atmosphere, and titrations were carried out at least in duplicate to assure reproducibility. The pH for all experiments remained constant throughout, without the addition of buffers, and the temperature was kept at 25 ºC by means of a Peltier PTC-351S apparatus.

The molecular mass of the Zn-, Cd-, and Cu-CRS5 species obtained *in vivo* and *in vitro* was determined by electrospray ionization mass spectrometry (ESI-MS) on a Fisons Platform II Instrument, equipped with MassLynx software and calibrated with horse-heart myoglobin (0.1 mg/ml). The assay conditions for the Zn- and Cd-containing species were as follows: 20 µl of protein solution injected at 60 µl/min; the use of an HPLC Kromasil-100 C_4 (3.5 µm, 5 x 0.21 cm) column to separate analytes; capillary counter-electrode voltage, 4.5 kV; lens counter-electrode voltage, 1.0 kV; cone potential, 60 V; source temperature, 120 ºC; m/z range, 850-1950; scanning rate, 3 s/scan; interscan delay, 0.3 s. The assay conditions for the Cu-containing species were: 20 µl of protein solution injected at 30 µl/min; capillary counter-electrode voltage, 3.5 kV; lens counter-electrode voltage, 1.0 kV; cone potential, 35 V; source temperature, 160 ºC; m/z range, 850-1950; scanning rate, 3 s/scan; interscan delay, 0.3 s. In all cases, the running buffer was an appropriate mixture of acetonitrile and 5 mM ammonium acetate/ammonia, pH 7.5. The molecular mass of the apo-forms was determined as for the Cu-containing species, except that the carrier was a 1:1 mixture of acetonitrile and trifluoroacetic acid, pH 1.5. Masses for the holo-species were calculated as described in (29).

RESULTS

After confirmation of the correctness of *CRS5* and *CRS5** cDNA sequences, preliminary expression assays allowed the recovery of the respective apo-forms by acidification (pH 1.5) of the corresponding zinc aggregates. ESI-MS measurements rendered the values: 7465.36 ± 3.02 Da (calculated molecular mass, 7465.48 Da) for Crs5 and XXX Da (calculated molecular mass, YYY Da) for Crs5*, which confirmed the identity and integrity of the recombinant peptides.

All the experiments and characterization strategies reported in this paper have been constantly carried

A

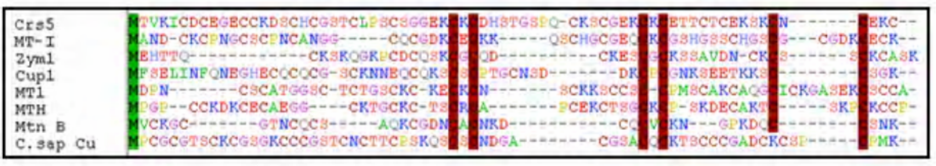

B

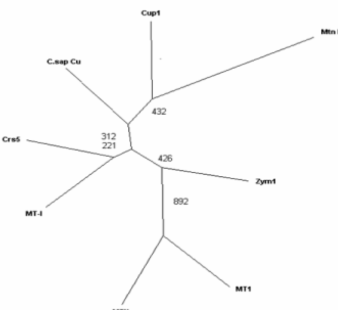

Fig 1: **Protein similarity analysis of Crs5 and some typical MTs.** (A) amino acid sequences shown according to their described alignment (see text). Residues conserved in more than 80% of the sequences are highlighted. (B) Fitch-Margoliash output tree of the alignment. Protein hosts are: Crs5 and Cup1, *S. cerevisiae*; MtnB, *D. melanogaster*; Zym1, *S. pombe*; MT1, *H. sapiens*; MTH, *H. americanus*; MT-I, *C. glabrata*; C.sap Cu, *C. sapidus*.

out for both the wild type, Crs5, and the mutated, Crs5*, forms. As results were invariably equivalent for all the parameters analyzed, from here on, they are only referred to Crs5.

Analysis of the primary structure of Crs5—When first reported, it was already made obvious that the Crs5 amino acid sequence was more similar to that of the mammalian MT forms that to its *S. cerevisiae* Cup1 counterpart (12). To further analyze the Crs5 protein similarities with other MTs, and significantly attempt its classification as Zn- or Cu-thionein following sequence distance criteria (4), we compared it with the following MTs: the yeast paradigmatic Cup1, for Cu-thioneins, and Zym1, for Zn-thioneins (ref 15??); the *Drosophila* MtnB Cu-thionein (ref 8 ??) and a representative of the crustacean Zn-thionein family (*H. americanus* MTH, (4) and of the crustacean Cu-thionein family (*C. sapidus Cu*-MT, ref??); the mammalian MT1 form (Zn-thionein) (ref??) and the MT1 form of *C. glabrata* (of unassigned classification, (30)). In spite of the apparently high divergence between these protein sequences (Fig. 1), with only some of their cysteine residues conserved, the distance tree still allows a clear correspondence with the metal binding abilities of all these MTs. In other words, the tree presented in Fig. 1 separates in two extreme branches those MTs exhibiting an absolute Zn-thionein and Cu-thionein behaviors: MTH, MT1, Zym1 and Cup1, MtnB and *Callinectes*-Cu, respectively. Then, the *S. cerevisiae* Crs5 and MT-I *C. glabrata* peptides, both having been described as copper-resistance proteins but with a secondary role in front of the main copper detoxifying systems of these organisms, are situated in an intermediate position between Zn- and Cu-thioneins. This result is in full concordance with the metal coordination results presented above, and with a possible role of

TABLE I

Molecular masses and metal (Zn, Cd or Cu) to protein ratios found for the in vivo synthesized Crs5 metal aggregates

Metal supplemented in culture media	MW_{exp}[a]	MW_{calc}[b]	M/Crs5[c]	M/Crs5[d]	M/Crs5[e]	S^{2-}/Crs5[f]
	Da	*Da*				
M = Zn	7911.6 ± 0.4	7909.1	Zn_7-Crs5 (S,e)	5.8 Zn	5.7 Zn	0.4
	7846.6 ± 1.2	7845.8	Zn_6-Crs5 (S,e)			
	7782.0 ± 1.7	7782.4	Zn_5-Crs5			
	7973.6 ± 0.8	7972.5	Zn_7S_2-Crs5 (s,e)			
	7717.4 ± 5.1	7719.0	Zn_4-Crs5 (s,e)			
M = Cd (Peaks 1 + 2)	8242.0 ± 0.5	8238.4	Cd_7-Crs5 (S)	0.1 Zn 3.2 Cd	---	2.03
	8193.5 ± 0.7	8191.3	Cd_6S_2-Crs5			
	8134.5 ± 0.0	8127.9	Cd_6-Crs5 (e)			
	8305.6 ± 0.0	8301.7	Cd_7S_2-Crs5 (e)			
	8353.7 ± 0.0	8348.8	Cd_8-Crs5 (s,ee)			
	8080.8 ± 0.0	8080.9	Cd_5S_2-Crs5 (s,ee)			
M = Cd (Peak 1)	8303.5 ± 3.8	8301.7	Cd_7S_2-Crs5 (S)	0.0 Zn 1.8 Cd	0.3 Zn 9.0 Cd	---
	8357.0 ± 7.2	8352.3	Cd_8-Crs5 (s)			
M = Cd (Peak 2)	8240.4 ± 2.6	8238.4	Cd_7-Crs5 (S)	0.1 Zn 3.1 Cd	0.1 Zn 7.4 Cd	1.81
	8301.7 ± 0.8	8301.7	Cd_7S_2-Crs5			
	8351.8 ± 1.8	8352.3	Cd_8-Crs5			
	8197.5 ± 2.3	8191.3	Cd_6S_2-Crs5			
	8147.3 ± 5.1	8145.7	Cd_5S_4-Crs5 (s)			
M = Cu (small-scale productions)	8087.0 ± 4.8	8090.5	Cu_{10}-Crs5 (S)	0.2 Zn 10.6 Cu	0.1 Zn 11.1 Cd	N/D[g]
	8024.5 ± 2.7	8027.9	Cu_9-Crs5			
	8146.3 ± 0.0	8153.0	Cu_{11}-Crs5			
	8215.9 ± 1.9	8215.6	Cu_{12}-Crs5			
	8285.7 ± 0.0	8278.6	Cu_{13}-Crs5			
	7965.5 ± 3.4	7965.4	Cu_8-Crs5			
M = Cu (large-scale productions)	8026.9 ± 1.1	8027.9	M_9-Crs5 (S,e)	1.8 Zn 5.1 Cu	1.9 Zn 5.6 Cu	N/D
	7963.2 ± 1.0	7965.4	M_8-Crs5 (S,e)			
	8090.6 ± 2.1	8090.5	M_{10}-Crs5			
	8153.4 ± 1.0	8153.0	M_{11}-Crs5 (ee)			
	8210.9 ± 1.6	8215.6	M_{12}-Crs5 (ee)			
	7837.0 ± 5.4	7840.3	M_6-Crs5 (s,eee)			
	7901.4 ± 3.1	7902.8	M_7-Crs5 (s,eee)			

[a] Experimental molecular masses for the Zn-, Cd- and Cu-Crs5 complexes.
[b] Calculated molecular mass for neutral species with loss of two protons/zinc or cadmium bound and of one proton/copper bound (29).
[c] Metal:Crs5 molar ratio calculated from the mass difference between holo- and apo-protein. (S) denotes a major species; (s) denotes a minor species; (e), (ee) and (eee) denote equimolarity.
[d] Metal:Crs5 molar ratio deduced from the metal content measured by *conventional* ICP-AES.
[e] Metal:Crs5 molar ratio deduced from the Zn, Cd, Cu and S content measured by acid ICP-AES.
[f] S^{2-} to MT ratio measured by GC-FPD.
[g] N/D means non detectable.

these forms in some cellular role involving zinc coordination.

Zn(II) binding abilities of Crs5—The biosynthesis of Crs5 in Zn-supplemented cultures renders a mixture of homometallic Zn-complexes with Zn_6- and Zn_7-Crs5 as the equimolar major species (Table I, Figure 2). The CD spectroscopic fingerprint of this sample (Figure 3) consists of a 240 nm centred gaussian band, characteristic of the $Zn(S_{Cys})_4$ chromophores, with a faint contribution at *ca.* 260 nm (31) of the minute amount of sulfide-containing clusters detected in this sample(Table I). Also, the lack of absorptions at *ca.* 230 nm provides spectroscopic evidence of the non participation of the two His residues in Zn binding (31).

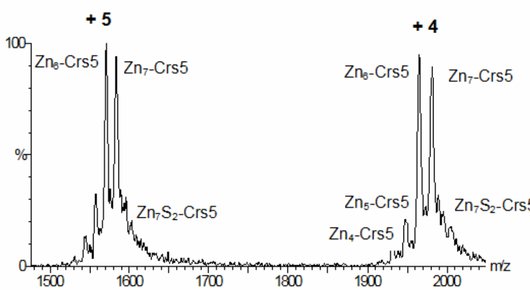

Fig. 2. **ESI-MS spectrum of the recombinant Zn-Crs5 preparation.** The two sets of peaks corresponding to two charge states (+4 and +5) illustrate the equimolarity of the Zn6- and n7-Crs5 biosynthesized species.

Cd(II) binding abilities of Crs5—All the syntheses of Crs5 performed in Cd-supplemented cultures gave rise to mixtures of homometallic Cd-complexes (Table I). The analysis of these syntheses was made difficult by the fractionation of the MT purified forms in two FPLC peaks. The joint characterization of peak 1 + peak 2 FPLC fractions in a single sample (Peaks 1+2 in Table I) affords a major Cd_7-Crs5 species followed by several under- and overloaded Cd-Crs5 species that contain or not sulfide ligands. Analysis of the separate FPLC peaks (Peak 1 and Peak 2 in Table I) gave further information on the composition of the Cd-Crs5 sample. The largest, and not very abundant, Cd_7S_2-Crs5 and Cd_8-Crs5 species are mainly eluted in peak 1, showing the conventional *vs.* acid ICP-AES results and the characteristic CD spectrum (Fig. 4A) that evidences the presence of sulfide ligands in the complexes (28). Conversely, peak 2 contains a major Cd_7-Crs5 species and some other minor S^{2-}-containing species, whose contribution to the CD fingerprint of the sample is quite negligible (Fig. 4A). The difference in the sulfide ligand content between peaks 1 and 2 is also patent in their UV-vis spectra (Fig 4B). Consideration of the CD fingerprints of peak 1 and peak 2 and the minor abundance of peak 1 yields a reasonable explanation to the CD spectrum recorded for the joint sample (Fig. 4A), which shows only a minor contribution in the 280-300 nm region.

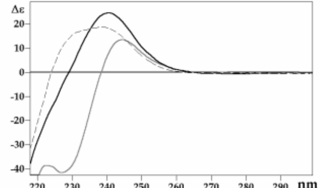

Fig. 3. **Circular dichroism spectrum of the in vivo synthesized Zn-CRS5**. The spectrum in gray and dashed correspond respectively to *in vivo* synthesized Zn_7-MT1 (18) and Zn-MTH samples (4) and are included to highlight the gaussian nature of Zn-Crs5 and Zn-MTH towards the derivative shaped envelope of Zn_7-MT1.

The *in vitro* Cd(II) titration of the Zn-Crs5 sample provided a further insight into the Cd-binding abilities of Crs5 (Fig. 5). In spite of the inherent difficulties of the system (initial mixture of Zn_6- and Zn_7-Crs5 complexes, the high number of Zn,Cd-Crs5 species coexisting at each point of the titration and the ESI-MS mass equivalence between 1 Zn^{2+} and 2 S^{2-}) the spectroscopic and spectrometric study of the Zn/Cd replacement reaction (Figures 5 and S1) has allowed to establish that: 1) there is an isomorphic replacement of Zn by Cd in the Zn-Crs5 complexes; 2) His do not contribute to Cd-binding even in an excess of Cd(II) ions; 3) Cd-Crs5 species are characterized by a gaussian CD envelope centred at 250 nm; 4) the preferred Cd:Crs5 stoichiometric ratio is of 7; and 5) as a consequence of the low sulfide content of the Zn-Crs5 preparations, the Cd-S^{2-} chromophores are practically inexistent. Furthermore, and in accordance with this later observation, only the

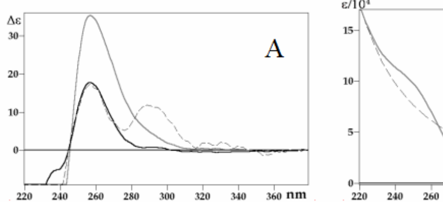

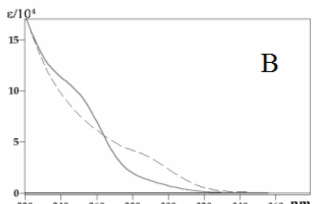

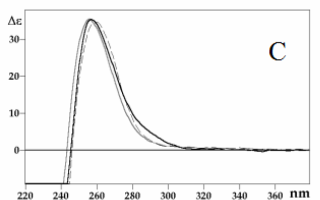

Fig. 4. **Comparison of the circular dichroism (A) and UV-vis (B) spectra of the of the *in vivo* synthesized Cd-Crs5 samples** corresponding to Peaks 1+2 sample (black), Peak 1 sample (dashed) and Peak 2 sample (gray). The normalized spectra superimposed in (C) correspond to those recorded after the addition of 6 (gray) and 7 (dashed) Cd(II) eq to the recombinant Zn-Crs5 preparation.

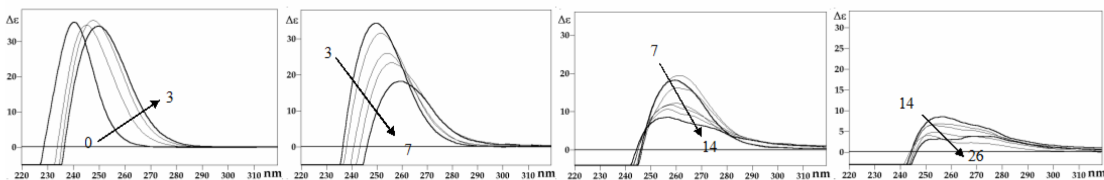

Fig. 5. **Circular dichroism spectra corresponding to the titration of recombinant Zn-Crs5 with Cd(II) at pH 7.** The arrows show the evolution of the spectra when the indicated number of Cd(II) equivalents were added.

features of the peak 2 preparations can be reproduced *in vitro* by Zn/Cd replacement in Zn-Crs5 samples, Fig. 4C.

Cu(I) binding abilities of Crs5—In order to analyze the features of the *in vivo*-folded Cu-Crs5 clusters, and to compare them with those generated *in vitro* from Zn-Crs5 by Zn/Cu displacement, two types of cultures were set up: small-scale 1.5-l cultures in 2-l Erlenmeyer flasks, and large-scale 10 l cultures. Both production types significantly differ in the degree of oxygenation of the cultures, being higher those of the large-scale productions, as the fermentator maintains a 70-80% oxygen saturation level.

Analysis of the results obtained in both types of syntheses revealed that the homo- or heterometallic nature of the Crs5 metal clusters obtained was culture-size dependent, as small-scale preparations rendered homometallic Cu-Crs5 complexes, while large-scale cultures yielded heterometallic Zn,Cu-Crs5 species (Table I). Both samples exhibited characteristic CD fingerprints (Fig. 6) that do not match any of those known for other Zn,Cu-MT complexes, Fig. 7. It is worth noting that sulfide ligands, if present, were not detected in any of the Cu-Crs5 preparations studied in correspondence with the scenarios found in other MTs (28),. Regarding the stoichiometry of the metal-Crs5 complexes synthesized, and contrasting with the Cu_{11-12}-Crs5 metal-to-protein ratios reported in the literature for native Cu-Crs5 preparations(13), we have found that in small-scale cultures, Cu_{10}-Crs5 is the major species of a continuum of metal-complexes ranging form Cu_8-Crs5 to Cu_{13}-Crs5 (Table I). The total metal-to-protein stoichiometry is lower in large-scale cultures, which yield an equimolar mixture of the heterometallic M_8- and M_9-Crs5 complexes together with other minor species.

DISCUSSION

Literature data (13) has shown that apo-CRS5 can bind *in vitro* up to 6 Cd(II) ions. Our results suggest that *in vivo* and in Zn-rich media, CRS5 exists as a mixture of several homometallic Zn-complexes with an average stoichiometry of 6 Zn per CRS5 protein (Table I), which includes a continuum of species ranging from Zn_4- to Zn_7-CRS5 but with a clear predominance of the equimolar Zn_6- and Zn_7-CRS5 complexes, which constitute the 80% of the sample. Consequently, the 19 Cys putative coordinating residues of CRS5 provide the protein with a Zn(II) binding capacity analogous to that of mammalian MTs, the 2 His residues not contributing to metal coordination. Interestingly, the Zn-CRS5 sample is, together with Zn-MTH, the only Zn-MT species described showing a CD spectrum with a gaussian band instead of the well known exciton coupling centred at 240 nm. Although this could suggest a poor degree of folding of the Zn-CRS5 clusters in comparison with other Zn-MT forms, it is important to highlight that the intensity of the CD spectrum, *i.e.* quirality of the ZnCrs5 complexes, is the highest ever reported for any Zn-MT (see for instance the comparison between Zn-CRS5, Zn-MTH and Zn_7-MT1 in Fig. 3). Finally, the low content in sulfide ligands of the Zn-CRS5 preparations (less than 1 S^{2-} per CRS5 molecule) is in accordance with the scenarios found for other Zn-MT samples (28), and the low oxidation degrees measured by the Ellmans method (32) (close to 0%, data not shown) suggest a high stability of these metal aggregates. All these data guarantee the already proposed (13) higher ability

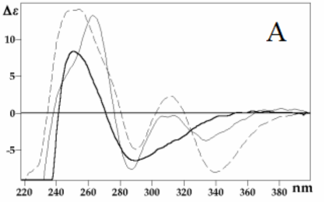

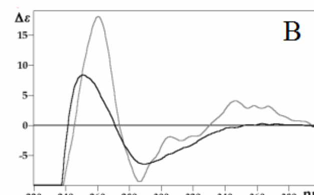

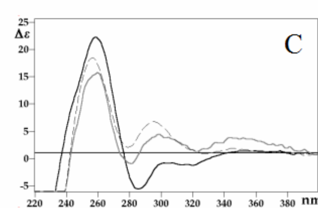

Fig. 6. Comparison of CD spectra of (A) homometallic Cu-Crs5 complexes (solid black line) with Cu_8-MTN (dashed) and Cu_9-MTO gray); (B) homometallic Cu-Crs5 complexes (solid black line) with Cu_{10}-MT4 (gray) and (C) heterometallic Zn,Cu-Crs5 complexes with Zn_3Cu_7-MT1 (dashed) and Zn_3Cu_7-MT4 (gray).

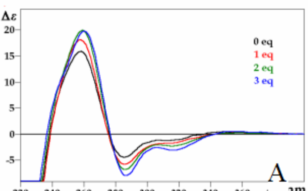

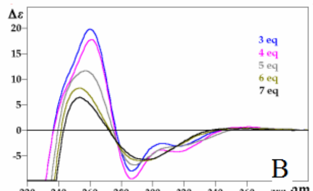

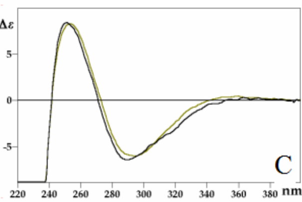

Fig. 9. (A,B) **Circular dichroism spectra corresponding to the titration of the *in vivo* heterometallic Zn,Cu-Crs5 sample with Cu(I) at pH 7.** Plate (C) correspond to the superimposition of the CD spectrum corresponding to the addition of 6 Cu(I) eq to the Zn,Cu-Crs5 of (B) and the biosinthesized homometallic Cu-Crs5 sample.

of CRS5 towards CUP1 for Zn binding.

The results of CRS5 synthesis in Cd-enriched cultures enhanced the hypothesis that CRS5 was optimized for divalent metal complexation as differing from MT4, the mammalian Cu-thionein (10), only homometallic Cd-CRS5 complexes were obtained (Table I). However, the presence of sulfide ligands in the Cd-CRS5 complexes cannot be underestimated. Fortunately, it has been possible to achieve separation of the high-sulfide-content species from those of low-sulfide-content by FPLC. This has allowed recording the CD spectra depicted in Figure 4A that can respectively be considered representative of the Cd_7S_2-CRS5 and Cd_7-CRS5 species. Consideration of these CD spectra allows to deduce that the Cd-CRS5 samples show the characteristic absorptions of the $Cd(S_{Cys})_4$ chromophores at *ca.* 250 nm plus those at the 280-300 nm assignable to the participation of sulfide ligands to Cd(II) binding (28) and to discard the participation of the two His residues in the metal clusters in contrast with the situations found in other His-containing MTs (9,33,34).

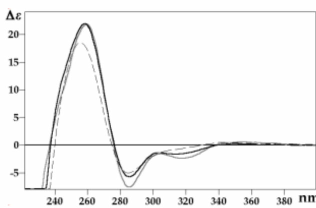

Fig. 7. Comparison of circular dichroism spectra of the *in vivo* heterometallic Zn,Cu-Crs5 …..

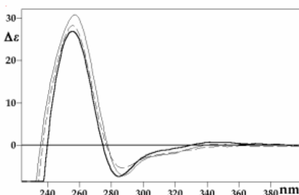

Fig. 8. ….

In respect to copper coordination to Crs5 ….

CONCLUDING REMARKS

……….

Acknowledgements-This work was supported by the *Spanish Ministerio de Ciencia y Tecnología* grants CTQ2004-00359/BQU to Mercè Capdevila and BIO2003-03892 to Silvia Atrian. We acknowledge the *Serveis Científico-Tècnics, Universitat de Barcelona* (DNA sequencing, ICP-AES, ESI-MS, GC-FPD) and the *Servei d'Anàlisi Química, Universitat Autònoma de Barcelona* (AAS, CD, UV-Vis) for allocating instrument time.

REFERENCES

1. revision 1
2. revision 2
3. revision 3
4. Valls, M., Bofill, R., Gonzalez-Duarte, R., Gonzalez-Duarte, P., Capdevila, M. and Atrian, S. (2001) *J. Biol. Chem.* **276**, 32835-32843
5. CUP1
6. MT1
7. Valls, M., Bofill, R., Romero-Isart, N., González-Duarte, R., Abián, J., Carrascal, M., González-Duarte, P., Capdevila, M. and Atrian, S. (2000) *FEBS Lett.* **467**, 189-194
8. Domenech, J., Palacios, O., Villarreal, L., González-Duarte, P., Capdevila, M. and Atrian, S. (2003) *FEBS Lett.* **533**, 72-78
9. Villarreal, L., Tío, L., Capdevila, M. and Atrian, S. (2005) *FEBS J.*, submitted
10. Tio, L., Villarreal, L., Atrian, S. and Capdevila, M. (2004) *J. Biol. Chem.* **279**, 24403-24413
11. Egli, D., Doménech, J., Selvaraj, A., Balamurugan, K., Hua, H., Yepiskoposyan, H., Vardanyan, A., Capdevila, M., Atrian, S., Georgiev, O. and Schaffner, W. (2005) *J. Biol. Chem.*, submitted
12. Culotta, V. C., Howard, W. R. and Liu X. F. (1994) *J. Biol. Chem.* **269**, 25295-25302
13. Jensen, L. T., Howard, W. R., Strain, J. J., Winge, D. R. and Culotta, V. C. (1996) *J. Biol. Chem.* **271**, 18514-18519
14. Strain, J. and Culotta, V. C. (1996) *Mol. Gen. Genet.* **251**, 139-145
15. Borrelly, G. P. M., Harrison, M. D., Robinson, A. K., Cox, S. G., Robinson, N. J. and Whitehall, S. K. (2002) *J. Biol. Chem.* **277**, 30394-30400
16. Fink, G. R., in H. Tabor and C. W. Tabor (Editors), *Methods in enzymology*, Vol. **17**, Part A, Academic Press, New York, 1970, p. 59.
17. Dujon, B., Albermann, K., Aldea, M., Alexandraki, D., Ansorge, W., Ariño, J., Benes, V., Bohn, C., Bolotin-Fukuhara, M.,

Bordonne, R., Boyer, J., Camasses, A., Casamayor, A., Casas, C., Cheret, G., Cziepluch, C., Daignan-Fornier, B., Dang, D.V., de Haan, M., Delius, H., Durand, P., Fairhead, C., Feldmann, H., Gaillon, L., Kleine, K., et al. (1997) *Nature*. **387**, 98-102.
18. Cols, N., Romero-Isart, N., Capdevila, M., Oliva, B., Gonzàlez-Duarte, P., Gonzàlez-Duarte, R. and Atrian, S. (1997) *J. Inorg. Biochem*. **68**, 157-166
19. Thompson, J.D., Higgins, D.G. and Gibson, T.J.(1994) *Nucleic Acids Res.* **22**, 4673-80.
20. Fitch, W.M. and Margoliash, E. (1967) *Science*. **155**, 279-84.
21. Felsenstein, J. (1989) *Cladistics* **5,** 164-166.
22. Longo, V.D., Gralla, E.B. and Valentine, J.S. (1996) *J. Biol. Chem*. **271**, 12275-12280.
23. Mumberg, D., Muller, R. And Funk, M. (1995) *Gene.* **156**, 119-122.
24. Stearns, T., Ma, H. and Botstein, D. (1991) *Methods in Enzymol*. **185**, 280-297.
25. Bofill, R., Capdevila, M., Cols, N., Atrian, S. and González-Duarte, P. (2001) *J. Biol. Inorg. Chem.* **6**, 408-417
26. Cols, N., Romero-Isart, N., Bofill, R., Capdevila, M., González-Duarte, P., González-Duarte, R. and Atrian, S. (1999) *Protein Eng.* **12**, 265-269.
27. Polec-Pawlak, K., Palacios, Ò., Capdevila, M., González-Duarte, P. and Lobinski, R. (2002) *Talanta* **57**, 1011-1017
28. Capdevila, M., Pagani, A., Domenech, J., Tio, L., Villarreal, L. and Atrian, S. (2005) *Angew. Chem. Int. Ed.* **44**, 4618-4622
29. Fabris, D., Zaia, J., Hathout, Y. and Fenselau, C. (1996) *J. Am. Chem. Soc.* **118**, 12242-12243
30. R.K. Mehra, J.R. Garey, T.R. Butt, W.R. Gray, D.R. Winge, (1989), J. Biol Chem., **264**, 19747-19753.
31. Kho, R., Nguyen, L., Torres-Martínez, C.L. and Mehra, R.K. (2000) *Biochem. Biophys. Res. Commun.* **272**, 29-35
32. Dameron, C.T. and Winge, D.R. (1990) *Inorg. Chem.* **29**, 1343-1348
33. Weber, D.N., Shaw III, C.F. and Petering, D.H. (1987) *J. Biol. Chem.* **262**, 6962-6964
34. Blindauer, C.A., Harrison, M.D., Parkinson, J.A., Robinson, A.K., Cavet, J.S., Robinson, N.J. and Sadler, P.J. (2001) *Proc. Natl. Acad. Sci. USA*, **98**, 9593-9598
35. Romero-Isart, N., Cols, N., Termansen, M.K., Gelpí, J.L., Gonzàlez-Duarte, R., Atrian, S., Capdevila, M. and Gonzàlez-Duarte, P. (1999) *Eur. J. Biochem*. **259**, 519-527
36. Peña, M-M. O., Koch, K. A. and Thiele, D. J. (1998) *Mol. Cell. Biol.* **18**, 2514-2523
37. Gross, C., Kelleher, M., Iyer, V. R., Brown, P. O. and Winge, D. R. (2000) *J. Biol. Chem.* **275**, 32310-32316
38.

SUPPLEMENTARY MATERIAL

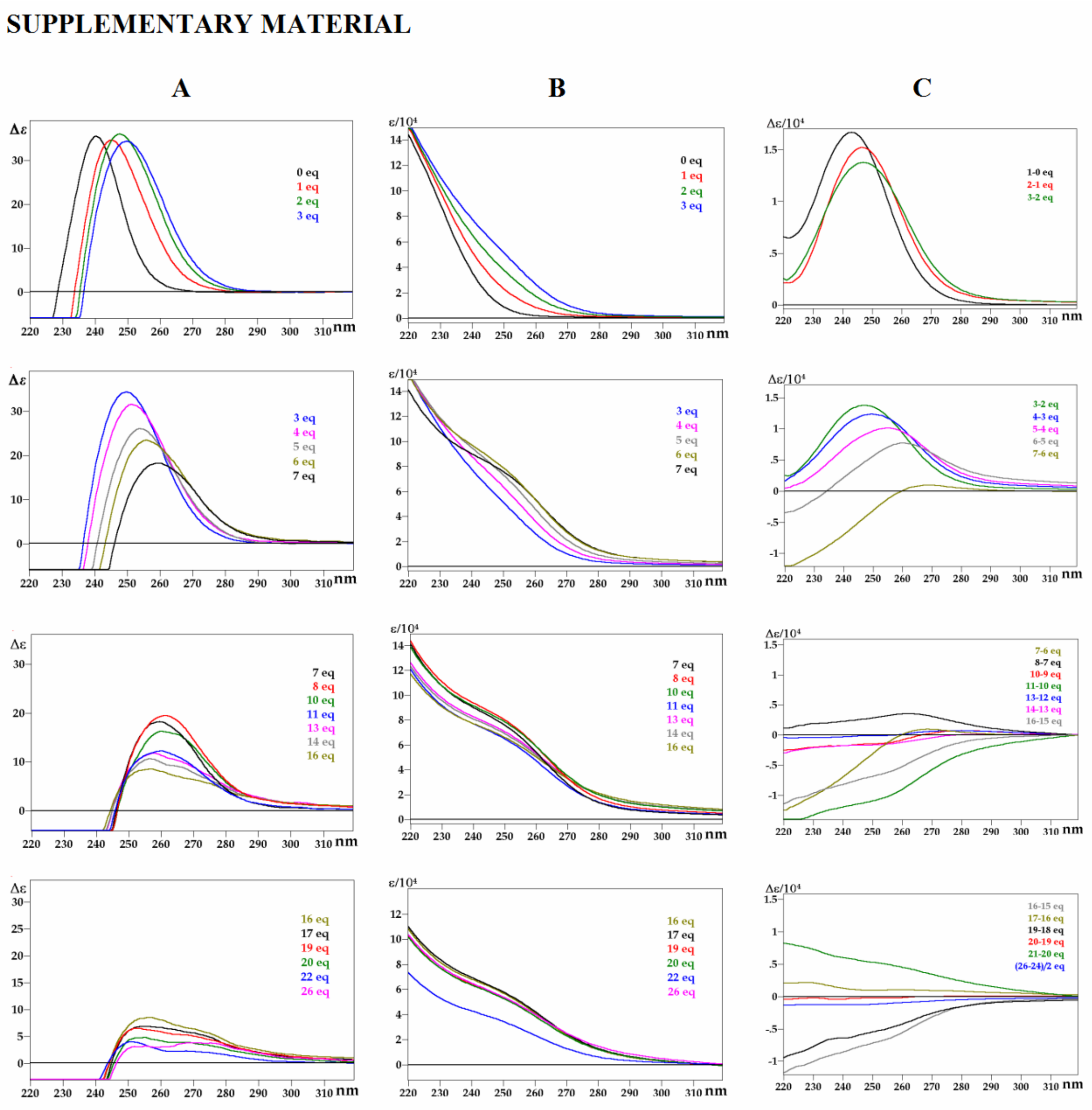

Fig. S1. Circular dichroism (A), UV-visible absorption (B) and UV-visible difference absorption (C) spectra corresponding to the titration of recombinant Zn-Crs5 with Cd(II) at pH 7. The UV-visible difference absorption spectra of (C) have been obtained by subtracting the successive spectra of (B). The Cd(II) to Crs5 molar ratios are indicated in each frame.

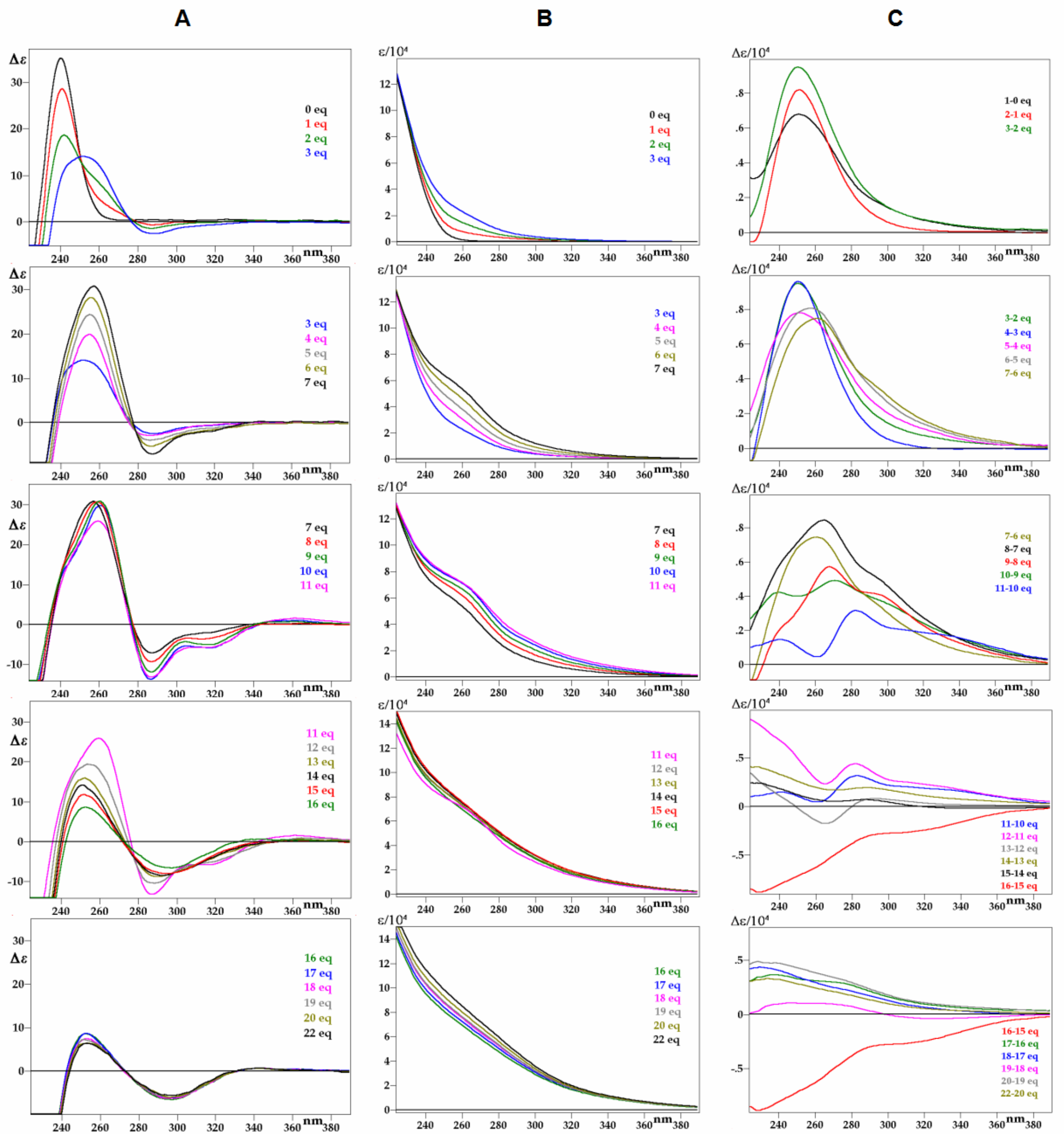

Fig. S2. Circular dichroism (A), UV-visible absorption (B) and UV-visible difference absorption (C) spectra corresponding to the titration of recombinant Zn-Crs5 with Cu(I) at pH 7. The UV-visible difference absorption spectra of (C) have been obtained by subtracting the successive spectra of (B). The Cu(I) to Crs5 molar ratios are indicated in each frame.

4. BIBLIOGRAFIA

[1].- M. Margoshes, B. Vallee, *J. Am. Chem. Soc.* (1957) **79**, 4813

[2].- P. Gonzàlez-Duarte., "Metallothioneins". Dins: J. A. McCleverty and T.J. Meyer, (eds.). *Comprehensive Coordination Chemistry II.* Oxford: Elsevier (2003) Secció 8.9, pag. 213

[3].- M.J. Stillman, *Coordination Chemistry Reviews* (1995) **144**, 461

[4].- J. F. Riordan, B. L. Vallee, eds. *Methods Enzymol.*, **vol. 205**, Academic Press, San Diego, (1991)

[5].- F.J. Kull, M.F. Reed, T.E. Elgren, T.L. Ciardelli, D.E. Wilcox, *J. Am. Chem. Soc.* (1990) **112**, 2291

[6].- A. Muñoz, D.H. Petering, C.F. Shaw III, *Inorg. Chem.* (2000) 39, 6114

[7].- Y. Nishiyama, S. Nakayama, Y. Okada, K.S. Min, S. Onosaka, K. Tanaka. *Chem. Pharm. Bull.* (1990) **38**, 2112

[8].- a) Y. Okada, N. Ohta, S. Iguchi, Y. Tsuda, H. Sasaki, T. Kitagawa, M. Yagyu, K.S. Min, S. Onosaka, K. Tanaka, *Chem. Pharm. Bull.* (1986) **34**, 986. b) H.J. Hartmann, Y.J. Li, U. Weser, *Biometals* (1992) **5**, 187 c) Y.J. Li, U. Weser, *Inorg. Chem.* (1992) **31**, 5526. d) A.K. Sewell, L.T. Jensen, J.C. Erikson, R.D. Palmiter, D.R. Winge, *Biochemistry* (1995) **34**, 4740

[9].- M. Capdevila, N. Cols, N. Romero-Isart, R. González-Duarte, S. Atrian, P. Gonzáles-Duarte, *Cell. Mol. Life Sci.* (1997) **53**, 681

[10].- M. Valls, R. Bofill, R. González-Duarte, P. González-Duarte, M. Capdevila, S. Atrian, *J. Biol. Chem.*(2001) **276**, 32835

[11].- P.A. Cobine, R.T. McKay, K. Zangger, C.T. Dameron, I.M. Armitage, *Eur. J. Biochem.* (2004) **271**, 4213

[12].- N. Romero-Isart, M. Vašák, *J. Inorg. Biochem.*, 2002, **88**, 388

[13].- P. Schultze, E. Worgotter, W. Braun, G. Wagner, M. Vašák, J.H.R. Kägi, K. Wüthrich, *J. Mol. Biol.* (1988) **203**, 251

[14].- A. Aseniev, P. Schultze, E. Wörgötter, W. Braun, G. Wagner, M. Vašák, J.H.R. Kägi, K. Wüthrich, *J. Mol. Biol.* (1988) **201**, 637

[15].- B.A. Messerle, A. Schäffer, M. Vašák, J.H.R. Kägi, K. Wüthrich, *J. Mol. Biol.* (1990) **214**, 765

[16].- K. Zangger, G. Öz, J.D. Otvos, I.M. Armitage, *Protein Sci.* (1999) 8, 2630

[17].- G. Öz, K. Zangger, I.M. Armitage, *Biochemistry* (2001) **40**, 11433

[18].- C. Capasso, V. Carginak, O. Crescanzi, D. Di Maro, E. Parisi, R. Spadaccini, P.A. Temussi, *Structure* (2003) **11**, 435

[19].- S.S. Narula, M. Brouwer, Y. Hua, I.M. Armitage, *Biochemistry* (1995) **34**, 620

[20].- A. Muñoz, F.H. Försterling, C.F. Shaw III, D.H. Petering, *J. Biol. Inorg. Chem.* (2002) 7, 713

[21].- R. Riek, B. Prêcheur, Y. Wang, E.A. Mackay, G. Wider, P. Güntert, A. Liu, J.H.R. Kägi, K. Wüthrich, *J. Mol. Biol.* (1999) **291**, 417

[22].- C.A. Blindauer, M.D. Harrison, J.A. Parkinson, A.K. Robinson, J.S. Cavet, N.J. Robinson, P.J. Sadler, *Proc. Natl. Acad. Sci. USA* (2001) **98**, 9593

[23].- Y.L. Li, U. Weser, *Inorg. Chem.* (1992) **31**, 5526

[24].- I. Bertini, H. -J. Hartmann, T. Klein, G. Liu, C. Luchinat, U. Weser, *Eur. J. Biochem.* (2000) **267**, 1008

[25].- V. Calderone, B. Dolderer, H.J. Hartmann, H. Echner, C. Luchinat, C. Del Bianco, S. Mangani, U. Weser, *Proc. Natl. Acad. Sci. USA* (2005) **102**, 51

[26].- T.A. Smith, K. Lerch, K.O. Hodgson, *Inorg. Chem.* (1986) **25**, 4677

[27].- B.A. Fowler, C.E. Hildebrand, Y. Kojima, M. Webb, Nomenclature of Metallothionein. A: *Metallothionein II.* J.H.R. Kägi, Y. Kojima, Eds., Birkhäuser Verlag, Basel (1987) **52**, 19

[28].- P.A. Binz, J.H.R. Kägi, In: *Metallothionein IV*, Birkhäuser Verlag, Basel (1999) **7**

[29].- http://www.unizh.ch/~mtpage/classif.html

[30].- R. Bofill, M. Capdevila, N. Cols, S. Atrian, P. González-Duarte, *J. Biol. Inorg. Chem.* (2001) **6**, 408

[31].- M. Valls, R. Bofill, N. Romero-Isart, R. González-Duarte, J. Abián, M. Carrascal, P. González-Duarte, M. Capdevila, S. Atrian, *FEBS Lett.* (2000) **467**, 189

[32].- J. Domenech, O. Palacios, L. Villarreal, P. González-Duarte, M. Capdevila, S. Atrian, *FEBS Lett.* (2003) 533, 72

[33].- D. Egli, J. Domenech, K. Balamurugan, H. Hua, A. Selvaraj, H. Yepiskoposyan, A. Vardanyan, M. Capdevila, S. Atrian, O. Georgiev, W. Schaffner, *J. Biol. Chem.* (2005), 000.

[34].- http://www.expasy.org/cgi-bin/lists?/metallo.txt

[35].- C.J. Quaife, S.D. Findley, J.C. Erikson, G.J. Froelick, E.J. Kelly, B.P. Zambrowicz, R.D. Palmiter, *Biochemistry* (1994) **33**, 7250
[36].- L. Liang, K. Fu, D.K. Lee, R.J. Sobieski, T. Dalton, G.K. Andrews, *Molecular Reproduction and Development* (1996) **43**, 25
[37].- M. Vašák, D.W. Hasler, *Curr. Opin. Chem. Biol.* (2000) ***4***, 177
[38].- B. Roschitzki, M. Vašák, *J. Biol. Inorg. Chem.* (2002) ***7***, 611
[39].- J. Hidalgo, M. Aschner, P. Zatta, M. Vašák, *Brain Res. Bull.* (2001) **55**, 133
[40].- N. Cols, N. Romero-Isart, R. Bofill, M. Capdevila, P. González-Duarte, R. González-Duarte, S. Atrian, *Protein Eng.*, (1999) **12**, 265
[41].- N. Cols, N. Romero-Isart, M. Capdevila, B. Oliva, P. Gonzàlez-Duarte, R. Gonzàlez-Duarte, S. Atrian, *J. Inorg. Biochem.* (1997) **68**, 157
[42].- International Chicken Genome Sequencing Consortion, *Nature* (2004) **432**, 695
[43].- http://www.biochem.unizh.ch/mtpage/poster/posterevol.html
[44].- C.C. McCormick, C.S. Fullmer, J.S. Garvey, *Proc. Natl. Acad. Sci.* USA (1988) **85**, 309
[45].- D. Wei, G.K. Andrews, Med. *Cent., Univ. Kansas City, KS, USA, Nuc. Acids Res.* (1988) **16**, 537
[46].- M.J. Daniels, J.S. Turner-Cavet, R. Selkirk, H. Sun, J.A. Parkinson, P.J. Sadler, N.J. Robinson, *J. Biol. Chem.* (1998) **273**, 22957
[47].- N. Romero-Isart, N. Cols, M.K. Termansen, J.L. Gelpí, R. González-Duarte, S. Atrian, M. Capdevila, P. González-Duarte, *Eur. J. Biochem.* (1999) **259**, 519
[48].- D. Wei, G.K. Andrews, *Nuc. Acids Res.* (1988) **16**, 537
[49].- U. Weser, F. Donay, H. Rupp, *FEBS Lett.* (1973) **32**, 171
[50].- H. Rupp, W. Voelter, U. Weser, *Hoppe-Seyler's Z. Physiol. Chem.* (1975) **356**, 755
[51].- R.K. Mehra, J.R. Garey, T.R. Butt, W.R. Gray, D.R. Winge, *J. Biol. Chem.* (1989) **264**, 19747
[52].- J.L. Thorvaldsen, R.K. Mehra, W. Yu, A.K. Sewell, D. R. Winge, *Yeast* (1995) **11**, 1501
[53].- R.K. Mehra, E.B. Tarbet, W.R. Gray, D.R. Winge, *Proc. Natl. Acad. Sci. USA* (1988) **85**, 8815
[54].- G.P.M. Borrelly, M.D. Harrison, A.K. Robinson, S.G. Cox, N.J. Robinson, S.K. Whitehall, *J. Biol. Chem.* (2002) **277**, 30394
[55].- R. Prinz and U. Weser, *Hoppe-Seyler's Z. Physiol. Chem.* (1975) **356**, 767-776
[56].- C. Luchinat, B. Dolderer, C. Del Bianco, H. Echner, H.J. Hartmann, W. Voelter, U. Weser, *J. Biol. Inorg. Chem.* (2003) **8**, 353
[57].- U. Weser, H.J. Hartmann, *Biochim. Biophys. Acta* (1988) **953**, 1
[58].- D.R. Winge, K.B. Nielson, W.R. Gray, D.H. Hamer, *J. Biol. Chem.* (1985) **260**, 14464
[59].- V.C. Culotta, W.R. Howard, X.F. Liu, *J. Biol. Chem.* (1994) **269**, 25295
[60].- L.T. Jensen, W.R. Howards, J.J. Strain, D.R. Winge, V.C. Culotta, *J. Biol. Chem.* (1996) **271**, 18514
[61].- J. Strain, V.C. Culotta, *Mol. Gen. Genet.* (1996) **251**, 139
[62].- R.N. Reese, D.R. Winge, *J. Biol. Chem.* (1988) **263**, 12832
[63].- D.N. Weber, F. Shaw III, D.H. Petering, *J. Biol. Chem.* (1987) **262**, 6962
[64].- R.N. Reese, R.M Mehra, E.B. Tarbet, D.R. Winge, *J. Biol. Chem.* (1988) **263**, 4186
[65].- D. Winge, C.T. Dameron, R.K. Mehra in *Metallothioneins* (Eds. M.J. Stillman, F.C. Shaw III, K.T. Suzuki), VCH Publishers Inc., New York (1992) **ch 11**, 257
[66].- C.T. Dameron, D.R. Winge, *Inorg. Chem.* (1990) 29, 1343
[67].- W. Maret, G. Heffron, H.A. Hill, D. Djuricic, L.J. Jiang, B.L. Vallee, *Biochemistry* (2002) **41**, 1689
[68].- D. H. Hamer, *Ann. Rev. Biochem.* (1986) **55**, 913
[69].- K. Polec, O. Palacios, M. Capdevila, P. González-Duarte, R. Lobinski, *Talanta* (2002) **57(5)**, 1011
[70].- R. Bofill, O. Palacios, M. Capdevila, N. Cols, R. González-Duarte, S. Atrian, P. González-Duarte, *J. Inorg. Biochem.* (1999) **73**, 57
[71].- K. Polec, J. Szpunar, O. Palacios, P. González-Duarte, S. Atrian, R. Lobinski, *J. Anal. At. Spectrom.* (2001) **16**, 567
[72].- W. Birchmeier, P. Christen, *FEBS Lett.* (1971) **18**, 209
[73]- J. Bongers, C.D. Walton, D.E. Richardson, J.U. Bell, *Anal. Chem.* (1988) **60**, 2683
[74].- In *Standard Methods for the Examination of Water and Wastewater* (Eds. L.S. Clesceri, A.E. Greenberg, A.D. Eaton), American Public Health Association, Washington D.C., (1998)
[75].- T.E. King, R.O. Morris, *Methods Enzymol.* (1967) **10**, 634

[76].- A. Marcó, R. Compañó, R. Rubio, I. Casals, L. Krotz, L. Ragaglia, G. Giazzi, *Analyst* (2001) **126**, 1820
[77].- H. Rupp, U. Weser, *Biochim. Biophys Acta* (1978) **533**, 209
[78].- P. Palumaa, E.A. Mackay, M. Vasák, *Biochemistry* (1992) **31**, 2181
[79].- Y. Hathout, K.J. Reynolds, Z. Szilagyi, C. Fenselau, *J. Inorg. Biochem.* (2002) **88**, 119
[80].- K. Zangger, I.M Armitage, *J. Inorg. Biochem.* (2002) **88**, 135
[81].- O. Palacios, K. Polec-Pawlak, R. Lobinski, M. Capdevila, P. Gonzàlez-Duarte, *J. Biol. Inorg. Chem.* (2003) **8**, 831